



HAL
open science

Development of micro and nanostructured systems for cutaneous leishmaniasis treatment

Ana Paula dos Santos Matos

► **To cite this version:**

Ana Paula dos Santos Matos. Development of micro and nanostructured systems for cutaneous leishmaniasis treatment. Chemical and Process Engineering. Ecole des Mines d'Albi-Carmaux; Universidade federal do Rio de Janeiro, 2018. English. NNT : 2018EMAC0021 . tel-03091971

HAL Id: tel-03091971

<https://theses.hal.science/tel-03091971v1>

Submitted on 1 Jan 2021

HAL is a multi-disciplinary open access archive for the deposit and dissemination of scientific research documents, whether they are published or not. The documents may come from teaching and research institutions in France or abroad, or from public or private research centers.

L'archive ouverte pluridisciplinaire **HAL**, est destinée au dépôt et à la diffusion de documents scientifiques de niveau recherche, publiés ou non, émanant des établissements d'enseignement et de recherche français ou étrangers, des laboratoires publics ou privés.



THÈSE

En vue de l'obtention du

DOCTORAT DE L'UNIVERSIT  DE TOULOUSE

D livr  par :

IMT -  cole Nationale Sup rieure des Mines d'Albi-Carmaux

Cotutelle internationale avec Universidade Federal do Rio de Janeiro, Brazil

Pr sent e et soutenue par :
Ana Paula DOS SANTOS MATOS

le 20 d cembre 2018

Titre :
Development of micro and nanostructured systems for cutaneous
leishmaniasis treatment

 cole doctorale et discipline ou sp cialit  :
ED MEGEP : G nie des proc d s et de l'Environnement

Unit  de recherche :
Centre RAPSODEE, UMR CNRS 5302, IMT Mines Albi

Directeur/trice(s) de Th se :
Maria In s R , Directrice de Recherche, IMT Mines Albi
Carla HOLANDINO QUARESMA, Professeur, UFRJ Brazil

Jury :
Carla HOLANDINO QUARESMA, Professeur, UFRJ Brazil, Pr sidente
Bruno Filipe CARMELINO CARDOSO SARMENTO, Professeur, Univ. do Porto,
Rapporteur
Lucas Antonio FERREIRA MIRANDA, Professeur, UFMG Brazil, Rapporteur
Bartira ROSSI BERGMANN, Professeur, UFRJ Brazil, Invit e



UNIVERSIDADE FEDERAL DO RIO DE JANEIRO
FACULDADE DE FARMÁCIA
PROGRAMA DE PÓS-GRADUAÇÃO EM CIÊNCIAS FARMACÊUTICAS
&
UNIVERSITÉ FÉDÉRALE TOULOUSE MIDI-PYRÉNÉES
ÉCOLE DOCTORALE MÉCANIQUE, ENERGÉTIQUE, GÉNIE CIVIL & PROCÉDÉS

**DEVELOPMENT OF MICRO AND
NANOSTRUCTURED SYSTEMS FOR CUTANEOUS
LEISHMANIASIS TREATMENT**

Ana Paula dos Santos Matos

SUPERVISORS: Prof. Dr. CARLA HOLANDINO QUARESMA

Prof. Dr. MARIA INÊS RE

CO-SUPERVISORS: Prof. Dr. EDUARDO RICCI JÚNIOR

Dr. ALESSANDRA LIFSITCH VIÇOSA

Rio de Janeiro

2018

ANA PAULA DOS SANTOS MATOS

**DEVELOPMENT OF MICRO AND NANOSTRUCTURED
SYSTEMS FOR CUTANEOUS LEISHMANIASIS
TREATMENT**

Thesis in international joint supervision submitted in partial fulfillment of the requirements for the degree of Doctor in Pharmaceutical Sciences (School of Pharmacy, Federal University of Rio de Janeiro, Brazil) and degree of Process Engineering, IMT Mines Albi, Federal University of Toulouse, France).

Supervisor in Brazil: Prof. Dr. Carla Holandino Quaresma

Supervisor in France: Prof. Dr. Maria Inês Ré

Co-supervisors in Brazil: Prof. Dr. Eduardo Ricci Junior

Dra. Alesssandra Lifsitch Viçosa

Rio de Janeiro

2018



FACULTY OF PHARMACY, FEDERAL UNIVERSITY OF RIO DE JANEIRO

SECRETARY OF THE GRADUATE PROGRAM IN PHARMACEUTICAL SCIENCES

THESIS DEFENSE DOCUMENT


At 11 am of December 20th, 2018, at the auditory Prof. Maria Thereza Loureiro Lima, located on the first floor of the Prof. Levy Gomes Ferreira building, occurred the thesis defense of the candidate **Ana Paula dos Santos Matos** to obtain the PhD title in Pharmaceutical Sciences. The session was opened by the Coordinator Graduate Program of Pharmaceutical Sciences from the Faculty of Pharmacy, Prof. Dr. Cláudia Pinto Figueiredo, who introduced the advisor, Prof. Carla Holandino Quaresma and nominated her the chair of the defense process. The other advisor of the student was present at the session, Prof. Dr. Maria Inês Ré and the other professors who constituted the approved Examining Board: Prof. Dr. Bruno Filipe Carmelino Cardoso Sarmiento, from the INEB of the University of Porto (Portugal) and Prof. Dr. Lucas Antonio Miranda Ferreira, from the Faculty of Pharmacy of UFMG and invited members Prof. Dr. Igor de Almeida Rodrigues, from the Faculty of Pharmacy of UFRJ; Prof. Dr. Bartira Rossi Bergmann, from IBCCF of UFRJ. The regulations of the Graduate Program were followed in terms of the candidate's presentation time and the candidate's arguments. After this stage, the Examining Board members asked the audience to leave the examining room and met to discuss the evaluation of the student, thus establishing the following result:

Prof. Dr. Carla Holandino Quaresma	Approved: (X) Not approved: ()
Prof. Dr. Maria Inês Ré	Approved: (X) Not approved: ()
Prof. Dr. Bruno Filipe Carmelino Cardoso Sarmiento	Approved: (X) Not approved: ()
Prof. Dr. Lucas Antonio Miranda Ferreira	Approved: (X) Not approved: ()


Based on the result above, it was determined that the candidate Ana Paula dos Santos Matos was approved to obtain her PhD title in Pharmaceutical Sciences, related to the presented work, entitled "**Development of micro and nanostructured systems for cutaneous leishmaniasis treatment**". Finally, this document is signed by the Coordinator of the Graduate Program in Pharmaceutical Sciences of the Faculty of Pharmacy and by the Examining Board members and Advisors.

Rio de Janeiro, December, 20th, 2018.

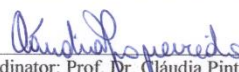

PhD candidate: Ana Paula dos Santos Matos


Supervisor: Prof. Dr. Maria Inês Ré


Prof. Dr. Lucas Antonio Miranda Ferreira


Supervisor: Prof. Dr. Carla Holandino Quaresma


Prof. Dr. Bruno Filipe Carmelino Cardoso Sarmiento


Coordinator: Prof. Dr. Cláudia Pinto Figueiredo

***To my Family for all the
support and affection***

ACKNOWLEDGEMENTS

First, I would like to thank *God* for give me the opportunity to develop this project, for guide me during all these years and for give me health and strength to make this project real.

I wish to dedicate my gratefulness to my parents *Ana Cristina and Paulo Roberto*, my “second father” *José Duarte*, my brothers *Rodrigo and Keila* and *all my family* for the understanding, encouragement, patience and love during all these years.

I would like to thank my *Supervisors (Prof. Carla, Prof. Eduardo, Prof. Maria Inês and Dr. Alessandra)* for all support, patience, guidance, advices and encouragement during all these years.

I would like to thank *Xellia Pharmaceuticals* (Denmark) for amphotericin B donation and *Farmanguinhos* for paromomycin donation.

I want to thank, in special, *Maria Luiza, Deise Drummond and Taísa Leiras* for all support and partnership to help me in experiments development.

I want to thank the first lab (LabCholandino) that receive me in Post-graduation, specially *Ana Paula Cajueiro, João Vitor da Costa, Juliana Paiva, Gleyce Barbosa, Fortune Homsani, Vania Bucco, Camila Siqueira, Adriana Oliveira, Michelle Nonato, Michelle Zanetti, Venicio Veiga* for all partnership, care, advices, aids and all the good moments that I passed there during this work.

I wish to dedicate my gratefulness for my other lab (LADEG), which was so important to me in the last year and thank, specially, for *Luciana Siqueira, Priscila Elias, Fiammeta Nigro, Iris Giovanini, Mayra Leal, Raphaela Schuenck, Leide Lene, Tatiana Zanella, Barbara Lorca, Prof. Ana Villa, Prof. Aline Guerra, Prof. Elisabete Santos, Prof. Zaida Freitas* for all care, aids, patience and good moments that I passed mostly in the last year.

I wish to dedicate my gratefulness for IMT Mines Albi and Rapsodee Research Center (*Sylvie Del Confetto, Christine Rolland, Laurent Devriendt, Rachel Calvet, Phillipe Accart, Véronique Nallet, Séverine Patry, Céline Boachon, Anne-Marie Fontes, Fabienne Espitalier*) for all technical support, patience and care. Moreover, I would like to thank all the PhD students and interns (*Lori Gonnet, Margot Chauvet, Yi Rong, Martin Giraud, Rajesh Munirathinam, Son Phan, Razac Sane, Lina Romero, Graciela Pacheco, Chaima Chaabani, Lucia Perez, Marwa Said, Bruna Rego, Hugo Hael, Thomas Blanchard, Théo Tellouk, Diana Avram, Diana Lucia and Issa Munu*) for friendship and good moments during the year that I passed there.

I would like to thank GALA Platform (*Angelique de Neiva, Antoine Perron, Laurène Haurie*) and *Jacqueline Azevedo* for all support, aids, partnership and attention gave to me during the development of my formulations.

I would like to thank, in specially, *Bhianca Lins, Roger Lima, Rababe Sani, Sinan Boztepe, Ercan Boztepe, Marion Boztepe, Ludovic Moulin, Augustina Ephrain and Audrey Trba* for all support, care, friendship and good moments that we spent together during my stay in France.

I want to thank Laboratório de Imunofarmacologia – IBCCF – UFRJ, specially *Maria Paula Borsodi, Ariane Batista, Felipe Gondim e Prof. Bartira Bergmann* for the support, expertise and aid in development of *in vitro* studies.

I want to thank *Luis* from LabCQ, which help me in some IR analysis and *Aline da Costa* for help me in HPLC analysis.

I would like to thank *Plataforma de Microscopia Eletrônica Rudolf Barth – IOC – Fiocruz* for SEM and TEM analyses.

I want to thank *Farmanguinhos – Fiocruz*, specially *Laboratório de Farmacotécnica Experimental* for care, support and parterneship during all these years.

I want to thank my friends *Amanda Dumani, Clarice Costa, Rafael Sá, Renato Costa, Fernanda Lima, Fernanda Paschoal, Lais Monteiro, Kalline Franco, Yuka Nakamura, Marlon Heggdorne, Natália Linhares, Jéssica Barbosa* for all support, care, friendship and patience for my absence during this work.

I wish to dedicate my gratefulness for *IMT Mines Albi, MEGEP, School of Pharmacy – UFRJ, Prof. Ana Luisa Pallhares, Prof. Yraima Cordeiro, Prof. Cláudia Figueiredo and Secretaria Pós-graduação (Marcelo and Valeria)* for all support, care and opportunities to belong of these Institutions.

I would like to thank *Prof. Alexandre Pyrrho, Prof. Helena Keiko and Prof. Flavia Almada* for all advices and suggestions in Qualification step.

I would like to thank the titular members of jury *Prof. Bruno Sarmiento, Prof. Lucas Miranda, Prof. Bartira Bergmann, Prof. Igor de Almeida* and the substitute members *Prof. Elisabete dos Santos and Prof. Alexandre Pyrrho* for availability and accept to be a part of this work.

I want to thank all the person that contribute direct or indirect for this work.

I would like to thank *Coordenação de Aperfeiçoamento de Pessoal de Nível Superior (CAPES)* for the financial support of my Ph.D. project and *Fundação Carlos Chagas Filho de Amparo à Pesquisa do Estado do Rio de Janeiro (FAPERJ)* for the financial support of a part of my Ph.D. Project developed in France.

RÉSUMÉ

Ana Paula dos Santos Matos. **Développement de systèmes micro et nanostructurés destinés au traitement de la leishmaniose cutanée.** Rio de Janeiro, 2018. Thèse (Doctorat Sciences Pharmaceutiques), Faculté de Pharmacie, Université Fédérale de Rio de Janeiro, Brésil ; (Doctorat en Génie des Procédés et de l'Environnement), IMT Mines Albi, Université de Toulouse, France, 2018.

La leishmaniose est une maladie négligée causée par des parasites protozoaires du genre *Leishmania* et affecte des millions de personnes dans plusieurs pays. Le traitement actuel pour la leishmaniose cutanée (LC) a de nombreux effets secondaires. Ces facteurs intensifient la recherche de nouvelles formulations et l'étude de différences voies d'administration principalement pour le traitement LC, pour lesquelles les micro- et nanotechnologies pourraient représenter des solutions technologiques intéressantes capables de moduler le relargage ou la biodisponibilité des principes actifs. Un des médicaments les plus étudiés pour le traitement LC est la paromomycine (PM), un antibiotique aminoglycoside utilisé par voie intraveineuse et topique. Un autre médicament important est l'amphotéricine B (AmB), un antibiotique macrolide injectable utilisé comme traitement de deuxième choix. Cette thèse porte sur le développement d'une nanoémulsion huile-dans-l'eau (HE) contenant AmB pour une administration topique et des microparticules polymériques contenant PM obtenues par séchage par atomisation pour une administration intralésionnelle pour le traitement LC. Les formulations ont été caractérisées en termes de taille et morphologie de particules et gouttelettes d'huile, contenu d'actif, stabilité, propriétés thermiques, relargage *in vitro*. L'activité biologique a été évaluée par sécurité *in vitro* sur des macrophages et par activité antileishmanienne sur des promastigotes de *Leishmania amazonensis*. Les nanoémulsions HE contenant AmB sont caractérisées par des tailles de gouttelettes d'huile de l'ordre d'environ 50 nm, avec un indice de polydispersité inférieur à 0,5 et une teneur en AmB de 0,5 mg/mL. Les nanoémulsions ont présenté un profil de relargage lent et une faible perméation cutanée. Malgré une bonne activité antileishmanienne, ces formulations s'avèrent toxiques. Elles présentent une bonne stabilité physique jusqu'à 365 jours, mais doivent être conservées dans la chaîne du froid. Pour les microparticules polymériques, différentes compositions ont été évaluées (PLGA et mélange PLGA-PLA). Les résultats ont montré que le profil de relargage de PM était influencé par le type de polymère utilisé, avec un relargage plus lent pour le mélange PLGA-PLA. Ces microparticules polymériques contenant PM ne sont pas toxiques et présentent une bonne activité leishmanienne. Par conséquent, les deux types de formulations étudiées présentent un potentiel en tant que nouvelles alternatives pour le traitement par LC. Néanmoins, d'autres études sont nécessaires pour leur optimisation comme l'activité antileishmanienne contre les amastigotes de *L. amazonensis* et des études *in vivo* sur des souris BALB/c.

Mots clés : Leishmaniose Cutanée, Amphotericine B, Paromomycine, Nanoémulsion, Microparticules, Mélanges Polymériques, PLGA, PLA, Séchage.

RESUMO

Ana Paula dos Santos Matos. **Desenvolvimento de sistemas nano e microestruturados para o tratamento da leishmaniose cutânea.** Rio de Janeiro, 2018. Tese (Doutorado em Ciências Farmacêuticas), Faculdade de Farmácia da Universidade Federal do Rio de Janeiro, Brasil; (Doutorado em Engenharia de Processos e Meio-ambiente), IMT Mines Albi, Universidade de Toulouse, França, 2018.

A leishmaniose é uma doença negligenciada causada por parasitas protozoários do gênero *Leishmania* e que afeta milhões de pessoas em vários países. O tratamento atual para a leishmaniose cutânea (LC) causa muitos efeitos colaterais. Com base neste cenário, há uma busca intensiva de novas formulações e o estudo de diferentes vias de administração, principalmente para o tratamento da LC. Desta forma, micro e nanotecnologia são tecnologias importantes, que podem ser úteis para a modulação do perfil de liberação dos fármacos, melhorando sua biodisponibilidade. Um dos fármacos mais investigados para o tratamento da LC é a paromomicina (PM), um antibiótico aminoglicosídeo administrado por via intravenosa e tópica. Outro fármaco importante é a anfotericina B (AmB), um antibiótico macrolídeo, administrado de forma injetável, como tratamento de segunda escolha. Os objetivos deste estudo foram desenvolver uma nanoemulsão óleo-água (O/A) contendo AmB para administração tópica e micropartículas poliméricas secas por atomização contendo PM para administração intralesional para o tratamento da LC. As formulações foram caracterizadas principalmente em termos de tamanho e morfologia de partículas ou gotículas de óleo, propriedades térmicas, teor de fármaco, estabilidade e perfil de liberação. A atividade biológica foi avaliada através da segurança *in vitro* em macrófagos e atividade antileishmanial contra promastigotas de *Leishmania amazonensis*. As nanoemulsões O/A contendo AmB, foram caracterizadas por gotículas de óleo com tamanho de cerca de 50 nm, com índice de polidispersão menor que 0,5 e teor de fármaco de 0,5 mg / mL. As nanoemulsões mostraram uma cinética de liberação lenta e controlada de AmB e baixa permeação cutânea. No entanto, essas formulações foram citotóxicas com boa atividade antileishmanial. Além disso, a melhor formulação mostrou estabilidade até os 365 dias com necessidade de armazenamento em câmara fria. Para as micropartículas poliméricas carregadas com PM, foram investigados diferentes transportadores (apenas PLGA ou uma mistura de PLGA-PLA). Verificou-se que a cinética de liberação de PM foi influenciada pela composição carreadora, com liberação lenta para a mistura de polímeros. As formulações investigadas foram não-tóxicas e revelaram boa atividade leishmanicida. Portanto, as nanoemulsões O/A contendo AmB e as micropartículas poliméricas carregadas com PM apresentaram potenciais de uso como novas alternativas para o tratamento da LC. No entanto, mais estudos são necessários para sua otimização como atividade antileishmanial contra amastigotas de *L. amazonensis* e estudos *in vivo* em camundongos BALB/c.

Palavras-chave: Leishmaniose Cutânea, Anfotericina B, Paromomicina, Nanoemulsões, Micropartículas, Misturas Poliméricas, PLGA, PLA, Spray Drying

LIST OF FIGURES

Figure 1. Thesis Structure.....	30
Figure 2. Biological cycle of Leishmania sp (REITHINGER <i>et al.</i> , 2007).....	33
Figure 3. Patient with hepatosplenomegaly caused by VL (MINISTÉRIO DA SAÚDE, 2006).	34
Figure 4. Status of endemicity of visceral leishmaniasis in the world in 2016 (http://apps.who.int/neglected_diseases/ntddata/leishmaniasis/leishmaniasis.html). 35	35
Figure 5. First lesion of cutaneous leishmaniasis (MINISTÉRIO DA SAÚDE, 2017).....	36
Figure 6. Status of endemicity of cutaneous leishmaniasis in the world in 2016 (http://apps.who.int/neglected_diseases/ntddata/leishmaniasis/leishmaniasis.html). 37	37
Figure 7. Nasal mucosa edema characteristic of mucocutaneous leishmaniasis (MINISTÉRIO DA SAÚDE, 2017).	38
Figure 8. Chemical structure of pentavalent antimonials salts (a) N-methyl glucamine or Glucantime®, (b) Sodium stibogluconate or Pentostam® (CHEMID PLUS, 2016).	39
Figure 9. Chemical structure of amphotericin B (CHEMID PLUS, 2016).	40
Figure 10. Chemical structure of pentamidine (CHEMID PLUS, 2016).	41
Figure 11. Chemical structure of paromomycin (CHEMID PLUS, 2016).....	42
Figure 12. Chemical structure of miltefosine (CHEMID PLUS, 2016).....	43
Figure 13. Chemical structure of sitamaquine (CHEMID PLUS, 2016).....	43
Figure 14. Different types of drug delivery system with micro and nanotechnology (adapted from Wen <i>et al.</i> , 2017).....	48
Figure 15. Different types of nanoemulsions (adapted from KATOUZIAN & JAFARI, 2016).....	53
Figure 16. Scheme for nanoemulgel preparation (CHOUDHURY <i>et al.</i> , 2017).	55
Figure 17. Poloxamers chemical general structure (a,b) ethylene oxide and	

propylene oxide units (ROWE, SHESKEY, QUINN, 2009).....	56
Figure 18. Scheme of methods of preparation of nanoemulsions (RAI <i>et al.</i> , 2018).....	59
Figure 19. – Relation between droplet size and sonication time to obtain nanoemulsions (CAMPOS, RICCI-JUNIOR, MANSUR, 2012)	62
Figure 20. Human skin composition (Source: http://www.naturallyhealthyskin.org/anatomy-of-the-skin/the-dermis/dermis-anatomy-of-the-skin/).....	63
Figure 21. Number of publications of amphotericin B (AmB) among 1997-2017 obtained from database ‘Web of Science’ using keywords as “AmB + Leishmaniasis”, “AmB + drug delivery system (DDS)”, “AmB + Nanoemulsions”, “AmB + Nanoemulsions + drug delivery systems (DDS)”.....	65
Figure 22. Main steps of the AmB nanoemulsions preparation method.....	68
Figure 23. Calibration curve of AmB in methanol.	70
Figure 24. Scheme of AmB nanoemulsions in vitro release study.	72
Figure 25. Calibration curve of AmB in PBS for in vitro release study.	73
Figure 26. Franz Vertical Cell Diffusion System.	74
Figure 27. Calibration curve of AmB in mobile phase for skin permeation study.	76
Figure 28. Chromatograms of (a) skin piece in mobile phase and (b) AmB solution extracted from skin piece.	77
Figure 29. Reduction reaction of resazurin (Alamar Blue®) (adapted from CSEPREGI <i>et al.</i> , 2018).....	78
Figure 30. SEM images of raw AmB in magnifications (a) 220x, (b) 650x, (c) 1300x.....	80
Figure 31. TGA curve of raw AmB.....	81
Figure 32. FTIR spectrum of raw AmB.....	82
Figure 33. AmB nanoemulsions prepared in this work.	84
Figure 34. AmB UV- spectrum.	88

Figure 35. UV spectrum of nanoemulsions F and H in methanol.	89
Figure 36. TEM images of nanoemulsions with AmB (a) B-NE, (b) F-NE and respectively nanoemulsions without drug (c) L-NE and (d) H-NE.	92
Figure 37. Droplets size in stability study of (a) B-NE and (b) L-NE. Legend: RT – room temperature (28°C), R – refrigerator (4°C). * - No statistically significant differences (P > 0.05); ** - No statistically significant differences (P > 0.05); *** - No statistically significant differences (P > 0.05) according to One-Way ANOVA with Tukey post-test.	94
Figure 38. Droplets size in stability study of (a) F-NE and (b) H-NE. Legend: RT – room temperature (28°C), R – refrigerator (4°C). * - No statistically significant differences (P > 0.05); ** - No statistically significant differences (P > 0.05); *** - No statistically significant differences (P > 0.05) according to One-way ANOVA with Tukey post-test.	95
Figure 39. Polydispersity index (Pdl) in stability study of (a) B-NE and (b) L-NE. Legend: RT – room temperature (28°C), R – refrigerator (4°C). * - No statistically significant differences (P > 0.05); ** - No statistically significant differences (P > 0.05); *** - No statistically significant differences (P > 0.05); **** - Statistically significant different (P < 0.05) according to One-way ANOVA with Tukey post-test.	98
Figure 40. Polydispersity index (Pdl) in stability study of (a) F-NE and (b) H-NE. Legend: RT – room temperature (28°C), R – refrigerator (4°C). * - No statistically significant differences (P > 0.05); ** - No statistically significant differences (P > 0.05); *** - Statistically significant differences (P < 0.05); **** - Statistically significant different (P < 0.05) according to One-way ANOVA with Tukey post-test.	101
Figure 41. Drug loading content in stability study of (a) B-NE at room temperature, (b) B-NE at refrigerator, (c) F-NE at room temperature and (d) F-NE at refrigerator. Legend: RT – room temperature (28°C), R – refrigerator (4°C). * - Statistically significant different (P < 0.05) according to One-way ANOVA with Tukey post-test.	102
Figure 42. <i>In vitro</i> release profile of (a) B-NE (blue) and F-NE (red) and (b) free AmB in solution (black) (n=4).	105
Figure 43. Amount of AmB (a) AmB permeated/area and (b) % AmB permeated present in receptor chamber (n=5).	108

Figure 44. Amount of AmB retained in (a) epidermis and (b) dermis after 8 hours of <i>in vitro</i> permeation study.	110
Figure 45. Cytotoxicity of (a) free AmB and (b) B-NE, (c) F-NE and (d) L-NE in BMDM cells. Legend: 0 – Negative Control, medium without treatment. Triton – Positive Control (4% Triton 100x). * - No statistically significant differences (P > 0.05); ** - No statistically significant differences (P > 0.05) according to One-way ANOVA with Tukey post-test.....	112
Figure 46. Antileishmanial activity of free AmB against promastigotes of <i>L. amazonensis</i> . Legend: Control – untreated parasites, only with Schneider’s medium supplemented with FBS; DMSO – amount of DMSO (5%) higher than used to dissolved AmB. * - No statistically significant differences (P > 0.05); ** - No statistically significant differences (P > 0.05) according to One-way ANOVA with Tukey post-test. Means ± SD (n=3).	115
Figure 47. Antileishmanial activity of clove oil against promastigotes of <i>L. amazonensis</i> . Legend: Control – untreated parasites, only with Schneider’s medium supplemented with FBS. * - Statistically significant difference (P < 0.05); ** - Statistically significant difference (P < 0.05) according to One-way ANOVA with Tukey post-test. Means ± SD (n=3).	116
Figure 48. Antileishmanial activity of AmB nanoemulsions (a) B-NE and L-NE, (b) F-NE and H-NE against promastigotes of <i>L. amazonensis</i> . Legend: B-NE – NE with AmB and Tween® 20; L-NE – NE without AmB with Tween® 20; F-NE – NE with AmB; H-NE – NE without AmB; C1- Positive Control – AmB solution (1 µg/mL); C2- Negative Control - untreated parasites, only with Schneider’s medium supplemented with FBS. * - No statistically significant differences (P > 0.05); ** - No statistically significant differences (P > 0.05); *** - Statistically significant difference (P < 0.05); **** - Statistically significant difference (P < 0.05) according to One-way ANOVA with Tukey post-test. Means ± SD (n=3).	118
Figure 49. Chemical structures of biodegradables polymers (PLA, PGA and PLGA) (LARRAÑETA <i>et al.</i> , 2016).	127
Figure 50. Types of microparticles (a) microcapsules with one core, (b) microcapsules with various core and (b) microspheres.	129
Figure 51. Emulsification methods based on the preparation of (a) an oil-in-	

water (O/W) or (b) water-in-oil-in-water (W/O/W) emulsion (HAN <i>et al.</i> , 2016).	131
Figure 52. Droplet formation and drying during spray drying process.	133
Figure 53. Typical spray drying process (SOSNIK & SEREMETA, 2015).	133
Figure 54. Types of spray drying nozzles (a) two-fluid and (b) three-fluid (adapted from KAŠPAR <i>et al.</i> , 2013b).	135
Figure 55. Scheme of possible PLGA particle degradation mechanism (a) initial particle, (b) water uptake into polymer matrix, (c) polymer degradation (adapted from YAO <i>et al.</i> , 2016).	137
Figure 56. Number of publications of paromomycin (PM) among 1997-2017 obtained from database 'Web of Science' using keywords as "Paromomycin + Leishmaniasis", "Paromomycin + Characterization", "Paromomycin + Drug delivery system (DDS)", "Paromomycin + PLGA", and "Paromomycin + Leishmaniasis + Drug delivery systems (DDS)"	141
Figure 57. Nozzle types used in this work (a) two-fluid nozzle and (b) three-fluid nozzle (in situ coating).	146
Figure 58. Nozzles design and diameters used (a) three diameters of two-fluid nozzle, (b) three-fluid nozzle 1.4 mm.	147
Figure 59. Possible derivatization reaction of PM with DNFB.	149
Figure 60. Calibration curve of derivatized PM in distilled water.	150
Figure 61. Scheme of <i>in vitro</i> release assay of PM-MS/PM-MC samples. Legend: RT – room temperature.	153
Figure 62. Calibration curve of derivatized PM in PBS for <i>in vitro</i> release study.	154
Figure 63. SEM images of raw PM in magnifications (a) 800x, (b) 3200x. ...	159
Figure 64. SEM images of atomized PM in magnifications (a) 800x, (b) 3200x.	160
Figure 65. MDSC of (a) raw PM and (b) spray-dried PM with two heating cycles.	162
Figure 66. Color change of free PM: (a) light yellow powder before DSC analysis at room temperature, (b) dark brown powder after submitted to 200°C in DSC analysis.	

.....	162
Figure 67. XR Diffractograms of PM powders.....	163
Figure 68. FTIR spectrum of PM.....	164
Figure 69. Raman spectrum of PM.	165
Figure 70. SEM Images of some batches prepared with ETHYL ACETATE in two different magnifications: (a) PM-MS01 800x, (b) PM-MS01 1600x, (c) PM-MS02 800x and (d) PM-MS02 1600x.	167
Figure 71. SEM Images of some batches prepared with ACETONE in two different magnifications: (a) PM-MS06 800x, (b) PM-MS06 1600x.	168
Figure 72. SEM Images of some batches prepared with acetone in two different magnifications varying the nozzle diameter size: (a) PM-MS05 1600x 0.7 mm, (b) PM-MS05 3200x 0.7 mm, (c) PM-MS06 1600x 1.4 mm, (d) PM-MS06 3200x 1.4 mm, (e) PM-MS07 1600x 2.0 mm and (f) PM-MS07 3200x 2.0 mm.	172
Figure 73. SEM Images of some batches prepared with acetone in two different magnifications varying the PM concentration in the initial formulation: (a) PM-MS07 1600x, (b) PM-MS07 3200x, (c) PM-MS08 1600x, (d) PM-MS08 3200x.	174
Figure 74. MDSC curves of (a) pure PLGA, (b) PM-loaded PLGA microspheres (PM-MS06) and (c) PM-loaded core-shell PLGA microcapsules (PM-MC12).	180
Figure 75. MDSC curves of (a) pure PLA, (b) PM-loaded core-shell PLGA/PLA microcapsules (PM-MC20) and (c) PLGA/PLA blend microparticles (MC24).	183
Figure 76. SEM Images of some batches prepared with acetone in two different magnifications varying the nozzle type: two-fluid PM-MS06 and three-fluid (PM-MC12 and PM-MC16).....	185
Figure 77. SEM images of some batches prepared from an aqueous of PM, three-fluid, with different compositions of PLGA/PLA blends: PM-MC19 (95:5), PM-MC20 (90:10) and PM-MC21 (60:40).	186
Figure 78. SEM Images of PM-MC22 prepared with dichloromethane: acetone in two different magnifications: (a) 1600x, (b) 3200x.	187
Figure 79. FTIR spectra of pure components (PLGA and PM), physical mixture PM+PLGA (30:70) and microparticles samples (PM-MS06, PM-MC12 and PM-MC18).	189

Figure 80. FTIR spectra of pure PLA, physical mixture PLGA+PLA (95:5), physical mixture PM+PLA+PLGA (30:5:65), PM microparticles (PM-MC19) and blank microparticles (MC23).	190
Figure 81. PM-MS06 microspheres, after contact with water for 24h.	197
Figure 82. PM-MC15 microcapsules, before and after contact with water for 24h.	198
Figure 83. PM-MC18 microcapsules, before and after contact with water for 24h.	199
Figure 84. Raman images of spatial distribution of some PM-MS/PM-MC batches (a) PM-MS06, (b) PM-MC12, (c) PM-MC16 and (d) PM-MC20; (e) Raman spectra of Paromomycin (red) and PLGA (blue) with correspondent colors to identify polymer and drug in spatial distribution.	202
Figure 85. Possible structure of PM-MS/PM-MC batches based on Raman analysis. Legend: red – corresponding PM and blue – corresponding polymer.	203
Figure 86. Cytotoxicity assay of (a) free PM, (b) PM-MC12, (c) PM-MC20 and (d) MC24 in BMDM cells. Legend: 0 – Negative Control without treatment, Triton – Positive Control (4% Triton 100x). * - No statistically significant differences ($P > 0.05$); ** - No statistically significant differences ($P > 0.05$); *** - No statistically significant differences ($P > 0.05$) according to One-way ANOVA with Tukey post-test.	206
Figure 87. Antileishmanial activity in <i>L. amazonensis</i> promastigotes. Legend: *- MC24 is statistically significant different ($P < 0.05$) than the others, ** - Statistically significant differences ($P < 0.05$) according to One-way ANOVA with Tukey post-test.	208

LIST OF TABLES

Table 1. Current treatments of leishmaniasis (adapted from ZULFIQAR, SHELPER, AVERY, 2017; LINDOSO <i>et al.</i> , 2012 and MENEZES <i>et al.</i> , 2015)..45	
Table 2. Physicochemical properties of some poloxamers used in pharmaceutical formulations (adapted from BODRATTI & ALEXANDRIDIS, 2018; adapted from DEVI, SANDHYA, HARI, 2013; adapted from ROWE, SHESKEY, QUINN, 2009).	57
Table 3. AmB nanoemulsions composition	69
Table 4. Physicochemical characterization of AmB nanoemulsions	86
Table 5. Drug Content of Nanoemulsions	90
Table 6. CC50, IC50 values and Selective Index of free AmB, free clove oil and nanoemulsions.	119
Table 7. Physical properties of some PLGAs (adapted from KAPOOR <i>et al.</i> , 2015; ANSARY <i>et al.</i> , 2014).	128
Table 8. Adjustable variables in a spray drying process (adapted from PATEL <i>et al.</i> , 2015; SOSNIK & SEREMETA, 2015; adapted from PAUDEL <i>et al.</i> , 2013).	134
Table 9. Drug delivery systems of paromomycin formulations.	142
Table 10. Dependent and independent kinetic models for study release profile of PM delivery systems (adapted from MEDEIROS <i>et al.</i> , 2017; adapted from COSTA, 2002).	155
Table 11. Formulation conditions, process and product characteristics of PM-loaded microspheres: solvent effect.	166
Table 12. Formulation conditions, process and product characteristics of PM-loaded microspheres: nozzle orifice diameter effect.	170
Table 13. Formulation conditions, process and product characteristics of PM-loaded microspheres: effect of PM concentration in the initial liquid formulation.	173
Table 14. Formulation conditions, process and product characteristics of PM-loaded core-shell microcapsules.	176
Table 15. Thermal properties of pure PLGA, PM-MS06 and PM-MC12.	179

Table 16. Thermal properties of PM-MC and MC (blank) batches prepared with PLGA/PLA as polymeric matrix.	181
Table 17. Particle size distribution and Span of some PM-MC batches.	191
Table 18. Composition of PM-MS/PM-MC batches selected and their characterization.....	193
Table 19. % PM released per hour of released test and dissolution efficiency after 4 hours (DE _{4h}).....	194
Table 20. Kinetic parameters of PM-MS/PM-MC batches using Korsmeyer-Peppas model.....	195
Table 21. In vitro antileishmanial activity and cytotoxicity results for PM-MC formulations (CC50, IC50 values and Selective Index of free PM and PM-MC batches) against <i>L. amazonensis</i> promastigotes	209

LIST OF EQUATIONS

Equation 1. Drug Content (DL %)	150
Equation 2. Encapsulation Efficiency (EE %)	150
Equation 3. Yield of batches	151
Equation 4. Polydispersity Index (Span)	151

ABBREVIATIONS

ACE - Acetone

AIC – Akaike Information Criterion

Abelcet – Lipid Complex of Amphotericin B

AmB – Amphotericin B

Ambisome – Liposomal Amphotericin B

Amphocil – Amphotericin B Colloidal Dispersion

Amphotec - Amphotericin B Colloidal Dispersion

ATL – American Tegumentary Leishmaniasis

BCS – Biopharmaceutical Classification System

BMDM – Bone Marrow derived Macrophages

CC₅₀ – Half Maximal Cytotoxic Concentration

CEUA – Ethics Committee for Animal Use

CL – Cutaneous Leishmaniasis

CMC – Critical Micelle Concentration

CMT – Critical Micelle Temperature

DCM - Dichloromethane

DDS – Drug Delivery System

DE – Dissolution Efficiency

DL – Drug Loading

DLS – Dynamic Light Scattering

DMSO – Dimethyl sulfoxide

DNFB - Dimethyl fluorobenzene

DSC – Differential Scanning Calorimetry

D_v – Volume Weighted Mean Diameter

EE – Encapsulation Efficiency

EMA – European Medicines Agency

FBS – Fetal Bovine Serum

FDA – Food and Drug Administration

Fiocruz – Fundação Oswaldo Cruz

FTIR – Fourier Transform Infrared Spectroscopy

Fungisome – Liposomal Amphotericin B Gel

Fungizone – Amphotericin B Sodium Deoxycholate

Glucantime - N-methylglucamine Antimoniate
HIV – Human Immunodeficiency Virus
HLB – Hydrophilic Lipophilic Balance
HPLC – High Performance Liquid Chromatography
IBCCF – Instituto de Biofísica Carlos Chagas Filho
ICH - International Conference on Harmonization of Technical Requirements
for Registration of Pharmaceuticals for Human Use
IC₅₀ - Half Maximal Inhibitory Concentration
IOC – Instituto Oswaldo Cruz / Oswald Cruz Foundation
Leishcutan – Ointment containing 15% Paromomycin + 12%
Methylbenzethonium Chloride
MCL – Muco Cutaneous Leishmaniasis
M-CSF – Macrophage Colony-stimulating Factor
MDSC – Modulated Differential Scanning Calorimetry
MS – Microparticles of PLGA without drug
NE – Nanoemulsion (s)
NMR – Nuclear Magnetic Resonance
O/W – Oil – Water
O/W/O – Oil – Water – Oil
PBS – Phosphate Buffer Solution
PDLA – Poly D-Lactide Acid
Pdl – Polydispersity Index
PEG – Polyethylene glycol
PIC – Phase Inversion Composition
PIT – Phase Inversion Temperature
Pentostam - Sodium Stibogluconate
PEO – Poly-ethylene Oxide
PGA – Poly Glycolide Acid
PLA – Poly Lactide Acid
PLGA – Poly Lactide co-Glycolide Acid
PLLA – Poly L-Lactide Acid
PEG – Polyethylene glycol
PM – Paromomycin
PM-MC – Microcapsules of PLGA and Paromomycin

PM-MS – Microspheres of PLGA and Paromomycin
PPO – Poly-propylene oxide
PVA – Polyvinyl Alcohol
R – Refrigerator
 R^2 – Coefficient of Determination
RESS – Rapid Expansion of Supercritical Solution
RMES – Root Mean Square Error
RPMI - Roswell Park Memorial Institute medium
RT – Room Temperature
SAS – Supercritical Antisolvent Crystallization
Sb V – Pentavalent Antimonial
SD – Standard Deviation
SEM – Scanning Electron Microscopy
SI – Selective Index
S/O – Solid -in-oil
TEM – Transmission Electron Microscopy
TGA - Thermogravimetry Analysis
Tg – Glass Transition Temperature
Tm – Melting Temperature
USP - The United States Pharmacopeia
VL – Visceral Leishmaniasis
WHO - World Health Organization
W/O – Water - Oil
W/O/W – Water – Oil - Water
XRD – X-ray Diffraction

CONTENTS

GENERAL INTRODUCTION	28
<u>CHAPTER 1</u> DISEASE LITERATURE REVIEW	31
<u>CHAPTER 2</u> OBJECTIVES	50
2.1. GENERAL OBJECTIVE	51
2.2. SPECIFIC OBJECTIVES	51
<u>CHAPTER 3</u> NANOEMULSIONS OF AMPHOTERICIN B.....	52
3.1. INTRODUCTION.....	53
3.1.1. Nanoemulsions	53
3.1.2. Poloxamers properties	55
3.1.3. Methods of nanoemulsion production	58
3.1.4. Topical administration	62
3.1.5. Amphotericin B.....	64
3.2. OBJECTIVES.....	66
3.3. MATERIALS AND METHODS.....	66
3.3.1. MATERIALS.....	66
3.3.2. METHODS.....	67
3.3.2.1. Physicochemical Characterization of Amphotericin B	67
3.3.2.1.1. Scanning Electron Microscopy (SEM).....	67
3.3.2.1.2. Thermogravimetry Analysis (TGA)	67
3.3.2.1.3. Fourier Transform Infrared Spectroscopy (FTIR)	67
3.3.2.2. Amphotericin B Nanoemulsions Development	68
3.3.2.3. Physicochemical Characterization of Amphotericin B Nanoemulsions.....	69
3.3.2.3.1. Determination of Droplet Size, Polydispersity Index and pH	69
3.3.2.3.2. Drug Content.....	70
3.3.2.4. Stability Study of Amphotericin B Nanoemulsions.....	70
3.3.2.4.1. Transmission Electron Microscopy (TEM).....	71
3.3.2.4.2. Determination of Droplet Size, Polydispersity Index and pH	71
3.3.2.4.3. Drug Content.....	71
3.3.2.5. In vitro Release of Amphotericin B Nanoemulsions	71

3.3.2.6. In vitro Skin Permeation Study of Amphotericin B Nanoemulsions	73
3.3.2.6.1. Skin Permeation Method	73
3.3.2.6.2. High Performance Liquid Chromatography (HPLC) Assay.....	75
3.3.2.7. BIOLOGICAL ASSAYS	77
3.3.2.7.1. Assessment of cytotoxicity of AmB nanoemulsions in BMDM cells.....	77
3.3.2.7.2. Antileishmanial Activity.....	79
3.3.2.8. Statistical Analysis	80
3.4. RESULTS AND DISCUSSION.....	80
3.4.1. PHYSICOCHEMICAL CHARACTERIZATION OF AMPHOTERICIN B ...	80
3.4.1.1. Scanning Electron Microscopy (SEM).....	80
3.4.1.2. Thermogravimetry Analysis (TGA).....	81
3.4.1.3. Fourier Transform Infrared Spectroscopy (FTIR)	82
3.4.2. AMPHOTERICIN B NANOEMULSIONS DEVELOPMENT	83
3.4.3. PHYSICOCHEMICAL CHARACTERIZATION OF AMPHOTERICIN B NANOEMULSIONS	85
3.4.3.1. Determination of Droplet Size, Polydispersity Index and pH	85
3.4.3.2. Drug Content.....	87
3.4.4. STABILITY STUDY OF AMPHOTERICIN B NANOEMULSIONS	91
3.4.4.1. Transmission Electron Microscopy (TEM).....	92
3.4.4.2. Determination of Droplet Size, Polydispersity Index and pH	93
3.4.4.3. Drug Content.....	102
3.4.5. IN VITRO RELEASE OF AMPHOTERICIN B NANOEMULSIONS	104
3.4.6. IN VITRO SKIN PERMEATION STUDY OF AMPHOTERICIN B NANOEMULSIONS	107
3.4.7. BIOLOGICAL ASSAYS	112
3.4.7.1. Assessment of cytotoxicity of AmB nanoemulsions in BMDM cells	112
3.4.7.2. Antileishmanial Activity.....	114
3.5. CONCLUSION	123
<u>CHAPTER 4</u> POLYMERIC MICROPARTICLES OF PAROMOMYCIN.....	125
4.1. INTRODUCTION.....	126
4.1.1. Biodegradable Polymeric Depots.....	126

4.1.2.	Physicochemical Properties of PLGA.....	127
4.1.3.	Preparation Methods of PLGA Microparticles	129
4.1.4.	Challenges in improving drug loading of PLGA microparticles with acceptable control over release rate profiles.....	134
4.1.5.	Release from PLGA microparticles	136
4.1.6.	PLGA microparticles for depot delivery	137
4.1.7.	Paromomycin	139
4.2.	OBJECTIVES.....	143
4.3.	MATERIAL AND METHODS	143
4.3.1.	MATERIAL	143
4.3.2.	METHODS.....	144
4.3.2.1.	PHYSICOCHEMICAL CHARACTERIZATION OF PAROMOMYCIN.....	144
4.3.2.1.1.	Scanning Electron Microscopy (SEM)	144
4.3.2.1.2.	Differential Scanning Calorimetry (DSC)	144
4.3.2.1.3.	X-ray Scattering Diffraction (XRD)	145
4.3.2.1.4.	Fourier Transform Infrared Spectroscopy (FTIR)	145
4.3.2.1.5.	Raman Spectroscopy.....	145
4.3.2.2.	PAROMOMYCIN POLYMERIC MICROPARTICLES DEVELOPMENT.	146
a)	Nozzle Design.....	146
b)	Type of Organic Solvent.....	147
c)	Type of Polymer.....	148
d)	PM Mass Concentration.....	148
e)	The Physical State of PM formulation	148
4.3.2.3.	PHYSICOCHEMICAL CHARACTERIZATION OF PAROMOMYCIN POLYMERIC MICROPARTICLES.....	148
4.3.2.3.1.	Scanning Electron Microscopy (SEM)	149
4.3.2.3.2.	Differential Scanning Calorimetry (DSC)	149
4.3.2.3.3.	Drug Content, Encapsulation Efficiency and Process Yield	149
4.3.2.3.4.	Fourier Transform Infrared Spectroscopy (FTIR)	151
4.3.2.3.5.	Particle Size	151
4.3.2.4.	IN VITRO RELEASE OF PAROMOMYCIN POLYMERIC MICROPARTICLES	

4.3.2.4.1. Methods used to compare drug release profiles from PM-loaded spray dried polymeric microparticles	154
4.3.2.5. SPATIAL DISTRIBUTION OF CONSTITUENTS IN THE MICROPARTICLES	155
4.3.2.5. BIOLOGICAL ASSAYS	156
4.3.2.5.1. Assessment of cytotoxicity of PM-loaded microparticles in BMDM cells	156
4.3.2.5.2. Antileishmanial Activity	157
4.3.2.6. STATISTICAL ANALYSIS	157
4.4. RESULTS AND DISCUSSION.....	158
4.4.1. PHYSICOCHEMICAL CHARACTERIZATION OF PAROMOMYCIN.....	158
4.4.1.1. Scanning Electron Microscopy (SEM)	158
4.4.1.2. Differential Scanning Calorimetry (DSC)	161
4.4.1.3. X-ray Scattering Diffraction (XRD)	163
4.4.1.4. Fourier Transform Infrared Spectroscopy (FTIR)	163
4.4.1.5. Raman Spectroscopy	164
4.4.2. PAROMOMYCIN POLYMERIC MICROSPHERES DEVELOPMENT	165
4.4.2.1. Development of PM-loaded PLGA microspheres.....	165
4.4.2.1.1. Solvent Choice	165
4.4.2.1.2. Nozzle Orifice Diameter Effect.....	169
4.4.2.1.3. Paromomycin Concentration	172
4.4.2.2. Development of PM-loaded core-shell PLGA microcapsules.....	175
4.4.2.2.1. Differential Scanning Calorimetry (DSC)	178
4.4.2.2.2. Scanning Electron Microscopy (SEM)	184
4.4.2.2.3. Fourier Transform Infrared Spectroscopy (FTIR)	188
4.4.2.2.4. Particle Size	191
4.4.3. IN VITRO RELEASE OF PAROMOMYCIN POLYMERIC MICROPARTICLES	192
4.4.4. SPATIAL DISTRIBUTION OF CONSTITUENTS IN PM-MS AND PM-MC MICROPARTICLES.....	196
4.4.4. BIOLOGICAL ASSAYS	205
4.4.4.1. Assessment of cytotoxicity of PM-loaded microparticles in BMDM cells	205
4.4.4.2. Antileishmanial Activity.....	208

4.5. CONCLUSION	211
<u>CHAPTER 5</u> GENERAL CONCLUSIONS AND PERSPECTIVES.....	214
<u>CHAPTER 6</u> BIBLIOGRAPHY	218
<u>CHAPTER 7</u> RÉSUMÉ LONG EN FRANÇAIS	254
<u>CHAPTER 8</u> ANNEXES	265
ANNEX 1 - Certificate of Analysis	266
ANNEX 2 - PM release fitting described by mathematical Korsmeyer-Peppas model.....	268
<u>CHAPTER 9</u> PUBLICATIONS RELATED TO THIS WORK.....	270
ABSTRACT	272

GENERAL INTRODUCTION

Leishmaniasis belongs of the group of neglected infectious diseases caused by protozoan parasites of the genus *Leishmania* (SINGH, KUMAR, SINGH, 2012; TRAN *et al.*, 2011) and is one of the major health problems in the world. This disease has many clinical manifestations and it is divided in visceral, muco-cutaneous and cutaneous leishmaniasis.

Cutaneous leishmaniasis is characterized by lesions on the skin, which appears, primarily, in the local of insect bite (MINISTÉRIO DA SAÚDE, 2017). In Brazil, is one of the most important dermatological illnesses and disseminate in the whole country.

The actual treatment for leishmaniasis, and particularly for cutaneous leishmaniasis, presents several side effects, which are motivating the development of new pharmaceutical formulations, as the study of different routes of administration. In this context, microtechnology and nanotechnology are interesting for modulate drug release profile and bioavailability providing more treatment effectiveness and low toxicity.

This PhD thesis was focused on the development of two new products aiming cutaneous leishmaniasis treatment: an oil-water nanoemulsion containing amphotericin B (one of the most drug studied for this disease) and polymeric microparticles containing paromomycin (drug that have been studied for topical administration) for intralesional administration for CL treatment. The work was undertaken under the framework of an international joint supervision between School of Pharmacy – Federal University of Rio de Janeiro in Brazil, and Mines Telecom Institute (IMT Mines Albi) in France.

This manuscript is divided in five chapters as shown in Figure 1.

Chapter 1 introduces a literature review on Leishmaniasis diseases, presenting types of clinical manifestations, treatment available and search of new formulations, focusing on micro and nanotechnologies. Chapter 2 describes the general and specifics objectives of this work.

Chapter 3 deals with amphotericin B (AmB) nanoemulsions. It starts with a literature review about the chosen drug followed by a review on nanoemulsions and more specifically, AmB nanoemulsions. In a second part, it describes all

material and methods used to produce AmB nanoemulsions and, finally the obtained results are presented and discussed.

Chapter 4 reports the development of PLGA-based microparticles loaded with paromomycin (PM), the second selected drug. Following the same report outline of Chapter 3, it presents paromomycin and then a review on polymeric depot deliveries, focusing on PLGA-based systems. In a second part, material and methods used to generate PLGA-based microparticles matrix type and core-shell structures are described. Results are presented and discussed in a third and last part of this chapter.

The concluding Chapter 5 summarizes the major findings of this thesis and gives suggestions for further studies.

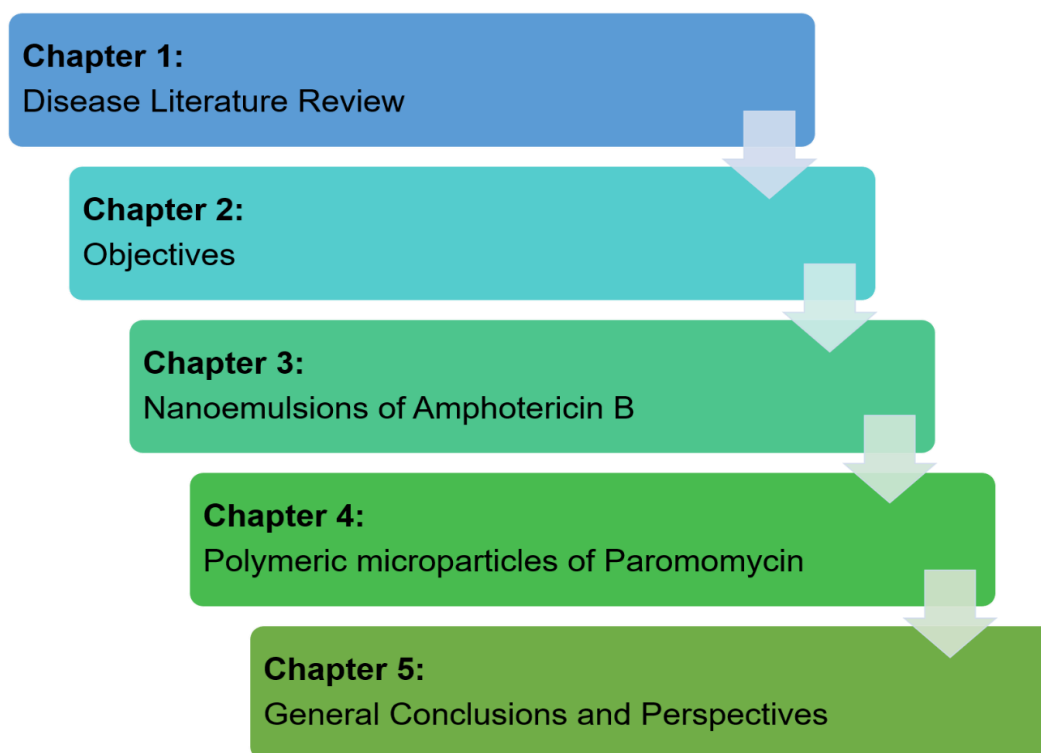


Figure 1. Thesis Structure

CHAPTER 1

DISEASE LITERATURE

REVIEW

Leishmaniasis is an anthroponosis caused by approximately 20 species of a protozoan of *Leishmania sp* genus, belongs to family Trypanosomatidae and transmitted by a bite of a hematophagous female sandflies belongs to a family Phlebotominae (AKBARI, ORYAN, HATAM, 2017; MINISTÉRIO DA SAÚDE, 2017; NASSIF *et al.*, 2017; MANSUETO *et al.*, 2014; WHO, 2017; SINGH, KUMAR, SINGH, 2012). This disease is considered a neglected disease, which affects 98 countries, 12 million cases and 350 million people are at risk to develop leishmaniasis with 1.5 to 2 million of new cases per year (AKBARI, ORYAN, HATAM, 2017; MINISTÉRIO DA SAÚDE, 2017; HUBERT *et al.*, 2013; YAHYA *et al.*, 2013; ALVAR *et al.*, 2012; CHATTOPADHYAY & JAFURULLA, 2011). Besides, cases of *Leishmania* with the co-infection human immunodeficiency virus (HIV) are increasing and have been described in 35 countries (SUNDAR & CHAKRAVARTY, 2015; PACE, 2014; TIUMAN *et al.*, 2011; SOARES *et al.*, 2007).

The etiological agent of leishmaniasis is an intracellular parasite of *Leishmania* genus, which presents a life cycle with two morphological forms: a flagellated or promastigote form, found in the insect vector organism and amastigote form found inside the macrophages of the vertebrate host. (MINISTÉRIO DA SAÚDE, 2017; SINGH, KUMAR, SINGH, 2012; TIUMAN *et al.*, 2011; REITHINGER *et al.*, 2007). The biological cycle of leishmaniasis is showed in Figure 2.

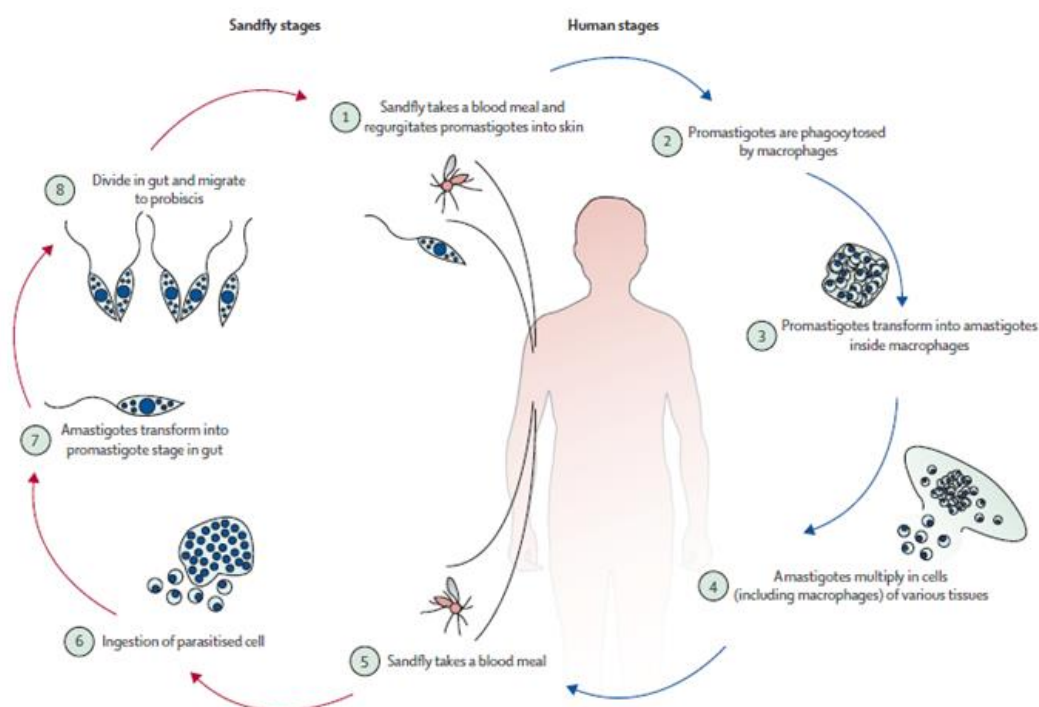


Figure 2. Biological cycle of *Leishmania* sp (REITHINGER *et al.*, 2007).

Leishmaniasis presents three major clinical manifestations as cutaneous, mucocutaneous and visceral (SINGH, KUMAR, SINGH, 2012; DUENAS-ROMERO, LOISEAU, CHAZALET, 2007; BATES, 2007), which depends on the infective specie and the host immunological response. Some authors consider diffuse cutaneous leishmaniasis form as the forth clinical patterns (CHAPPUIS *et al.*, 2007; REITHINGER *et al.*, 2007, KHATAMI *et al.*, 2007).

The visceral leishmaniasis (VL), also known as kala-azar, is the most serious leishmaniasis form and can be fatal when not treated (WHO, 2017; NO, 2016; MINISTÉRIO DA SAÚDE, 2006). The clinical diagnosis is complex because this disease shows nonspecific symptoms. However, in general, the patients with VL present prolonged fever, weight loss, anemia, abdominal pain, hepatomegaly and splenomegaly (WHO, 2017). These last two symptoms are the most characteristic of this clinical manifestation. The Figure 3 shows one patient with hepatosplenomegaly caused by VL.



Figure 3. Patient with hepatosplenomegaly caused by VL (MINISTÉRIO DA SAÚDE, 2006).

VL is endemic in more than 65 countries with widespread distribution around the world (MANSUETO *et al.*, 2014; MINISTÉRIO DA SAÚDE, 2006). The main species of *Leishmania*, which causes this type of leishmaniasis, are: *Leishmania infantum* and *Leishmania donovani* (NO, 2016; SINGH, KUMAR, SINGH, 2012). Kala-azar presents the incidence rate, approximately, 2 million cases and 500.000 new cases each year. Around 90% of visceral leishmaniasis cases in the world occur in five countries: India, Bangladesh, Nepal, Sudan and Brazil (NO, 2016; SINGH, KUMAR, SINGH, 2012; TIUMAN *et al.*, 2011). Each year, an estimated 50,000 to 90,000 new cases of VL take place worldwide (WHO, 2017) and an estimative between 20,000 and 40,000 cases of deaths happen per year (ALVAR *et al.*, 2012). The status of endemicity of VL in the world, in 2016, is showed in Figure 4. In Brazil, VL affects specially babies and small children. However, there is an increase of number of cases in adults, which were HIV-positive or were immunosuppressed (SUNDAR & CHAKRAVARTY, 2015, MANSUETO *et al.*, 2014; PACE, 2014; MINISTÉRIO DA SAÚDE, 2006).

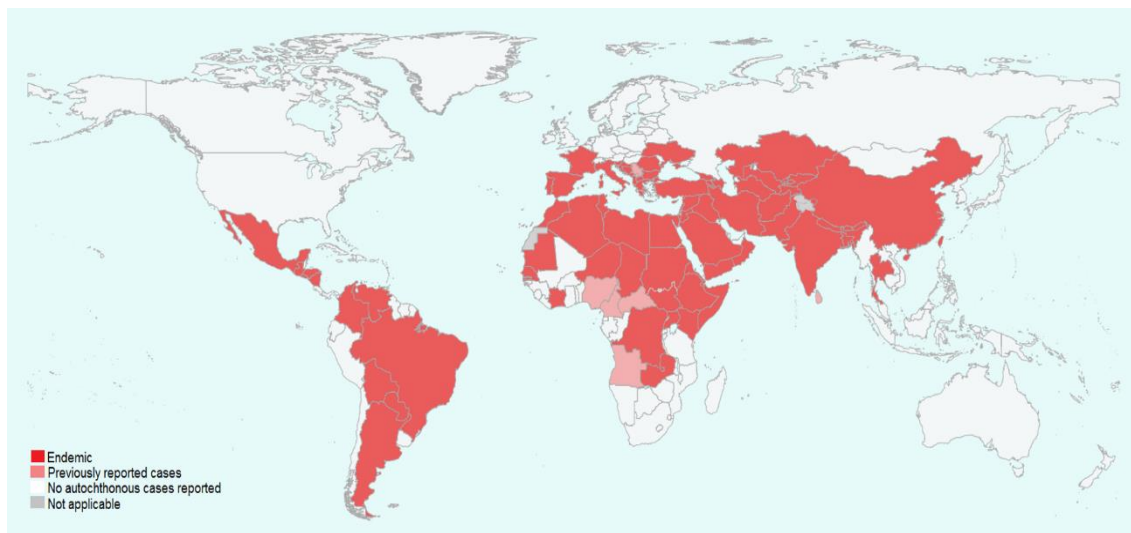


Figure 4. Status of endemicity of visceral leishmaniasis in the world in 2016 (http://apps.who.int/neglected_diseases/ntddata/leishmaniasis/leishmaniasis.html).

The cutaneous leishmaniasis (CL) or American tegumentary leishmaniasis (ATL) is usually characterized by the presence of rounded or oval skin lesions, which arise, primarily at the insect bite site (MINISTÉRIO DA SAÚDE, 2017; CARNEIRO *et al.*, 2012). The first lesion is, in general, single and painless (Figure 5). After a period of 1 to 12 weeks, arise one lesion as a papule erythematous that develops into a nodule with necrotic base and raised edges in a period of two weeks to six months (MINISTÉRIO DA SAÚDE, 2017; REITHINGER *et al.*, 2007; HEPBURN, 2000). Sometimes, CL lesion may be leave life-long scars (WHO, 2017). The clinical features of CL present many variables, as: patient location, parasite specie, type of zoonotic cycle of leishmania, immunological and also genetics responses of patients (SUNDAR & CHAKRAVARTY, 2015; WHO, 2010).



Figure 5. First lesion of cutaneous leishmaniasis (MINISTÉRIO DA SAÚDE, 2017).

CL is endemic in more than 70 countries with 90% reported cases occurred in seven countries (Afghanistan, Saudi Arabia, Algeria, Brazil, Pakistan, Peru and Syria) (SINGH, KUMAR, SINGH, 2012; TIUMAN *et al.*, 2011; REITHINGER, 2007). The status of endemicity of CL in the world, in 2016, is showed in Figure 6. The species of *Leishmania* most common are: *Leishmania major*, *Leishmania tropica*, *Leishmania mexicana*, *Leishmania guyanensis*, *Leishmania braziliensis*, *Leishmania amazonensis* and *Leishmania panamensis* (CARNEIRO *et al.*, 2012). According to the WHO, this type of leishmaniasis is considered one of the six infectious diseases most important because CL shows high capacity to cause deformations and high detection coefficient (MINISTÉRIO DA SAÚDE, 2017).

In Brazil, is one of the most important dermatological affection diseases with slight drop of number of cases in the last years, but with an incidence still very high being widely disseminated in brazilian territory (MINISTÉRIO DA SAÚDE, 2017).



Figure 6. Status of endemicity of cutaneous leishmaniasis in the world in 2016 (http://apps.who.int/neglected_diseases/ntddata/leishmaniasis/leishmaniasis.html).

The mucocutaneous form (MCL) presents destructive lesions located in the mucous membranes of the mouth and upper respiratory tract (Figure 7). It is believed that occur a hematogenous or lymphatic spread of the parasites from a cutaneous lesion. In most cases, MCL results from a chronic evolution of cured CL lesion without adequate treatment or without treatment (MINISTÉRIO DA SAÚDE, 2017; PACE, 2014; WHO, 2010). Some studies in Brazil indicated that MCL can happen months or more than 20 years after CL lesion (WHO, 2010). In severe cases, MCL lesion can lead to mutilations with partial or total loss of the nose and lips induced serious deformations and severe social problems (AKBARI, ORYAN, HATAM, 2017; PACE, 2014; WHO, 2010). Moreover, secondary infections may increase the patient's death risk and may lead to death (WHO, 2010).



Figure 7. Nasal mucosa edema characteristic of mucocutaneous leishmaniasis (MINISTÉRIO DA SAÚDE, 2017).

The species of *Leishmania* responsible for MCL are: *Leishmania braziliensis*, *Leishmania amazonensis* and *Leishmania guyanensis* (MINISTÉRIO DA SAÚDE, 2007). This type of leishmaniasis occurs mainly in the Americas with the highest number of reported cases in Bolivia, Peru and Brazil (WHO, 2010). There are rare reports of cases of mucocutaneous leishmaniasis in Europe affecting only elderly and immunocompromised individuals (PACE, 2014).

The first line treatment of leishmaniasis is an intravenous, intralesional or intramuscular administration of pentavalent antimonials (Figure 8), as N-methylglucamine antimoniate (Glucantime®) and sodium stibogluconate (Pentostam®) (SUNDAR & CHAKRAVARTY, 2015). This last one is not marketed in Brazil (MINISTÉRIO DA SAÚDE, 2017). The antimonials still present a questionable mechanism of action, although they have been on the market for a long time. It is believed that the mechanism of action can be related to the transformation of pentavalent antimoniate into trivalent. The pentavalent and trivalent antimonials induced parasite DNA fragmentation (MINISTÉRIO DA SAÚDE, 2017; SINGH, KUMAR, SINGH, 2012; KHATAMI *et al.*, 2007), inhibition of glycolysis step of metabolism and fatty acid oxidation of the parasite (PACE, 2014; LINDOSO *et al.*, 2012; SINGH, KUMAR, SINGH, 2012; GOTO & LINDOSO, 2010).

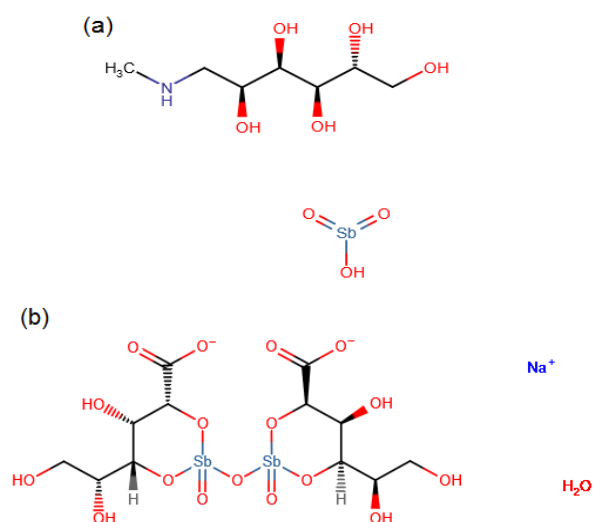


Figure 8. Chemical structure of pentavalent antimonials salts (a) N-methyl glucamine or Glucantime®, (b) Sodium stibogluconate or Pentostam® (CHEMID PLUS, 2016).

The antimonials follow therapeutic scheme preconized by WHO through intravenous or intramuscular injection use of 10 to 20 mg (Sb V)/ kg/ day for 20 or 30 days depending on the leishmaniasis form developed by patient (MINISTÉRIO DA SAÚDE, 2017; REITHINGER, 2007). Intralesional administration therapeutic scheme uses one to three applications, subcutaneously, of antimonials solution every 15 days (MINISTÉRIO DA SAÚDE, 2017). This type of medicines has not to be use for pregnant and elderly people because they induce severe side effects such as hepatotoxicity, nephrotoxicity and cardiotoxicity (AKBARI, ORYAN, HATAM, 2017; ESPUELAS *et al.*, 2003). Intralesional administration can cause a local reaction and systemic side effects similar as intravenous and intramuscular administration, but of mild to moderate intensity and reversible after end of treatment (MINISTÉRIO DA SAÚDE, 2017). Besides side effects, there are some reports of parasite resistance to these drugs (SINGH, KUMAR, SINGH, 2012).

The second-choice treatment involves the administration of amphotericin B and pentamidine (NASSIF *et al.*, 2017; TIUMAN *et al.*, 2011).

Amphotericin B (AmB) (Figure 9) is a polyene antifungal of the macrolide class produced by *Streptomyces nosodus* (CHEMID PLUS, 2016; THE INTERNATIONAL PHARMACOPEIA, 2017a; USP, 2012a; EUROPEAN

PHARMACOPEIA 7.0, 2009; GOLENSER & DOMB, 2006). This drug acts by binding the ergosterol molecules present in the cytoplasmic membrane of parasites, being the most active leishmanicidal on the market nowadays (MINISTÉRIO DA SAÚDE, 2017; SINGH, KUMAR, SINGH, 2012; GOLENSER & DOMB, 2006, BERMAN, 1997). Although AmB shows high affinity to ergosterol, it can also bind cholesterol molecules, which induces the side effects (SINGH, KUMAR, SINGH, 2012). The recommended dosage of AmB, in leishmaniasis treatment, is 0.7 to 1 mg/ kg/ day by intravenous route for 20 days (MINISTÉRIO DA SAÚDE, 2017).

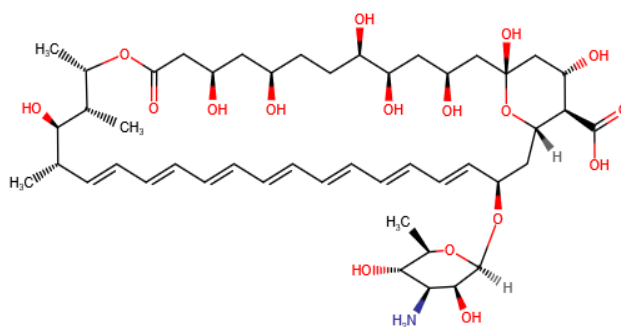


Figure 9. Chemical structure of amphotericin B (CHEMID PLUS, 2016).

Nowadays, there are 4 commercial formulations of amphotericin B available on the market for hospital use: an amphotericin B deoxycholate (Fungizone[®]), a liposomal amphotericin B (Ambisome[®]), cholesterol dispersion amphotericin B (Amphocil[®]/Amphotec[®]) and lipid complex of amphotericin B (Abelcet[®]) (CALDEIRA *et al.*, 2015; IBRAHIM *et al.*, 2012; LINDOSO *et al.*, 2012; GOTO & LINDOSO, 2010).

Although its higher efficacy than antimonial pentavalent based-products, AmB, in all commercial forms available, still presents high toxicity (nephrotoxicity) and several side effects such as fever, headache, nausea, vomiting, tremors, hypotension among others (MINISTÉRIO DA SAÚDE, 2017; FILIPPIN, SOUZA, MARANHÃO, 2008; GOLENSER & DOMB, 2006). Commercial AmB lipid formulations (Ambisome[®], Abelcet[®] and Amphocil[®]/Amphotec[®]) are less toxic than Fungizone[®], however the high cost and difficulty of production restrict their widespread use (CALDEIRA *et al.*, 2015; SINGH, KUMAR, SINGH, 2012).

It is well known that the pharmacokinetics parameters are dependent on the composition of the AmB lipid formulations. Some examples: Ambisome® has the lower size, negative charge and presents higher peak plasma level (C_{max}) and larger area under curve (AUC) than Fungizone®; Abelcet® has the largest size and the highest volume of distribution and clearance of all AmB formulations; Amphocil® /Amphotec® shows fast elimination from the body circulation by phagocytosis and achieves the lowest C_{max} , which requires larger therapeutic doses and consequently, higher toxicity; Amphocil® /Amphotec® has a toxicity similar to Fungizone®, reason why the FDA suspended its distribution in 2011 (HAMILL, 2013).

Pentamidine (Figure 10) is an aromatic diamidine, which has been marketed in the form of two salts: isethionate (di-b-hydroxyethane sulfonate) and mesylate (di-b-hydroxymethyl sulfonate) (MINISTÉRIO DA SAÚDE, 2017; SINGH, KUMAR, SINGH, 2012;). The mechanism of action may be related to a decrease of mitochondrial membrane potential by drug accumulation in the mitochondria (LINDOSO *et al.*, 2012; SINGH, KUMAR, SINGH, 2012; GOTO & LINDOSO, 2010).

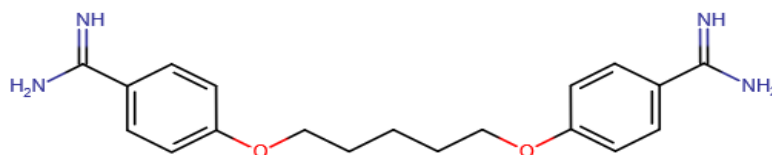


Figure 10. Chemical structure of pentamidine (CHEMID PLUS, 2016).

The pentamidine is administered by intravenously or intramuscularly with recommended dose of 3 to 4 mg/ kg/ day. This drug can be cause different side effects such as hypoglycemia, hyperglycemia, nephrotoxicity and hepatotoxicity. Furthermore, pentamidine may be induced insulin dependent diabetes. There are already reports of parasite resistance (LINDOSO *et al.*, 2012).

There is an alternative treatment using paromomycin, miltefosine (PACE, 2014; SINGH, KUMAR, SINGH, 2012; TIUMAN *et al.*, 2011) and sitamaquine (Phase II study) (SUNDAR & CHAKRAVARTY, 2015).

Paromomycin (PM) (Figure 11) is an aminoglycoside antibiotic (PUJOL-BRUGUÉS *et al.*, 2014; SINGH, KUMAR, SINGH, 2012, TIUMAN *et al.*, 2011), produced by *Streptomyces rimosus* (PUJOL-BRUGUÉS *et al.*, 2014; USP, 2012b). The mechanism of action is not yet well known, but it is believed that paromomycin acts in the inhibition of protein synthesis (inhibition of translocation and recycling of ribosome subunits) and cause mitochondria disturb (modification in mitochondrial membrane potential) (BRUGUÉS *et al.*, 2015; KHARAJI *et al.*, 2015; LINDOSO *et al.*, 2012; SINGH, KUMAR, SINGH, 2012). PM has been used with alternative drug in leishmaniasis treatment at a dose of 15 mg/ kg/ day for 20 days (DAVIDSON, DEN BOER, RITMEIJER, 2009).

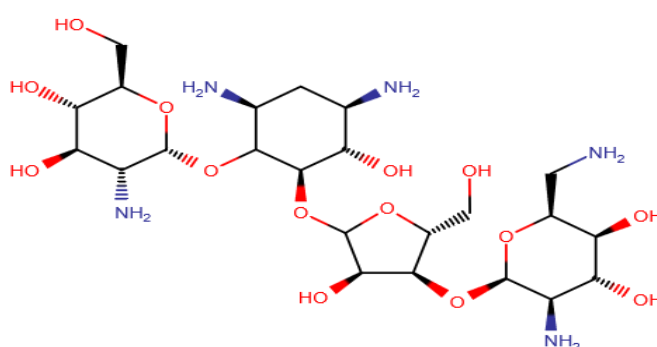


Figure 11. Chemical structure of paromomycin (CHEMID PLUS, 2016).

Nowadays, there is an ointment for topical application containing 15% paromomycin with 12% methylbenzethonium chloride (Leishcutan®), available only in Israel market, which was developed in 1984 by El-On and colleagues. This formulation presents a local toxicity that was described as local irritancy associated with the use of methylbenzethonium chloride (SALAH *et al.*, 2013). There is, also, one study involving an ointment with 15% paromomycin and 10% urea, which further studies are required in order to confirm the effectiveness (BRYCESON, MURPHY, MOODY, 1994). Another formulation was developed as a cream containing 15% of paromomycin and 0.5% gentamicin, which had the same efficacy as paromomycin cream against *L. major* (SALAH *et al.*, 2009, 2013). In Brazil, there is one gel formulation containing 15% paromomycin under development for topical use (GONÇALVES *et al.*, 2005).

Miltefosine (Figure 12) is, originally, an antitumor drug

(hexadecylphosphocholine), which shows interesting results in leishmaniasis treatment and has been considered a progress in the research of new treatment of this disease. Its mechanism of action is based on drug intracellular accumulation in parasites through transporters (LINDOSO *et al.*, 2012; SINGH, KUMAR, SINGH, 2012).

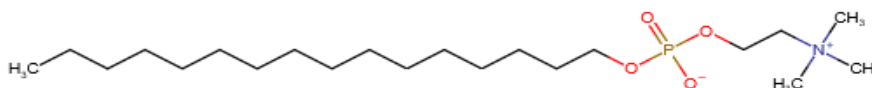


Figure 12. Chemical structure of miltefosine (CHEMID PLUS, 2016).

It is the first drug approved for leishmaniasis treatment that is used orally with a dose between 2 and 5 mg/ kg/ day for 28 days (SINGH, KUMAR, SINGH, 2012; REITHINGER, 2007). This drug shows several side effects such as vomiting, diarrhea, toxicity in gastrointestinal tract. Furthermore, presents a teratogenic effect and is forbidden to use in pregnant women (AKBARI, ORYAN, HATAM, 2017; MENEZES *et al.*, 2015; SINGH, KUMAR, SINGH, 2012). As other drugs used to treat leishmaniasis, miltefosine is already triggering resistance in parasites (AKBARI, ORYAN, HATAM, 2017; SINGH, KUMAR, SINGH, 2012).

Sitamaquine (Figure 13), an aminoquinoline, is the only drug developed for visceral leishmaniasis treatment. Its mechanism of action affects the mobility, morphology and growth of the protozoans, through an electrostatic interaction between polar ionic groups of the phospholipids present in the parasite membrane and positive charge of the drug (IMBERT *et al.*, 2014; SINGH, KUMAR, SINGH, 2012).

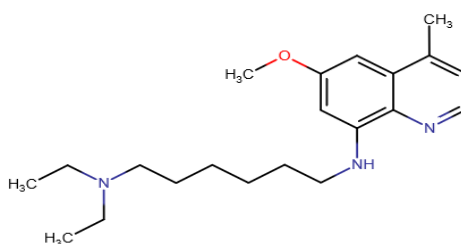


Figure 13. Chemical structure of sitamaquine (CHEMID PLUS, 2016).

It is a new medicine, used orally, which is in clinical studies (Phase II study in India and Kenya), but presents promising results (IMBERT *et al.*, 2014). The worst problem of sitamaquine is the poor knowledge of the toxicity of its metabolism (SINGH, KUMAR, SINGH, 2012; KULSHRESTHA *et al.*, 2011).

Table 1 shows the advantages and disadvantages of current leishmaniasis treatment.

In addition to these treatments, there are some drugs of other therapeutic classes that are used as alternative treatments such as ketoconazole, imiquimod, itraconazole, allopurinol among others (HANDLER *et al.*, 2015; MITROPOULOS, KONIDAS, DURKIN-KONIDAS, 2010).

Imidazoles (ketoconazole) and triazoles (fluconazole, itraconazole) are antifungal compounds with same mechanism of action. These drugs act binding to the ergosterol molecules in the cytoplasmic membrane of parasites increasing membrane permeability. These compounds can be administered orally and present lower toxic side effects than pentavalent antimonials (MITROPOULOS, KONIDAS, DURKIN-KONIDAS, 2010). Furthermore, triazoles are less toxic, interfere less with human synthesis of cholesterol and are slower metabolized than imidazoles (LINDOSO, 2012; GOTO & LINDOSO, 2010; MITROPOULOS, KONIDAS, DURKIN-KONIDAS, 2010).

Pentoxifylline is a methyl-xanthine derivate drug belongs to peripheral vasodilator class with hemorheological effects (MINISTÉRIO DA SAÚDE, 2017; HASSAN, DORJAY, ANWAR, 2014). Some researchers have been demonstrated successful using pentoxifylline as adjunct drug as immunomodulate in cutaneous leishmaniasis reducing treatment time. This drug is available in extended release tablets and is recommended one tablet of 400 mg, three times a day for 30 days (MINISTÉRIO DA SAÚDE, 2017).

Table 1. Current treatments of leishmaniasis (adapted from ZULFIQAR, SHELPER, AVERY, 2017; LINDOSO *et al.*, 2012 and MENEZES *et al.*, 2015).

Drugs	Administration route	Dosage	Advantages	Disadvantages	Resistance
Amphotericin B	Intravenous	0.75-1mg/kg/day (15 or 20 days daily or alternately)	Primary resistance is unknown	Need slow intravenous infusion, toxicity, unstable in high temperatures	Laboratory strains
Liposomal amphotericin B	Intravenous	3-5mg/kg single dose or 10-30mg/kg total dose	High effective and low toxicity	Need slow intravenous infusion, high cost, unstable in high temperatures	Not documented
Miltefosine	Oral	100-150mg/day for 28 days	Effective and safe	Cost, poor patient compliance	Laboratory strains, some cases reported in India
Paromomycin	Intramuscular, intravenous or topic	15mg/day for 21 days or 20mg/kg for 17 days	Low cost	Efficacy varies between and within regions	Laboratory strains
Pentamidine	Intramuscular	3mg/kg/day every other day for 4 injections	Short treatment	Efficacy varies between <i>Leishmania</i> species	Not documented
Pentavalent antimonials	Intramuscular, intravenous or intralesional	20mg/kg/day for 28-30 days	Easily availability and low cost	Length treatment, painful injection and toxicity	Common
Sitamaquine*	Oral	2mg/kg/day for 21 days	Effective	Toxicity	Not documented

*- Sitamaquine is in phase II study for leishmaniasis treatment.

Another alternative option to treat cutaneous leishmaniasis, already described in literature, is Heat Therapy or Thermotherapy (LOBO *et al.*, 2006). In general, this therapy consists a local heat application, on the edge of lesion, at 50°C for 30 seconds, varying methods and devices (CARDONA-ARIAS *et al.*, 2018; ARONSON *et al.*, 2010; LOBO *et al.*, 2006). One of the devices, ThermoMed® was approved by Food Drug and Administration (FDA) for CL treatment (LOBO *et al.*, 2006). There are some studies that compared the efficacy of thermotherapy with meglumine antimoniate and showed efficacy similar than pentavalent antimonials with safety results (CARDONA-ARIAS *et al.*, 2018; LÓPEZ *et al.*, 2012; ARONSON *et al.*, 2010). However, this therapy cannot be applied in cutaneous lesions near mucosa or in lesions (LÓPEZ *et al.*, 2012).

In addition to other drugs treatment and heat treatment, there are, also, combination therapies studies as: intralesional injections of pentavalent antimonials and paromomycin, antimonials with imiquimod, miltefosine and liposomal amphotericin B, amphotericin B with miltefosine and paromomycin among others (ZULFIQAR, SHELPER, AVERY, 2017; SUNDAR & CHAKRAVARTY, 2015).

The actual treatment for leishmaniasis, in particular for cutaneous leishmaniasis, presents several side effects (toxic drugs), parasite resistance and low patients' adhesion (injectable treatment, painful and for long period of time). These factors are motivating the development of new pharmaceutical formulations, as the study of different routes of administration, especially for cutaneous leishmaniasis treatment. In this context, microtechnology and nanotechnology have presented a large potential to promote various advantages in new formulations development. For this reason, many governments and industries around the world are investing in this area. Micro and nanotechnologies encompass the development, production, characterization and application of structures, systems and dispositive in micrometer scale and nanometer scale, respectively (STEVENSON, SANTINI JUNIOR, LANGER, 2012; DOWLING, 2004).

Micro and nanotechnologies can be used in drugs delivery, in vaccines

development, in cosmetics, in genetic material, in implants and in diagnosis (PARVEEN, MISRA, SAHOO, 2012; TAO & DESAI, 2003). In relation to drugs delivery, one of the main advantages is the drug targeting in specific cells (PARVEEN, MISRA, SAHOO, 2012). Moreover, these systems allow improve drug solubility by increase the surface area, improve permeability or transport of drugs with low permeation (class III and IV of Biopharmaceutical Classification System), increase the bioavailability, improve pharmacokinetics and protect drugs for physicochemical and/or biologicals degradations (LI *et al.*, 2011; DATE *et al.*, 2010; DATE, JOSHI, PATRAVALE, 2007).

There are several types of micro and nano-sized systems already described in the literature for drug delivery, such as: cyclodextrins, dendrimers, liposomes, polymeric micro or nanoparticles, solid lipid micro or nanoparticles, magnetic micro or nanoparticles and micro or nanoemulsion (HERRERO-VANRELL *et al.*, 2013; MEI *et al.*, 2013) (Figure 14). Although, some marketed products can be find in countries such as India and Bangladesh in conventional pharmaceutical forms (ointment), cutaneous leishmaniasis treatment has also been approached in research studies with liposomal forms (for antimonials compounds), solid lipid nanoparticles (for AmB or paromomycin molecules), and nanoparticles (metallic or polymeric) (ISLAN *et al.*, 2017).

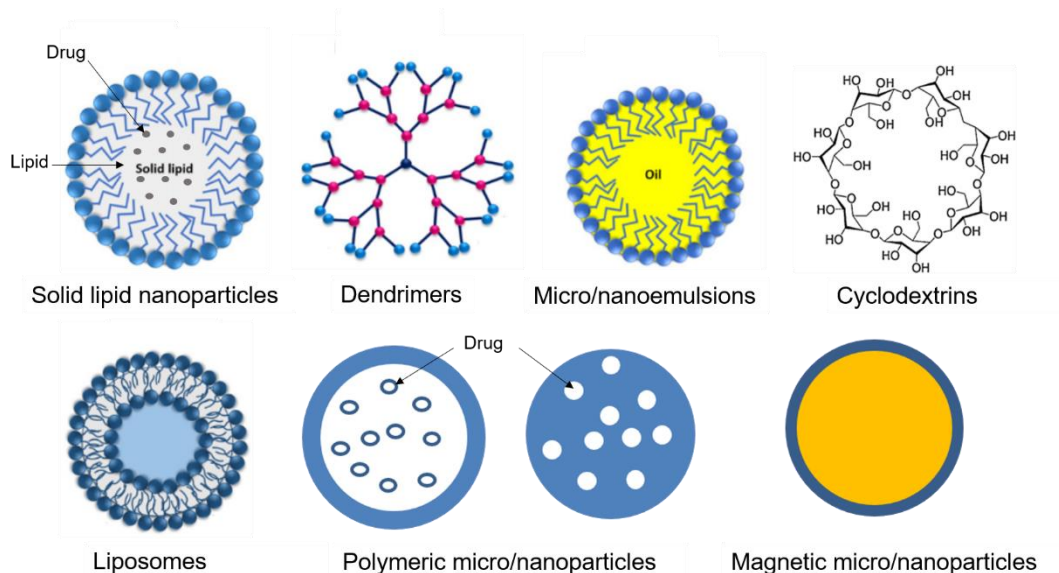


Figure 14. Different types of drug delivery system with micro and nanotechnology (adapted from Wen *et al.*, 2017).

Whatever the route of administration for a given disease treatment, the vehicle used (drug delivery system) should be able to deliver the good drug dosage to the targeted site. Topical and intralesional are two interesting routes for CL treatment. From one side, topical administration shows some advantages as easy of administration, low cost, few side effects and can be used for local treatment (GARNIER & CROFT, 2002). However, stratum corneum barrier difficult drug permeation across the skin and decrease the efficacy of drugs (SENGUPTA & CHATTERJEE, 2017). In addition, the high molecular weight of drugs (BOS & MEINARDI, 2000) and the location of leishmania parasites, in the dermis layer, increase the challenges of developing effective topical formulations for CL (SINGH & SIVAKUMAR, 2004).

From the other side, intralesional administration presents some advantages as lower total dose, less toxic effects, local application and more adjustable schedule for drug administration (BRITO, RABELLO, COTA, 2017). However, repeated dose injections, rapid clearance, sporadically systemic effects, risk of late mucosal complications and efficacy rate difficult the patient compliance and the implementation of this kind of administration in large scale (SILVA *et al.*, 2018; BRITO, RABELLO, COTA, 2017; SOUSA-BATISTA *et al.*,

2017).

Intralesional treatment is recommended, since 2013, for patients with single lesion (not in face or joints) and with contraindications to systemic treatment by Pan American Health Organization (PAHO) (BRITO, RABELLO, COTA, 2017; DUQUE *et al.*, 2016). In Brazil, intralesional administration of meglumine antimoniate has been used without a standard protocol to evaluate the efficacy of this treatment (SILVA *et al.*, 2018).

Thereby, the search of new therapies and the improvement of current therapy for CL treatment are still required. Based on this emergency situation, this thesis work focuses on polymeric microparticles and nanoemulsions, aiming to develop useful formulations respectively for intralesional use of Paromomycin and topical administration of AmB-based formulation, both for cutaneous leishmaniasis treatment.

CHAPTER 2

OBJECTIVES

2.1. GENERAL OBJECTIVE

This work aims to develop two different formulations for cutaneous leishmaniasis treatment, one using Amphotericin B for topical administration and other using Paromomycin for intralesional administration.

2.2. SPECIFIC OBJECTIVES

- ✓ Better knowledge of the chosen drugs thanks to raw material characterizations (size and morphology of raw material, thermal properties, chemical structure from FT-IR spectra);
- ✓ Formulation, generation (by an ultrasonication method) and characterization of nanoemulsions of amphotericin B (size distribution, morphology, encapsulation efficiency, drug load, stability, *in vitro* skin permeation, *in vitro* AmB release, cytotoxicity and leishmanicidal activity);
- ✓ Formulation, generation (by spray drying as manufacturing process) and characterization of PLGA-based microparticles containing paromomycin (size distribution, morphology, encapsulation efficiency, drug load, stability, *in vitro* PM release, cytotoxicity and leishmanicidal activity).

CHAPTER 3

NANOEMULSIONS OF AMPHOTERICIN B

3.1. INTRODUCTION

3.1.1. Nanoemulsions

Nanoemulsions (NE) are transparent or translucent heterogenous systems formed by a dispersion of two immiscible phases (oil-in-water or water-in-oil) or by a dispersion of three phases (O/W/O or W/O/W) (RAI *et al.*, 2018; CAMPOS, RICCI-JUNIOR, MANSUR, 2012; DATE *et al.*, 2010) (Figure 15). Multiple emulsion O/W/O is very unusual (SINGH *et al.*, 2017). They are kinetically and thermodynamically stable with a droplet size between 20-400 nm and can be considered nanoemulsion until 500 nm (RAI *et al.*, 2018; SINGH *et al.*, 2017).

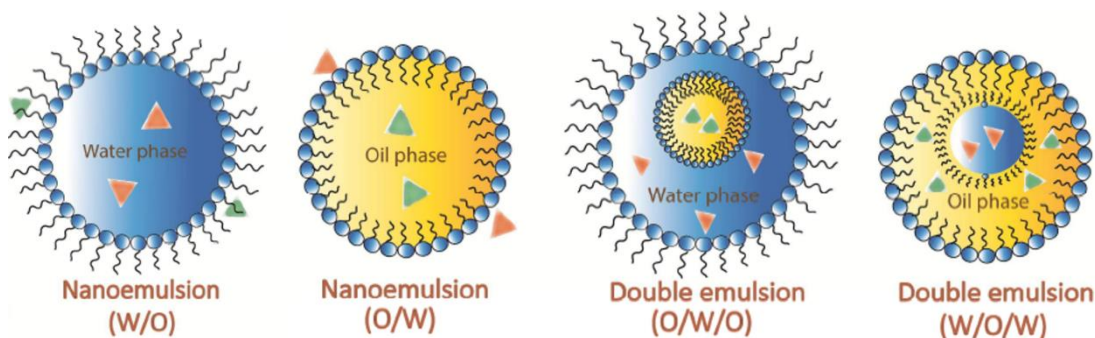


Figure 15. Different types of nanoemulsions (adapted from KATOUZIAN & JAFARI, 2016).

Nanoemulsions could be classified as neutral, anionic and cationic nanoemulsion based on the surface charge presents in droplets (RAI *et al.*, 2018). NE droplets are prepared considering the optimal hydrophilic-lipophilic relation and the greatest surfactant concentration (Lu *et al.*, 2018), being oil phase, surfactant/cosurfactant and aqueous phase important ingredients in this type of formulation (JAISWAL, DUDHE, SHARMA, 2015).

The oil phase is used to solubilize lipophilic drugs and varies from 2% to 20% (w/w) in O/W nanoemulsions. This type of emulsion is indicated, mainly, for drugs belongs to class II and IV of biopharmaceutical classification system (BCS). The oils most used in NE formulations are: isopropyl myristate, triacetin, soybean oil, sesame oil, coconut oil, triacyl glycerides, vitamin E (RAI *et al.*, 2018; SINGH *et al.*, 2017) and essential oils. Essential oils can cross the cell membrane and permeate due to chemical composition (lipophilic mixture) (DHIFI *et al.*, 2016). One of essential oils used in nanoemulsions is clove oil, which has eugenol as

the major constituent and has analgesic, anti-inflammatory, antioxidant and antimicrobial properties (TEIXEIRA *et al.*, 2018; CHOUDHURY *et al.*, 2017; SHARMA *et al.*, 2017; SHAHAVI *et al.*, 2015; MORAIS *et al.*, 2014).

Surfactants are amphiphilic molecules selected by their solubility in oil and aqueous phases, emulsification ability and lower toxicity profile. They reduce interfacial tension and avoid droplets agglomeration. Non-ionic surfactants have lower toxicity and irritability than anionic or cationic emulsifiers (RAI *et al.*, 2018; SINGH *et al.*, 2017). Sodium deoxycholate and cremophor EL have been used in parenteral formulations. Other surfactants as polyoxyethylene sorbitan monolaurate family (Tween® 20, 40, 60, 80), sorbitan monolaurate family (Span® 20, 40, 60, 80), polyoxyethylene 660 hydroxystearate (Solutol HS 15), polyoxyethylene-polyoxypropylene triblock copolymer (poloxamer) family (Pluronic® F127, F68), sodium dodecyl sulfate, casein and polyethylene glycol containing block copolymers are also applied (SINGH *et al.*, 2017). Sometimes, cosurfactants are chosen to aid interfacial tension stability. Cosurfactants can be propylene glycol, polyethylene glycol, ethanol, propanol, glycerin and transcutool IP (HALNOR *et al.*, 2018; RAI *et al.*, 2018; SINGH *et al.*, 2017).

The aqueous phase can affect the droplet size and the stability of nanoemulsions. The pH and presence of electrolytes in this phase must be considered for good formulation development (HALNOR *et al.*, 2018; SETYA, TALEGAONKAR, RAZDAN, 2014).

The selection of ingredients, their concentration, the appropriate preparation method and the optimal process parameters are important to produce a good nanoemulsion (RAI *et al.*, 2018). One option to evaluate the best correlation and ingredients concentration is plot a pseudo-ternary phase diagram, which is based on surfactant, oil and water proportions (HALNOR *et al.*, 2018).

NE have some advantages compared to conventional emulsions, such as: high stability, increase of interfacial area, improve of drug solubility and bioavailability, increase of drug absorption through biological membranes, ease to produce and scale-up (RAI *et al.*, 2018; CAMPOS, RICCI-JUNIOR, MANSUR, 2012; DATE *et al.*, 2010). Despite the several advantages, NE systems have low viscosity and low spreadability, which difficult their topical use. Based on these

problems, some studies suggested an increment in NE formulations through gelling agent addition. Thus, nanoemulsions can be transformed into nanoemulgel (CHOUDHURY *et al.*, 2017) (Figure 16).

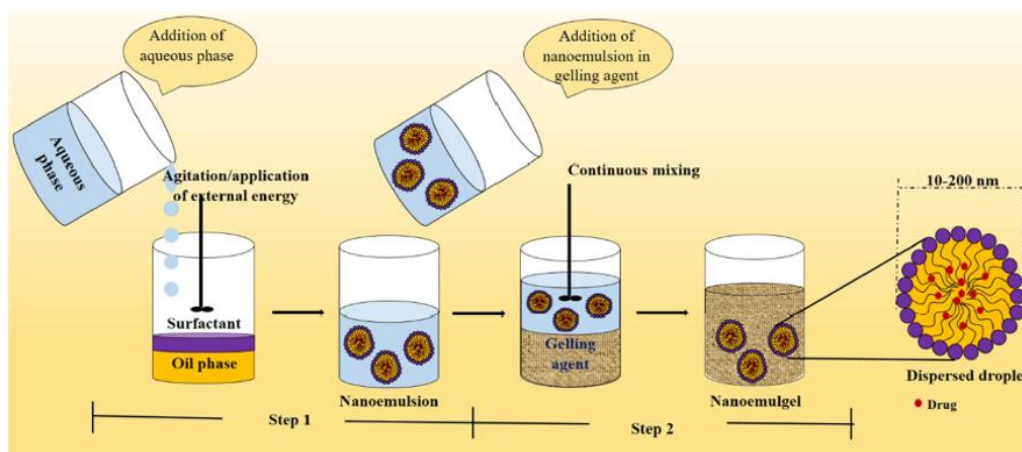


Figure 16. Scheme for nanoemulgel preparation (CHOUDHURY *et al.*, 2017).

There are some gelling agents commonly used in nanoemulgel formations, such as chitosan, carbopol family, methyl cellulose and poloxamer 407. The gelling agent's incorporation in NE change formulation physical state and some modifications in pharmacokinetic properties of NE system. Nanoemulgels containing drugs have already been described (CHOUDHURY *et al.*, 2017; SENGUPTA & CHATTERJEE, 2017).

There are some articles describing nanoemulsions with gelling agents. Arantes and co-workers (2017) prepared nifedipine nanoemulsions with poloxamer 407 for topical administration. Hussain and co-workers (2016a) developed AmB nanoemulsion gel or nanoemulgel (AmB nanoemulsion incorporated into carbopol gel) for topical delivery to antifungal treatment. Zheng and co-workers (2016) developed nanoemulsions gel, using carbopol 934 as gelling agent, for topical and transdermal drug delivery of terbinafine and citral.

3.1.2. Poloxamers properties

Poloxamers (Figure 17), also known with trademark Pluronic[®], are a non-ionic, non-toxic, water-soluble triblock copolymers family composed of hydrophilic

poly-(ethylene oxide) (PEO) and hydrophobic poly-(propylene oxide) (PPO) (BODRATTI & ALEXANDRIDIS, 2018; FAKHARI, CORCORAN, SCHWARZ, 2017; DEVI, SANDHYA, HARI, 2013; PATEL, PATEL, PATEL, 2009). These copolymers have been used since 1950s in several pharmaceutical applications as surfactant, dispersing agent, tablet lubricant, wetting agent, gelling agent and emulsifying agent (DEVI, SANDHYA, HARI, 2013; ROWE, SHESKEY, QUINN, 2009).

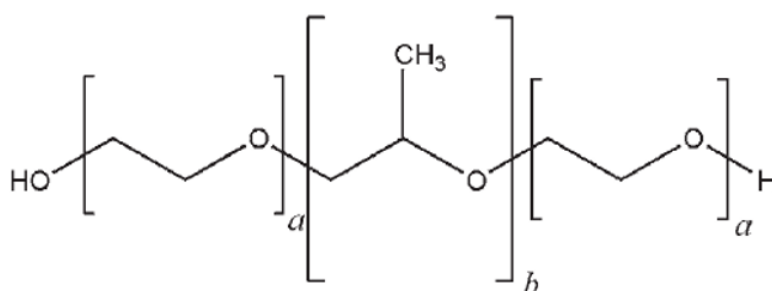


Figure 17. Poloxamers chemical general structure (a,b) ethylene oxide and propylene oxide units (ROWE, SHESKEY, QUINN, 2009).

Poloxamers have some advantages for their use, as commercial availability, wide range of molecular weights and PEO/PPO composition (BODRATTI & ALEXANDRIDIS, 2018; DEVI, SANDHYA, HARI, 2013). These copolymers have an interesting thermoreversible property, in which at low temperatures (or below sol-gel transition temperature) remain as solution and at high temperatures (or above sol-gel transition temperature) become gel (DEVI, SANDHYA, HARI, 2013; PATEL, PATEL, PATEL, 2009). Moreover, some poloxamers have been approval for pharmaceutical formulations by Food and Drug Administration (FDA) as Poloxamer 407 and Poloxamer 188 (FAKHARI, CORCORAN, SCHWARZ, 2017). Table 2 presents some Poloxamers, used in pharmaceutical formulations, with some physicochemical properties.

Table 2. Physicochemical properties of some poloxamers used in pharmaceutical formulations (adapted from BODRATTI & ALEXANDRIDIS, 2018; adapted from DEVI, SANDHYA, HARI, 2013; adapted from ALVAREZ-LORENZO, SOSNIK, CONCHEIRO, 2011; adapted from ROWE, SHESKEY, QUINN, 2009).

Poloxamer	Pluronic® Notation	Physical Form	Molecular Weight	Melting Point (°C)	Ethylene Oxide Units*	Propylene Oxide Units*	CMC** (mM)
124	L44	Liquid	2090- 2360	16	10-15	18-23	3.60
188	F68	Solid	7680- 9510	52-57	75-85	25-40	0.48
237	F87	Solid	6840- 8830	49	60-68	35-40	0.0910
338	F108	Solid	12700- 17400	57	137-146	42-47	0.0220
407	F127	Solid	9840- 14600	52-57	95-105	54-60	0.0028

Legend: * - based on average molecular weight; ** - CMC – Critical micellar concentration at 37°C.

In aqueous solution, poloxamers exhibit micelles structures. The micellization process starts when the concentration of copolymer in solution achieve critical micellar concentration (CMC) at certain temperature or when increases temperature to achieve critical micellar temperature (CMT) at fixed polymer concentration. Then, occurs the reduction of PPO chains solubility resulting into micelles formations (BODRATTI & ALEXANDRIDIS, 2018; DEVI, SANDHYA, HARI, 2013). The micellization is a spontaneous process with spherical micelles are core-shell structure, in which micelles core have hydrophobic characteristic and micelles shell hydrophilic characteristic (BODRATTI & ALEXANDRIDIS, 2018). Micelles formation allow hydrophobic

drug introduction into aqueous solution (DEVI, SANDHYA, HARI, 2013). The addition of drugs, salts, excipients or polar organic solvents into poloxamers solution can affect the micellization process (BODRATTI & ALEXANDRIDIS, 2018; FAKHARI, CORCORAN, SCHWARZ, 2017).

There are some methods for prepare drug-loaded poloxamers formulations as direct solubilization (simplest method), thin film hydration, temperature-induced emulsification, solvent displacement and kinetically frozen micelles (BODRATTI & ALEXANDRIDIS, 2018).

One of the most studied poloxamer is Poloxamer 407 (Pluronic® F127) due to this copolymer can form hydrogels with low polymer concentration in water, around 20% w/w (BODRATTI & ALEXANDRIDIS, 2018). Poloxamer 407 formulations can be used for drug, small molecules, peptides, biological molecules deliveries, especially for controlled release (FAKHARI, CORCORAN, SCHWARZ, 2017). Moreover, some studies have been described that poloxamer 407 gel has properties to promote wound healing (PATEL, PATEL, PATEL, 2009).

There are some studies using poloxamer 407 for several pharmaceutical applications. Ali and Hussein (2017) prepared nanoemulsions containing candesartan cilexetil for oral use using different poloxamers, including poloxamer 407. Chauhan and Batra (2018) developed diclofenac sodium nanoemulsions dispersed in poloxamer 407 for ocular application. Inal and Yapar (2013) evaluated the mechanical properties on meloxicam release from poloxamers (407 and 188) alone or combined. Pereira and co-workers (2013) produced poloxamer 407 gel containing polymeric microparticles and hyaluronic acid for burn wounds treatment.

3.1.3. Methods of nanoemulsion production

NE can be prepared by methods, which involve low energy emulsification (spontaneous emulsification, phase inversion method and emulsion inversion method) or high energy emulsification (microfluidizer, high pressure homogenizer and ultrasonication) (MUNGURE *et al.*, 2018; RAI *et al.*, 2018; SINGH *et al.*, 2017; KATOZIAN & JAFARI, 2016; CAMPOS, RICCI-JUNIOR, MANSUR, 2012;

DATE et al., 2010). The methods to prepare nanoemulsions are simple and fast when compared to other techniques to produce nanosystems (CALDEIRA *et al.*, 2015; CAMPOS, RICCI-JUNIOR, MANSUR, 2012). Figure 18 shows a scheme, which represents all methods used to obtain nanoemulsions.

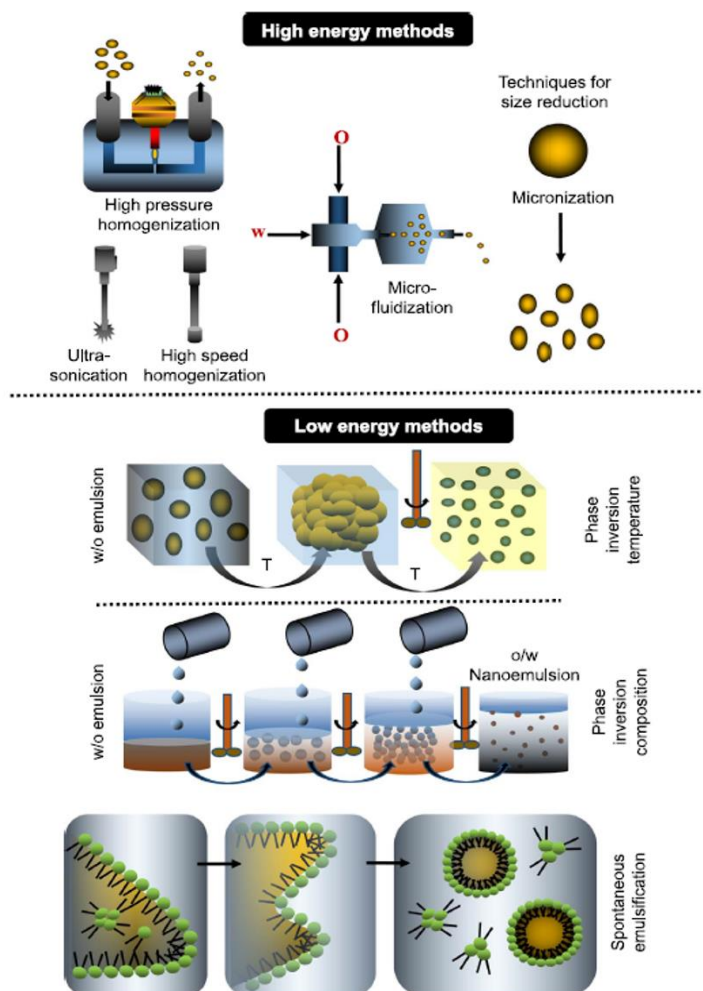


Figure 18. Scheme of methods of preparation of nanoemulsions (RAI *et al.*, 2018).

Low-energy methods utilize the internal chemical energy of the system to produce small droplets. There are two types of phase inversion method: phase inversion temperature (PIT) and phase inversion composition (PIC) (RAI *et al.*, 2018; CAMPOS, RICCI-JUNIOR, MANSUR, 2012; SOLANS & SOLE, 2012).

PIT is based on changes in aqueous/oil solubility of surfactants induced by temperature changes (RAI *et al.*, 2018; SINGH *et al.*, 2017; CAMPOS, RICCI-

JUNIOR, MANSUR, 2012; SOLANS & SOLE, 2012). Polyoxyethylene-type nonionic surfactants are the most used surfactant in this method. At high temperatures, these emulsifiers stay lipophilic due to aliphatic groups presence, which results in W/O emulsions. Nevertheless, these ingredients remain hydrophilic at low temperatures due to hydration of polar groups producing O/W emulsions. The disadvantage of this technique is the risk of generate unstable emulsion, which can be avoid with fast cooling or fast heating the emulsion prepared at hydrophilic-lipophilic balance (HLB) temperature (RAI *et al.*, 2018; CAMPOS, RICCI-JUNIOR, MANSUR, 2012; SOLANS & SOLE, 2012).

PIC method consists of changes in volumetric fractions. In O/W formulation, the aqueous phase is added progressively over a mixture of oil phase with surfactant, while in W/O emulsion, the oil phase is added over a mixture of aqueous phase with surfactant. In both case there is a spontaneous inversion of curvature of the surfactant monolayers (RAI *et al.*, 2018; CAMPOS, RICCI-JUNIOR, MANSUR, 2012; SOLANS & SOLE, 2012). PIC method has high potential for large scale production compared to PIT method (SOLANS & SOLE, 2012).

Spontaneous emulsification or self-emulsification method involves an addition of oil phase with surfactant/cosurfactant and drug into aqueous phase under continuous agitation. This technique is good for oral delivery hydrophobic drugs and the components can be able to oral administration as nonionic surfactants and medium chain triglycerides (oil phase) (SINGH *et al.*, 2017; EID *et al.*, 2014; SOLANS & SOLE, 2012). Emulsification happens immediately because of negative/positive and low free energy (EID *et al.*, 2014).

High energy methods depend on mechanical devices able to create high degree forces to disrupt the oil phase into small oil droplets (MUNGURE *et al.*, 2018; RAI *et al.*, 2018; SINGH *et al.*, 2017; SOLANS & SOLE, 2012).

Microfluidization technique is based on emulsification through collision of two immiscible phases moving in microchannels under high pressure. Usually to obtain the desire droplet size and dispersity, NE is passed many times in microfluidizer. The correct surface device (hydrophobic or hydrophilic) is chosen considering the type of nanoemulsion required (W/O or O/W, respectively). The

advantages of this technique are high scalability and zero contamination of feed material (RAI *et al.*, 2018; SINGH *et al.*, 2017).

High pressure homogenizers technique depends on the emulsion pass through a gap between a fixed rotor and high-speed rotor. The emulsion is submitted to hydraulic shear and intense turbulence resulting in small droplets of emulsion (HALNOR *et al.*, 2018; RAI *et al.*, 2018; SINGH *et al.*, 2017). This method has high efficiency and scalable, but consumes much energy and temperature, which can be promote drug or excipients degradation (SETYA, TALEGAONKAR, RAZDAN, 2014).

The method of nanoemulsion preparation by ultrasonication is based on ultrasonic waves caused by a sonicator probe introduced in formulation. These waves promote cavitation bubbles that collapse generating high energy into the system, which break the internal phase in small droplets (LU *et al.*, 2018; RAI *et al.*, 2018; SINGH *et al.*, 2017; JAISWAL, DUDHE, SHARMA, 2015; CAMPOS, RICCI-JUNIOR, MANSUR, 2012). Ultrasonication is the high energy method, which requires less energy. However, this technique can be induced contamination by sonicator probe. Furthermore, the scale up is not easy, but commercial homogenizers using ultrasonication have already been developed (SINGH *et al.*, 2017). The sonication time and the ultrasonic wave amplitude affect directly the droplet size of formulation (CAMPOS, RICCI-JUNIOR, MANSUR, 2012). Figure 19 shows the relation between droplet size and sonication time to obtain nanoemulsions.

Nanoemulsions can be administered in different routes as topical, parenteral, intranasal, pulmonary, oral and ocular (HALNOR *et al.*, 2018; SINGH *et al.*, 2017).

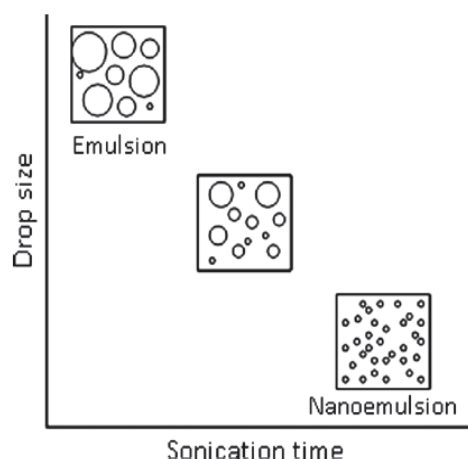


Figure 19. – Relation between droplet size and sonication time to obtain nanoemulsions (CAMPOS, RICCI-JUNIOR, MANSUR, 2012)

3.1.4. Topical administration

Topical administration is an interesting non-invasive route of drugs administration, which can be used for local or systemic effects. This route has many advantages, such as: painless self-medication, improved drugs permeation avoiding hepatic first-pass effects or gastric degradation, reduction of dose frequency (constant drug delivery for a prolonged period) and hydrophilic or lipophilic drugs administration. However, the major problem of this administration is the skin barrier that difficult drugs penetration (RAI *et al.*, 2018; SENGUPTA & CHATTERJEE, 2017; MONTENEGRO *et al.*, 2016; BHOWMIK *et al.*, 2012), mainly hydrophobic drugs (CHOUDHURY *et al.*, 2017).

The skin is the largest organ of the human body with a surface area around 2 m² and composes the natural barrier between the body and external environment. It is composed by three functional layers (Figure 20): epidermis, dermis and hypodermis. The epidermis is most superficial layer and provides protective and sensory properties. In this layer, there are keratinocytes cells divided in four different layers (*stratum corneum*, *stratum granulosum*, *stratum spinosum* and *stratum basale*). The *stratum corneum* represents the major barrier to drugs permeation. The dermis provides the skin mechanical properties and presents high vascularization. The hypodermis (subcutaneous layer) has the

adipose tissue, nerves and blood vessels and connect the skin with deeper tissues (muscles and bones) (RAI *et al.*, 2018; MORONKEJI *et al.*, 2017; MONTENEGRO *et al.*, 2016; RUELA *et al.*, 2016).

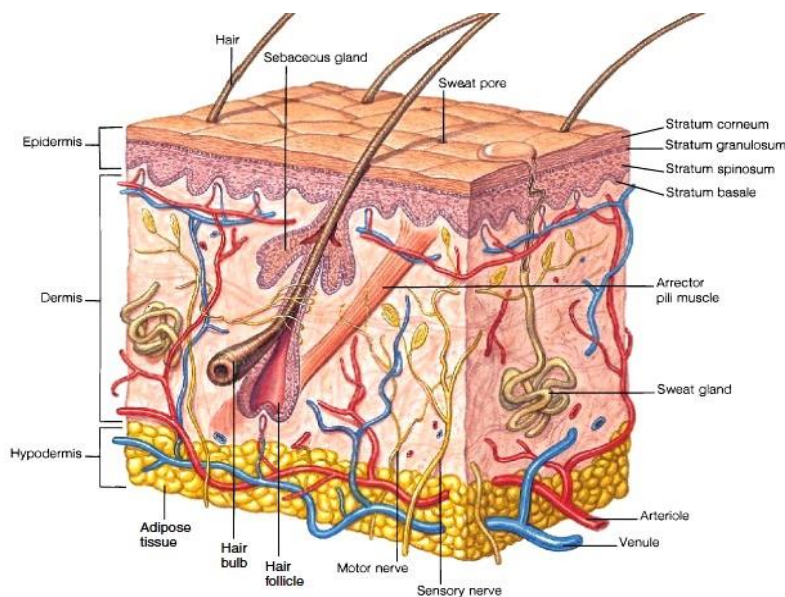


Figure 20. Human skin composition (Source: <http://www.naturallyhealthyskin.org/anatomy-of-the-skin/the-dermis/dermis-anatomy-of-the-skin/>).

The small droplet size, low skin irritation, high permeation ability (NE can disrupt lipid bilayer) and increase drug retention at the site of action provide nanoemulsions an interesting system for topical and transdermal drug delivery (RAI *et al.*, 2018; CHOUDHURY *et al.*, 2017; SINGH *et al.*, 2017; MOU *et al.*, 2008). For this reason, NE is a promising alternative for skin diseases treatment (MATTOS *et al.*, 2015).

One of the most important skin diseases in the world is cutaneous leishmaniasis. For CL topical treatment, the drug needs to achieve the dermis, where occurs parasites phagocytosis by macrophages (MATTOS *et al.*, 2015). NE can be used as drug delivery system for improve topical cutaneous leishmaniasis treatment, because can reduces the drugs toxicity, is easy to prepare and has low-cost production (CALDEIRA *et al.*, 2015; MATTOS *et al.*, 2015). Moreover, nanoemulsions prepared with poloxamer 407 (Pluronic® F127) promote wound healing and can be improve cutaneous leishmaniasis treatment. Amphotericin B (AmB) is an effective second-line drug in CL treatment

(CALDEIRA *et al.*, 2015; SANTOS *et al.*, 2012) and has been chosen as model drug for this work.

3.1.5. Amphotericin B

AmB is a yellow-orange powder (THE INTERNATIONAL PHARMACOPEIA, 2017a; EUROPEAN PHARMACOPEIA 7.0, 2009), hygroscopic (EUROPEAN PHARMACOPEIA 7.0, 2009), that presents molecular formula $C_{47}H_{73}NO_{17}$ and molecular weight of 924.08 g (CHEMID PLUS, 2016; THE INTERNATIONAL PHARMACOPEIA, 2017a; USP, 2012a; EUROPEAN PHARMACOPEIA 7.0, 2009). It has very low solubility in water around 0.75 $\mu\text{g}/\text{mL}$ (CHEMID PLUS, 2016), soluble in dimethyl sulfoxide (DMSO) and propylene glycol, insoluble in ethanol and slightly soluble in methanol and dimethylformamide (THE INTERNATIONAL PHARMACOPEIA, 2017a; EUROPEAN PHARMACOPEIA 7.0, 2009, GOLENSER & DOMB, 2006). This drug is sensitive to light and must be stored in places protected from light (THE INTERNATIONAL PHARMACOPEIA, 2017a; EUROPEAN PHARMACOPEIA 7.0, 2009; CONNORS, AMIDON, STELLA, 1986) and in low temperatures (between 2°C – 8°C) (THE INTERNATIONAL PHARMACOPEIA, 2017a).

Besides has low solubility, AmB has a low permeability, being classified with drug belongs to class IV of biopharmaceutics classification system (BCS). For this reason, presents low bioavailability for oral use and it is administered intravenously (IBRAHIM *et al.*, 2012). Furthermore, this drug has high toxicity and topical administration could be a useful alternative to reduce this problem (SANTOS *et al.*, 2012).

Several studies involving amphotericin B in new topical formulations, mainly lipid-based formulation, as liposomes, complexes with cholesterol, emulsions, microemulsions, nanoemulsions have been developed to improve leishmaniasis treatment (CALDEIRA *et al.*, 2015; SANTOS *et al.*, 2012). Another studies focused on AmB nanoemulgel or emulgel production to treat cutaneous leishmaniasis (MENDONÇA *et al.*, 2016; PINHEIRO *et al.*, 2016) Figure 21 shows a review of number of publications, obtained in database “Web of

Science”, related to AmB physicochemical characterization or AmB drug delivery systems between 1997 and 2017 using keywords as “AmB + Leishmaniasis”, “AmB + drug delivery system (DDS)”, “AmB + Nanoemulsions”, “AmB + Nanoemulsions + drug delivery systems (DDS)” and “AmB + Leishmaniasis + drug delivery systems (DDS)”.

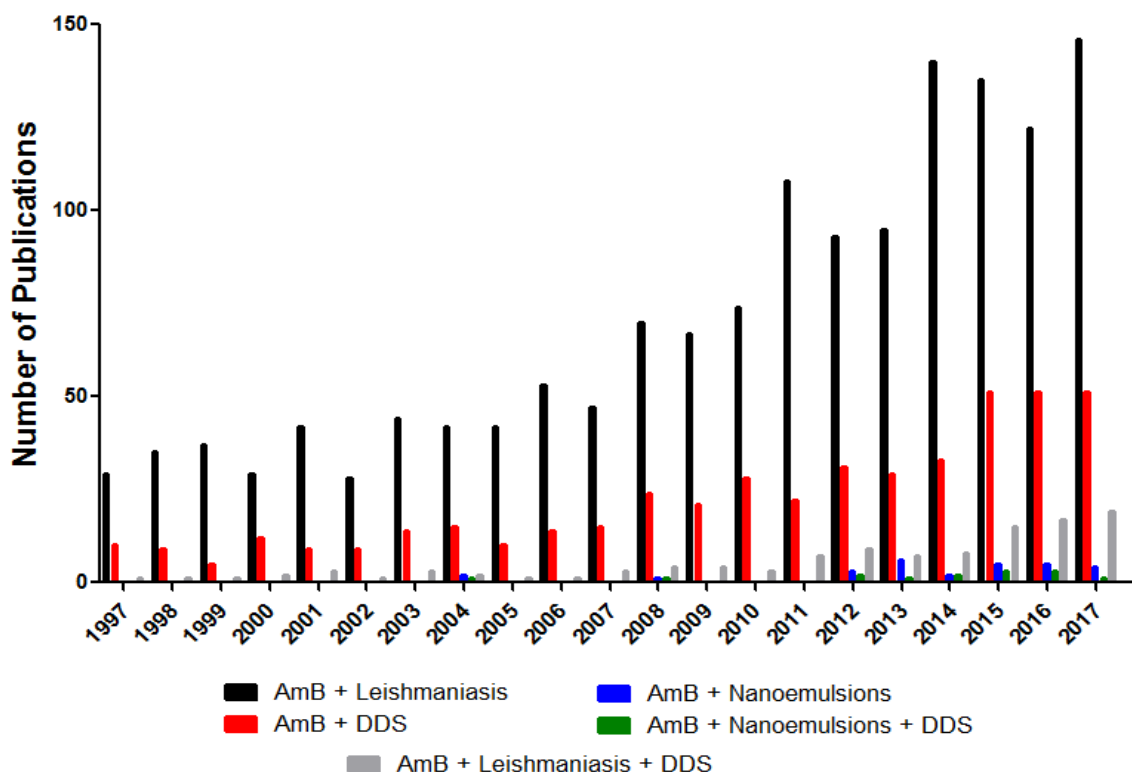


Figure 21. Number of publications of amphotericin B (AmB) among 1997-2017 obtained from database ‘Web of Science’ using keywords as “AmB + Leishmaniasis”, “AmB + drug delivery system (DDS)”, “AmB + Nanoemulsions”, “AmB + Nanoemulsions + drug delivery systems (DDS)”.

It can be observed a several publications about amphotericin B plus leishmaniasis with an increase of number of publications after 2011. In the last three years, there are more researches involving AmB and drug delivery systems. Furthermore, there is an increase of number of publications after 2011 involving drug delivery systems, AmB and leishmaniasis. It can also be observed that are few studies about nanoemulsions and AmB, which began in 2012. Therefore, this work aims to develop nanoemulsions of amphotericin B prepared by ultrasonication method for topical administration for CL treatment.

3.2. OBJECTIVES

This chapter was developed in School of Pharmacy at Federal University of Rio de Janeiro (Brazil) and aims:

- Physicochemical characterization of amphotericin B;
- AmB nanoemulsions development;
- Physicochemical characterization of amphotericin B nanoemulsions;
- Stability study of AmB nanoemulsions;
- *In vitro* release profile of AmB nanoemulsions;
- *In vitro* skin permeation study of AmB nanoemulsions;
- *In vitro* cytotoxicity assay of AmB nanoemulsions;
- *In vitro* antileishmanial activity of AmB nanoemulsions.

3.3. MATERIALS AND METHODS

3.3.1. MATERIALS

Amphotericin B (AmB) was kindly donated by Xellia Pharmaceuticals (Denmark).

Clove oil and mint oil were purchased from Ferquima (Brazil) and were obtained from *Eugenia caryophyllata* flower oil and *Mentha piperita* leaf oil, respectively.

Poloxamer 407 (Pluronic® F127) was purchased from Sigma-Aldrich (Brazil). Polysorbate 20 was obtained from Tedia Brazil (Brazil) and imidazolidinyl urea was obtained from All Chemistry (Brazil). All other materials were of analytical reagent grade.

3.3.2. METHODS

3.3.2.1. Physicochemical Characterization of Amphotericin B

The drug amphotericin B was physicochemically characterized to verify the quality of the sample and evaluate its physicochemical properties. This analysis followed amphotericin B monography of United States Pharmacopeia (USP, 2012a) with adequate potency (see Annex 1 – Xellia certificate of analysis).

3.3.2.1.1. Scanning Electron Microscopy (SEM)

Morphologic evaluation was performed using scanning electronic microscope (Jeol - JSM6390LV, Japan) belonging to the electron microscopy platform Rudolf Barth from Oswaldo Cruz Institute – Fiocruz. Amphotericin B sample was added on a SEM stub with a double-sided carbon adhesive tape. After that, the sample was coated in a sputter coater equipment Denton Vacuum Desk (USA) with a gold-palladium thin layer for 8 minutes in 10 mA under Argon gas atmosphere.

3.3.2.1.2. Thermogravimetry Analysis (TGA)

Thermal gravimetric analysis of AmB was performed using an equipment TGA-QR500 (TA Instruments, USA) at heating rate of 10 K/min under synthetic air atmosphere. Approximately 8 mg of sample were weighed and placed into standard aluminum pan, which was hermetically sealed. The heating temperature ranged from 25 °C to 700 °C.

3.3.2.1.3. Fourier Transform Infrared Spectroscopy (FTIR)

The FTIR spectrum of the pure AmB was analyzed using a FTIR spectrophotometer (Perkin Elmer Frontier, USA) in the range of 4000 cm^{-1} to 600 cm^{-1} . The AmB sample was diluted with KBr powder at 1% and analysed as powder mixture at room temperature (adapted from ZU *et al.*, 2014).

3.3.2.2. Amphotericin B Nanoemulsions Development

AmB nanoemulsions were prepared by high emulsification energy method using ultrasonic processor UP 100H (Hielscher, Germany) (CAMPOS, RICCI-JUNIOR, MANSUR, 2012). Firstly, the drug was solubilized in dimethyl sulfoxide (DMSO) to obtain a 20 mg/mL solution. Then, concentrated AmB solution was diluted in oil phase (1:3 v/v ratio). Oil phase containing AmB was dispersed in aqueous phase with or without surfactant under ultrasound device for 5 minutes in ice bath (SHAHAVI *et al.*, 2015). Figure 22 shows the main steps of AmB nanoemulsions preparation.

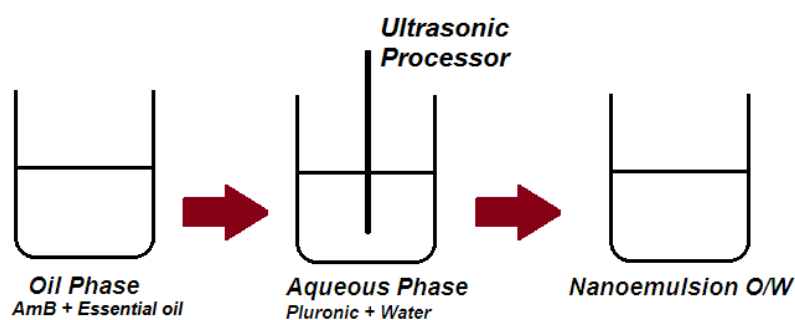


Figure 22. Main steps of the AmB nanoemulsions preparation method.

Twelve batches of nanoemulsions (NE) were prepared, codified from A to L, varying the essential oil used in the oil phase (clove oil or mint oil), the presence of surfactant (0 to 5% w/w), the presence of AmB and the amount of polymer used in the aqueous phase (10 and 15% w/w). Essential oils were chosen for oil phase due to their ability to increase drugs permeation. Nanoemulsions containing drug presented a theoretical final concentration of 0.5 mg/mL and the final nanoemulsions volume were 10 mL (1 mL of oil phase and 9 mL of aqueous phase). The final concentration of DMSO in nanoemulsions were lower than 2.5%. The composition of each formulation is described in Table 3.

Table 3. AmB nanoemulsions composition

Sample	Essential Oil	Surfactant (%)	Polymer (%)	AmB theoretical concentration
A-NE	Clove	0	15	0.5 mg/mL
B-NE	Clove	1.5	15	0.5 mg/mL
C-NE	Mint	0	15	0.5 mg/mL
D-NE	Clove	0	10	0.5 mg/mL
E-NE	Clove	1.5	10	0.5 mg/mL
F-NE	Clove	0	15	0.5 mg/mL
G-NE	Clove	1.5	10	0.5 mg/mL
H-NE	Clove	0	15	-
I-NE	Mint	1.5	15	0.5 mg/mL
J-NE	Mint	5	10	0.5 mg/mL
K-NE	Clove	5	10	0.5 mg/mL
L-NE	Clove	1.5	15	-

3.3.2.3. Physicochemical Characterization of Amphotericin B Nanoemulsions

The following characteristics of nanoemulsions A to L were determined: mean oil droplet size and polydispersity index, pH and drug content.

3.3.2.3.1. Determination of Droplet Size, Polydispersity Index and pH

The droplet size and polydispersity index of developed formulations were analyzed following method previous described in the literature (CAMPOS, RICCI-JUNIOR, MANSUR, 2012; CAMPOS *et al.*, 2010) in Zetasizer Nano Model S90 (Malvern Instruments, UK) equipment. The pH was verified in pH-indicator strips pH 0 - 14 Universal indicator (Merck, Germany).

3.3.2.3.2. Drug Content

The AmB concentration in the nanoemulsions was determined by UV-vis (UV-vis model V-630, Jasco, Brazil) spectrophotometric method adapted from THE INTERNATIONAL PHARMACOPEIA, 2017a and USP, 2012a using methanol as a solvent and wavelength of 410 nm. The calibration curve (Figure 23) was prepared in methanol in the range of 0.5 to 8 $\mu\text{g/mL}$, corresponding to a regression equation ($y= 0.1063x + 0.0118$) with linearity $r^2 = 0.9989$. A preweighed amount of each nanoemulsion was diluted in methanol (1:40 v/v) and evaluated in duplicate.

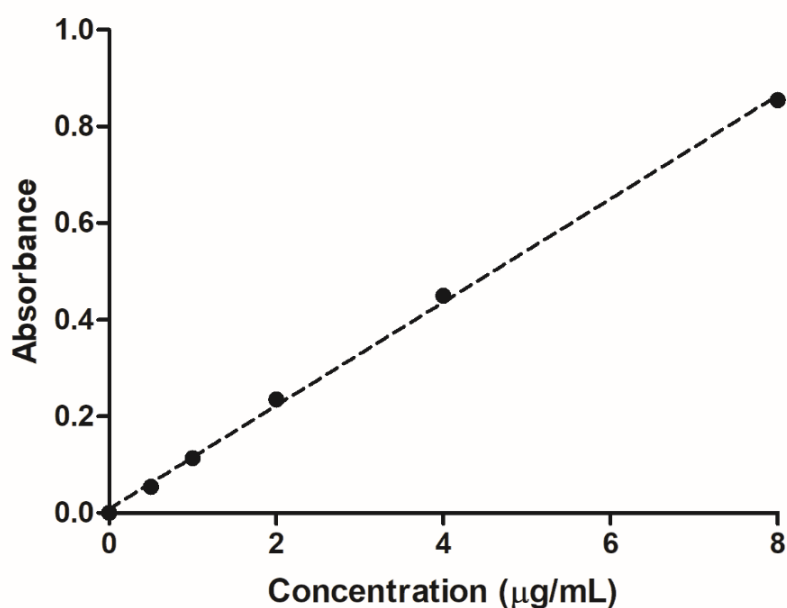


Figure 23. Calibration curve of AmB in methanol.

3.3.2.4. Stability Study of Amphotericin B Nanoemulsions

The NE that presented the best physicochemical properties were chosen and submitted to stability study. The stability study was conducted by one year. The samples were stored under two different conditions: $4^{\circ}\text{C} \pm 2^{\circ}\text{C}$ (refrigerator) and $28^{\circ}\text{C} \pm 2^{\circ}\text{C}$ (room temperature) in amber glass flasks hermetically sealed.

3.3.2.4.1. Transmission Electron Microscopy (TEM)

The morphology of AmB nanoemulsions was analyzed by transmission electron microscopy (TEM) in Jeol JEM 1011 (JEOL Inc., Peabody, USA) equipment available in Rudolf Barth Electronic Microscopy Platform (IOC - Fiocruz). The samples were diluted in distilled water at 1:4 and 1:8. Then, 5 μ L of diluted NE was added through a 300-mesh copper grid with sterile 2% of Collodion (Parlodion strips) in amyl acetate coating (adapted from MATTOS *et al.*, 2015; adapted from FUKUI *et al.*, 2003). The excess was removed with filter paper and the samples deposited on the grid were analyzed in the microscopy.

3.3.2.4.2. Determination of Droplet Size, Polydispersity Index and pH

The droplet size and polydispersity index of developed formulations were analyzed in Zetasizer Nano Model S90 (Malvern Instruments, UK) equipment following method described before in item 3.3.2.3.1. The pH was verified in pH-indicator strips pH 0 - 14 Universal indicator (Merck, Germany). The measurements were performed at 0, 7, 15, 30, 60, 90, 180, 365 days in two storage conditions (room temperature – 28°C and refrigerator - 4°C).

3.3.2.4.3. Drug Content

The AmB concentration in the nanoemulsions was determined by UV-vis (UV-vis model V-630, Jasco, Brazil) spectrophotometric method previously described in item 3.3.2.3.2. The AmB concentration was evaluated at 7, 30, 60, 90, 180, 365 days in two storage conditions (room temperature – 28°C and refrigerator - 4°C).

3.3.2.5. In vitro Release of Amphotericin B Nanoemulsions

AmB nanoemulsions were submitted to *in vitro* release study as well as free AmB. Free AmB dissolved in 1 ml of DMSO was analyzed in the same amount of AmB contained in nanoemulsions. In brief, 300 mg of NE were weighted and then inserted on cellulose acetate membrane (Sigma-Aldrich,

Brazil), previously attached to a cut falcon tube. The cellulose acetate membrane was hydrated in distilled water for, at least, 12 hours before use. Therefore, the tubes with membrane and material were inserted on the surface of 20 mL of receptor medium. The receptor medium was phosphate buffer pH 7.4 (USP, 2012c) containing 2% of Tween® 20. Experiments were carried out at 37°C under constant stirring (300 rpm) for 48 hours. Hence, 3 mL of receptor medium was collected at 1, 2, 4, 6, 24, 30 and 48h with sample return to collected recipient. The AmB concentration was determined by UV-visible spectrophotometry method (adapted from SANTOS *et al.*, 2012) in wavelength 410 nm. The experiments were conducted in quadruplicate. Furthermore, free AmB sample dissolved in DMSO was also evaluated in the same system used for NE release. A previous study (data not shown) showed good solubility of AmB solution in the receptor medium. Figure 24 presents a scheme of *in vitro* release study.

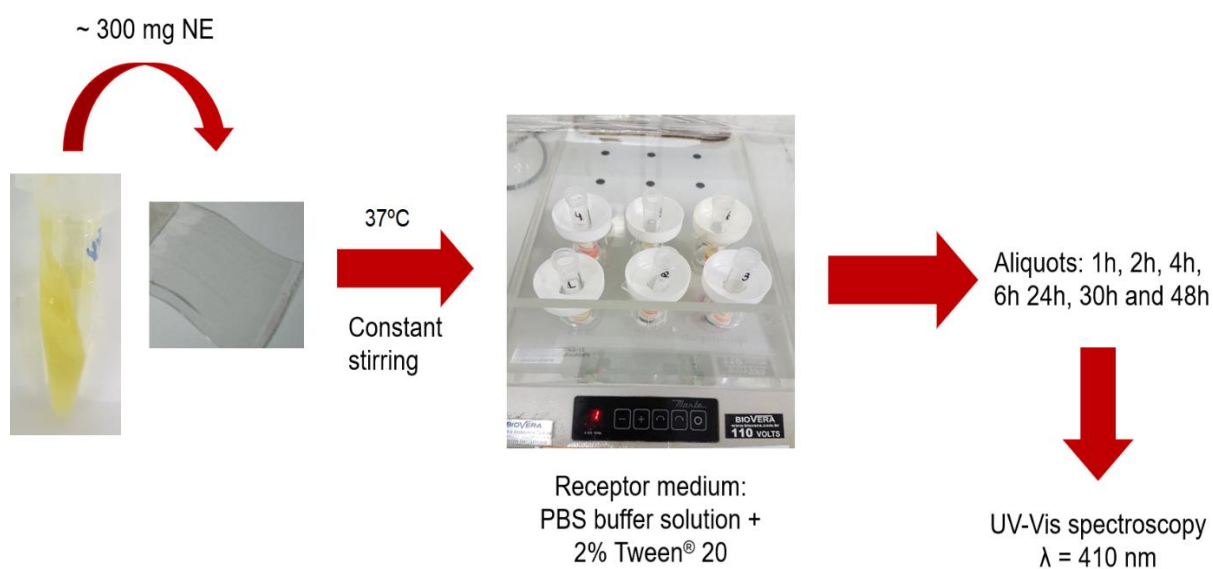


Figure 24. Scheme of AmB nanoemulsions *in vitro* release study.

The calibration curve (Figure 25) was prepared in phosphate buffer solution (PBS) in the range of 0.05 to 10 $\mu\text{g/mL}$ and a regression equation ($y = 0.07449x + 0.00033$) was obtained with linearity $r^2 = 0.9979$.

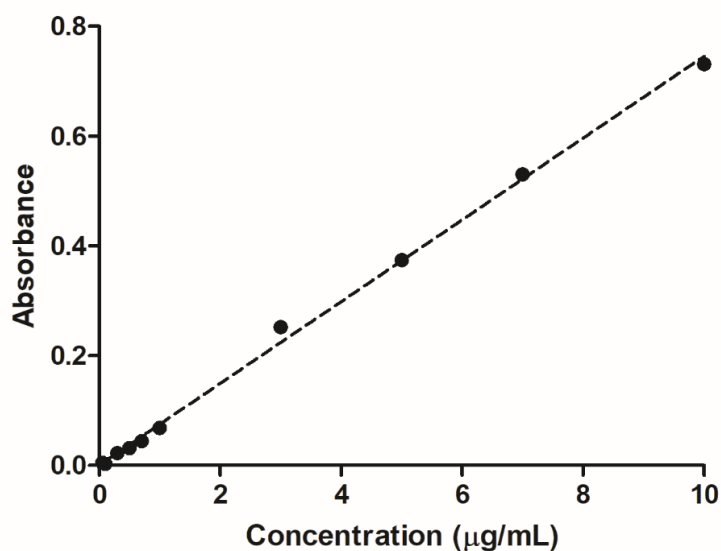


Figure 25. Calibration curve of AmB in PBS for in vitro release study.

3.3.2.6. *In vitro* Skin Permeation Study of Amphotericin B Nanoemulsions

3.3.2.6.1. Skin Permeation Method

The *in vitro* skin permeation study of AmB nanoemulsions were evaluated in a Franz vertical cell diffusion system (Figure 26), composed of a donor compartment with diffusional area of 1.54 cm² and receptor compartment with 7 mL corresponding to maximum volume. The experiments were carried out following method described before by our group (MARQUES *et al.*, 2018; ARANTES *et al.*, 2017) and adapted from Santos and co-workers (2012).



Figure 26. Franz Vertical Cell Diffusion System.

It was chosen pig ear skin for experiments because it presents similarity of human skin. The pig ears were obtained from a local slaughterhouse, cleaned with water and the skin was separated using a scalpel. The subcutaneous tissue (hypodermis) was removed. Pig skin samples were put with the epidermis tuned up to the donor compartment. The receptor medium was phosphate buffer pH 7.4 (USP, 2012c) containing 2% of Tween[®] 20. Experiments were carried out at 32°C under constant stirring (500 rpm) for 8 hours. 300 mg of sample was applied on each cell and the system was enclosed. It was used five Franz diffusion cells in each experiment. Previous experiment showed no differences between results of AmB penetrated in 1, 2, 4 and 6h (data not shown). For this reason, 1 mL of the receptor medium was collected after 6h and after 8h with refilling with 1 mL of fresh buffer solution. The aliquots were filtered through 0.20 µm pore diameter filters discs (Chromafil[®] Xtra PES – 20/25) and analyzed by High Performance Liquid Chromatography (HPLC).

After 8h, the permeation study was finished. The pig ear skins were removed from Franz diffusion cell and nanoemulsions excess were removed with a cotton swab dipped in distilled water. In order to evaluate the drug retained in epidermis and in dermis, the layers were separated using a scalpel to collect the epidermis following method standardized by our group. Thereafter, the epidermis and dermis (cut into small pieces) were inserted in eppendorf containing 1 mL of mobile phase (sodium acetate buffer solution pH 5.0 + acetonitrile – 60:40 v/v

respectively) for AmB extraction. The eppendorfs were vortexed for 60 seconds three times and centrifuged for 10 minutes in 8000 rpm. Then, all samples were filtered through 0.20 µm pore diameter filters discs (Chromafil® Xtra PES – 20/25) and analyzed by HPLC. The results were expressed as mean of triplicates.

3.3.2.6.2. High Performance Liquid Chromatography (HPLC) Assay

The quantification of AmB in the skin permeation study was measured by reverse phase HPLC using a Kromasil C18 column (250 mm X 4.6 mm; 5 µm) using method adapted from Santos and co-workers (2012). HPLC equipment was Flexar™ Conventional LC Manual Injection HPLC System (Perkin Elmer, USA) with Flexar LC manual injection valve, Flexar LC UV/VIS detector, Flexar isocratic LC pump and software system Chromera CDS. The system was maintained at room temperature (25°C). Moreover, the mobile phase was a mixture of sodium acetate buffer solution pH 5.0 (USP, 2012c) and acetonitrile (60:40 v/v). The flow rate was 1.0 mL/min, with 20 µL as injection volume and UV detection at 410 nm. The calibration curve (Figure 27) was prepared in mobile phase in the range of 0.01 to 20 µg/mL and was obtained a regression equation ($y = 141692x$) and linearity ($r^2 = 0.9992$) with retention time of AmB around 3.2 minutes.

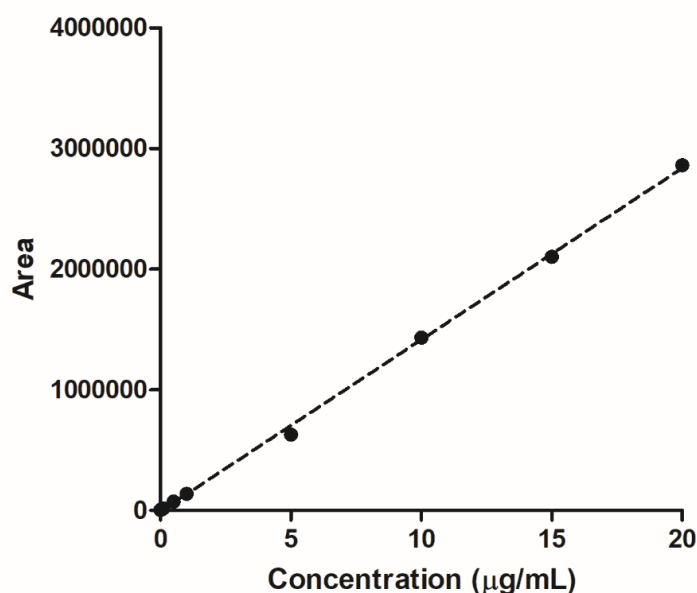


Figure 27. Calibration curve of AmB in mobile phase for skin permeation study.

Pig ear skin pieces without contact with nanoemulsions were cut and inserted in Eppendorf containing 1mL of mobile phase. The eppendorfs were vortexed for 1 minute three times and centrifuged for 10 minutes in 8000 rpm. Then, all samples were filtered through 0.20 µm pore diameter filters discs (Chromafil® Xtra PES – 20/25) and analyzed by HPLC. Moreover, three different solutions containing AmB in higher concentration used for calibration curve (20 µg/mL) were placed on pig ear skin pieces and added 1 mL of mobile phase. Then, the eppendorfs were submitted to method described for blank analyses. These quantifications showed the retention time of AmB around 3.2 minutes after peaks corresponding to skin interferences. Figure 28 shows the blank chromatogram (skins pieces only in mobile phase) and AmB solution chromatogram (extracted from skin pieces).

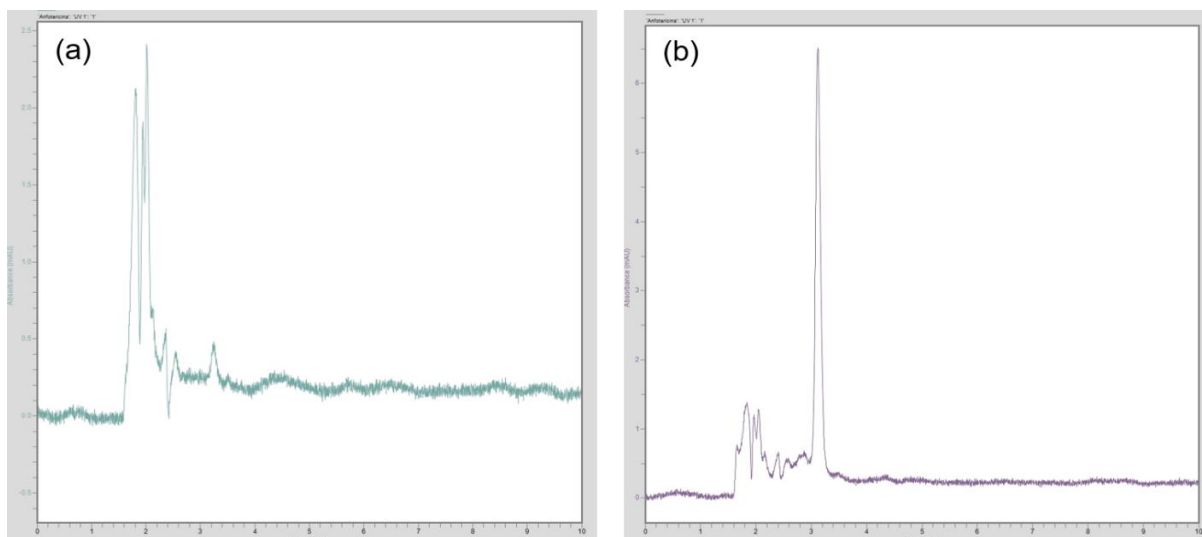


Figure 28. Chromatograms of (a) skin piece in mobile phase and (b) AmB solution extracted from skin piece.

3.3.2.7. BIOLOGICAL ASSAYS

3.3.2.7.1. Assessment of cytotoxicity of AmB nanoemulsions in BMDM cells

Bone marrow-derived macrophages (BMDM) were obtained from femurs and tibia of BALB/c mice as described by Marim and co-workers (2010). Mice were anaesthetized with 5% of isoflurane and euthanized as approved by Ethics Committee of Animal Use (CEUA) of the Instituto de Biofísica Carlos Chagas Filho (IBCCF) under number IBCCF-118.

Marrow cells were centrifuged (100 rpm for 10 minutes), the concentration was adjusted to 5×10^6 cells per Petri dish and resuspended in Roswell Park Memorial Institute (RPMI) medium with 10% of inactivated fetal bovine serum (FBS), 50 U/mL of penicillin, 50 $\mu\text{g}/\text{mL}$ of streptomycin, 2 mM of L-glutamine, 1 mM of sodium pyruvate and 20% of L-cell conditioned media as source of macrophage colony stimulating factor (M-CSF). Petri dishes (90 x 15 mm) were maintained at 37°C in a 5% CO₂ atmosphere until completely differentiation in seven days. Differentiated cells were removed with ice-cold PBS. Then, the cells (1×10^5 cells/100 μL) were seeded on 96-well microtiter plates and maintained in RPMI medium with 10% of inactivated FBS, at 37°C in a 5% CO₂ atmosphere for 24 hours for further treatment (adapted from MARIM *et al.*, 2010).

BMDM (1×10^5 cells/100 μ L) were incubated with different concentrations of free AmB and AmB nanoemulsions (0.05, 0.2, 0.8, 3.2 μ g/mL) for 48 hours at 37°C in a 5% CO₂ atmosphere. The range of AmB concentration was based on previous studies and in CC₅₀ values already described in literature (CARDOSO *et al.*, 2018; SIQUEIRA *et al.*, 2017). Moreover, the negative control was RPMI medium without treatment and positive control was Triton 100x. Triton 100x is a nonionic surfactant most used for lysing cells (KOLEY & BARD, 2010) and can be used as positive control in cytotoxicity assays. After incubation time, the cytotoxicity assay was investigated using resazurin method (RAMPERSAD, 2012). Resazurin (7-hydroxy-10-oxidophenoxazin-10-ium-3-one), also known Alamar Blue®, is a redox indicator, which is reduced to resorufin (7-hydroxy-3H-phenoxazin-3-one) by viable cells (CSEPREGI *et al.*, 2018; RAMPERSAD, 2012). Figure 29 shows the reduction reaction of resazurin.

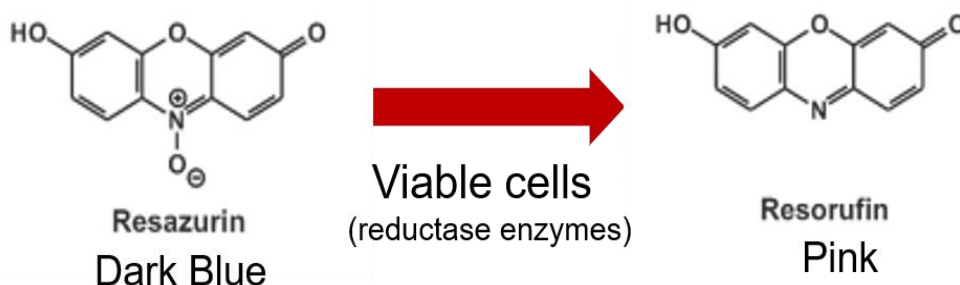


Figure 29. Reduction reaction of resazurin (Alamar Blue®) (adapted from CSEPREGI *et al.*, 2018).

20 μ L of resazurin solution were added and the plate was incubated for more 4 hours at 36°C. Following incubation, the fluorescence was measured using microplate Fluorimeter Spectra Max M5 (Molecular Devices, USA) at 560 nm for excitation and 590 nm for emission. The results were reported as % cell viability. The 50% cytotoxicity concentration (CC₅₀), which represents the concentration of drug or formulation that reduces 50% cell viability when compared to negative control/untreated control, were determined by logarithmic regression analysis.

3.3.2.7.2. Antileishmanial Activity

The promastigotes form of *Leishmania L. amazonensis* (IFLA/BR/1967/PH8) were obtained from Leishmania Collection of Oswaldo Cruz Institute (IOC-Fiocruz). The parasites were maintained in Schneider's Insect medium with 10% of inactivated FBS and 1% of antibiotics (penicillin + streptomycin). Promastigotes were grown at 28°C in climatic chamber (adapted from FREITAS *et al.*, 2015). The antileishmanial activity of AmB nanoemulsions was investigated in promastigotes of *L. amazonensis* by resazurin reduction method (KULSHRESTHA *et al.*, 2013; ROLÓN *et al.*, 2006).

Promastigotes (10^7 parasites/mL) were seeded on 96-well microtiter plates. 180 μ L of samples (AmB nanoemulsions, nanoemulsions without drug, AmB in DMSO solution and medium with FBS + antibiotics) were added on 96-well microtiter plates containing promastigotes. AmB solution was tested in following concentrations: 0.05, 0.1, 0.5, 1, 5 μ g/mL. AmB nanoemulsions and blank nanoemulsions were evaluated in concentrations between 0.1 and 5 μ g/mL. Moreover, the essential oil was analyzed in various concentrations (0.3, 1.5, 3, 7.5 and 15 μ g/mL) in order to investigate the effect of this substance alone. DMSO was evaluated, also, in concentration used to dissolve AmB. Negative control was only medium and positive control in nanoemulsions tests was AmB solution in concentration that promotes lesser than 50% of viable promastigotes.

Thereafter, the plate was incubated for 24 hours at 28°C. After incubation time, 20 μ L of resazurin solution 0.05% were added and the plate was incubated for more 4 hours at 28°C. Following incubation, the fluorescence was measured using microplate Fluorimeter Spectra Max M2e (Molecular Devices, USA) at 560 nm for excitation and 590 nm for emission. The results were reported as % parasite viability. The 50% inhibitory concentration (IC_{50}), which represents the concentration of drug or formulation that promote 50% of parasite's death in comparison with negative control/untreated control, were determined by logarithmic regression analysis.

The selective index (SI) was calculated as the ratio between cytotoxicity (CC_{50}) and activity (IC_{50}) against *Leishmania amazonensis* promastigotes.

3.3.2.8. Statistical Analysis

One-Way ANOVA with Tukey Post-test, T test paired, CC_{50} and IC_{50} were calculated using GraphPad Prism 5.0 (GraphPad Software, USA). The P value < 0.05 was considered significant.

3.4. RESULTS AND DISCUSSION

3.4.1. PHYSICOCHEMICAL CHARACTERIZATION OF AMPHOTERICIN B

3.4.1.1. Scanning Electron Microscopy (SEM)

The SEM images of AmB raw material were evaluated in three different magnifications (220x, 650x and 1300x) and were shown in Figure 30.

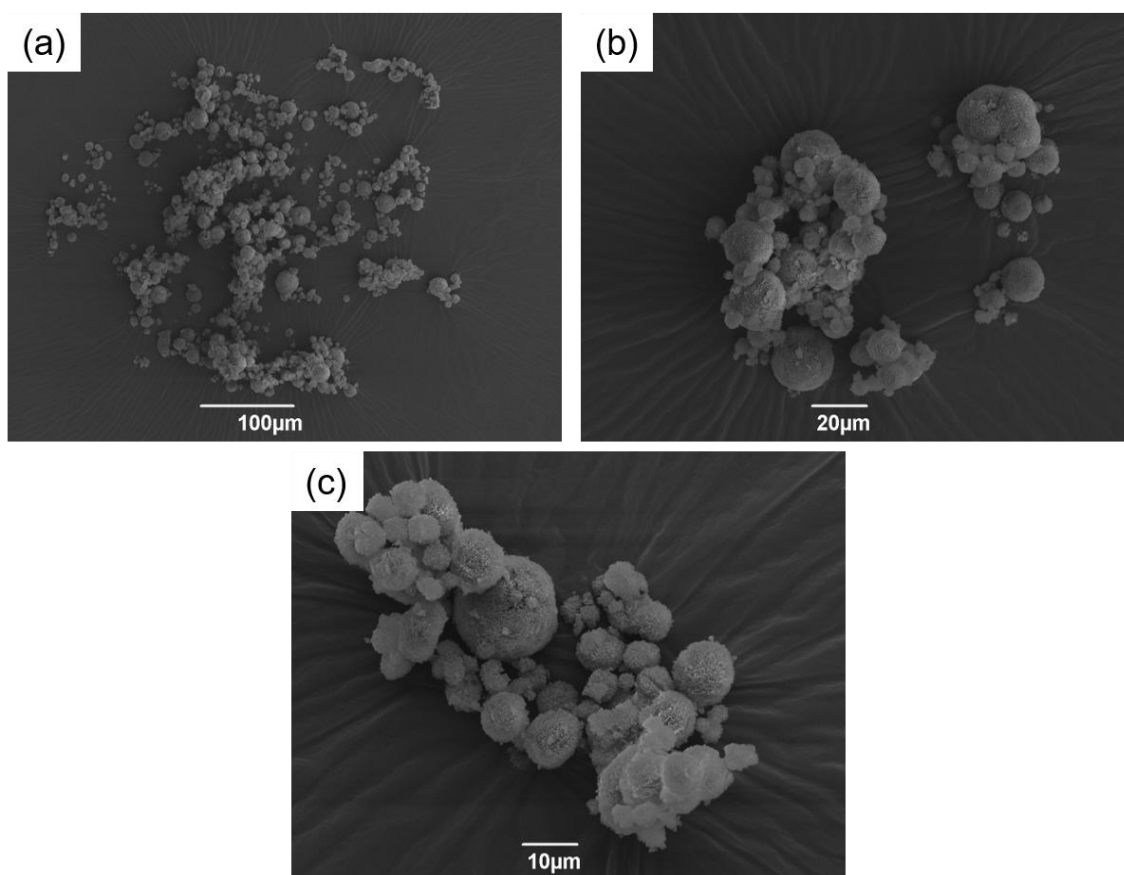


Figure 30. SEM images of raw AmB in magnifications (a) 220x, (b) 650x, (c) 1300x.

AmB powder showed a spherical shape with porous surface and varied sizes between 2 μm and 20 μm (measures held in Figure 30c, data not shown). Additionally, AmB powder presented some agglomerates. Rodríguez (2011) evaluated the influence of sodium deoxycholate addition in AmB formulations and the physicochemical, kinetical and toxicological effects. In this study, AmB raw material showed scaly agglomerate particles with particle size under 15 μm and short particles adhered on surface. Zu and co-workers (2014) produced AmB nanoparticles and evaluated some physicochemical properties. It was detected irregular crystals with mean particle size around 14 μm . These two works showed raw AmB with similar morphology than observed in Figure 30, which confirms AmB raw material structure.

3.4.1.2. Thermogravimetry Analysis (TGA)

Figure 31 shows the Thermogravimetric Analysis (TGA) of AmB raw material. AmB TGA presents two lines, being the black one related to mass loss (%) and the blue the first derivation of mass loss ($\%/^{\circ}\text{C}$).

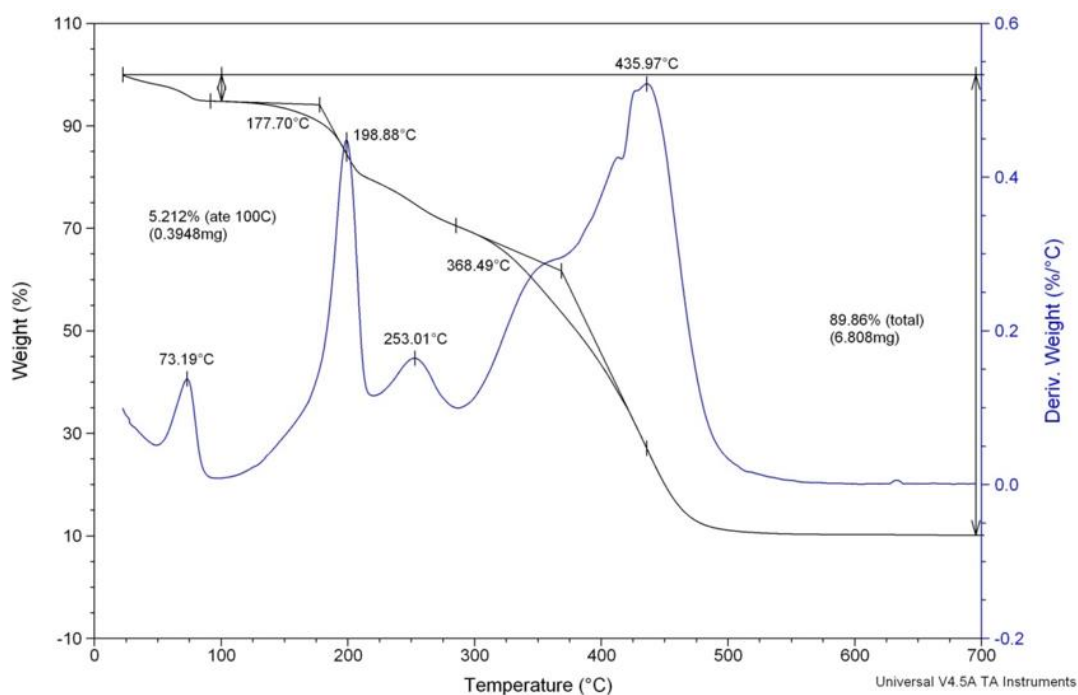


Figure 31. TGA curve of raw AmB.

According to TGA curve, raw AmB presented two mass loss events, being the first at 177.70°C and the second at 368.49°C. Connors and co-workers (1986) described a gradual decomposition of AmB above 170°C. Zu and co-workers (2014) prepared and characterized AmB nanoparticles. They evaluated thermal properties of nanoparticles comparing with raw drug and observed, in TGA curve of raw AmB, only one mass loss event at 168°C due to TGA was held between 25°C and 250°C. Ghosh and co-workers (2017) developed and investigated some properties of mannose modified PLGA nanoparticles containing AmB. In Thermal Analysis held in the range of 30-360°C, TGA curve of raw drug presented a mass loss event around 80°C corresponding to drug dehydration followed by a high mass loss event around 195°C corresponding to drug degradation.

Franzini (2010) studied AmB complexes with cyclodextrin and their incorporation in microemulsions. During the study of the thermal behavior of complexes and AmB, three mass loss events for AmB in the range of 151-245°C, 245-303°C and 303-542°C were observed, also attributed to drug degradation. Based on this information, the two events shown in Figure 31 are attributed to drug degradation in high temperatures.

3.4.1.3. *Fourier Transform Infrared Spectroscopy (FTIR)*

Figure 32 presents the FTIR spectrum of raw AmB.

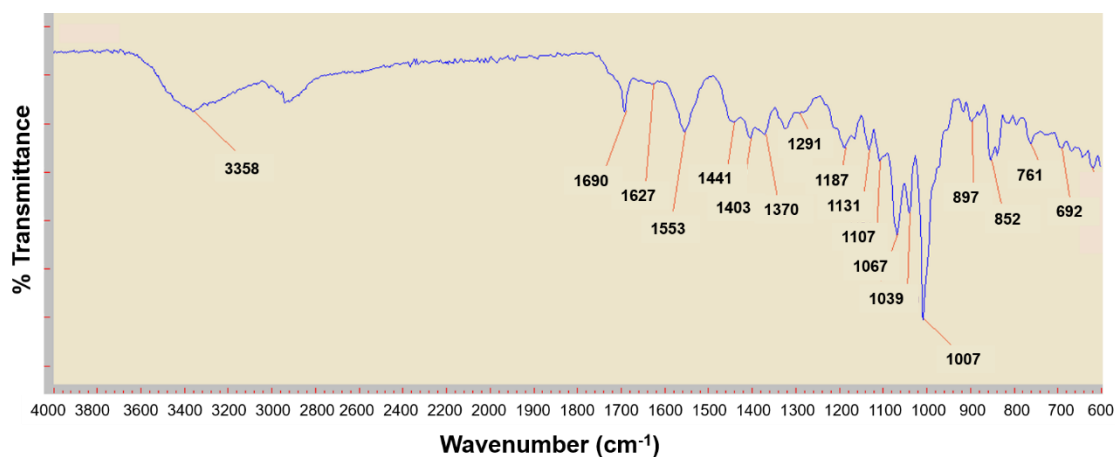


Figure 32. FTIR spectrum of raw AmB.

AmB spectrum showed characteristics peaks at 3358 cm^{-1} corresponding to hydroxyl group (OH), at 1690 cm^{-1} (C=O stretching), at 1553 cm^{-1} (C=C stretching), at 1068 cm^{-1} (C-O asymmetric stretching) and at 1007 cm^{-1} (C-H bending). Chhonker and co-workers (2015) developed and characterized lecithin/chitosan nanoparticles of AmB. It was observed strong characteristics peaks at 3401 cm^{-1} corresponding to hydroxyl group (OH) and at 1645 cm^{-1} corresponding to C=O stretching in AmB FTIR spectrum. Ghosh and co-workers (2017) identified some AmB characteristics peaks, in FTIR analysis, at $3416\text{-}3382\text{ cm}^{-1}$ (N-H stretching), at $2936\text{-}2916\text{ cm}^{-1}$ (long alkane chains asymmetric stretching), at 1680 cm^{-1} (C=C non-conjugated stretching) and one peak near 1100 cm^{-1} (C-O stretching). Zia and co-workers (2017) investigated the physicochemical properties and fungal activity of nanoparticles of AmB produced using *Aloe vera* leaf extract. Raw AmB spectrum presented some peaks as at 3440 cm^{-1} (OH stretching), at 2936 cm^{-1} (C-H stretching), at 1657 cm^{-1} (C=O stretching), at 1579 cm^{-1} (C=C stretching), at 1095 cm^{-1} (C-O asymmetric stretching) and at 994 cm^{-1} (C-H bending). FTIR spectrum of AmB used in this study, showed in Figure 32, presents the same characteristic peaks reported in these studies for AmB.

3.4.2. AMPHOTERICIN B NANOEMULSIONS DEVELOPMENT

The AmB nanoemulsions prepared were stored in amber glass flasks hermetically sealed at room temperature (Figure 33) in order to protect from light.

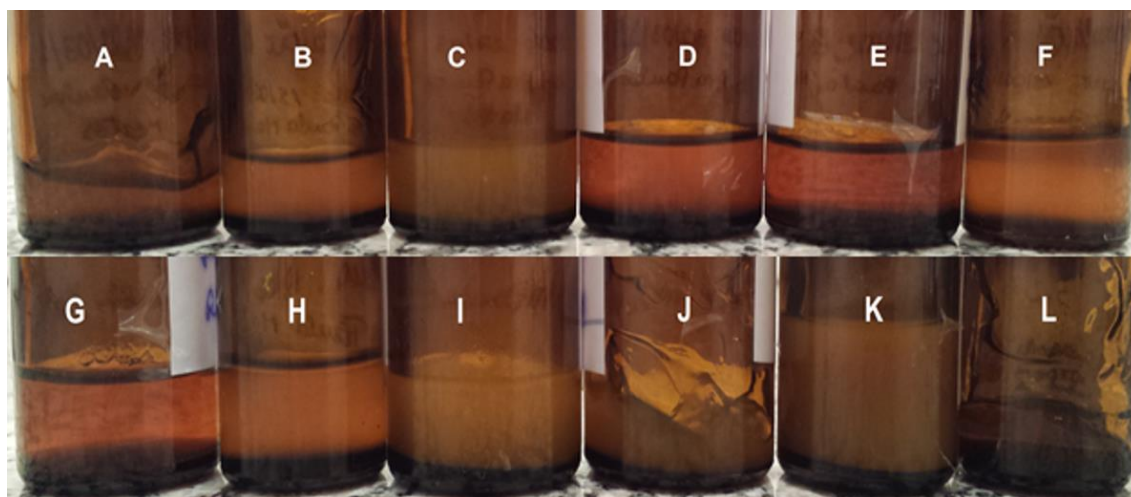


Figure 33. AmB nanoemulsions prepared in this work.

From a visual analysis of Figure 33, it can be seen that nanoemulsions A, B, J and K presented different physical aspects, from liquid to gelled formulations. More specifically, A-NE, B-NE and J-NE samples showed yellow color, stable and limpid aspect, while K-NE exhibited yellow color with cloudy aspect.

Yellow color may be related to AmB color. C-NE and I-NE samples, prepared with mint oil, exhibited polydisperse system with dispersed cloudy yellow particles indicating instable system. D-NE, E-NE, F-NE and G-NE were liquid, while A-NE, B-NE, J-NE and K-NE were gel-like. D-NE, E-NE, F-NE and G-NE presented stable aspect and yellow color. H-NE and L-NE samples, prepared without drug, showed whiter color than NE containing AmB, visually stable and gel-like aspect.

There are no literature reports about AmB nanoemulsions using essential oils, even if AmB nanoemulsions have already been described before, prepared by different methods and, with the oil phase generally composed by triglycerides. As examples, Filippin and co-workers (2008) developed and characterized AmB nanoemulsions using caprylic/capric triglycerides, cholesterol and soy bean lecithin for candidiasis treatment. Caldeira and co-workers (2015) studied AmB nanoemulsions containing oil phase prepared with medium chain triglycerides, Tween 80, cholesterol, stearylamine and α -tocopherol by hot homogenization method. Hussain and colleagues (2016b) focused on AmB nanoemulsions

formulations for antifungal use by oil phase slow titration in aqueous phase. The oil phase contained propylene glycol monocaprylate (Capmul PG8) as a lipid, caprylocaproyl polyoxyl-8 glycerides (Labrasol[®]) and polyethylene glycol 400 as surfactant and co-surfactant, respectively. Sosa and colleagues (2017) developed AmB nanoemulsions for antifungal treatment using different lipids composition and nanoemulsion prepared with castor oil, Labrasol[®]: Plurol[®] oleique (polyglyceryl-3 dioleate) mixture and Transcutol[®] P (highly purified diethylene glycol monoethyl ether EP/NF) showed the best results.

Mendonça and colleagues (2016) prepared AmB polymeric micelles using Pluronic[®] F127 and evaluated *in vitro* and *in vivo* response against murine tegumentary leishmaniasis. The polymeric micelles were produced under vigorous magnetic agitation of AmB solution (AmB dissolved in dichloromethane) addition in Pluronic[®] F127 solution. Then, dichloromethane was evaporated under rotary evaporation and, after dispersed in water. They used the same polymer selected for this thesis. However, they used more steps and organic solvent to produce AmB polymeric micelles, while here we are using ultrasonic processor (one step formulation) with an organic solvent of Class 3 (DMSO) instead Class 2 (dichloromethane). Solvents in Class 2 (ICH Guidelines) should be limited in pharmaceutical products because of their inherent toxicity. Ideally, less toxic solvents (Class 3) should be used where practical (ICH, 2016).

3.4.3. PHYSICOCHEMICAL CHARACTERIZATION OF AMPHOTERICIN B NANOEMULSIONS

3.4.3.1. Determination of Droplet Size, Polydispersity Index and pH

The physicochemical characterization of twelve batches of AmB nanoemulsions is shown in Table 4.

Table 4. Physicochemical characterization of AmB nanoemulsions

Samples	Mean droplet size (nm) ± SD	Polydispersity index (Pdl) ± SD	pH
A-NE	32.63 ± 1.81	0.19 ± 0.06	5.0
B-NE	43.50 ± 3.14	0.26 ± 0.01	5.0
C-NE	294.27 ± 2.03	0.45 ± 0.03	4.5
D-NE	85.88 ± 1.82	0.37 ± 0.05	4.5
E-NE	46.83 ± 0.44	0.37 ± 0.00	4.5
F-NE	93.91 ± 2.63	0.36 ± 0.04	5.0
G-NE	51.27 ± 0.51	0.43 ± 0.00	4.5
H-NE	78.50 ± 1.20	0.33 ± 0.04	5.0
I-NE	371.40 ± 8.77	0.63 ± 0.04	4.5
J-NE	56.65 ± 3.42	0.61 ± 0.01	5.0
K-NE	112.10 ± 0.40	0.31 ± 0.01	5.0
L-NE	31.43 ± 0.43	0.16 ± 0.03	5.0

Legend: SD – standard deviation

C-NE and I-NE, prepared with mint oil and showed the highest mean droplet size (294.27 ± 2.03 nm and 371.40 ± 8.77 nm, respectively) and elevated values of Pdl (0.454 ± 0.030 and 0.633 ± 0.041 , respectively). They presented a visual instable aspect (Figure 33) and these data confirmed an unstable behavior. J-NE, also prepared with mint oil, presented lower mean droplet size (56.65 ± 3.42 nm) than formulations C and I, but presented elevated Pdl (0.609 ± 0.014) as formulations C and I.

NE A showed the lowest mean particle droplet size and the lowest Pdl of formulations prepared with drug suggesting a more stable formulation. B-NE, D-NE, E-NE, F-NE and G-NE exhibited mean droplet size lower than 100 nm. However, formulation G showed elevated Pdl (0.432 ± 0.002), suggesting an

instable system. The batches H-NE and L-NE, which had not AmB, exhibited average droplet size lower than 100 nm and lower than respectively formulations produced with AmB (F and B). The Pdl of these nanoemulsions were lower than Pdl values of respectively nanoemulsions containing drug. Formulation K presented an average droplet size higher than 100 nm and a moderate value of Pdl.

The achievement of nanoemulsions containing droplet size lower than 100 nm allows their characterization in nanoscale formulations, since nanoscale concept is controversial in literature (CAMPOS, RICCI-JUNIOR, MANSUR, 2012). However, in general, nanoemulsions are defined as oil-water emulsions with droplet size below 500 nm (RAI *et al.*, 2018). Thus, the twelve batches prepared can be consider in nanoscale.

The small droplets size observed in nanoemulsions prepared with clove oil (Table 4) was related to the ultrasonication time used (5 minutes). It is known that the ultrasonication time interferes in average droplets size. For example, Shahavi and co-workers (2015) evaluated physicochemical parameters for clove oil nanoemulsions. They prepared nanoemulsions containing between 2.5% and 15% of clove oil and 5% of Tween[®] 80/Span[®] 80, under ultrasonication. Ultrasonication times higher than 2.5 minutes allowed average droplets sizes lower than 80 nm.

In relation to pH values of nanoemulsions, the values remained 4.5 and 5.0, which correspond to a compatible pH with human skin pH. The pH of human skin has a value in the range of 4.0 to 6.0 (ALI & YOSIPOVITCH, 2013; LAMBERS *et al.*, 2006). Furthermore, the values of pH allow topical administration of AmB nanoemulsions, which it is the objective of this development.

3.4.3.2. Drug Content

Prior to drug content assay of nanoemulsions, the AmB ultraviolet spectrum was identified in the range of 200 to 800 nm (Figure 34). Four peaks can be seen respectively at 333 nm, 360 nm, 389 nm and 415 nm.

According to European Pharmacopeia (2009), AmB UV spectrum is characterized by three peaks at 362 nm, 381 nm and 405 nm. Some studies have related these peaks to the presence of AmB aggregates or AmB monomers: AmB aggregates at 328 nm followed by three peaks at 365 nm, 384 nm and 408 nm (RODRIGUES *et al.*, 2013); AmB aggregates at 340 nm, followed by three peaks at 365 nm, 388 nm and at 410 nm corresponding to AmB monomers (CALDEIRA *et al.*, 2015). Based on these data, the AmB UV spectrum obtained in our study are considered to be related to the self-association of AmB (peak at 333 nm) and the presence of AmB monomers (peaks at 360 nm, 389 nm and 415 nm).

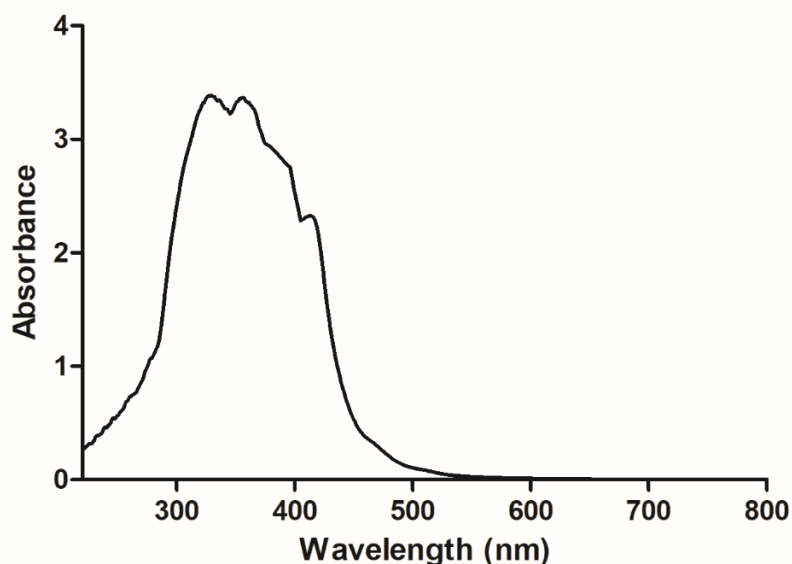


Figure 34. AmB UV- spectrum.

In the following, UV spectra of two nanoemulsions were obtained in order to evaluate the best wavelength for drug content assay. The nanoemulsions selected were F-NE (nanoemulsion with AmB) and H-NE (blank nanoemulsion). Figure 35 shows the UV spectra of these formulations in the range of 220 to 500 nm. This range of wavelength was chosen due to previous identification of AmB absorption peaks between 300 and 420 nm (Figure 34).

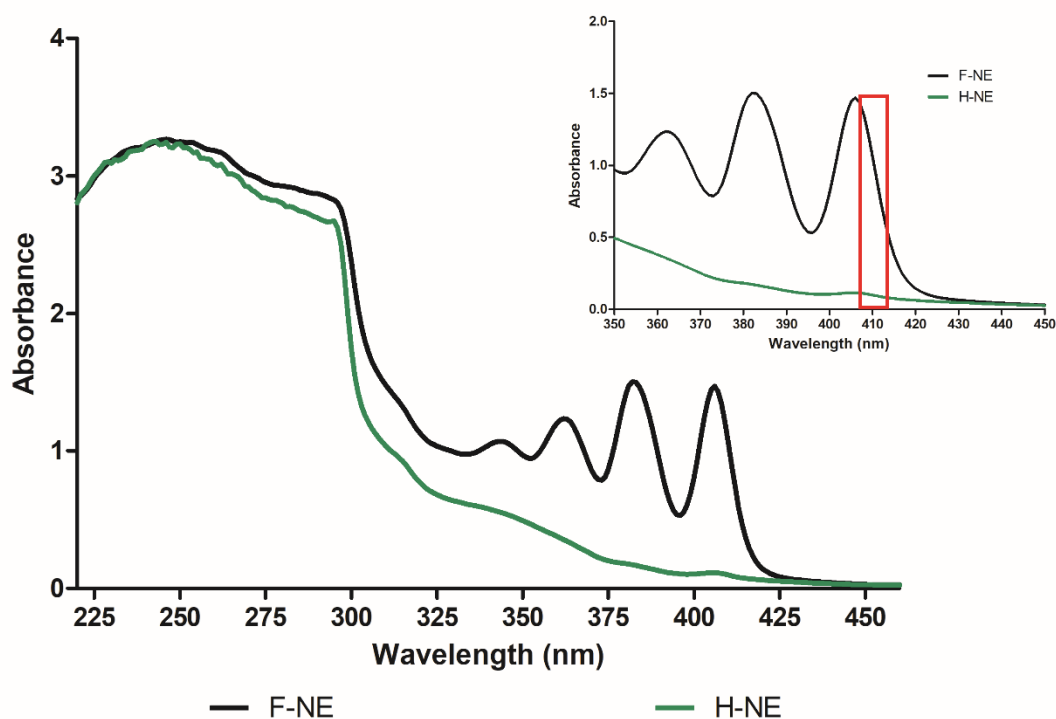


Figure 35. UV spectrum of nanoemulsions F and H in methanol.

It could be observed that F-NE, which contains AmB, presented four peaks in the range of 340-420 nm, corresponding to AmB peaks. H-NE (formulation without drug) presented no peaks in the range of 340-420 nm, which confirmed the absence of AmB in this sample. However, some absorption between 300 and 400 nm was also detected in H-NE spectrum, suggesting that other material used to produce nanoemulsions had some absorption in the same region as AmB. This interference allowed the choice of 410 nm as the wavelength for drug content assay. In this wavelength, the absorbance value was related to AmB presence in the formulations. Moreover, in the UV spectra of two other samples, it could be identified highest absorbance values in the range of 220-300 nm, which are probable related to other constituents as essential oil or polymer in the formulations.

Table 5 presents the drug content of twelve batches of nanoemulsions. These batches were stored at room temperature for seven days before the drug content analysis. The theoretical concentration of AmB was 0.5 mg/mL.

Table 5. Drug Content of Nanoemulsions

Batch	Concentration of AmB (mg/mL) \pm SD¹	% DC²
A-NE	0.26 \pm 0.00	51.2
B-NE	0.38 \pm 0.00	76.8
C-NE	0.02 \pm 0.00	4.2
D-NE	0.30 \pm 0.00	60.2
E-NE	0.39 \pm 0.00	78.2
F-NE	0.39 \pm 0.00	77.2
G-NE	0.36 \pm 0.00	72.0
H-NE	-	-
I-NE	0.01 \pm 0.00	1.2
J-NE	0.02 \pm 0.01	3.2
K-NE	0.28 \pm 0.00	55.4
L-NE	-	-

Legend: ¹ Standard deviation; ² Drug content in percentage

H-NE and L-NE are blank without drug. C-NE, I-NE and J-NE, prepared with mint oil, had the lowest values of %DC, which suggested no drug encapsulation supporting the instability of these systems observed in visual analysis and through high Pdl probably related to phase separation. Thus, samples prepared with mint oil were discarded from the AmB nanoemulsions development.

A-NE, D-NE and K-NE presented lower values of %DC than B-NE, E-NE, F-NE and G-NE being also discarded from this study. It is worth pointing out K-NE showed high droplet size as well. Although %DC of G-NE was good (72%),

this formulation was discarded due to Pdl higher than 0.4.

Finally, B-NE, E-NE and F-NE showed the best %DC compared with the other batches. Furthermore, they presented satisfactory droplet sizes and Pdl.

Referring to the literature, it can be confirmed that others AmB nanoemulsions have reached higher loads of AmB. For example, Santos and co-workers (2012) developed AmB nanoemulsions with triglycerides and stearylamine and obtained 95% of drug content in their formulations for topical application. Santos and co-workers (2017) prepared AmB nanoemulsions, for intravenous administration, with triglycerides, Tween[®] 80 and glycerol and with a higher drug content than the best values observed for our AmB nanoemulsions (around 77%), probably due to the differences in the formulations (presence of stearylamine formed ion pairing with drug), affecting, among other things, the stability of AmB nanoemulsions. Another possibility for lower drug content values observed in this work is the storage time at room temperature (7 days) before the analysis indicating a possible drug degradation.

To summarize, the AmB nanoemulsions selected for further studies (stability and *in vitro* analyses) showed, on average, 77% of drug content.

3.4.4. STABILITY STUDY OF AMPHOTERICIN B NANOEMULSIONS

New batches (B-NE, E-NE and F-NE, H-NE and L-NE) were prepared for stability study. These new nanoemulsions were prepared with 0.3% of antimicrobial preservative (imidazolidinyl urea) to protect the formulations. E-NE was discarded from the study due to its visual changes (became more fluid and cloudier) in seven days of storage. Then, B-NE and F-NE (with AmB) and H-NE and L-NE (without drug) were submitted for one year of storage in two different temperature conditions: at room temperature (28°C) and in refrigerator (4°C), in amber flasks hermetically sealed.

3.4.4.1. Transmission Electron Microscopy (TEM)

Prior to stability study, the recent nanoemulsions were evaluated by TEM to investigate the morphology of droplets. Figure 36 presents the TEM images of nanoemulsions using 100K for B-NE and L-NE as magnification and 80K magnification for F-NE and H-NE.

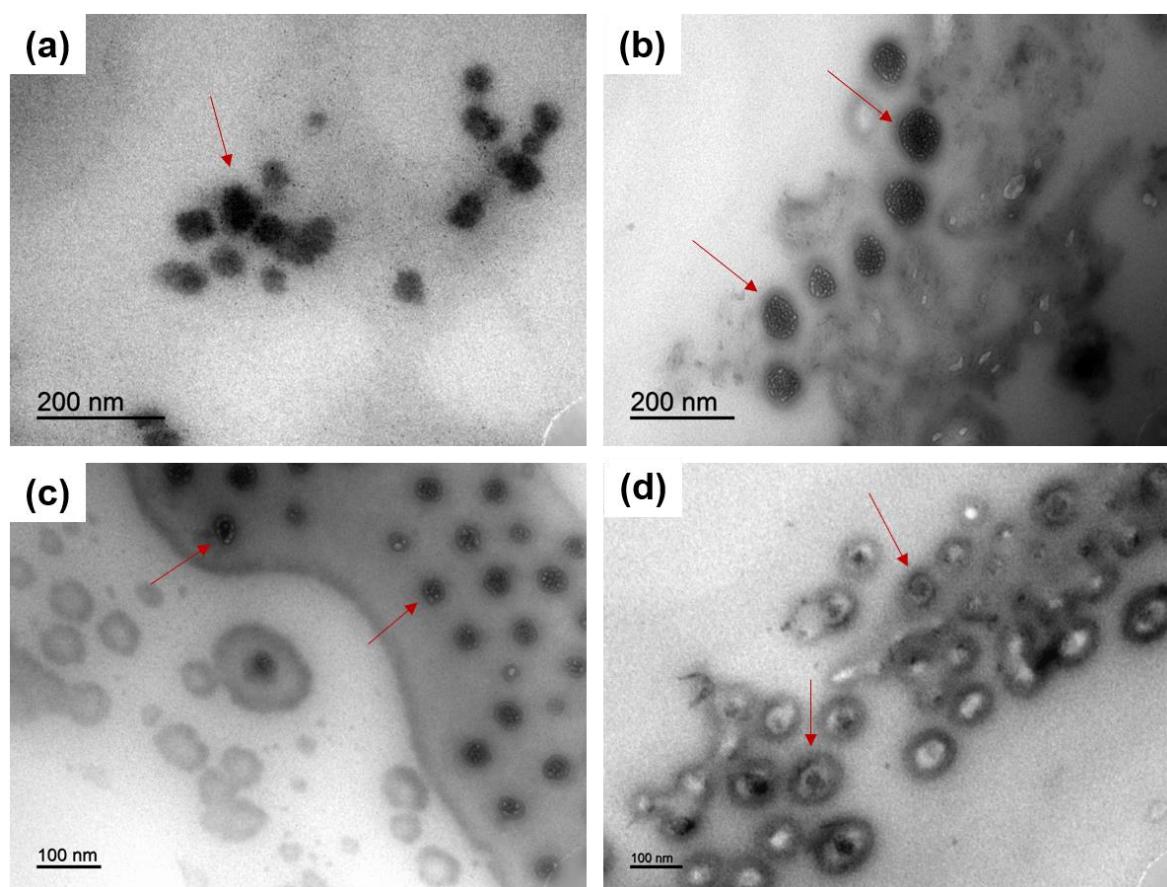


Figure 36. TEM images of nanoemulsions with AmB (a) B-NE, (b) F-NE and respectively nanoemulsions without drug (c) L-NE and (d) H-NE.

TEM images of four nanoemulsions showed spherical shaped droplets. Moreover, droplets lower than 100 nm in size were observed, according to the average droplets size determined by dynamic light scattering analysis.

This is the range of droplet size of dispersed phase frequently reported in the literature: AmB microemulsion comprising various lipids, Span[®] and Tween[®] as surfactants with an average droplet size around 120 nm were described by Silva and co-workers (2013); AmB nanoemulsions with variable compositions of

surfactant and co-surfactant with an average droplet size lower than 100 nm were developed by Hussain and co-workers (2013 and 2016), while AmB nanoemulsions prepared with various lipids were characterized by monodispersed oil droplets with spherical shape and sizes lower than 150 nm (SOSA *et al.*, 2017). These studies have described similar morphology than that observed in our work. Moreover, they supported the use of TEM analysis to investigate the morphology and average size of nanoemulsions confirmed by dynamic light scattering analysis.

3.4.4.2. Determination of Droplet Size, Polydispersity Index and pH

The AmB nanoemulsions, stored at 0, 7, 15, 30, 60, 90, 180, 365 days under two storage conditions (room temperature – RT and refrigerator – R) and placed into amber glass flasks in order to protect to light due to AmB is photo sensible (EUROPEAN PHARMACOPEIA, 2009), were evaluated in terms of their average droplet size over time.

The results were given in Figure 37 for B-NE and its blank L-NE and in Figure 38 for others two AmB nanoemulsions, F-NE and its blank H-NE.

In Figure 37, B-NE and L-NE presented droplets size, on average, lower than 60 nm. Moreover, B-NE (which have AmB) showed higher droplets size (around 40 nm) than L-NE, which was prepared without drug and had droplets size around 30 nm. It was possible to observe an increase of droplets size at 90 days of storage, when samples were storage under refrigeration. This can be explained by droplets agglomeration and/or no efficacy of droplets dispersion in distilled water for DLS measurements. The two nanoemulsions were considered physically stable until 365 days, even if an enhancement of droplet sizes was detected (B-NE – around 200 nm and L-NE 130 nm).

However, L-NE stored in refrigerator (4°C) remained more stable than sample stored at room temperature in the same period (365 days). Based on these results, it seems that AmB nanoemulsion (B-NE) and blank nanoemulsion (L-NE) can be produced, stored in room temperature or under refrigeration (4°C), and used until 365 days from their manufacturing data.

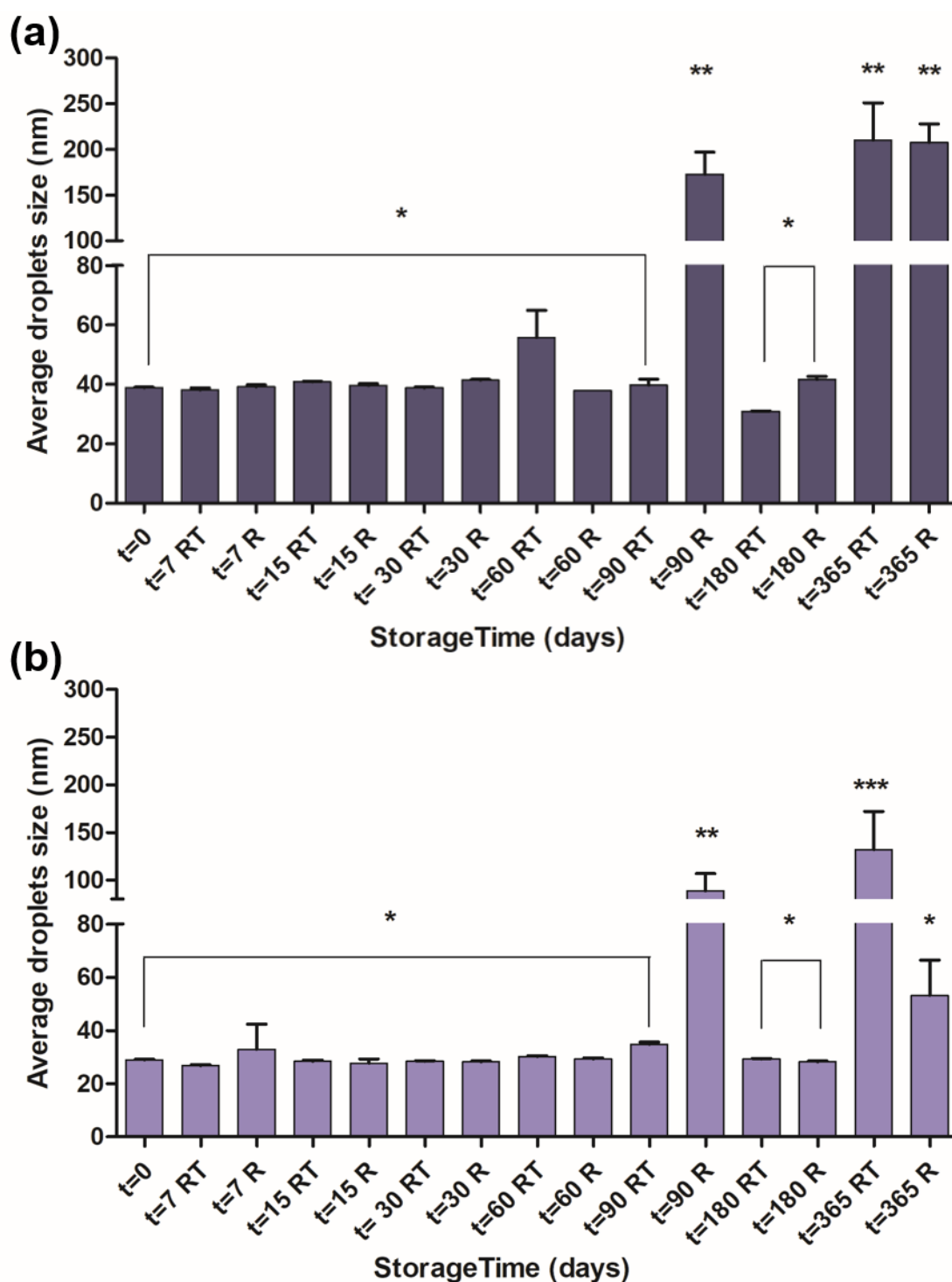


Figure 37. Droplets size in stability study of (a) B-NE and (b) L-NE. Legend: RT – room temperature (28°C), R – refrigerator (4°C). * - No statistically significant differences ($P > 0.05$); ** - No statistically significant differences ($P > 0.05$); *** - No statistically significant differences ($P > 0.05$) according to One-Way ANOVA with Tukey post-test.

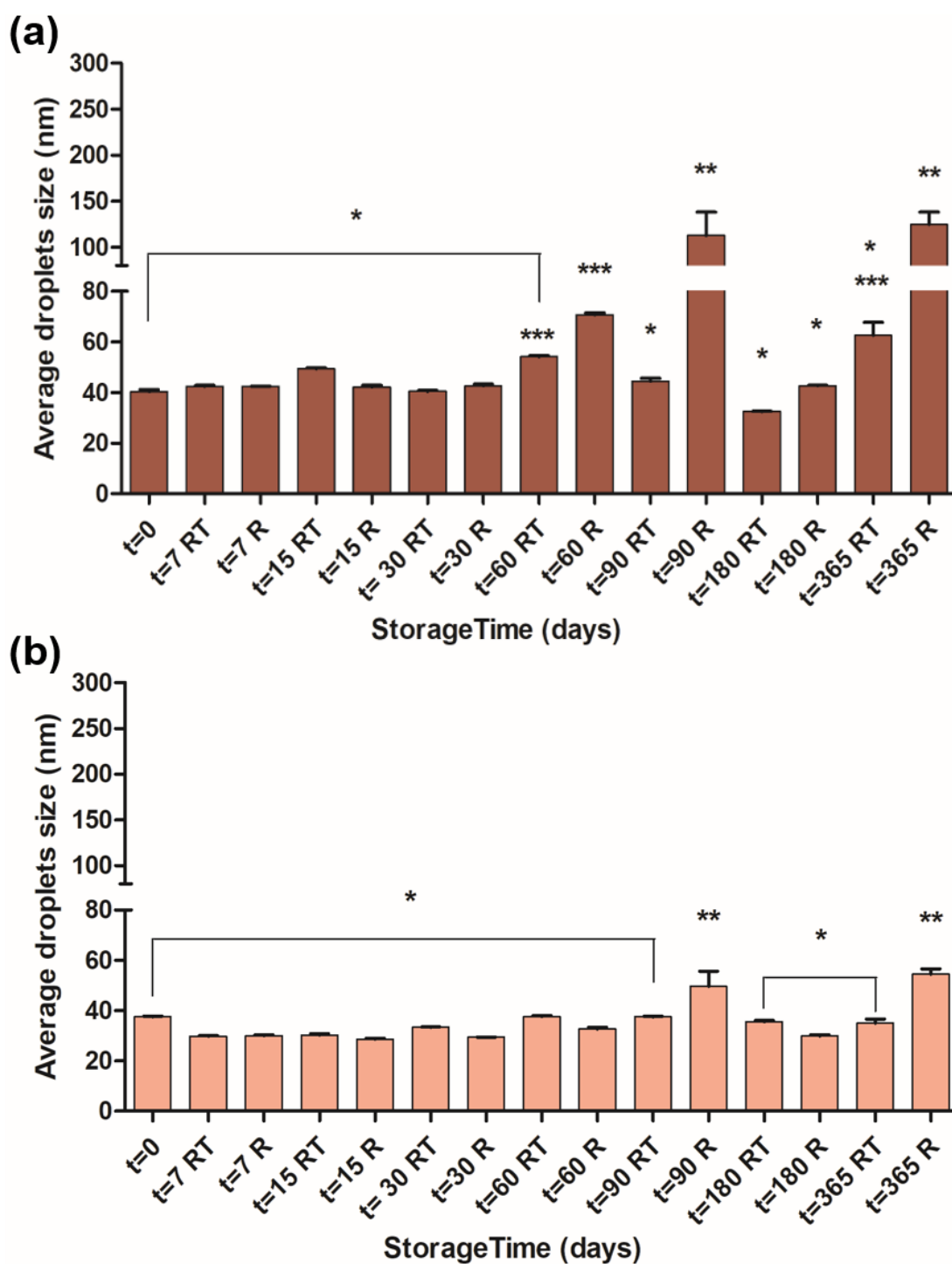


Figure 38. Droplets size in stability study of (a) F-NE and (b) H-NE. Legend: RT – room temperature (28°C), R – refrigerator (4°C). * - No statistically significant differences ($P > 0.05$); ** - No statistically significant differences ($P > 0.05$); *** - No statistically significant differences ($P > 0.05$) according to One-way ANOVA with Tukey post-test.

In Figure 38, F-NE and H-NE showed droplets size, on average, lower than 60 nm as observed to B-NE and L-NE as well.

F-NE (with AmB) presented droplets size around 43 nm, while H-NE (blank) were around 33 nm. The same trend was observed with B-NE (with AmB) and L-NE (without AmB). Therefore, the presence of drug in nanoemulsion formulation increased the droplets size when compared to blank formulations.

As for B-NE and L-NE, F-NE and H-NE presented a good stability and remained stable until 365 days of storage. Furthermore, when samples were stored in refrigerator, it was possible to detect:

- An increase of droplets size in 90 days of storage. A possible explanation, as already mentioned, could be some droplets agglomeration and/or no homogeneous dispersion in distilled water to DLS measurements;

- An enhancement of droplets size in F-NE (droplet size around 120 nm) in the last storage time;

- A slight increase of droplets size in H-NE (droplets around 55 nm).

Results from the literature have shown that AmB nanoemulsions may represent stable systems, even varying the components and the preparation method. Taking some examples:

Santos and co-workers (2012) developed AmB nanoemulsions using triglycerides, Tween[®] 80, Span[®] 80 and stearylamine and investigated the stability of formulations for 15 and 30 days. The formulations were stored into amber glass containers. They obtained nanoemulsions (with or without AmB) with droplet size around 200 nm and stable for 30 days. However, the storage condition of these formulations was not described. Singh and co-workers (2017) developed AmB nanoemulsions using Pluronic[®] F127 and chitosan. The formulations were submitted to a stability study during 6 months at 4°C. They obtained stable nanoemulsions with droplets size around 110 nm. Shahavi and co-workers (2015) evaluated physicochemical parameters and the stability of clove oil nanoemulsions (containing between 2.5% and 15% of clove oil and 5% of Tween[®] 80/Span[®] 80) for 180 days. They observed a better stabilization in nanoemulsions with higher concentrations of oil. Moreover, droplets size

increased during storage.

It is important to emphasize here that our study evaluated two different storage temperature conditions over longer period than those reported in the literature.

In addition to droplets size evaluation, the polydispersity index (Pdl) of four NE were determined and are presented in Figure 39 for B-NE and L-NE.

B-NE presented, during the stability study, 0.337 of Pdl on average. The sample stored for 180 days at room temperature showed the lowest value of Pdl (around 0.113). This value, statistically different of all others, could be explained by an error of analysis, probably related to non-representative aliquot or high sample dilution. The samples stored for 60 days (RT), 90 days (R) and 365 days (RT and R) presented higher values of Pdl. The high values observed in samples stored for 365 days ($Pdl > 0.390$) are probably due to an instability of the nanoemulsion, in according to the increase of droplets size observed in the same conditions. Thus, B-NE showed stability until 365 days of storage.

L-NE, without drug, showed a Pdl value of 0.183 (on average) during the stability study. As observed in stability of B-NE, samples stored for 90 days (R) and 365 days (RT and R) presented higher values of Pdl. The high values observed in samples stored for 365 days ($Pdl > 0.440$) suggested an instability of nanoemulsion as described for B-NE and in accordance with the enhancement of droplets size in this storage period. As for B-NE, L-NE was stable until 365 days. However, the values of Pdl, on average, obtained for L-NE were lower than those found for B-NE. This can be explained by the drug presence in system, which increased the droplets size and the polydispersity. Pdl values close to 0 indicates monodisperse systems and values near 1 indicates large distribution (TANG *et al.*, 2012). Nonetheless, the two nanoemulsions prepared (B-NE and L-NE) presented Pdl values closer to zero than one, indicating stable systems.

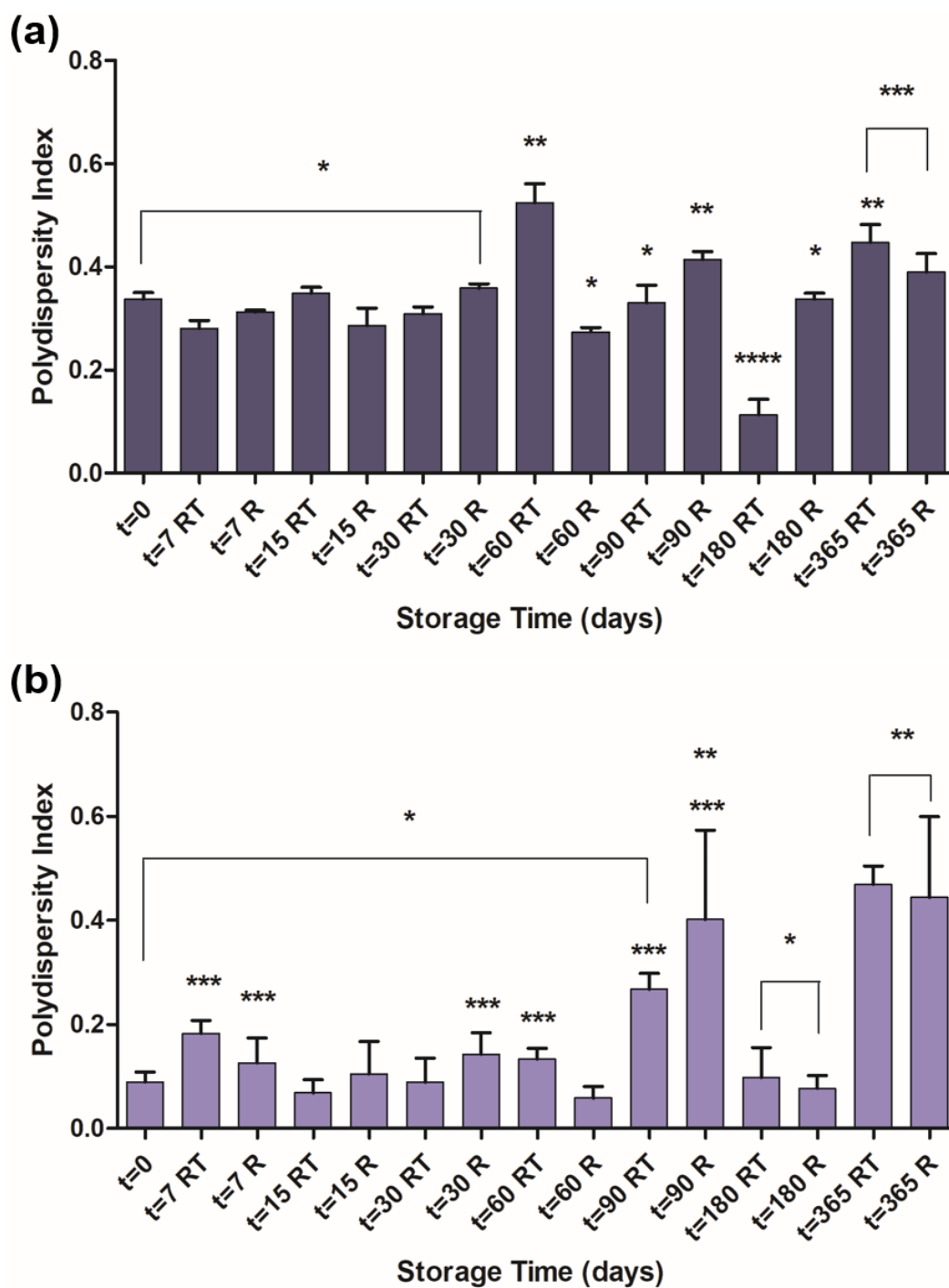


Figure 39. Polydispersity index (PDI) in stability study of (a) B-NE and (b) L-NE. Legend: RT – room temperature (28°C), R – refrigerator (4°C). * - No statistically significant differences ($P > 0.05$); ** - No statistically significant differences ($P > 0.05$); *** - No statistically significant differences ($P > 0.05$); **** - Statistically significant different ($P < 0.05$) according to One-way ANOVA with Tukey post-test.

Figure 40 gives Pdl evolution during storage for two other nanoemulsions, F-NE (with AmB) and H-NE (without AmB).

F-NE presented, on average, 0.396 of Pdl during the stability study. This value is higher than observed for NE B (0.337), which could be explained by Tween[®] 20 absence in F-NE. Tween[®] 20 is a non-ionic surfactant, which presents a good efficiency in emulsions stabilization (POLYCHNIATOU & TZIA, 2014). Moreover, Pluronic[®] and Tween[®] 20 work synergistically as surfactant promoting nanoemulsions stability (ARANTES *et al.*, 2017).

Sample stored 180 days at room temperature showed the lowest value of Pdl (around 0.140). As already observed for B-NE, this sample was statistically different of others and this result could be explained by an error of analysis (non-representative aliquot or high sample dilution). The samples stored for 90 days (R) and 365 days (RT) presented higher values of Pdl. The sample stored for 365 days, at room temperature, showed a Pdl value higher than 0.600, suggesting formulation instability, which is supported by the larger droplet size of this sample.

H-NE (without AmB), showed a Pdl value of 0.172 (on average) during the storage period. Samples stored for 90 days (R) and 365 days (RT and R) presented higher values of Pdl. As observed for other nanoemulsions (B-NE, F-NE and L-NE), samples storage for 365 days presented instability with high values of Pdl and high droplets size. Therefore, the four nanoemulsions prepared and submitted to stability test were stable until 365 days. In addition, the values of Pdl obtained for H-NE were lower than values of F-NE and could be explained by the absence of drug as described before for B-NE and L-NE.

There are some studies that described the stability of AmB nanoemulsions evaluating the Pdl. Santos and co-workers (2012) investigated the stability of AmB nanoemulsions for 30 days. They observed that blank nanoemulsions and AmB nanoemulsions showed values of Pdl very similar varying between 0.2 and 0.3 and concluded that these systems were stable and homogeneous. Singh and co-workers (2017) evaluated the stability of AmB nanoemulsions with or without chitosan for 180 days. The nanoemulsions produced without chitosan showed values of Pdl between 0.120 and 0.200 while nanoemulsions with chitosan presented values of Pdl varying from 0.100 to 0.300. However, it was not

statistically different and all nanoemulsions were considered stable for 180 days.

In addition to droplets size and Pdl values, the pH of the four nanoemulsions (B-NE, F-NE, H-NE and L-NE) were evaluated in stability study.

The values of pH during all storage period under two storage conditions for all four samples were maintained 5.0 without any variation. This value of pH is in agreement of desired for topical formulations due to belongs the range of human skin pH, which is between 4.0 and 6.0 (ALI & YOSIPOVITCH, 2013; LAMBERS *et al.*, 2006).

One study evaluated the pH values during stability of AmB nanoemulsions for topical administration. Santos and co-workers (2012) observed that nanoemulsions, with and without AmB, presented no significant differences of pH values, which were in the range of 7.3 to 7.7. These values were higher than consider optimal pH for topical application and higher than values obtained in this work. This difference is related to the formulation composition, which is different between this work and work of Santos and colleagues (2012).

Other studies investigated the pH values for intravenous administration. Filippin and co-workers (2008) developed AmB nanoemulsions using triglycerides and evaluated the stability of formulations for 180 days stored in two conditions (4°C and 25°C) protected from light. It was observed no differences in pH values, maintained between 6.2 and 6.6, during stability study in the two conditions of storage. Caldeira and co-workers (2015) developed nanoemulsions of AmB using triglycerides, cholesterol and with or without stearylamine. They investigated the stability of these formulations for 180 days and analyzed pH one day after preparation and after 180 days. It was observed that pH of nanoemulsions (with or without stearylamine) was between 7.2 and 7.4, while after 180 days the pH decreased to 6.2-6.4. This reduction in pH values can be explained by fatty acids formation with triglycerides hydrolysis.

From these studies, the control of pH at values desired for topical application is formulation-dependent. The NE formulations developed here seemed satisfied this criterion.

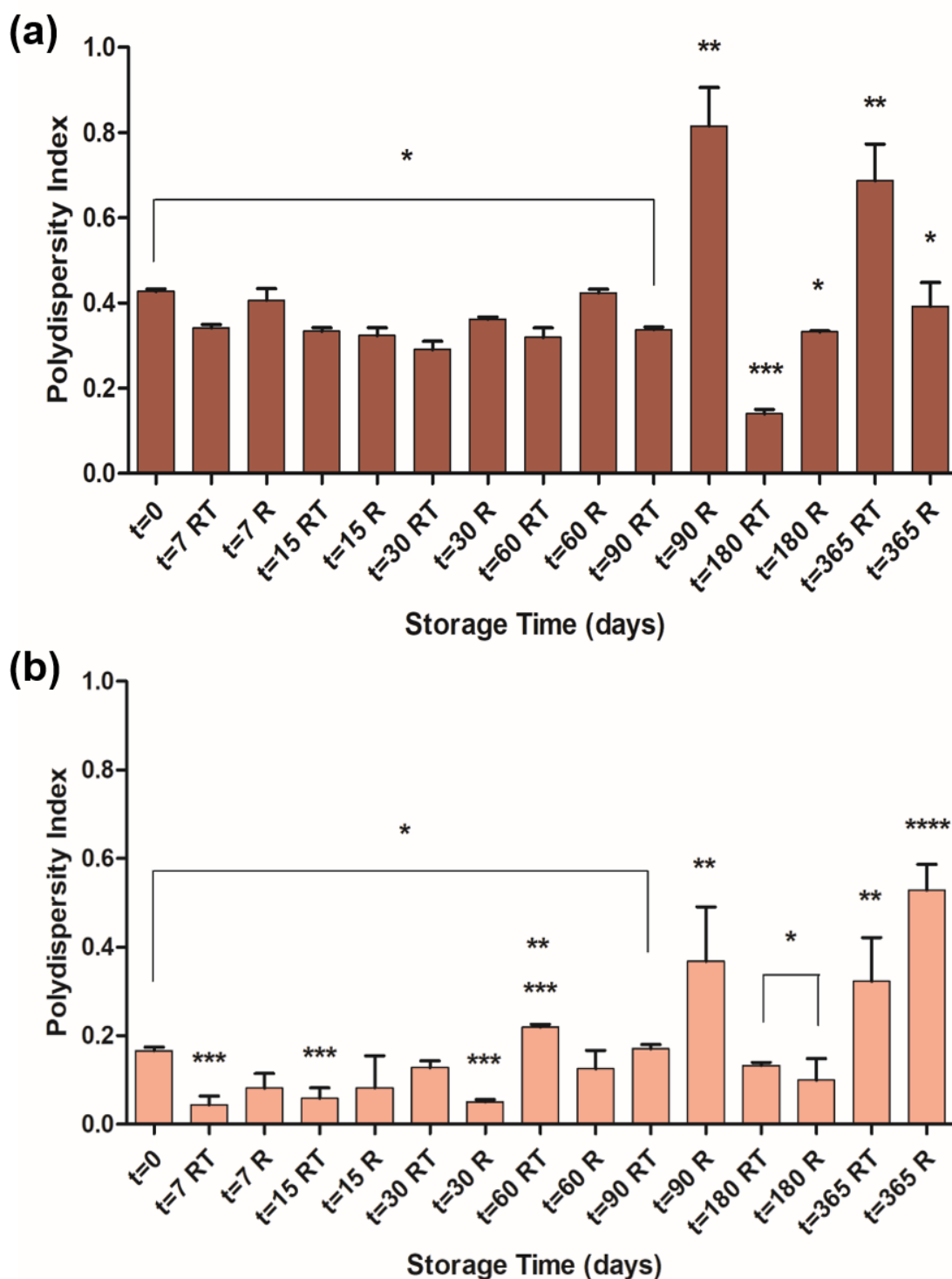


Figure 40. Polydispersity index (PDI) in stability study of (a) F-NE and (b) H-NE. Legend: RT – room temperature (28°C), R – refrigerator (4°C). * - No statistically significant differences ($P > 0.05$); ** - No statistically significant differences ($P > 0.05$); *** - Statistically significant differences ($P < 0.05$); **** - Statistically significant different ($P < 0.05$) according to One-way ANOVA with Tukey post-test.

3.4.4.3. Drug Content

Besides monitoring droplet size, Pdl and pH during storage (365 days under two different temperature conditions), the drug content was investigated in B-NE and F-NE. Figure 41 shows the results of drug content in these nanoemulsions.

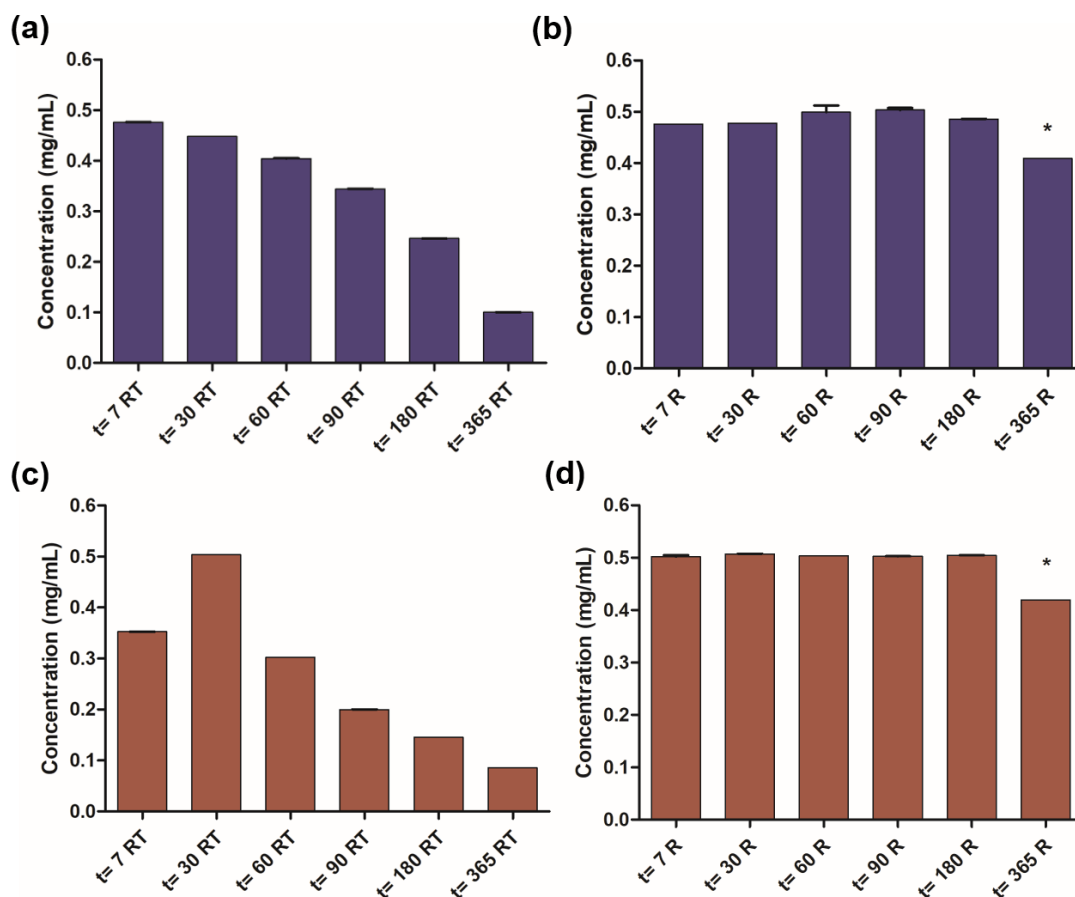


Figure 41. Drug loading content in stability study of (a) B-NE at room temperature, (b) B-NE at refrigerator, (c) F-NE at room temperature and (d) F-NE at refrigerator. Legend: RT – room temperature (28°C), R – refrigerator (4°C). * - Statistically significant different ($P < 0.05$) according to One-way ANOVA with Tukey post-test.

B-NE and F-NE stored at room temperature (Figure 41a and 41c, respectively) showed a considerable reduction of AmB concentration during storage. Furthermore, B-NE samples were statistically different among them as observed for F-NE samples. F-NE presented higher value of AmB concentration in sample stored for 30 days than that for sample stored for 7 days. An error of

analysis can explain this difference. B-NE showed a drug content around 95% for sample stored 7 days at room temperature, while sample stored for 365 days in the same condition presented only 20% of drug content.

F-NE showed 71% of drug content in sample stored 7 days, while sample stored for 365 days had only 17% of AmB content. This reduction of AmB concentration in samples storage at room temperature can be related to AmB degradation. AmB exhibits poor stability already described in literature when exposed to light, heat, ultraviolet irradiation, extremes of pH and suffers oxidation in presence of oxygen (BONNER, MECHLINSKI, SCHAFFNER, 1975). Moreover, there are, also, reports about AmB degradation when incorporated in oil-water systems (WALKER *et al.*, 1998). The possible AmB degradation observed in nanoemulsions stored at room temperature will be investigate through HPLC in a complementary study.

B-NE and F-NE stored in refrigerator (4°C) (Figure 41b and 41d, respectively) presented unchanged AmB concentration over whole storage period, presenting only a statistically significant reduction at the end of the experiment (365 days). However, the reduction was lower than reduction observed in samples stored at room temperature. B-NE presented 95% of drug content in 7 days of storage and maintained this value until 365 days, in which AmB concentration was reduced to 82%. F-NE had 100% of drug content in 7 days of storage while the last analysis (365 days) showed 83% of drug content.

According to these results, it is advisable to store AmB nanoemulsions at 4°C to maintain their stability until 365 days. The nanoemulsions prepared for *in vitro* studies were then maintained at 4°C.

Filippin and co-workers (2008) evaluated the AmB content during 180 days of storage at 25°C and 4°C. They observed that drug content was 98% in the beginning of stability study and was maintained around 90% AmB content during stability tests. It was, also, verified that nanoemulsions stored in both conditions remained stable chemically and physically, which was explained by the high purity of soybean phosphatidylcholine.

Santos and co-workers (2012) analyzed the stability of AmB

nanoemulsions prepared with or without stearylamine for 90 days of storage. The AmB concentration remained constant during stability study for nanoemulsion prepared with stearylamine while a significant reduction of AmB content after 90 days was observed for formulation without stearylamine. The presence of stearylamine promotes ion pairing formation between this amine and carboxylic group of AmB, which stabilized oil-water interface and increase the nanoemulsions stability. The same group, in 2015, evaluated the stability of AmB nanoemulsions (with or without stearylamine) for 180 days stored at 4°C using cholesterol instead of sorbitan monooleate used before. It was observed that NE with or without stearylamine presented a constant AmB content after 180 days, suggesting that both formulations were stable (CALDEIRA *et al.*, 2015).

Singh and co-workers (2017) investigated the stability of AmB nanoemulsions containing chitosan or not during 180 days at 4°C. The encapsulation efficiency remained around 60% for nanoemulsions with or without chitosan and during whole storage period, suggesting stable formulations.

It is possible to observe that, in general, AmB nanoemulsions described in literature were stable and submitted to stability studies corresponding to a period of 180 days at 4°C. These results support the results obtained in this work that AmB nanoemulsions remained stable until 365 days and storage under refrigeration is advisable.

Comparing our formulation with AmB formulations presented on the market, our nanoemulsions are more stable than Ambisome® and Anforicin® B, formulations for intravenous administration. These market formulations have stability for 24 hours after reconstitution under refrigeration (2°C – 8°C), while our formulation remains stable for 365 days under same temperature (4°C).

3.4.5. IN VITRO RELEASE OF AMPHOTERICIN B NANOEMULSIONS

New AmB nanoemulsions (B-NE and F-NE) were prepared and stored at 4°C for *in vitro* studies. These formulations presented oil droplets size around 45 nm and AmB content around 98%wt. Free AmB (AmB dissolved in DMSO), B-NE and F-NE *in vitro* release profiles are shown in Figure 42.

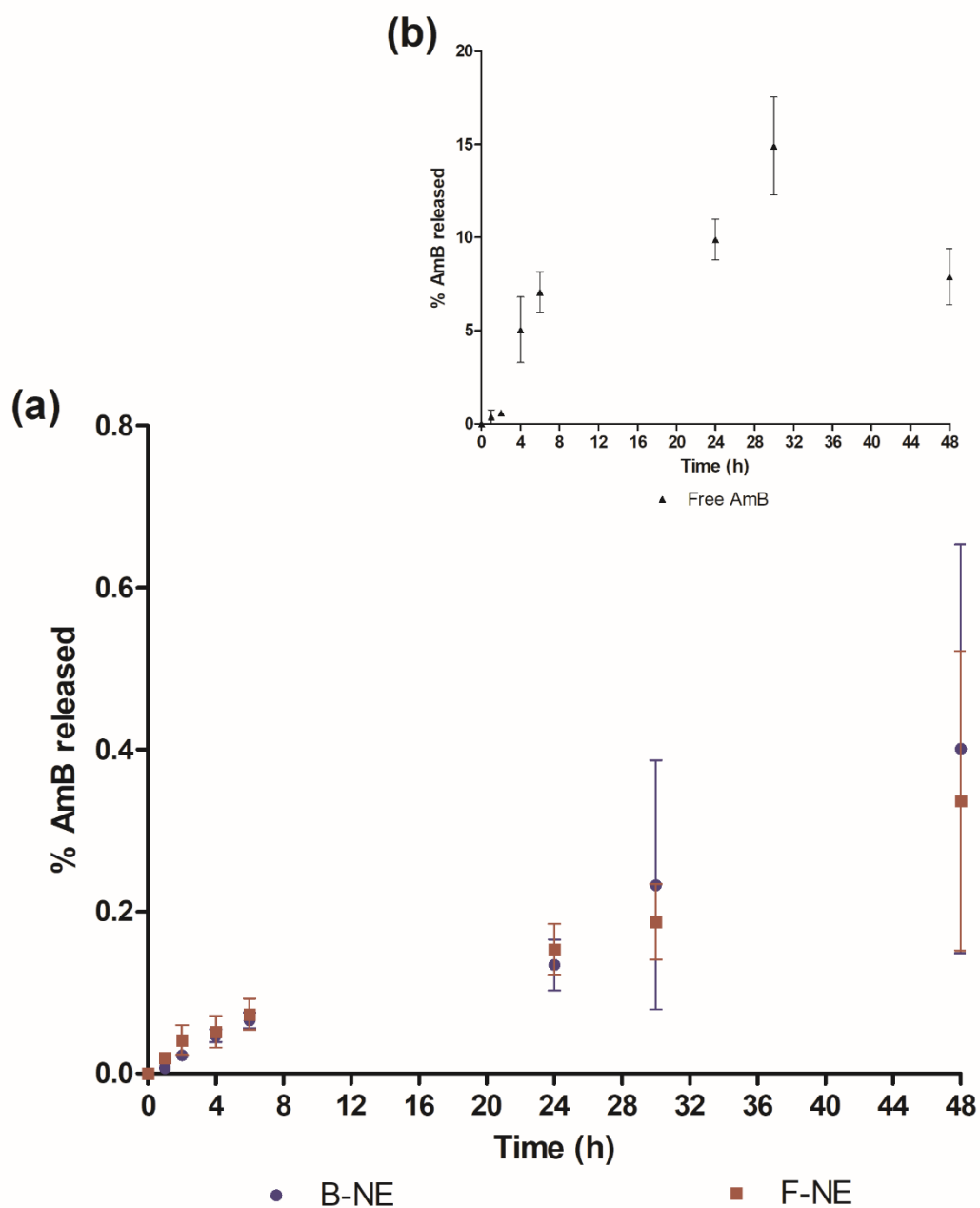


Figure 42. *In vitro* release profile of (a) B-NE (blue) and F-NE (red) and (b) free AmB in solution (black) (n=4).

Figure 42 shows similar and very slow release profile of AmB from B-NE and F-NE formulations. Moreover, it can be observed (Fig 4b) that free AmB showed faster release than nanoemulsions (around 15% of drug released in 30h, against 0.2% from B-NE and F-NE formulations). However, after 30 hours, free AmB presented a decrease of release profile, possible due to some drug

degradation. In fact, AmB degradation in phosphate buffer solution maintained at 37°C has already report by Connors and co-workers (1986).

AmB toxicity is one of the challenges for conventional therapy to leishmaniasis treatment. A slow release of AmB nanoemulsions should be interesting for a controlled drug release, decreasing the drug toxicity and protecting it from degradation. Due to the very slow AmB release from our nanoemulsions (lower than 1%wt), these systems were not submitted to a mathematical kinetic analysis.

Santos and co-workers (2012) evaluated and compared the *in vitro* release profile, for 8 hours, of three formulations containing AmB: AmB in solution (methanol/DMSO), Fungizone® and AmB nanoemulsion developed by the authors. They verified that AmB solution presented the highest percentage of drug release after 8 hours (around 69%), while AmB nanoemulsion presented the lowest percentage (only 8%). The low release profile of nanoemulsion may be explained by the strong absorption of AmB at the oil-water interface and this property allows a reduction of AmB toxicity in comparison to Fungizone® toxicity.

Sosa and co-workers (2017) developed AmB nanoemulsion for topical application for antifungal treatment. The physicochemical properties, drug release, permeation and antifungal activity were evaluated. The release of AmB from AmB nanoemulsions (prepared with triglycerides) was evaluated for 75 hours and compared with AmB solution (in DMSO). AmB nanoemulsions released 100% of drug after 75 hours, while AmB solution released only 10%. The percentage of AmB released from nanoemulsions increased over time until 100%. Therefore, AmB nanoemulsion presented a higher and extended drug release than AmB solution.

These results indicated that nanoemulsions is an interesting formulation for topical delivery of AmB. Despite two different formulations, this work and the work of Santos and colleagues (2012) suggested a slow release of AmB from this kind of formulation. A controlled release was also demonstrated by the nanoemulsion formulation of Sosa and colleagues (2017), even if with higher drug release rate.

Furthermore, there are some more recent studies, which described *in vitro* release profiles from AmB nanoparticles. Al-Quadeib and co-workers (2015) developed PEG-PLGA nanoparticles of AmB for oral delivery and evaluated the *in vitro* release profile of different batches prepared for 24 hours. They observed a biphasic release profile with a rapid release in the first 6 hours (varying 21-51% of drug released) and a slow release after 6 hours until 24 hours with 11% of drug released. This release profile was explained, in the first 6 hours (fast release) by the dissolution and diffusion of AmB not entrapped, followed by a continuous and slow release attributed to a drug diffusion from the particle core.

Chhonker and co-workers (2015) developed a lecithin AmB nanoparticles with or without chitosan for ocular application and analyzed the *in vitro* release profile for 10 hours. They observed a biphasic release with a burst release in the first hours followed by a continuous release. The initial fast release was related to desorption and diffusion of AmB adhered to nanoparticles surface. The continuous release was explained by drug diffusion from nanoparticles matrix. However, the amount of AmB released after 10 hours was higher than 80%.

It can be verified that AmB release is dependent on formulation types. Nanoparticles presented a biphasic release while nanoemulsions promoted a slow and continuous release. The two type of formulations are interesting for prolonged release of drugs.

3.4.6. IN VITRO SKIN PERMEATION STUDY OF AMPHOTERICIN B NANOEMULSIONS

In vitro skin permeation study evaluated the amount of AmB permeated across the pig ear skin and presented in the receptor chamber after 6 and 8 hours of experiment (Figure 43).

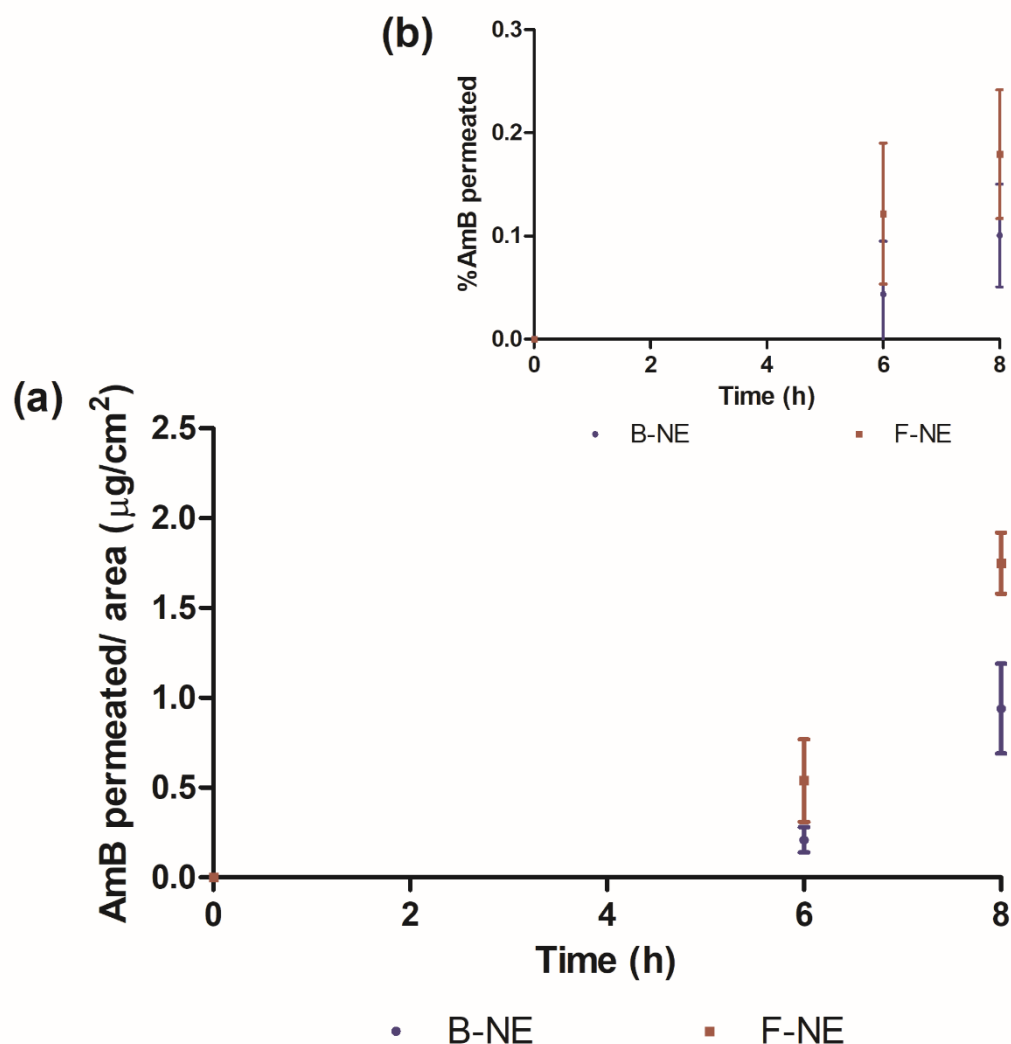


Figure 43. Amount of AmB (a) AmB permeated/area and (b) % AmB permeated present in receptor chamber (n=5).

The amount of AmB permeated from the two nanoemulsions was lower than $2 \mu\text{g}/\text{cm}^2$ (or lower than 0.2%) after 8 hours. A higher amount of AmB was permeated from F-NE than from B-NE. The lower values of AmB permeated after 8 hours can be related to the *in vitro* release profile of these formulations, which showed very slow release. Furthermore, the low amount of AmB permeated could suggest a possible low systemic action of these formulations, decreasing the toxicity and side effects of AmB and supporting the local action desired for these formulations.

Santos and co-workers (2012) evaluated *in vitro* skin permeation study for different formulations containing AmB (AmB in solution, Fungizone[®], Amphocil[®], AmB nanoemulsion and Fungizone[®]- Lipofundin[®] mixture) and investigated the amount of drug permeated after 24 hours. It was observed no amount of AmB (concentration lower than 0.02 µg/mL) detectable in receptor chamber for all formulations. This might probably be explained by the drug hydrophobicity and high molecular weight, which difficult the drug passage through dermis hydrophilic barrier. This article confirmed the results observed in Figure 43 that AmB nanoemulsions presented a low permeation across skin.

There are some articles that use albino rat skin as skin model instead of pig ear skin. Hussain and co-workers (2013) investigated the *in vitro* permeation study of three oil-water AmB nanoemulsions, Fungisome[®] (liposomal AmB gel) and drug solution for 24 hours. It was collected aliquots in various times (1, 2, 4, 6, 8, 10, 12, 16, 20 and 24 hours) to evaluate the amount of AmB presented in receptor chamber. Nanoemulsions prepared with polyethylene glycol 400 (PEG-400) as co-surfactant showed a higher cumulative amount of AmB (higher than 950 µg) after 24 hours than nanoemulsion prepared with propylene glycol, drug solution and Fungisome[®]. The presence of PEG-400 allowed the increase of drug penetration due to increases the drug solubility in *stratum corneum* layer. Butani and co-workers (2014) developed AmB microemulsions and evaluated the *in vitro* skin permeation of these formulations. Microemulsions showed higher amount of AmB permeated (higher than 95 µg/cm²) than drug solution (around 50 µg/cm²) after 24 hours. The microemulsions increased the drug permeability. This finding was explained by the authors by the water content in microemulsions, which allowed the drug permeation due to stratum corneum hydration promoting the enlargement of channels in keratin layer.

In addition to evaluation the amount of AmB presented in the receptor chamber, it was investigated the amount of AmB presented in epidermis and in dermis after 8 hours of experiment. Figure 44 shows the amounts of AmB retained in each skin layer (epidermis and dermis).

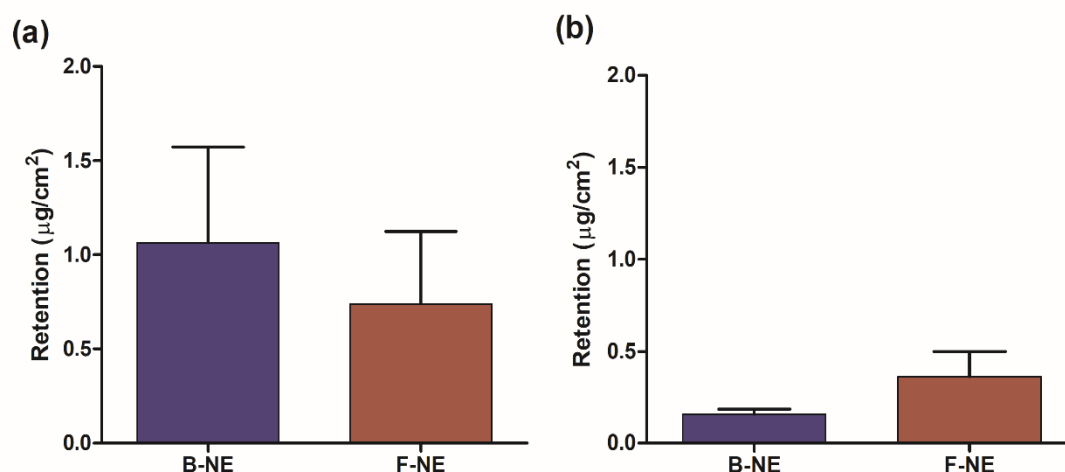


Figure 44. Amount of AmB retained in (a) epidermis and (b) dermis after 8 hours of *in vitro* permeation study.

B-NE and F-NE showed some amount of AmB retained in epidermis and dermis. However, epidermis presented more AmB retained than dermis, which can be explained by the *stratum corneum* layer presence in the epidermis that is the major barrier to drug permeation (RUELA *et al.*, 2016). The two formulations presented AmB retention higher than $0.7 \mu\text{g}/\text{cm}^2$ in epidermis and between 0.16 - $0.36 \mu\text{g}/\text{cm}^2$ in dermis. Nanoemulsions showed no statistically differences ($p > 0.05$) between them conforming to T test in relation to AmB retention in epidermis and in dermis. Moreover, no statistically differences ($p > 0.05$) was observed comparing AmB retention in epidermis and dermis for each NE based on T test. Although these results suggested low permeation of AmB from nanoemulsions, there is some amount of drug retained in dermis that can be promote the CL treatment as the parasites are located. Thus, these results were compared with *in vitro* antileishmanial activity in order to evaluate if this low amount of drug retained in dermis can be able to treat CL.

Despite this experiment was conducted in intact skin, which has skin composition different from skin with cutaneous leishmaniasis lesions, it is not possible investigate *in vitro* skin permeation with skin containing lesion. Therefore, skin permeation study allows have an idea of formulations behavior on skin.

Our results demonstrated low penetration across the skin with some AmB retention in dermis and epidermis. A low AmB penetration across the skin was already described in literature, as well as high amounts of drug retained into skin layers. Among them:

Santos and co-workers (2012) evaluated the amount of AmB penetrated into dermal membranes from various formulations (AmB in solution, Fungizone[®], Amphocil[®], AmB nanoemulsion and Fungizone[®]- Lipofundin[®] mixture). These experiments were investigated in pig ear skin without epidermis. It was observed that AmB solution showed the highest value of penetration into dermal membranes, around 18 $\mu\text{g}/\text{cm}^2$, while nanoemulsion and Fungizone[®]- Lipofundin[®] mixture presented the lowest values (1.1 $\mu\text{g}/\text{cm}^2$ and 1.7 $\mu\text{g}/\text{cm}^2$, respectively). This may be justified by the water-oil interface of these formulations, which allows slow release of drug. These results showed higher penetration into dermal membranes than those observed in Figure 44(b). However, in our work, the penetration study was evaluated in intact skin with epidermis while Santos and co-workers evaluated in skin without epidermis.

Some studies evaluated *in vitro* skin permeation of AmB formulations in different skin models. Butani and co-workers (2014) evaluated the amount of AmB retained in the rat skin from four AmB microemulsions and AmB solution after 24 hours. It was investigated the drug retained in the skin (epidermis + dermis). They verified that microemulsions had high drug retained in the skin (higher than 80 μg) than drug solution (lower than 40 μg). Perez and co-workers (2016) evaluated the amount of AmB retained in the *stratum corneum* and viable epidermis (epidermis without *stratum corneum*) of two liposomal formulations (Ambisome[®] and AmB-ultradeformable liposome) after 1 hour in excised human skin for topical administration. The AmB-ultradeformable liposome presented higher drug retention in the *stratum corneum* (around 33%) and in the viable epidermis (around 7%) than Ambisome[®], suggesting an improvement in ultradeformable liposome development for increase AmB target delivery to viable epidermis and dermis.

3.4.7. BIOLOGICAL ASSAYS

The free AmB, free clove oil and four AmB nanoemulsions (B, F, H and L) were submitted to cytotoxicity and antileishmanial study.

3.4.7.1. Assessment of cytotoxicity of AmB nanoemulsions in BMDM cells

The cytotoxicity results of free AmB and AmB nanoemulsions are shown in Figure 45.

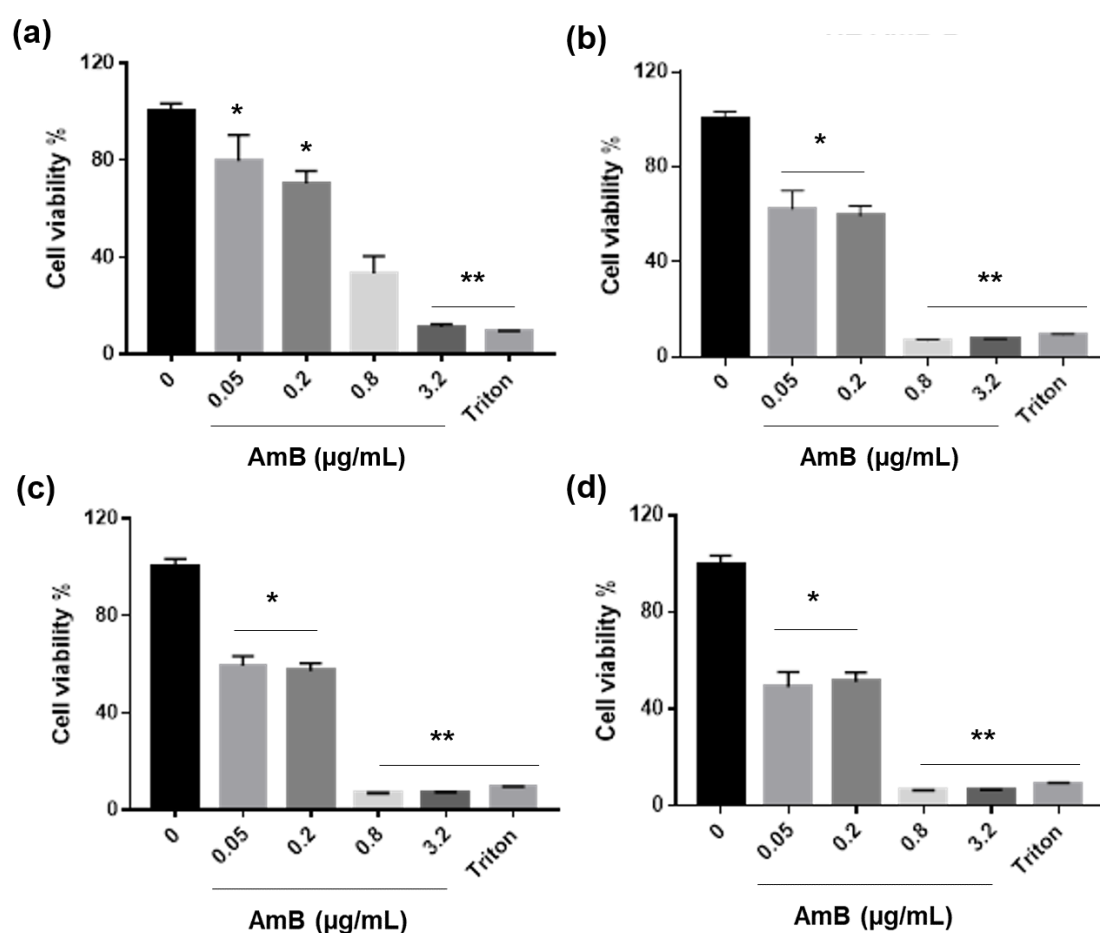


Figure 45. Cytotoxicity of (a) free AmB and (b) B-NE, (c) F-NE and (d) L-NE in BMDM cells. Legend: 0 – Negative Control, medium without treatment. Triton – Positive Control (4% Triton 100x). * - No statistically significant differences ($P > 0.05$); ** - No statistically significant differences ($P > 0.05$) according to One-way ANOVA with Tukey post-test.

Figure 45 shows a dose-dependent relation to cytotoxicity, especially for free AmB. Free AmB showed high toxicity in concentrations higher than 0.2 µg/mL while AmB nanoemulsions and blank nanoemulsion presented toxicity in all concentrations tested.

L-NE showed toxicity similar than B-NE and F-NE, indicating that NE formulations had some ingredients which promote toxicity. H-NE (blank formulation of F-NE) was not evaluated in this experiment because all NE had elevated toxicity. The two higher concentrations (0.8 µg/mL and 3.2 µg/mL) of nanoemulsions presented no statistically differences ($P > 0.05$) to positive control while free AmB presented only the highest concentration (3.2 µg/mL) without statistically differences ($P > 0.05$) to positive control. The two-lower concentration (0.05 µg/mL and 0.2 µg/mL) of free AmB and nanoemulsions presented no statistically differences ($P > 0.05$) between them. However, all concentrations are statistically different ($P < 0.05$) in comparison with Negative Control.

The ingredient in all NE that can be the cause of high toxicity is clove oil. The high cytotoxicity of clove oil has already described in literature. Prashar and co-workers (2006) evaluated the cytotoxicity of clove oil in human fibroblasts and endothelial cells. It was observed that at concentration of 0.03%, clove oil promotes more than 90% of cell death. Furthermore, it was suggested that clove oil cytotoxicity can be attributed to eugenol, which is the major constituent of this oil. Kouidhi and co-workers (2010) investigated clove oil cytotoxicity in different cells type (macrophages RAW 264.7, adenocarcinoma cells – A549 and HT-29, human epidermoid cancer Hep-2, human fibroblast-like fetal lung cell MRC-5). They found higher oil toxicity in cells MRC-5, HT29 and RAW 264.7 (IC_{50} values lower than 30 µg/mL) than Hep-2 and A549 cells (IC_{50} 500 and 112 µg/mL, respectively). The decrease of oil droplet size of nanoemulsions may increase the cytotoxicity of this ingredient, by enlarging the surface area of contact of macrophages cells.

Caldeira and co-workers (2015) developed AmB nanoemulsions and investigated the cytotoxicity in macrophages J774. AmB nanoemulsion and blank nanoemulsion with two concentration of stearylamine (0.1% or 0.2%) were used in these studies. The results were compared with conventional AmB formulation

(AmB deoxycholate). It was found that nanoemulsion with and without AmB presented high cytotoxicity and similar values of CC_{50} . Moreover, nanoemulsions prepared with 0.2% stearylamine showed higher toxicity than nanoemulsions with 0.1%. AmB presence in formulation promoted low influence in cytotoxicity values. However, when the concentration of stearylamine in nanoemulsions was increased, the cytotoxicity was also increased. This was attributed to electrostatic interactions between stearylamine and anionic components of the cell membrane. Despite high toxicity of nanoemulsions, conventional AmB presented higher toxicity, suggesting that nanoemulsions decreased the drug toxicity.

Mendonça and co-workers (2016) produced AmB polymeric micelles formulations using Pluronic[®] F127 and investigated the cytotoxicity of this formulations in murine peritoneal macrophages. It was verified that blank formulation and AmB formulation presented similar values of CC_{50} (around 120 μ M) and lesser toxicity than free AmB. These formulations presented no essential oil as nanoemulsions produced in this work. For this reason, the formulations presented more safety than nanoemulsions. Furthermore, it was possible to identify the most cytotoxicity component in nanoemulsions, which was clove oil.

Silva and co-workers (2013) studied the cytotoxicity of microemulsions (with and without AmB) and free AmB in macrophages J774. They observed a dose-dependent relation for toxicity as well as observed in Figure 45. Moreover, microemulsion with or without drug showed similar results and lesser toxicity than free AmB when AmB concentration was lower than 10 μ g/mL. However, when AmB concentration was 25 μ g/mL, microemulsions presented toxicity similar than free drug.

3.4.7.2. Antileishmanial Activity

The antileishmanial activity of AmB nanoemulsions was investigated against *L. amazonensis* promastigotes as well as free AmB and free clove oil. Figure 46 shows the results of antileishmanial activity of free AmB.

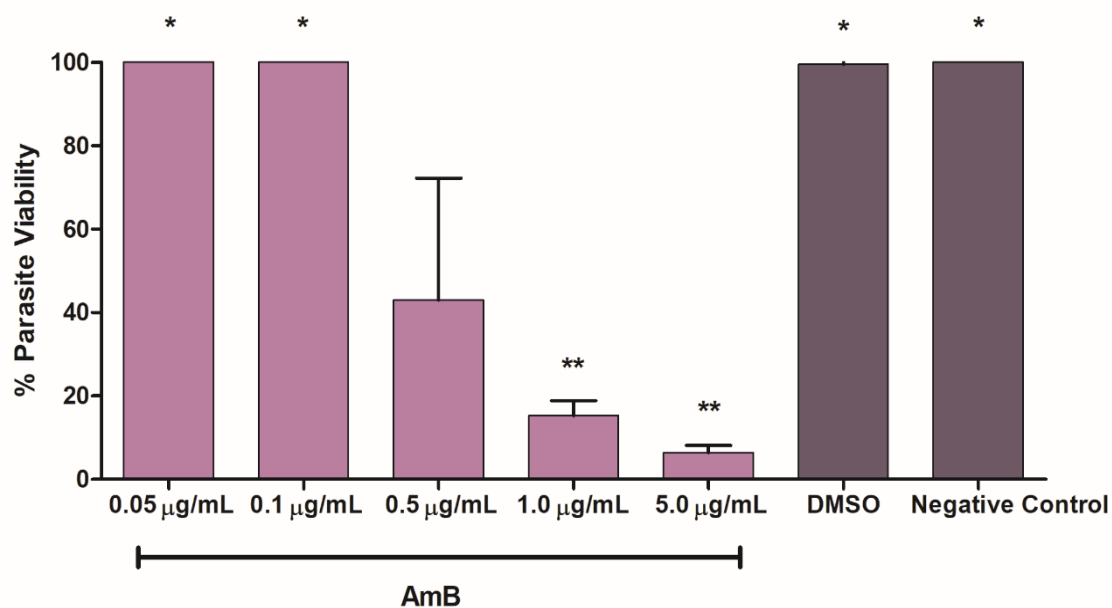


Figure 46. Antileishmanial activity of free AmB against promastigotes of *L. amazonensis*.
 Legend: Control – untreated parasites, only with Schneider's medium supplemented with FBS;
 DMSO – amount of DMSO (5%) higher than used to dissolved AmB. * - No statistically significant differences ($P > 0.05$); ** - No statistically significant differences ($P > 0.05$) according to One-way ANOVA with Tukey post-test. Means \pm SD ($n=3$).

Free AmB showed an antileishmanial activity against promastigotes in concentrations higher than 0.1 $\mu\text{g/mL}$. The lower concentrations of AmB analyzed in this study (0.05 $\mu\text{g/mL}$ and 0.1 $\mu\text{g/mL}$) presented no statistically significant differences ($P > 0.05$) in comparison with DMSO solution (amount higher than used to dissolved AmB) and with control (without treatment).

Based on these results, it was possible to observe no interference of DMSO in parasites viability then the antileishmanial activity was related only to drug effects. Furthermore, the two higher concentrations of AmB (1 $\mu\text{g/mL}$ and 5 $\mu\text{g/mL}$) promoted more the 70% of parasites death and presented no statistically significant differences ($P > 0.05$) between then.

Thereafter free AmB antileishmanial activity, free clove oil was submitted to antileishmanial assay. Figure 47 presents the results of clove oil antileishmanial activity against *L. amazonensis* promastigotes.

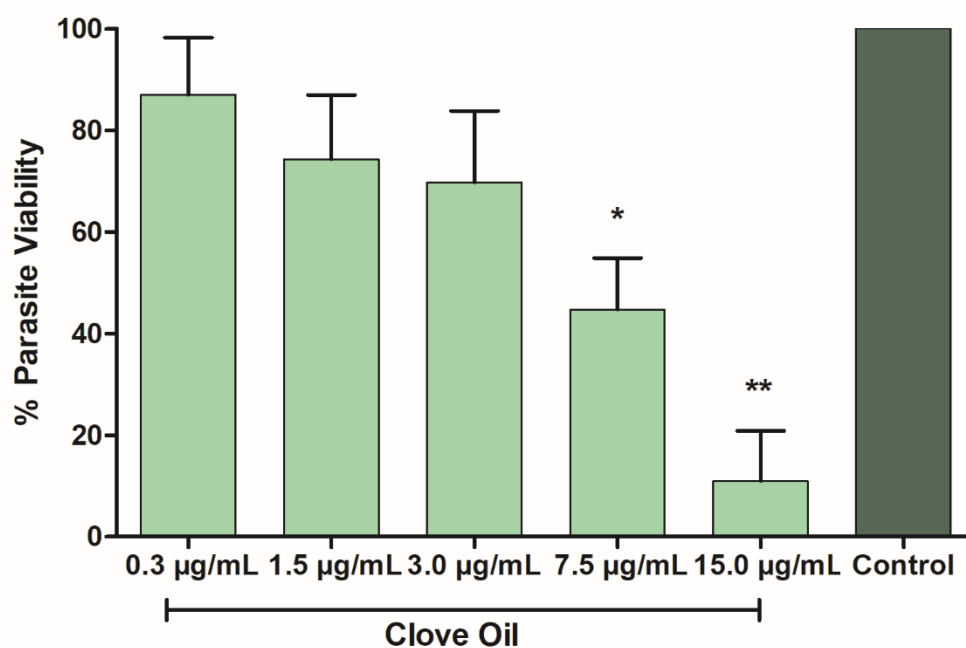


Figure 47. Antileishmanial activity of clove oil against promastigotes of *L. amazonensis*. Legend: Control – untreated parasites, only with Schneider's medium supplemented with FBS. * - Statistically significant difference ($P < 0.05$); ** - Statistically significant difference ($P < 0.05$) according to One-way ANOVA with Tukey post-test. Means \pm SD ($n=3$).

Clove oil showed an antileishmanial activity against promastigotes in concentrations higher than 3 $\mu\text{g/mL}$. The antileishmanial activity of clove oil was previously described in literature, which correlate the effect to eugenol, the major constituent of clove oil (MORAIS *et al.*, 2014). Lower concentrations (0.3 $\mu\text{g/mL}$, 1.5 $\mu\text{g/mL}$ and 3 $\mu\text{g/mL}$) presented no statistically significant differences ($P > 0.05$) in comparison with control. However, the highest concentrations of clove oil (7.5 $\mu\text{g/mL}$ and 15 $\mu\text{g/mL}$) were statistically significant differences ($P < 0.05$) compared with other concentrations, control and between them. The highest concentration of clove oil analyzed was lower than oil concentration in nanoemulsions (around 78 $\mu\text{g/mL}$). Nonetheless, it was observed a high amount of oil in wells that contained 15 $\mu\text{g/mL}$. For this reason, it was not investigated higher concentrations than 15 $\mu\text{g/mL}$ and not analyzed the real oil concentration present in nanoemulsions.

The antileishmanial activity of all nanoemulsions (B, F, H and L) is illustrated in Figure 48. The positive control (C1) used in these experiments was free AmB in concentration (1 $\mu\text{g}/\text{mL}$) that promotes higher than 50% of parasites death based on assay showed in Figure 45.

According to Figure 48(a), it was possible to observe that antileishmanial activity of negative control (C2) was statistically significant different ($P < 0.05$) than positive control (C1) and nanoemulsions in all concentrations.

B-NE presented high leishmanicidal effect in all four concentrations analyzed with higher than 70% of parasite death. The four concentrations of B-NE showed no statistically significant differences ($P > 0.05$) among them, positive control and L-NE in two higher concentrations (1 $\mu\text{g}/\text{mL}$ and 5 $\mu\text{g}/\text{mL}$). These results showed a greater leishmanicidal effect on B-NE than free AmB, which can be explained by the presence of clove oil, besides the low droplet size of nanoemulsions. Moreover, lower concentrations of L-NE (0.1 $\mu\text{g}/\text{mL}$ and 0.5 $\mu\text{g}/\text{mL}$) had no statistically significant differences ($P > 0.05$) between them.

In relation to Figure 48(b), Negative control was statistically significant different ($P < 0.05$) than nanoemulsions and positive control as observed in Figure 48(a). The lowest concentration of F-NE (0.1 $\mu\text{g}/\text{mL}$) and two concentrations of H-NE (0.1 $\mu\text{g}/\text{mL}$ and 0.5 $\mu\text{g}/\text{mL}$) presented no statistically significant differences ($P > 0.05$) among them. Furthermore, three concentrations of F-NE (0.5 $\mu\text{g}/\text{mL}$, 1 $\mu\text{g}/\text{mL}$ and 5 $\mu\text{g}/\text{mL}$), the highest concentration of H-NE (5 $\mu\text{g}/\text{mL}$) and positive control presented no statistically significant differences ($P > 0.05$) among them.

F-NE and H-NE as B-NE and L-NE showed antileishmanial activity. However, F-NE showed smaller leishmanicidal effect in comparison with B-NE as well as H-NE showed smaller leishmanicidal effect in comparison with L-NE. This can be due to the Tween[®] 20 presence in B-NE and L-NE, which can be cytotoxicity. Although L-NE and H-NE were prepared without drug, these nanoemulsions presented leishmanicidal effect similar as observed for free AmB, confirming the antileishmanial activity of clove oil.

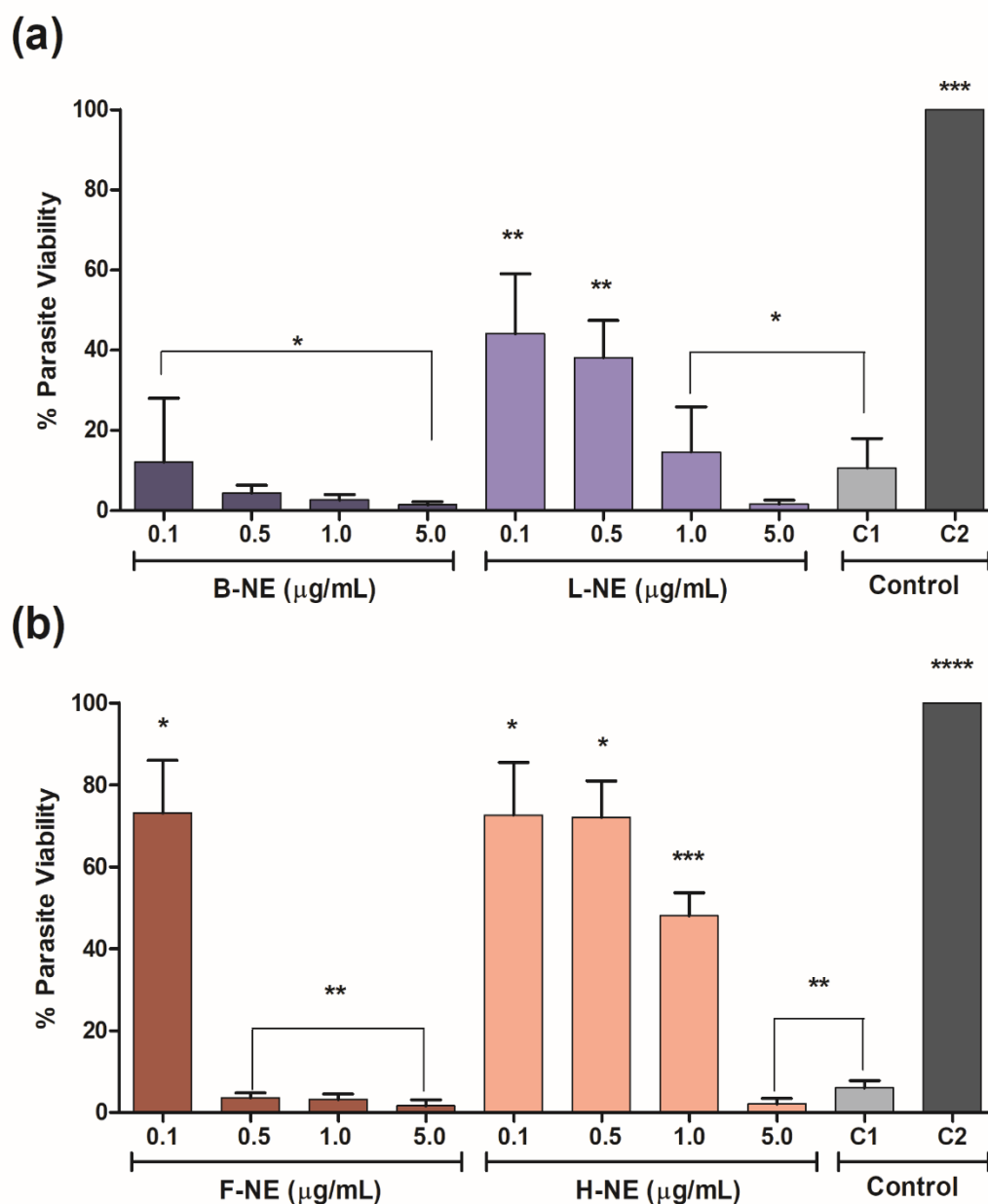


Figure 48. Antileishmanial activity of AmB nanoemulsions (a) B-NE and L-NE, (b) F-NE and H-NE against promastigotes of *L. amazonensis*. Legend: B-NE – NE with AmB and Tween[®] 20; L-NE – NE without AmB with Tween[®] 20; F-NE – NE with AmB; H-NE – NE without AmB; C1- Positive Control – AmB solution (1 µg/mL); C2- Negative Control - untreated parasites, only with Schneider's medium supplemented with FBS. * - No statistically significant differences ($P > 0.05$); ** - No statistically significant differences ($P > 0.05$); *** - Statistically significant difference ($P < 0.05$); **** - Statistically significant difference ($P < 0.05$) according to One-way ANOVA with Tukey post-test. Means \pm SD (n=3).

Based on cytotoxicity assay and anti-promastigotes activity, it was calculated the CC₅₀, IC₅₀ and the selective index of free AmB, free clove oil and of the four nanoemulsions. The values of CC₅₀, IC₅₀ and selective index are shown in Table 6.

Table 6. CC₅₀, IC₅₀ values and Selective Index of free AmB, free clove oil and nanoemulsions.

Formulation	CC ₅₀ [*]	IC ₅₀ ^{**}	Selective Index (SI) ^{***}
AmB	0.50 µg/mL	0.48 µg/mL	1.04
Clove oil	18.80 µg/mL [#]	5.26 µg/mL	3.57
B-NE	0.19 µg/mL	0.03 µg/mL	6.33
L-NE	0.11 µg/mL	0.14 µg/mL	0.79
F-NE	0.17 µg/mL	0.14 µg/mL	1.21
H-NE	-	0.84 µg/mL	-

Legend: * - concentration in µg/mL cytotoxicity for 50% of BMDM; ****** - concentration in µg/mL which reduce 50% of viability of *L. amazonensis* promastigotes; ******* - Selective Index: CC₅₀/IC₅₀; **#** - literature data obtained from macrophages RAW 264.7 (KOUIDHI, ZMANTAR, BAKHROUF, 2010).

Table 6 shows lower CC₅₀ values for B-NE, F-NE and L-NE than free AmB. The nanoemulsions had lower CC₅₀ than CC₅₀ described in literature for clove oil. This suggests that nanoemulsions had higher toxicity due to their small oil droplets size, which increases the interaction between formulation and cells membrane.

In relation to IC₅₀ values, free AmB showed value higher than observed for NE containing drug (B-NE = 0.03 µg/mL and F-NE = 0.14 µg/mL) and lower than values for blank NE (H-NE = 0.84 µg/mL). However, L-NE showed higher activity than free drug, which may be explained by the presence of Tween[®]20 in formulation. Moreover, clove oil showed IC₅₀ around 5.26 µg/mL suggesting that

free oil had a good leishmanicidal effect, which was already described in the literature. It was possible to notice an increase of antileishmanial activity of AmB nanoemulsion in comparison with free drug. This can be explained by the small size of oil droplets, which facilitates the uptake from parasites as well as observed in the cytotoxicity study. Furthermore, the presence of clove oil and AmB combined in nanoemulsions increased the leishmanicidal activity. Although blank NE presented IC_{50} higher than AmB nanoemulsions, these values showed interesting antileishmanial activity. Nevertheless, the problem of clove oil nanoemulsions is its high cytotoxicity.

In order to investigate the selectivity of these formulations, the selective index (SI) was calculated. Free AmB and F-NE showed values of 1.03 and 1.25 respectively, indicating low selectivity with cytotoxicity dose close to the effective dose to promote parasite death.

L-NE presented $SI=0.79$, which suggests that effective dose against *L. amazonensis* promastigotes is higher than the cytotoxicity dose. SI for free clove oil and B-NE are respectively 3.58 and 6.33, which means that effective dose against promastigotes is lower than cytotoxicity dose.

As already discussed, formulations B-NE and F-NE had retained in dermis 0.25 $\mu\text{g/mL}$ and 0.56 $\mu\text{g/mL}$, respectively, which are higher than their IC_{50} (0.03 $\mu\text{g/mL}$ and 0.13 $\mu\text{g/mL}$, respectively). It should be noted that dermis retention was evaluated after 8 hours of experiment, that could represent an extended period of exposition for topical application. For this reason and considering the slow drug release from these formulations, more studies are required to investigate their cytotoxicity nature.

Comparing with SI of AmB nanoemulsions from other studies: Caldeira and co-workers (2015) developed AmB nanoemulsions with and without stearylamine and investigated CC_{50} in macrophages J774, IC_{50} (in *L. amazonensis* amastigotes) and SI of nanoemulsions and compared with conventional AmB (AmB deoxycholate). The CC_{50} of nanoemulsions with and without stearylamine (6.3 $\mu\text{g/mL}$ and $> 200 \mu\text{g/mL}$, respectively) were higher than CC_{50} of conventional AmB (1 $\mu\text{g/mL}$), showing that stearylamine increased the cytotoxicity of nanoemulsion. IC_{50} of the two nanoemulsions were 0.11 $\mu\text{g/mL}$ and

0.21 µg/mL, close to IC₅₀ of conventional AmB (0.06 µg/mL). The SI index were: 57 (AmB nanoemulsion with stearylamine), 952 (AmB nanoemulsion without stearylamine) and 16 (conventional AmB). All SI index were higher than 10 for all formulations, showing that nanoemulsions with or without stearylamine were selective for Leishmania and more safe than conventional AmB.

Mendonça and co-workers (2016) analyzed *in vitro* antileishmanial activity of free AmB and AmB in polymeric micelles system against *L. amazonensis* promastigotes and amastigotes. Moreover, the cytotoxicity of these formulations was investigated in peritoneal macrophages. The CC₅₀ values were 9.5 µM, 119.5 µM and 134.7 µM for free AmB, AmB-polymeric micelles and blank-formulation, respectively. These results showed that blank and AmB formulation had lower toxicity than the free drug. The values of IC₅₀ detected for free AmB was 1.2 µM, for AmB micelles was 1.8 µM and blank micelles was 22.1 µM against promastigotes. The presence of AmB increases the antileishmanial effect of polymeric micelles. The SI index corresponded to 61.5 for AmB polymeric micelles, in comparison with blank formulation (SI = 5.4) and free drug (SI = 7.9). From these results, the AmB polymeric micelles were considered a safe formulation and with low toxicity than the free drug.

Our results (see Table 6) and the previous studies reported here (MENDONÇA *et al.*, 2016, CALDEIRA *et al.*, 2015) agreed on the toxicity and high antileishmanial activity of free AmB. However, the two mentioned studies obtained nanoemulsions with lower toxicity than the free drug and safe (SI higher than 10), while our AmB nanoemulsions are more cytotoxic than free AmB and need more studies and perhaps optimization (in particular B-NE), to be considered safe (at present, their SI are lower than 10).

There are some studies described in literature, which developed nanoemulsions using clove oil as oil phase. Siqueira and co-workers (2017) investigated *in vitro* antileishmanial activity of free AmB and different nanoemulsions against *L. amazonensis*. The cytotoxicity of free drug and formulations were evaluated in macrophages RAW 264.7. The blank nanoemulsion contained 5% of clove oil and Pluronic® F127. Blank nanoemulsion and free AmB presented IC₅₀ of 4000 µg/mL and 0.55 µg/mL, respectively.

Furthermore, CC_{50} of free AmB was 0.99 $\mu\text{g/mL}$, while blank nanoemulsion showed no activity in macrophages. These results indicated lower toxicity and lower antileishmanial activity of blank nanoemulsion in comparison with free drug. The results obtained for blank nanoemulsion were different than those obtained in our work (see Table 6). The differences in cytotoxicity assay can be explained by the different macrophage cells used and the method to quantify toxicity.

Cardoso and co-workers (2018) produced different sulphonamide nanoemulsions with clove oil and Pluronic[®] F127 using the same method described in this work. It was evaluated the antileishmanial activity against *L. amazonensis* promastigotes and *L. infantum* promastigotes as the cytotoxicity in macrophages RAW 264.7 of sulphonamide nanoemulsions and compared with free AmB. Six nanoemulsions presented CC_{50} between 2.24 and 18.26 $\mu\text{g/mL}$ and IC_{50} between 3.21 and 8.13 $\mu\text{g/mL}$. Free AmB showed CC_{50} of 1.07 $\mu\text{g/mL}$ and IC_{50} of 0.61 $\mu\text{g/mL}$. The SI values of free AmB and sulphonamide nanoemulsions were lower than 2.5, then nanoemulsions presented cytotoxicity similar to free AmB. The *in vitro* response for blank nanoemulsion (that could be compared to the cytotoxicity of clove oil given in Table 6) was not investigated.

Furthermore, the cytotoxicity and antileishmanial activity of clove oil were studied in previous works. Kouidhi and co-workers (2010) investigated the cytotoxicity of clove oil in different cells. The CC_{50} of clove oil in macrophages RAW 264.7 was 18.8 $\mu\text{g/mL}$. Morais and co-workers (2014) investigated the cytotoxicity and antileishmanial activity against *L. chagasi* of thymol, eugenol and its derivatives. The two eugenol derivatives presented higher IC_{50} values (23.21 $\mu\text{g/mL}$ and 10.58 $\mu\text{g/mL}$) than eugenol (56.13 $\mu\text{g/mL}$). Moreover, eugenol derivatives had lower toxicity in macrophages RAW 264.7 (around 100% of cell viability using 100 $\mu\text{g/mL}$), while eugenol presented only 29% of cell viability in the same concentration.

3.5. CONCLUSION

In this chapter, AmB nanoemulsion using clove oil and Pluronic® F127 were proposed for topical cutaneous leishmaniasis treatment. The development of AmB nanoemulsions was already described in the literature, but the formulation (essential oil, polymer and AmB) proposed in this work was not held before.

The choice of clove oil as oil phase is based on its several pharmacology activities already described including antileishmanial activity. Moreover, the use of Pluronic® F127 is related to the thermoreversible property of this compound and its gelling ability in high concentrations favoring a simple formulation for topical administration.

After a first characterization study of the raw AmB (SEM images, FTIR analysis), the development of the AmB nanoemulsions started with their preparation, during which several parameters were varied: - the presence of surfactant (Tween® 20); - the amount of polymer used in aqueous phase (10% w/w or 15% w/w); - the essential oil (mint oil or clove oil). The nanoemulsions were characterized in terms of physicochemical properties, release behavior, skin permeation and biological assays.

It could be demonstrated that the type of essential oil influenced the nanoemulsion stability, with nanoemulsions produced with clove oil being more stable than those produced with mint oil. Furthermore, the pH for all formulations was in the ideal range for topical application. Based on some preliminary results, two nanoemulsions containing AmB (B-NE – with Tween® 20 as surfactant and F-NE- without surfactant) and respectively blank-formulation (L-NE - with Tween® 20 as surfactant and H-NE- without surfactant) were chosen for further studies.

The nanoemulsions submitted to a stability study presented droplets size lower than 60 nm and polydispersity index lower than 0.400 until 365 days of storage. The drug content in formulations stored at room temperature was reduced over storage time, probably related to the AmB degradation. Then, these formulations need to be stored under refrigeration (approximately 4°C).

In vitro release tests showed a very slow release profile (lower than 1% released in 48 hours). Furthermore, in skin permeation study, the nanoemulsions showed low values of drug permeated after 8 hours, which confirms the slow release profile. The slow drug permeation could be an indicative that nanoemulsions could promote a local treatment without a systemic effect.

The cytotoxicity of nanoemulsions were investigated in bone marrow-derived macrophages cells and compared with antileishmanial activity against *Leishmania amazonensis* promastigotes. The results revealed a higher cytotoxicity but a higher antileishmanial activity of nanoemulsions in comparison to the free drug. The increased antileishmanial activity of AmB nanoemulsions related to free drug was attributed to the small oil droplets of nanoemulsions that could increase the contact of the drug with the macrophage cells.

The selective index was calculated, and the values were lower than 10, which correlated free drug, clove oil and nanoemulsions with or without AmB as cytotoxicity products with low selectivity for leishmanicidal effect.

CHAPTER 4

**POLYMERIC
MICROPARTICLES OF
PAROMOMYCIN**

4.1. INTRODUCTION

4.1.1. Biodegradable Polymeric Depots

Over the past few years, drug delivery systems development received considerable attention, specially depot formulations. Depot formulations offer some advantages, such as localized delivery, ease of application, drug-controlled release, reduce dosing frequency, enhance patient compliance. Moreover, these formulations reduce side effects and toxicity in comparison with conventional and oral therapies (ABADI, MOIN, VEERABHADRAPPA, 2016; KEMPE & MÄDER, 2012; PILANIYA, KHATRI, PATIL, 2011; BARI, 2010).

One of the most drug carrier study for depot formulation is biodegradable polymeric particles, which have been used for biomedical applications. These particles require polymers, which present several properties as biodegradability, *in vivo* toxicological safety with ease elimination of degradation products by the metabolic pathways (SWIDER *et al.*, 2018).

Poly (lactic acid) (PLA), poly(glycolic acid) (PGA), and their copolymer poly(lactic-co-glycolic acid) (PLGA) are appropriate polymers to prepare depot deliveries due to their favorable biocompatibility and biodegradability (SWIPER *et al.*, 2018; FREDENBERG *et al.*, 2011). They are the most commonly polymers investigated for controlled or sustained release and some have been approved by Food Drug Administration (FDA) (WANG & YANG, 2016; KAPOOR *et al.*, 2015; ANSARY, AWANG, RAHMAN, 2014; WANG *et al.*, 2013; RE, 2006) and by European Medicines Agency (EMA) for pharmaceutical products development and can be administered orally or parenterally and as implant without surgery (HAN *et al.*, 2016; WANG & YANG, 2016). Since the 1970s, PLGA is used as a biomaterial, when it was developed as biodegradable sutures and artificial prostheses, followed by advances use in devices production as implants and therapeutic devices (SWIDER *et al.*, 2018; KAPPOR *et al.*, 2015).

4.1.2. Physicochemical Properties of PLGA

PLGA is a synthetic linear copolymer composed of lactic and glycolic acid monomers, which can be organized as a block-copolymer or statistical copolymer. This copolymer can be synthesized by several methods, which the most used methods are ring opening polymerization and polycondensation reactions. The conditions of reactions and process parameters strongly affect the physicochemical properties of final product (PLGA) (MIR, AHMED, REHMAN, 2017; SHARMA *et al.*, 2016; KAPOOR *et al.*, 2015; LÜ *et al.*, 2009). Figure 49 shows its molecular structure, besides those of PGA and PLA.

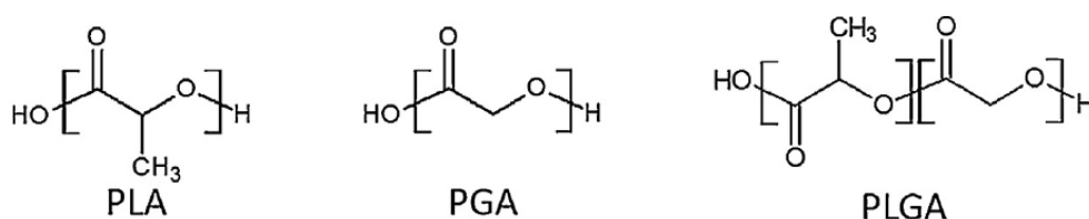


Figure 49. Chemical structures of biodegradable polymers (PLA, PGA and PLGA) (LARRAÑETA *et al.*, 2016).

PLGA is available on the market with different molecular weight, different ratios of lactic acid to glycolic acid, different end-group functionalization, PLA stereochemistry variation and PEGylation (WAN & YANG, 2016; DANHIER *et al.*, 2012). The physicochemical properties of PLGA may be varied systematically by changing the ratio of lactic acid to glycolic acid, including polymer degradation rate, crystallinity, and hydrophilicity (DING & ZHU, 2018; KAPOOR *et al.*, 2015; FREDENBERG *et al.*, 2011). This in turn alters the release rate of microencapsulated therapeutic molecules from PLGA microparticle formulations (BUSATTO *et al.*, 2018; ANSARY, AWANG, RAHMAN, 2014).

Table 7 shows some physical properties of some PLGAs. It can be seen that the biodegradation rate of PLGA depends on several factors, among them, the composition of the polymer. The degradation of PLGA is faster for polymers with the increased amount of glycolic acid units. Polymers with a 50:50 ratio of lactic and glycolic acids have the fastest degradation rate. PLGA with the 50:50 ratio has the degradation rate of around two months *in vivo* and has the fastest

release rate when compared to other ratios (DING & ZHU, 2018; KAPOOR *et al.*, 2015).

Table 7. Physical properties of some PLGAs (adapted from KAPOOR *et al.*, 2015; ANSARY *et al.*, 2014).

Polymer (lactide/glycolide ratio)	Molecular Weight range	Glass Transition (<i>T_g</i>) temperature (°C)	Physical state	Degradation time (months)
PLGA (50:50)	7,000-54,000	42-50	Amorphous	1-2
PLGA (65:35)	24,000-38,000	45-50	Amorphous	3-4
PLGA (75:25)	4,000-116,000	42-50	Amorphous	4-5
PLGA (85:15)	190,000- 240,000	50-55	Amorphous	5-6

Generally, a range of common organic solvents can dissolve PLGA, depending on its composition. Chlorinated solvents, like dichloromethane or chloroform, and water-miscible solvents, like acetone or tetrahydrofuran, can dissolve PLGA with a higher amount of lactic acid. However, PLGA with a higher amount of glycolic acid is dissolved by fluorinated solvents, like hexafluoroisopropanol (SWIDER *et al.*, 2018; MAKADIA & SIEGEL, 2011). It is also possible to use organic solvent combinations in order to regulate the polymer solubility (SOSNIK & SEREMETA, 2015).

In addition, the glass transition temperature of PLGA can also be explored. Usually, PLGA has glass transition above body temperature, between 42 and 55°C. The glass transition temperature increases with an increase of PLA content and an increase of molecular weight (see Table 7).

4.1.3. Preparation Methods of PLGA Microparticles

According to the internal structure, PLGA microparticles are classified into two types: microcapsules (one drug core or various drug core in a polymer layer) and microspheres (drug dispersed in a polymeric matrix) (Figure 50) (BRAVO-OSUNA *et al.*, 2016; HERRERO-VANRELL *et al.*, 2013, SINGH *et al.*, 2010).

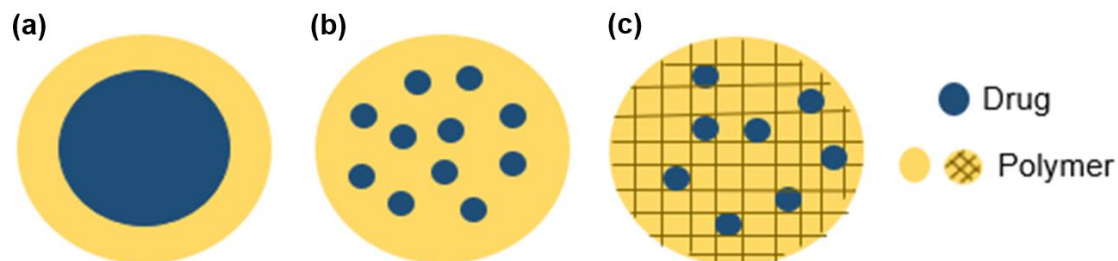


Figure 50. Types of microparticles (a) microcapsules with one core, (b) microcapsules with various core and (b) microspheres.

PLGA microspheres are the most commonly particles type produced due to their ease development. Unfortunately, the structure of microspheres is, mainly, adequate for hydrophobic drugs encapsulation. This particle type presents some difficulties for peptides, proteins and water-soluble drugs encapsulation, such as our drug of interest, paromomycin, due to low encapsulation (ABULATEEFEH & ALKILANY, 2015). Prior and co-workers (2000) developed gentamicin (water-soluble drug) PLGA microspheres by two different techniques, solvent evaporation and spray drying, and obtained low encapsulation efficiency and drug content.

In fact, production of aqueous core-PLGA shell microcapsules is an evident challenge and few studies have addressed this point in the literature. Han and co-workers (2016) reported some strategies to improve water-soluble drugs in PLGA microparticles as drug conversion into hydrophobic form (complexation with ionic surfactant), solid dispersion in polymer solution or use of double-emulsion method. Abulateefeh and Alkilany (2015) synthesized and characterized core-PLGA shell microcapsules containing risedronate (water-soluble drug) prepared with internal phase separation and obtained higher encapsulation efficiency in comparison with conventional PLGA microspheres.

Gasparini and co-workers (2010) investigated the encapsulation of model water-soluble drug, blue-dextran, using double-emulsion method and PLGA as polymer. It was observed that encapsulation efficiency can be increased varying production parameters as polymer concentration. Lin and co-workers (2005) evaluated the doxorubicin, water-soluble drug, PLGA/PLLA microparticles prepared by spray-dried varying organic solvent and polymer composition and obtained encapsulation efficiency lower than 30%.

There are several methods of particle preparation from PLGA copolymers and can be divided in chemical methods (emulsion solvent extraction/evaporation, polymerization), physical methods (pan coating, extrusion, fluid-bed, spray drying) and physicochemical methods (coacervation, gelation, supercritical fluid) (DESHMUKH, WAGH, NAIK, 2016; HERRERO-VANRELL *et al.*, 2013; TOMARO-DUCHESNEAU *et al.*, 2013; JYOTHI *et al.*, 2010; SINGH *et al.*, 2010; RE, 1998). One the most conventional methods refers to single and double emulsion–solvent evaporation methods (RAMAZANI *et al.*, 2016; SHARMA *et al.*, 2016). Single and double emulsification methods are based on the preparation of an oil-in-water (O/W) or water-in-oil-in-water (W/O/W) emulsion, respectively, as schematically illustrated in Figure 51. These techniques are suitable to encapsulate different types of lipophilic and hydrophilic drugs (SWIDER *et al.*, 2018).

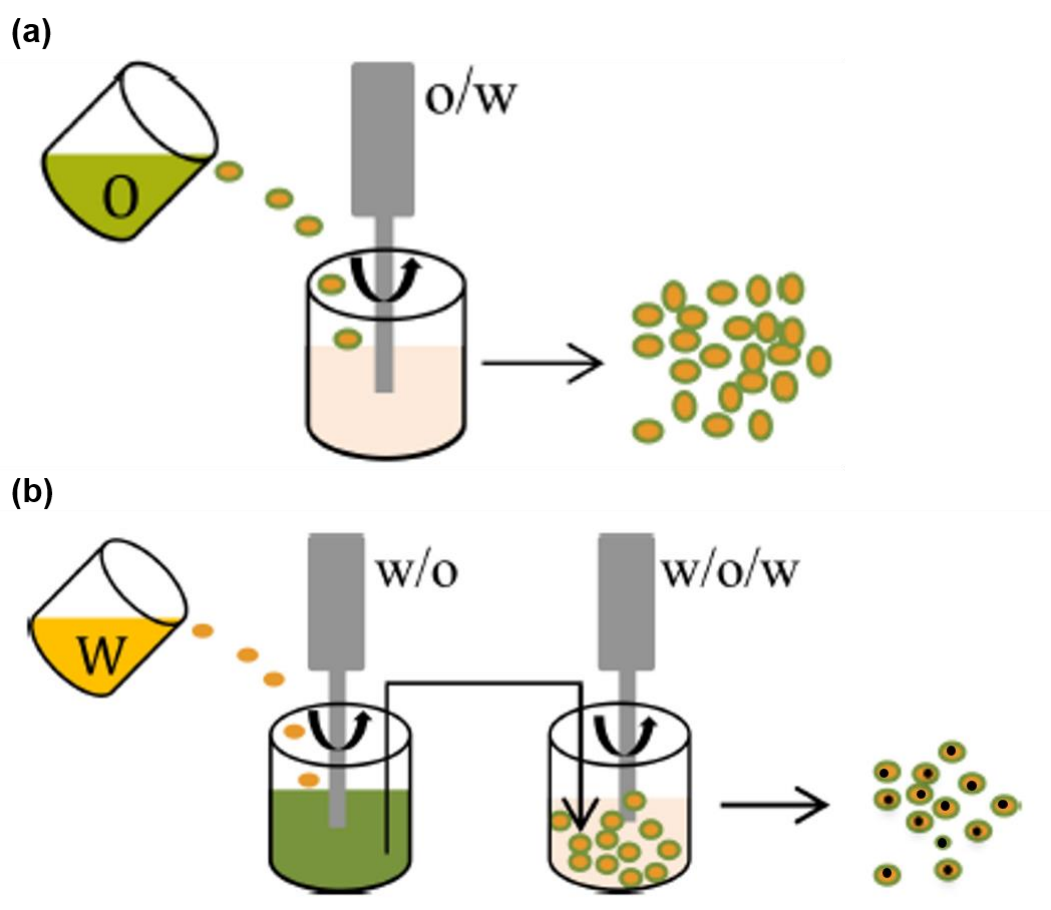


Figure 51. Emulsification methods based on the preparation of (a) an oil-in-water (O/W) or (b) water-in-oil-in-water (W/O/W) emulsion (HAN *et al.*, 2016).

Single-emulsion method consists of an organic phase containing PLGA and the lipophilic agent (e.g. drug) in a volatile organic solvent, and an aqueous phase with a surfactant, usually poly vinyl alcohol (PVA). The organic phase is added, under homogenization or sonication, to the aqueous phase with surfactant. Then, organic solvent is removed by evaporation and particles are collected after washing (to remove the surfactant), separation generally by centrifugation and, finally, freeze-drying as last step (DING & ZHU, 2018; SWIDER *et al.*, 2018; RAMAZANI *et al.*, 2016; SHARMA *et al.*, 2016; WISCHKE & SCHWENDEMAN, 2008). Double-emulsion method, commonly $W_1/O/W_2$, consists in a water-soluble drug dissolved in a first water phase (W_1), which is dispersed in an oil phase O (polymer dissolved in an organic solvent), then dispersed in a second water phase (W_2). The W_1 phase is added under stirring

into the organic phase, forming the first W_1/O emulsion. Then, W_1/O emulsion is emulsified in the W_2 phase, followed by extraction/evaporation of the organic solvent and collection of polymeric hardened particles (DING & ZHU, 2018; SWIDER *et al.*, 2018; SHARMA *et al.*, 2016).

To prepare particles with controlled properties, such as size or degradation rate, it is important to choose not only the right materials but also the right synthesis parameters. For example, the polymer concentration and the stirring speed, time of stirring and temperature (sonication, homogenization) can affect particles size (SWIDER *et al.*, 2018; RAMAZANI *et al.*, 2016; SHARMA *et al.*, 2016).

The single and double emulsion technique can be scaled up by adjusting process parameters, such as the amount of polymer, type of solvents, type of surfactant, speed and temperature of sonication or homogenization (SHARMA *et al.*, 2016). Single-emulsion method is applicable for hydrophobic drugs encapsulation, while double-emulsion method is used to the encapsulation of more hydrophilic drugs (SWIDER *et al.*, 2018; RAMAZANI *et al.*, 2016; MAKADIA & SIEGEL, 2011; LÜ *et al.*, 2009; WISCHKE & SCHWENDEMAN, 2008).

Spray drying is a rapid, well-established, reproducible, scalable and one-step process, which can be used in a closed system (organic solvents using inert gas) or an open system (aqueous mode using compressed air) (PATEL *et al.*, 2015; SOSNIK & SEREMETA, 2015; WAN *et al.*, 2014a). Moreover, spray-drying can be used to encapsulate both hydrophilic and lipophilic drugs, peptides and proteins into a biodegradable polymer like PLGA (DAS *et al.*, 2011).

Drug-loaded particles are prepared by spraying a solid-in-oil (S/O) dispersion or W/O emulsion in a hot stream gas (DING & ZHU, 2018; SWIDER *et al.*, 2018; WANG & YANG, 2016; PATEL *et al.*, 2015; SOSNIK & SEREMETA, 2015; KAŠPAR, JAKUBEC, ŠTĚPÁNEK, 2013a; RE, 2006) as shown in Figure 52. This method may induce particles agglomeration (JAMEKHORSHID, SADRAMELI, FARID, 2014). Furthermore, encapsulation by spray drying depends on solubility and diffusion coefficient of materials (KONDO, NIWA, DANJO, 2014).

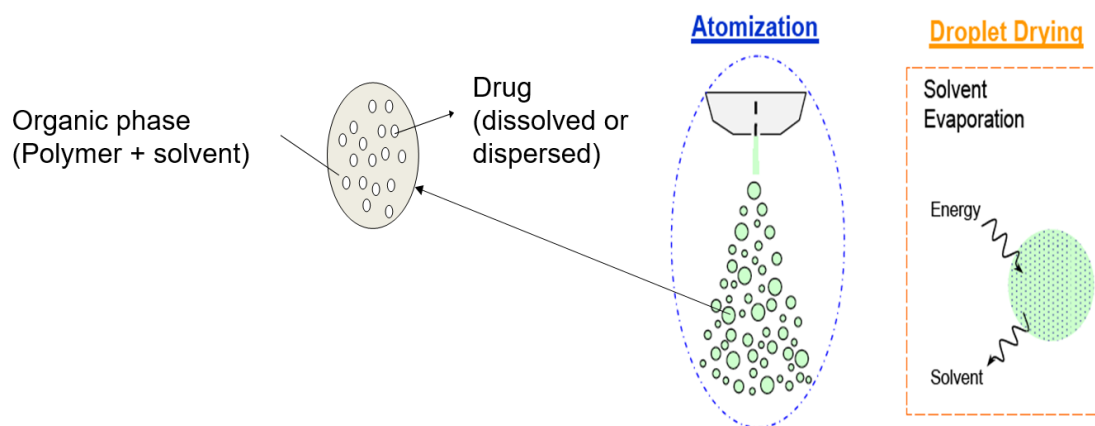


Figure 52. Droplet formation and drying during spray drying process.

Figure 53 shows a scheme of a typical spray-drying process and the different steps: liquid feed into the atomizing nozzle, droplets formation (atomization), gas-droplets contact in the drying chamber and solvent evaporation, gas-dried particles separation in a cyclone.

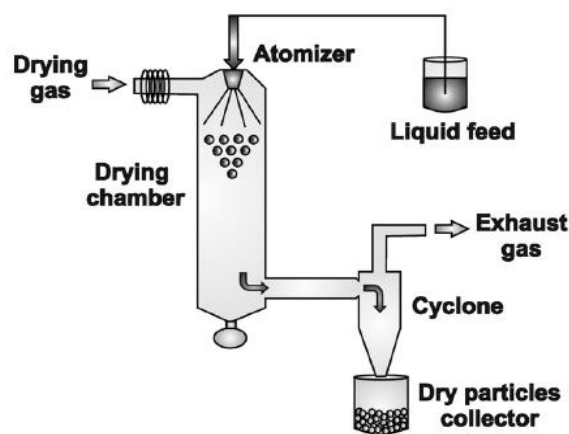


Figure 53. Typical spray drying process (SOSNIK & SEREMETA, 2015).

The characteristics of spray-dried microparticles can be influenced by different parameters related to the process, the formulation and the equipment design (SINGH & VAN DEN MOOTER, 2016; PATEL *et al.*, 2015; SOSNIK & SEREMETA, 2015). The choice of the solvent is influenced by the type of drug (hydrophilic or hydrophobic) to be encapsulated (DING & ZHU, 2018). Table 8 presents the different adjustable variables in a spray drying process.

Table 8. Adjustable variables in a spray drying process (adapted from PATEL *et al.*, 2015; SOSNIK & SEREMETA, 2015; adapted from PAUDEL *et al.*, 2013).

Process Parameters	Formulation Parameters	Equipment Parameters
Inlet gas temperature	Concentration	Type of equipment
Liquid feed flow rate	Viscosity	Type of nozzle
Drying gas flow rate	Type of solvent	Nozzle orifice diameter size
Drying rate	Density	
Pressure	Surface tension	
% Aspiration		

There are some types of nozzles, which can be used for spray drying, such as rotary atomizer, pressure nozzle, ultrasonic nozzle and pneumatic nozzle (PATEL *et al.*, 2015; SUNDERLAND, KELLY, RAMTOOLA, 2015; KAŠPAR, JAKUBEC, ŠTĚPÁNEK, 2013a; PAUDEL *et al.*, 2013; CAL & SOLLOHUB, 2010).

4.1.4. Challenges in improving drug loading of PLGA microparticles with acceptable control over release rate profiles

The encapsulation of hydrophilic drugs in PLGA microparticles has some challenges as low encapsulation, high initial burst drug release (HAN *et al.*, 2016). Most studies came mainly in an attempt to overcome drawbacks related to the conventional $W_1/O/W_2$ double-emulsion method in conventional emulsification-evaporation methods (ABULATEEFEH & ALKILANY, 2016).

When using a spray drying process, different nozzles can be employed for droplets formation. In two-fluid nozzles, only one liquid feed (containing drug and polymer) is atomized through the nozzle orifice. The name ‘two-fluid’ is due to the use of a second fluid (gas) in the nozzle flowing through a second passage and

that encounters the liquid feed transferring the energy for its disintegration in liquid droplets. Generally, this configuration produces microspheres (drug dispersed in a polymer matrix) as shown in Figure 54a (SUNDERLAND, KELLY, RAMTOOLA, 2015; KONDO, NIWA, DANJO, 2014).

In three-fluid nozzles, two liquid feeds are pumped separately through two liquid passages and the hot gas is flowing through a third passage (Figure 54b). This configuration allows immiscible liquids encapsulation because the two liquids come into contact only at the nozzle tip. Therefore, three-fluid nozzles can produce microcapsules (core-shell system) (SUNDERLAND, KELLY, RAMTOOLA, 2015; KONDO, NIWA, DANJO, 2014).

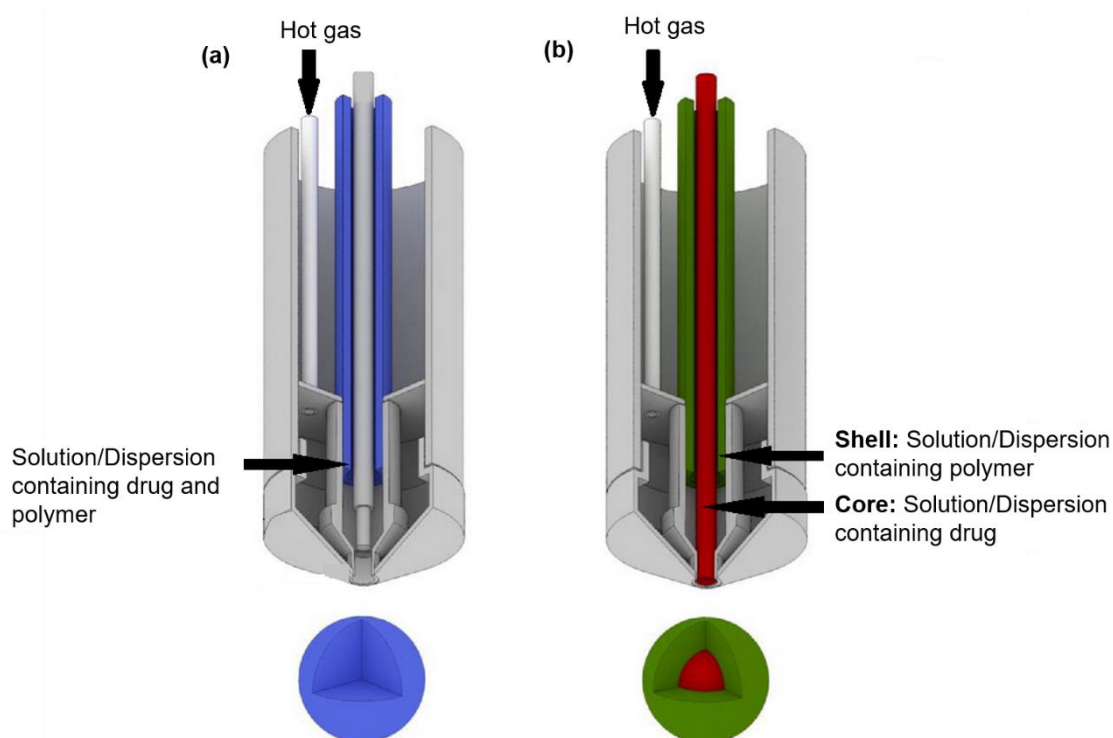


Figure 54. Types of spray drying nozzles (a) two-fluid and (b) three-fluid (adapted from KAŠPAR *et al.*, 2013b).

Some examples of studies focusing on core-shell microparticles produced by spray drying equipped with three-fluid nozzles are giving here: Son and McConville (2012) developed rifampicin PLGA microparticles using three-fluid nozzle to produce a sustained release and reduce the burst release effect. Kašpar and co-workers (2013a) produced spray-dried tripolyphosphate chitosan

microparticles by two-fluid and three-fluid nozzles. Wan and co-workers (2014a) prepared lysozyme and trehalose PLGA microparticles using a three-fluid nozzle and investigated the mechanism of particle formation process. They obtained irregular microparticles aggregates and observed that the feeding rate ratio (outer feed: inner feed) is important to encapsulate proteins in PLGA microparticles. The same group (WAN *et al.*, 2014b) investigated the release profiles of spray-dried bovine serum albumin PLGA microparticles obtained with three-fluid nozzle. The microcapsule structure contributed to protection and modulation of the protein release profile.

4.1.5. Release from PLGA microparticles

In aqueous medium, PLGA copolymer suffers degradation/biodegradation by hydrolysis through breakage of polymer backbone ester linkages into oligomers, which increase polymer hydrophilicity, and then are cleavage into monomers (lactic and glycolic acids). These monomers are breakage into energy, carbon dioxide and water (DING & ZHU, 2018; KAPOOR *et al.*, 2015; MAKADIA & SIEGEL, 2011). PLGA is consider a bulk-eroding polymer and during the polymer erosion, the water uptake into matrix is higher than polymer degradation rate (hydrolysis) (HAN *et al.*, 2016; KAPOOR *et al.*, 2015; MAKADIA & SIEGEL, 2011).

PLGA particles follow some of three degradation mechanism: erosion of polymer surface with drug physically release, splitting of drug-polymer bonding with drug diffusion release and/or drug release by diffusion followed by polymer erosion (HAN *et al.*, 2016; KAPOOR *et al.*, 2015). The degradation rate of PLGA can regulate the drug release (SWIDER *et al.*, 2018; FREDENBERG *et al.*, 2011).

Figure 55 gives a schematically representation of possible degradation mechanisms for PLGA particles. Generally, PLGA particles show a biphasic release profile. In phase I, occurs the water penetration into polymer matrix forming pores corresponding to an initial burst drug release; the polymer degradation that follows corresponds to a slower release (phase II) (HAN *et al.*, 2016; SHARMA *et al.*, 2016; MAKADIA & SIEGEL, 2011).

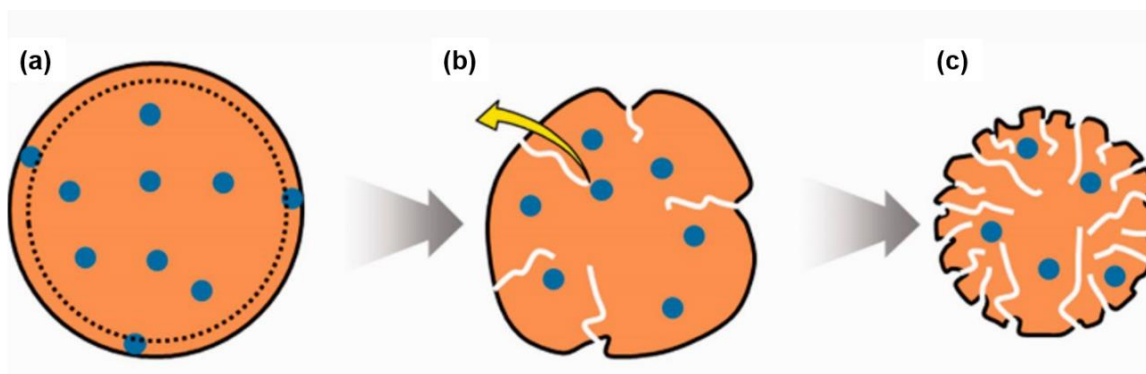


Figure 55. Scheme of possible PLGA particle degradation mechanism (a) initial particle, (b) water uptake into polymer matrix, (c) polymer degradation (adapted from YAO *et al.*, 2016).

There are several factors, which can affect the PLGA particles degradation, such as polymer properties, drug properties (type of drug) and formulation properties.

Polymer properties influencing particles degradation and drug release profile are composition, crystallinity (T_g) and molecular weight. In general, a polymer with more glycolic acid has higher hydrophilicity and fast degradation; indeed, PLGA with high molecular weight has slower degradation.

Formulations properties affecting PLGA particles degradation, include size and shape of matrix (large particles have small initial burst release with slow release than smaller particles) and drug load (low drug content allows slow burst release). The presence of enzymes and pH (alkaline or acid) can, also, affect PLGA particles release (DING & ZHU, 2018; SWIDER *et al.*, 2018; SHARMA *et al.*, 2016; KAPOOR *et al.*, 2015; MAKADIA & SIEGEL, 2011).

4.1.6. PLGA microparticles for depot delivery

There are several published reviews focusing on the PLGA particles formulation due to the polymer broad use and acceptance. Ding and Zhu (2018) discussed the recent advances of PLGA micro and nanoparticles for bio macromolecular molecules delivery, as preparation methods, drug release and macromolecular compounds deliveries. Swiper and co-workers (2018) focused on PLGA particles preparation, novels particles design and how to improve

effects on treatments using these particles. Mir and co-workers (2017) discussed the recent application of PLGA particles in drug delivery for different diseases treatment. Moreover, they introduced the products prepared with PLGA in clinical trials and on market. Han and co-workers (2016), described some examples of PLGA microparticles for sustained release design and some strategies to improve drug loading in particles. Sharma and co-workers (2016) focused on helping to explain the preparation methods to obtain PLGA-based nanoparticles for biomedical applications. They also discussed the mechanisms of drug release, factors affecting particles degradation and targets strategies for efficient drug delivery. Wan and Yang (2016) reported PLGA-based depot delivery systems prepared by spray drying and discussed some aspects of the spray drying technology as the critical solvent properties, novel types of nozzles for atomization and their applications. Kappor and co-workers (2015) addressed the synthesis, physicochemical properties and biodegradation of PLGA, microencapsulation methods, problems with drug delivery and PLGA formulations in drug delivery systems.

PLGA microparticles can be administered by different routes such as pulmonary, ocular, parenteral, oral, intramuscular, subcutaneous, nasal and topical (WANG & YANG, 2016; WANG *et al.*, 2013). There are already some marketed formulations using PLGA, especially for cancer treatment, as: Lupron Depot[®], Suprecur[®] MP, Somatuline[®] LA, Trelstar[™] Depot and others (ANSARY, AWANG, RAHMAN, 2014). Moreover, the preparation method fully influences in the properties of PLGA particles. Particles, used in specific function such as therapeutic delivery or cell imaging/targeting, require accurate physicochemical properties (SWIDER *et al.*, 2018; KAPPOR *et al.*, 2015).

One of alternative administration route, which has been studied is intralesional administration. This alternative route has some advantages as decrease of drug dose and/or the administration frequency, reduction of side effects, improvement of treatment efficiency (PINERO *et al.*, 2006). Moreover, it can be a potential route for treat complex diseases (ANGAMUTHU *et al.*, 2014). A positive example is the formulation containing PLGA and terbinafine for intralesional administration to treat fungal nail infections, which had good results

(ANGAMUTHU *et al.*, 2014). A poorer result was obtained with one formulation called OncoGel™ (PLGA-PEG-PLGA triblock copolymer with paclitaxel) for local tumor treatment, which failed in phase IIb (JAIN *et al.*, 2016).

Intralesional administration has already been described in literature for leishmaniasis treatment (BATISTA *et al.*, 2018). In 2013, it was included in leishmaniasis guidelines intralesional treatment using pentavalent antimonials to decrease antimonials dose and decrease side effects in comparison with traditional treatment using intramuscular or intravenous routes (BRITO, RABELLO, COTA, 2017). Moreover, there are studies involving PLGA formulations with chalcones (natural product with a broad spectrum of biological activities including antileishmanial) for this type of administration, which showed interesting results (BATISTA *et al.*, 2018; PINERO *et al.*, 2006).

The present thesis aims to develop PLGA microspheres and PLGA core-shell microcapsules to encapsulate paromomycin, a water-soluble drug to be tested in leishmaniasis treatment by intralesional administration. The process of choice is spray drying.

The production of PLGA microparticles by spray drying seems represent a promising way for depot deliveries development, including with water-soluble drugs (RE, 2006).

4.1.7. Paromomycin

Paromomycin (PM) is a white or slightly yellow powder, which is in salt form (paromomycin sulfate) with molecular formula $C_{23}H_{45}N_5O_{14} \cdot xH_2SO_4$ and molecular weight of 615.6 g of PM base and 896.86 g in sulfate form salt (CHEMID PLUS, 2016; THE INTERNATIONAL PHARMACOPEIA, 2017b; USP, 2012b; DAVIDSON, DEN BOER, RITMEIJER, 2009).

PM presents high solubility in water and low solubility in ethanol (THE INTERNATIONAL PHARMACOPEIA, 2017b). PM is hygroscopic and undergo degradation in moist environment and degrades rapidly when exposed to high temperatures (THE INTERNATIONAL PHARMACOPEIA, 2017b).

The efficacy of PM formulations against *Leishmania* species from 'New World' still controversial and several clinical studies are required to evaluate their performance (GONÇALVES *et al.*, 2005). The controversy is generated by less efficacy showed by these studies compared to parenteral meglumine antimoniate (KIM *et al.*, 2009). In Brazil, paromomycin has not been yet approved to use in leishmaniasis treatment (DNDi, 2018), probably related to PM low efficacy reported against *Leishmania* "New World" species. Furthermore, PM current topical formulations present low permeability because this drug belongs to class III of BCS. Moreover, the parasite resistance of paromomycin current formulations has been reported and it is related to decrease of PM uptake by *Leishmania* (JHINGRAN *et al.*, 2009).

The parasite resistance, the few studies of PM efficacy in New World, the few numbers of clinical studies, the toxicity of formulations presented on the market and the poor permeability of this drug are motivating the development of new PM formulations for leishmaniasis treatment.

However, there are still few studies described in literature about PM physicochemical characterization or paromomycin drug delivery systems. Figure 56 shows the number of publications, obtained in database "Web of Science", related to PM physicochemical characterization or paromomycin drug delivery systems between 1997 and 2017 using keywords as "Paromomycin + Leishmaniasis", "Paromomycin + Characterization", "Paromomycin + Drug delivery system (DDS)", "Paromomycin + PLGA" and "Paromomycin + Leishmaniasis + Drug delivery systems (DDS)".

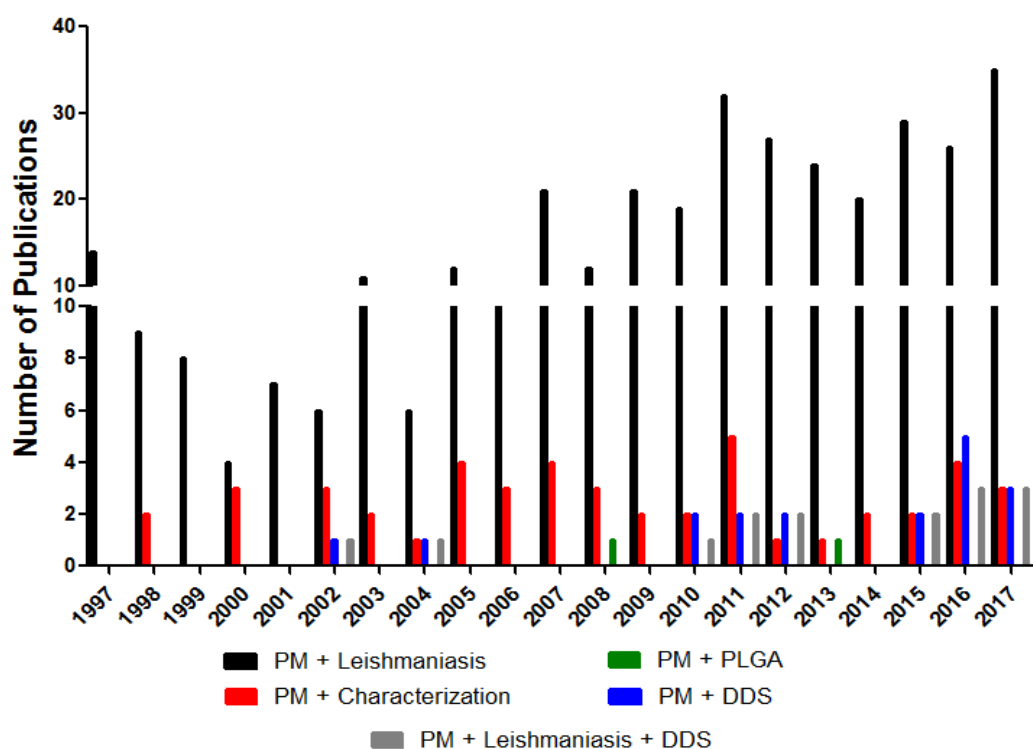


Figure 56. Number of publications of paromomycin (PM) among 1997-2017 obtained from database 'Web of Science' using keywords as "Paromomycin + Leishmaniasis", "Paromomycin + Characterization", "Paromomycin + Drug delivery system (DDS)", "Paromomycin + PLGA", and "Paromomycin + Leishmaniasis + Drug delivery systems (DDS)".

Table 9 shows PM drug delivery systems described in literature, including information about the preparation methods and some product characteristics. It can be observed that studies on PM drug delivery systems for leishmaniasis were not numerous before 2009. However, an increasing interest on this topic has been observed from 2010, mainly in the last three years. There are, also, few studies about PM formulations for subcutaneous administration, which is one of objectives of this work.

Table 9. Drug delivery systems of paromomycin formulations.

Formulation	Administration route	Method	Physicochemical characterization	Reference
Nanoparticles of PM + PLGA	-	Nanoprecipitation	Particle size, encapsulation efficiency, DSC	Kalimoultou <i>et al.</i> , 2008.
PM liposomes	Topical	Fusion and homogenization	Particle size	Jaafari <i>et al.</i> , 2009.
PM liposomes	Topical	Reverse phase evaporation	Particle size, zeta potential, encapsulation efficiency	Carneiro <i>et al.</i> , 2010.
Microspheres of albumin containing PM	Parenteral	Spray drying	Particle size, encapsulation efficiency, drug release, SEM, DSC, TGA, FTIR, contact angle	Khan <i>et al.</i> , 2011a.
Ionic complexation	Topical	Ion pairing	NMR, thermal analysis, solubility	Nogueira <i>et al.</i> , 2011.
PM Solid lipid nanoparticles	-	Microemulsion and solvent diffusion	Particle size, encapsulation efficiency, drug release, DSC	Ghadiri <i>et al.</i> , 2012.
Microspheres of albumin containing PM	Parenteral	Spray drying	Stability study	Khan <i>et al.</i> , 2013.
PM liposomes and PM+miltefosine liposomes	Subcutaneous	Double emulsion and lyophilization	Particle size, zeta potential, encapsulation efficiency, drug loading	Momeni <i>et al.</i> , 2013.
PM nanogel	Transdermal	Hydrogel formation	Particle size, zeta potential, pH, rheological study, spreadability test, gelation time, drug efficiency, stability study, thermal analysis	Brugués <i>et al.</i> , 2015.
PM liposomes	Parenteral	Dehydration and rehydration	Particle size, zeta potential, encapsulation efficiency, stability study, DSC	Gaspar <i>et al.</i> , 2015.
PM Solid lipid nanoparticles	Intramuscular	Modified high shear homogenization microemulsion	Particle size, zeta potential, encapsulation efficiency	Kharaji <i>et al.</i> , 2016.
Microspheres of chitosan containing PM	Oral	Spray drying	Particle size, zeta potential, encapsulation efficiency, drug release	Blanco-Garcia <i>et al.</i> , 2016.

Legend: PM – Paromomycin, SEM – Scanning Electron Microscopy, DSC – Differential Scanning Calorimetry, TGA – Thermogravimetric Analysis; FTIR – Fourier Transform Infrared Spectroscopy, NMR – Nuclear Magnetic Resonance.

4.2. OBJECTIVES

The chapter presents the part of this thesis developed at RAPSODEE Research Centre (France) related to:

- The development of new formulations of PM loaded in biodegradable polymeric microparticles, intending intralesional administration;
- The physicochemical characterization of pure PM and PM-loaded polymeric microparticles;
- The study of their performance behavior under the following *in vitro* studies:
 - In vitro* PM release profile;
 - In vitro* cytotoxicity assay;
 - In vitro* antileishmanial activity.

4.3. MATERIAL AND METHODS

4.3.1. MATERIAL

Paromomycin sulfate (PM) was obtained from Biovet (Bulgaria).

Polymer poly lactic co-glycolic acid (PLGA) (Purasorb[®] PDLG 5004 – ester terminated) was purchased from Corbion (Netherlands). PLGA has 0.4 dl/g of inherent viscosity midpoint, 44 kg/mol of molecular weight and 50:50 lactide/glycolide ratio.

Poly lactic acid (PLA) (Resomer[®] L206S – ester terminated) was purchased from Sigma-Aldrich (France).

All other materials were of analytical reagent grade.

4.3.2. METHODS

4.3.2.1. PHYSICOCHEMICAL CHARACTERIZATION OF PAROMOMYCIN

Very little information is found in the literature concerning the physicochemical properties of this molecule. PM alone was then firstly characterized by applying several techniques.

Two different samples of pure PM were characterized: the raw PM obtained from Biovet and the same molecule reprocessed by spray drying.

The second sample was produced by solubilizing approximately 50 g of PM powder in 62 g of water. The resultant solution was then spray-dried using the same spray dryer used to produce the PM-loaded polymeric microparticles. i.e., a spray dryer B-290 (Büchi, Switzerland), equipped with a two-fluid nozzle, nozzle size 0.7 mm. Compressed air at flow rate of 600 L/h was the drying/carrying gas. The inlet temperature was $119^{\circ}\text{C} \pm 1^{\circ}\text{C}$, outlet temperature $87^{\circ}\text{C} \pm 2^{\circ}\text{C}$ and PM solution flow rate was 114.23 g/h.

4.3.2.1.1. Scanning Electron Microscopy (SEM)

SEM images of PM powders were taken with scanning electronic microscope (Philips XL30 ESEM-FEG, Netherlands). Raw and reprocessed PM powders were dispersed on a SEM stub with a double-sided carbon adhesive tape. After that, the sample was coated in a sputter coater equipment Sputter Coater (Polaron Range SC7640, United Kingdom) with a platinum thin layer for 2 minutes in 10 mA under Argon gas atmosphere.

4.3.2.1.2. Differential Scanning Calorimetry (DSC)

DSC analysis of PM powders were performed using an equipment DSC-Q200 (TA Instruments, USA) in modulated mode (MDSC) at heating rate of $2^{\circ}\text{C}/\text{min}$ under dry nitrogen atmosphere ($50\text{ mL}/\text{min}$). Approximately 7 mg of sample were weighed and placed into standard non-hermetic aluminum pan. The heating temperature ranged from 25°C to 200°C following adapted method

(KHAN & KUMAR, 2011a,b; KALIMOUTTOU *et al.*, 2008). The DSC was calibrated with indium for temperature and enthalpy calibration and with sapphire for heat capacity calibration. The sample was submitted to two heating cycles.

4.3.2.1.3. X-ray Scattering Diffraction (XRD)

The solid state of PM powders was evaluated in an X-ray Diffraction equipment Philips X'Pert (Philips, USA). The measurements were made with Cu K α radiation at scanning speed of 0.02°/sec, in 2 θ , from 5 to 80°. Furthermore, the analyses were performed at 40 KV and 40 mA (adapted from KANG *et al.*, 2008).

4.3.2.1.4. Fourier Transform Infrared Spectroscopy (FTIR)

The FTIR spectra of the raw and reprocessed PM were analyzed using a FTIR spectrophotometer (Thermo Scientific Nicolet iS10, Thermo Fisher Scientific, France) in the range of 4000 cm⁻¹ to 450 cm⁻¹. The PM samples were diluted with KBr powder using conventional KBr discs method (KHAN & KUMAR, 2011a, b). The peaks identification was based on published data describing characteristic infrared bands (SILVERSTEIN, WEBSTER, KIEMLE, 2005; LARKAN, 2011).

4.3.2.1.5. Raman Spectroscopy

Raman mapping of PM powders was performed with a Raman microscopy (Alpha 300R Raman-AFM spectrophotometer, WITEC GmbH, Germany). The measurements were obtained at room temperature with 50X magnification using a confocal laser wavelength of 532 nm. The PM Raman spectra were analyzed four times, collected for 1s of integration using ten accumulations.

4.3.2.2. PAROMOMYCIN POLYMERIC MICROPARTICLES DEVELOPMENT

PM-loaded microparticles were prepared by spray dryer B-290 (Büchi, Switzerland) equipped with an inert loop B-295. Heated nitrogen gas was used as drying/carrying gas with flow rate of 600 L/h. Twenty-five batches of spray-dried powders were generated. The batches differed in relation to:

a) Nozzle Design

Two types of nozzles were used, two- and three-fluids, as represented in Figure 57. The three-fluid nozzle have some advantages in comparison with two-fluid nozzle, such as the use of two solvents immiscible and solutions with high concentrations (KAUPPINEN *et al.*, 2018).

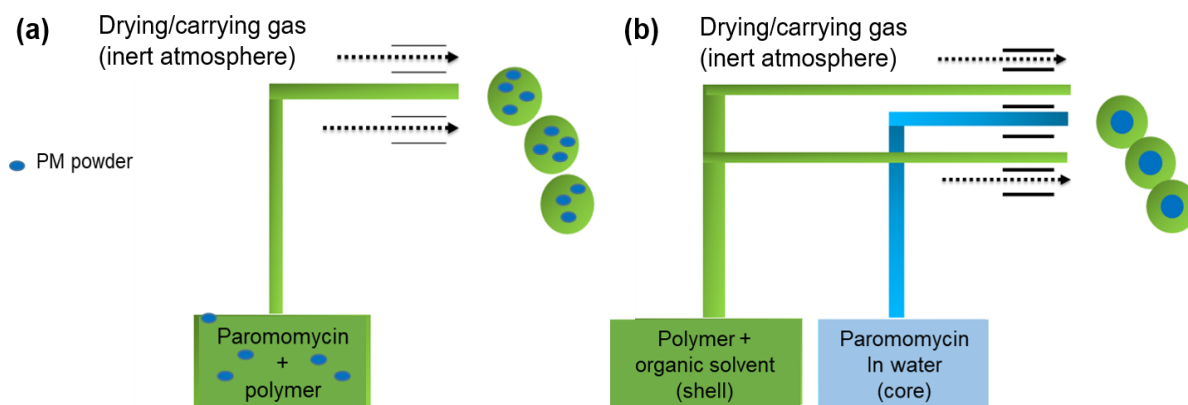


Figure 57. Nozzle types used in this work (a) two-fluid nozzle and (b) three-fluid nozzle (in situ coating).

When using a two-fluid nozzle (Figure 57a), only one liquid formulation was spray dried in contact with the drying/carrying gas. This formulation contains both compounds, PM and polymer. Firstly, an organic solution was prepared by dissolving the polymer in a selected solvent (1.5% w/w). The drug (PM powder) was then mixed to the organic solution (6.8 mg/mL).

With this nozzle design, the nozzle orifice diameter was varied in the study (0.7 mm, 1.4 mm and 2.0 mm).

When three-fluid nozzle was used (Figure 53b), the outer solution was the

organic solution of polymer. In turn, the inner feed was constituted by an aqueous solution of PM in a concentration of 20.2 mg/mL. The nozzle orifice diameter was fixed (1.4 mm). In this configuration, two solutions (PM in water and PLGA in organic solvent) or one solution (PLGA in organic solvent) and one dispersion (PM dispersed in organic solvent) were pumped separately and joined at the nozzle tip, where they are mixed and atomized by pressurized gas provided by the third channel. Subsequently, the solvents evaporate from the droplets by a stream of hot gas and the particles are formed.

The ratio of flow ratio desired was the proportion 1:4 (core: shell), corresponding to a flow rate of 2.6 mL/min for inner (core) and 10.4 mL/min for out (shell).

Figure 58 shows the different nozzles used in this work.

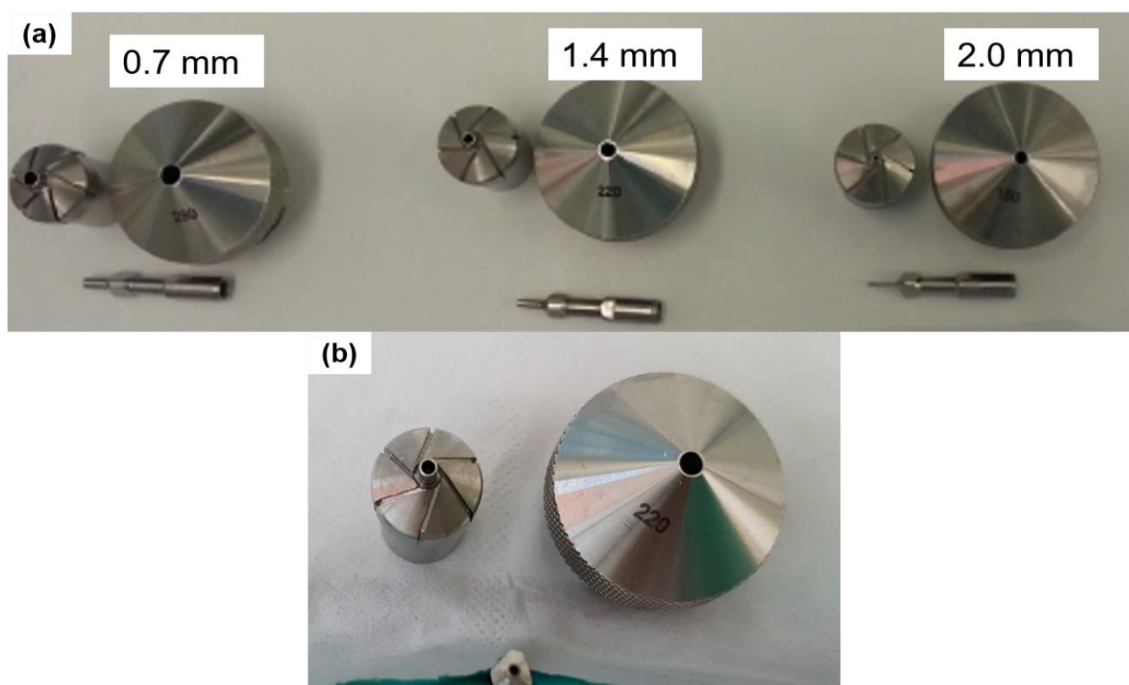


Figure 58. Nozzles design and diameters used (a) three diameters of two-fluid nozzle, (b) three-fluid nozzle 1.4 mm.

b) Type of Organic Solvent

Two organic solvents were used to dissolve the polymeric carrier, PLGA alone or a mixture of PLGA and PLA. The solvents used were ethyl acetate or acetone.

Inlet gas temperature used in all batches varied from 60 to 72 °C and the outlet temperature varied from 60 to 66 °C when ethyl acetate was chosen as organic solvent, and from 35 to 50 °C, when acetone was chosen.

c) Type of Polymer

Most of formulations were generated with a single polymer, PLGA. However, the use of a mixture of PLGA and PLA were also tested in different mass proportions in relation to the total polymer amount: PLGA 95%- PLA 5%; PLGA 90%- PLA 10%; 60%- PLA 40%; PLA 100%.

d) PM Mass Concentration

Different PM mass percentage in the binary mixtures constituted of PM and polymer: 30% and 70% wt. for two-fluid batches and 15%, 30%, 45% and 60% wt. for three-fluid batches.

e) The Physical State of PM formulation

PM-loaded polymeric microparticles were generated from different physical states of the drug: dispersed in water (with two-fluid nozzle) or dissolved in water (with the three-fluid nozzle). Blank particles were also generated. They will be presented and discussed in detail in the next sections.

4.3.2.3. PHYSICOCHEMICAL CHARACTERIZATION OF PAROMOMYCIN POLYMERIC MICROPARTICLES

PM- loaded polymeric microparticles produced by the two-fluid nozzle will be named 'PM-MS', while those produced by the three-fluid nozzle will be named 'PM-MC' from this point of the manuscript.

The PM-MS and PM-MC batches were characterized with respect to some physical characteristics (particle size and morphology), thermal properties, FT-IR and Raman spectra as described below.

4.3.2.3.1. Scanning Electron Microscopy (SEM)

The PM-MS/PM-MC samples images were performed using scanning electronic microscope (Philips XL30 ESEM-FEG, Netherlands) following method described previously in item 4.3.2.1.1.

4.3.2.3.2. Differential Scanning Calorimetry (DSC)

DSC analysis of PM-MS/PM-MC samples were performed using an equipment DSC-Q200 (TA Instruments, USA) in modulated mode (MDSC) following method already described previously in item 4.3.2.1.2.

4.3.2.3.3. Drug Content, Encapsulation Efficiency and Process Yield

The PM concentration in the microparticles was determined by UV-vis (UV-vis model V-630, Jasco, Brazil) spectrophotometric method using PM derivatization with 1-fluoro-2,4-dinitrobenzene (DNFB) (Figure 59) in distilled water as a solvent at 415 nm (adapted from RYAN, 1984) and previous validated by this research group (data not yet published).

The PM derivatization have to be done to promotes PM UV detectability because PM lacks UV chromophores (FAROUK, AZZAZY, NIESSEN, 2015; ISOHERRANEN & SOBACK, 1999) and derivatized PM presents yellow color.

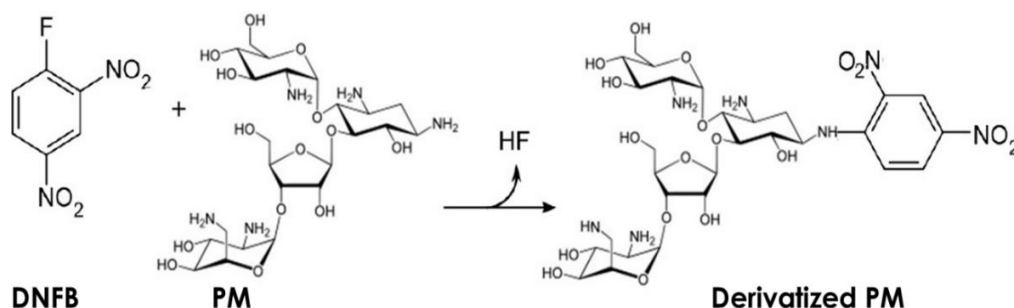


Figure 59. Possible derivatization reaction of PM with DNFB.

The calibration curve (Figure 60) was prepared in distilled water in the range of 0.25 to 10 mg/mL and a regression equation ($y = 0.1171x + 0.4844$) was obtained (linearity $r^2 = 0.9735$).

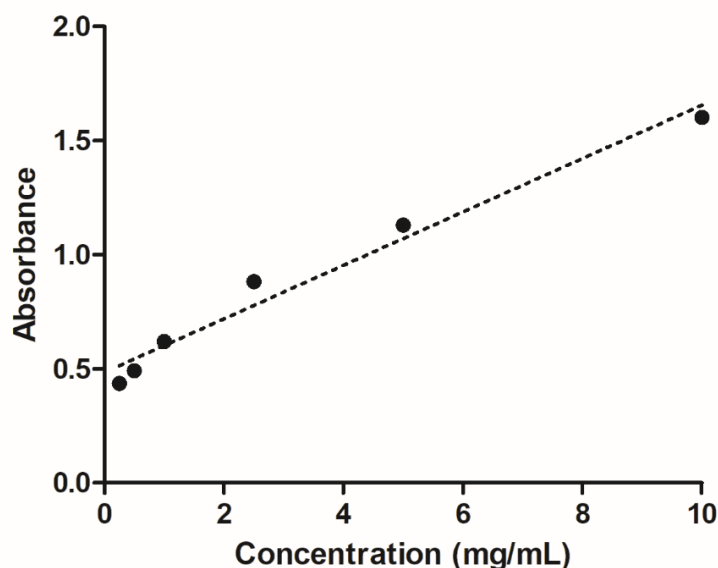


Figure 60. Calibration curve of derivatized PM in distilled water.

In short, 100 mg of PM-MS or PM-MC samples were weighed and 1% of micronized Pluronic (dispersing agent) were mixed. Then, 5 mL of dichloromethane was added and homogenized using vortex mixer during approximately 2 minutes. After homogenization, 5 mL of distilled water was added and homogenized for another 2 minutes using vortex mixer. Subsequently, the suspension was added into separatory funnel for a liquid-liquid extraction. The material was left until complete phase's separation. The organic phase was discarded and the aqueous phase, containing PM extracted from PM-MS samples, was collected and submitted to derivatization reaction with DNFB (adapted from RYAN,1984). The absorbance values were evaluated at 415 nm.

The drug content, DL (%), in PM-MS and PM-MC products was then calculated by Equation 1:

$$\text{DL (\%)} = \frac{\text{Mass of drug loaded in microparticles}}{\text{Mass of microparticles recovered}} \times 100 \quad \text{Equation 1}$$

The encapsulation efficiency, EE (%), was defined by Equation 2:

$$\text{EE (\%)} = \frac{\text{Drug concentration in the microparticles}}{\text{Theoretical drug concentration in the microparticles}} \times 100 \quad \text{Equation 2}$$

The yield of batches (%) was calculated following the Equation 3:

$$\text{Yield (\%)} = \frac{\text{Total mass of microparticles}}{\text{Mass of drug} + \text{Mass of polymer}} \times 100 \quad \text{Equation 3}$$

4.3.2.3.4. Fourier Transform Infrared Spectroscopy (FTIR)

The FTIR spectra of PM-MS/PM-MC samples were analyzed using a FTIR spectrophotometer (Thermo Scientific Nicolet iS10, Thermo Fisher Scientific, France) following method described previously in item 4.3.2.1.4.

4.3.2.3.5. Particle Size

The particle size and polydispersity index of PM microparticles were investigated in equipment Mastersizer 3000 (Malvern Instruments, United Kingdom). The microparticles were dispersed in distilled water containing 0.01% (w/v) of Tween® 80 and sonicating 1 min in a water bath to prevent aggregation phenomena at room temperature (WANG *et al.*, 2015; adapted from BONIATTI, PITALUGA, SEICEIRA, 2011). The particle size distribution, exhibited as volume weighted mean diameter (Dv), was showed based on values of d10, d50 and d90, which represent the accumulated diameters of 10, 50 and 90% of the particles, respectively. Furthermore, it was calculated polydispersity index (Span) following equation below:

$$\text{Span} = \frac{(d_{90} - d_{10})}{d_{50}} \quad \text{Equation 4}$$

Where d10, d50 and d90 were the diameters at 10%, 50% and 90% cumulative volumes, respectively.

4.3.2.4. IN VITRO RELEASE OF PAROMOMYCIN POLYMERIC MICROPARTICLES

In vitro release assay has been used for investigating the drug release profile from micro and nano formulations. Membrane diffusion method, also known as dialysis method, is an appropriate method for drug release determination and several adaptations for this method is already described in literature (JUG *et al.*, 2018). In this work, to evaluate the *in vitro* release profile of PM-MS and PM-MC batches, it was chosen an adapted dialysis method, which have been adopted by the Brazilian research group for similar *in vitro* release studies.

In brief, 10 mg of PM-MS or PM-MC samples were weighed and mixed to 1 mg of micronized Pluronic (dispersing agent). These powders were inserted on a cellulose acetate membrane (Sigma-Aldrich, Brazil), previously attached to a cut falcon tube. The cellulose acetate membrane was hydrated in distilled water for, at least, 12 hours before use. Thereafter, 0.5 mL of distilled water was added inside each tube containing powder. Therefore, the tubes with membrane and material were inserted on the surface of 10 mL of receptor medium. The receptor medium was phosphate buffer pH 7.4 (USP, 2012c) containing 2% of Tween® 20. Experiments were carried out at room temperature under constant stirring (100 rpm) for 4 hours. Hence, 1 mL of receptor medium was collected at 1, 2, and 4 hours with refilling with 1 mL of fresh buffer solution.

Furthermore, two other samples were also evaluated:

1. A physical mixture of PM and PLGA in the same mass proportion of the PM-MS/PM-MC particles;
2. A free PM sample in the same amount of PM contained in PM-MS/PM-MC particles. Figure 61 shows a scheme of the *in vitro* release assay used in this study.

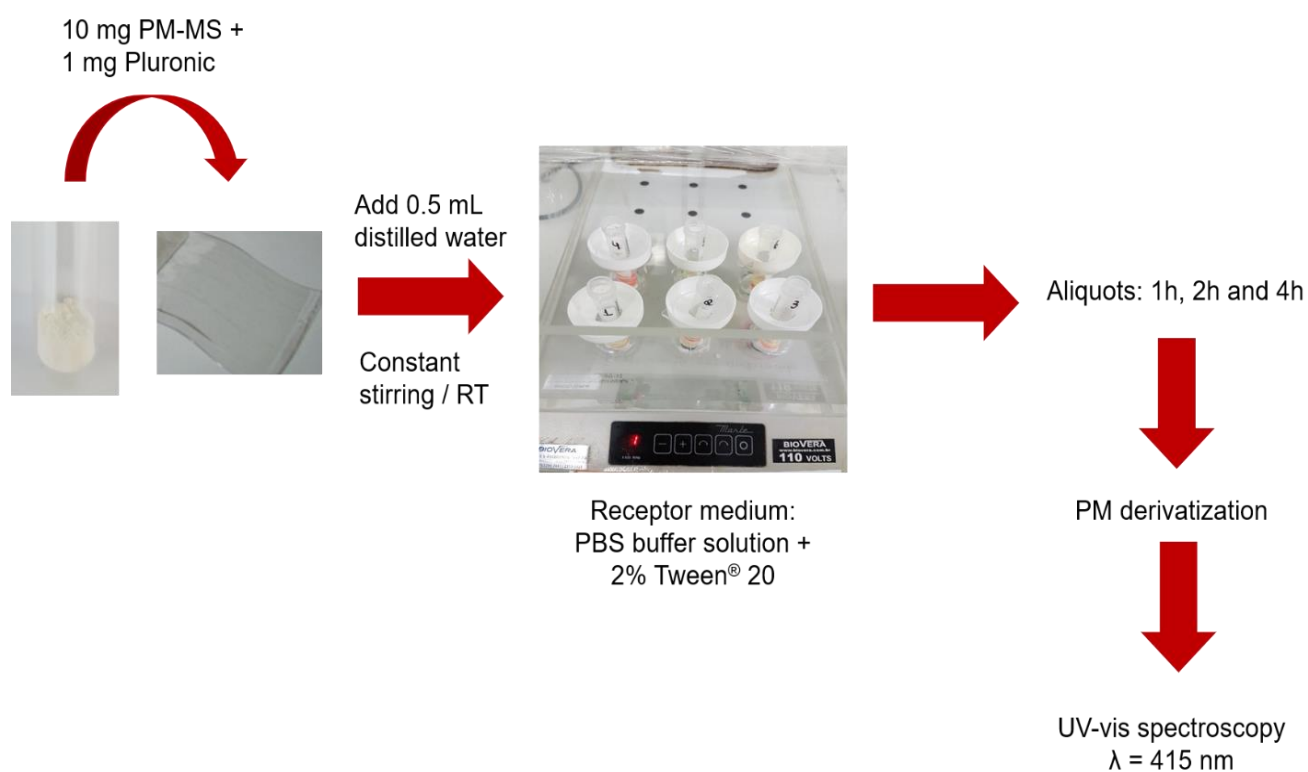


Figure 61. Scheme of *in vitro* release assay of PM-MS/PM-MC samples. Legend: RT – room temperature.

The PM concentration was determined by UV-visible spectrophotometry method (adapted from RYAN, 1984) in wavelength 415 nm. The experiments were conducted in triplicate for samples (free PM, physical mixture and PM-MS or PM-MC batches). The calibration curve (Figure 62) was prepared in PBS with PM derivatized in the range of 25 to 500 $\mu\text{g/mL}$ and a regression equation ($y = 0.0028x$) was obtained (linearity $r^2 = 0.9941$).

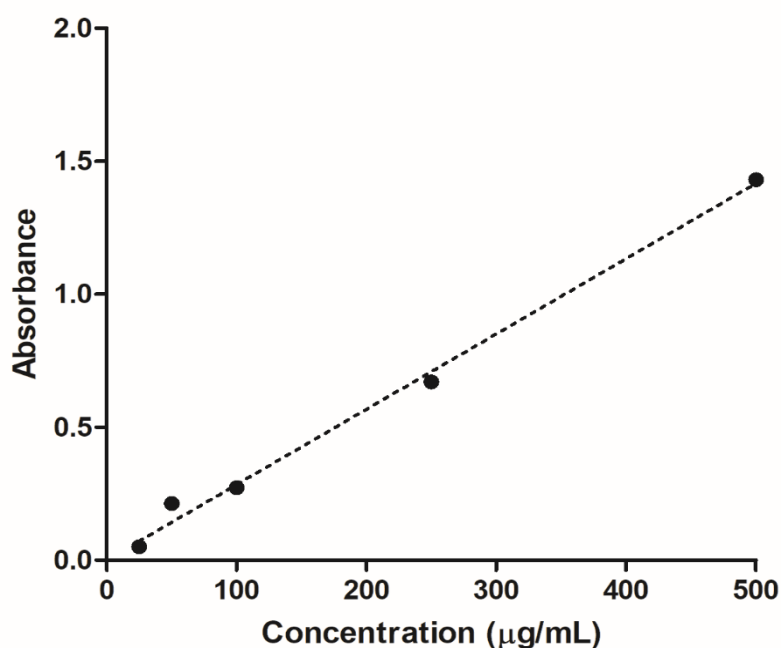


Figure 62. Calibration curve of derivatized PM in PBS for in vitro release study.

4.3.2.4.1. Methods used to compare drug release profiles from PM-loaded spray dried polymeric microparticles

Drug release profiles were analyzed using independent [dissolution efficiency (DE)] and a model-dependent (curve-fitting) approach, the Korsmeyer-Peppas model.

The DE was calculated by the free open source software Kinet DS 3.0 rev. 2010 software (Krakow, Poland) according to Equation 4 in Table 10.

Korsmeyer–Peppas model is a semi-empirical model, relating exponentially the drug release to the elapsed time. It is used to analyze the release of pharmaceutical polymeric dosage forms, when the release mechanism is not well known or when more than one type of release phenomenon could be involved (BRUSCHI, 2015; RAMTEKE *et al.*, 2014; COSTA, 2002; COSTA & LOBO, 2001). Nonlinear regressions were applied for cumulative dissolved drug. The coefficient of determination (R^2), root-mean-square error (RMSE, Equation 2, Table 10) and Akaike's information criterion (AIC, Equation 3, Table 10) values were determined using the same software Kinet DS 3.0 rev. 2010.

Table 10. Dependent and independent kinetic models for study release profile of PM delivery systems (adapted from MEDEIROS et al., 2017; adapted from COSTA, 2002).

Approach	Model	Mathematical Equation
Dependent	Korsmeyer-Peppas	$\frac{Q_t}{Q_\infty} = Kk t^n$ (1)
	RMSE	$RMSE = \frac{\sqrt{\sum_{i=1}^n (y_{iobs} - y_{ipred})^2}}{n}$ (2)
	AIC	$AIC = 2k + n[\ln(\sum_{i=1}^n (y_{iobs} - y_{ipred})^2)]$ (3)
Independent	Dissolution Efficiency (DE)	$DE = \left(\frac{\int_0^t Q_t dt}{Q_{tmax} t} \right) \times 100$ (4)

Legend: Q_t – amount of drug released in time t ; Q_{tmax} – maximal amount of drug released (=100%); Q_∞ - amount of drug released at an infinite time; Q_0 – initial amount of drug in dosage form; K_K – release rate constant; n – diffusional exponent.

4.3.2.5. SPATIAL DISTRIBUTION OF CONSTITUENTS IN THE MICROPARTICLES

In order to investigate the spatial localization of the constituents, polymer and drug in the microparticles, different techniques were associated. They are:

Raman mapping - following method described in item 4.3.2.1.5. Each spectral scan was collected for 0.05 s of integration using ten accumulations and each sample was analyzed three times. 2D (surface) and 3D (depth) analyses were performed on the samples.

SEM observation - following method described previously in item 4.3.2.1.1. PM-loaded polymer microparticles were observed just after manufacturing. Some microparticles were then added to water and exposed to the contact with this medium during 24h (to solubilize and remove PM not protected by PLGA), after which they were centrifuged in a microcentrifuge (HMAC CT15RE, Hitachi,

Japan) for 15 minutes (12000 rpm, 21°C). The water was discarded, the powder was dried at room temperature for 48 hours in desiccator and observed by SEM.

4.3.2.5. BIOLOGICAL ASSAYS

4.3.2.5.1. Assessment of cytotoxicity of PM-loaded microparticles in BMDM cells

Bone marrow-derived macrophages (BMDM) were obtained from femurs and tibia of BALB/c mice as described by Marim and co-workers (2010). Mice were anaesthetized with 5% of isoflurane and euthanized as approved by Ethics Committee of Animal Use (CEUA) of the Instituto de Biofísica Carlos Chagas Filho (IBCCF) under number IBCCF-118. The protocol to obtain BMDM was described in chapter 3, item 3.3.2.7.1.

BMDM (1×10^5 cells/100 μ L) were seeded on 96-well microtiter plate and incubated with different concentrations of free PM, two PM-MS batches and respective blank microparticles (812, 1625, 3250, 7500 μ g/mL) for 48 hours at 36°C in a 5% CO₂ atmosphere. The range of PM concentration selected for cytotoxicity was based on previous studies described in literature (BRUGUÉS *et al.*, 2015; KHARAJI *et al.*, 2015). Moreover, the negative control was RPMI medium without treatment and positive control was Triton 100X. After incubation time, the cytotoxicity assay was investigated using resazurin method (RAMPERSAD, 2012).

20 μ L of resazurin solution were added and the plate was incubated for more 4 hours at 36°C. After 4 hours, the fluorescence was measured using microplate Fluorimeter Spectra Max M5 (Molecular Devices, USA) at 560 nm for excitation and 590 nm for emission. The results were reported as % cell viability. The 50% cytotoxicity concentration (CC₅₀) values were determined by logarithmic regression analysis as previously described in item 3.3.2.7.1.

4.3.2.5.2. Antileishmanial Activity

The promastigotes metacyclic form of *Leishmania L. amazonensis* (WHOM/BR/75/JOSEFA) were maintained in M-199 medium with 10% of inactivated FBS and 1% of antibiotics (penicillin + streptomycin). Promastigotes were grown at 26°C in climatic chamber (adapted from TORRES-SANTOS *et al.*, 2009). The antileishmanial activity of free PM and best PM-MS was investigated by resazurin reduction method (KULSHRESTHA *et al.*, 2013; ROLÓN *et al.*, 2006).

Promastigotes (5×10^5 parasites/ 200 μ L) were seeded on 96-well microtiter plate. Different concentrations of free PM and PM-MS batches (40, 120, 361, 1083 and 3250 μ g/mL) were evaluated and the plate was incubated for 48 hours at 26°C. The negative control was M-199 medium without treatment and positive control was free PM in microparticles analysis.

After incubation time, 20 μ L of resazurin solution were added and the plate was incubated for more 4 hours at 26°C. After that, the fluorescence was measured using microplate Fluorimeter Spectra Max M5 (Molecular Devices, USA) at 560 nm for excitation and 590 nm for emission. The results were reported as % parasite viability. The 50% inhibitory concentration (IC₅₀) values were determined by logarithmic regression analysis and the selectivity index (SI) was calculated as the ratio CC₅₀/IC₅₀, as previously described in item 3.3.2.7.2.

4.3.2.6. STATISTICAL ANALYSIS

Statistical analysis, CC₅₀ and IC₅₀ were calculated using GraphPad Prism 5.0 (GraphPad Software, USA). The *P* value < 0.05 was considered significant.

4.4. RESULTS AND DISCUSSION

4.4.1. PHYSICOCHEMICAL CHARACTERIZATION OF PAROMOMYCIN

4.4.1.1. Scanning Electron Microscopy (SEM)

SEM images of raw PM are shown in two different magnifications (800x and 3200x) in Figure 63. PM powder presents a smooth shriveled spherical morphology. This morphology suggested that PM powder was probably produced by spray drying.

As spray drying was our process of choice to produce PM-loaded polymeric microparticles, the raw PM powder was also reprocessed alone by in the bench scale spray dryer used in our study. The reprocessed spray-dried PM powder can be visualized as SEM images in Figure 64. It can be observed that spray-dried PM particles has the shape (predominantly spherical and shriveled morphology) already showed by the raw PM powder. However, reprocessed spray-dried PM particles are smaller in size with an apparently large particle size distribution, which could be explained by different scales of production (industrial versus bench scale).

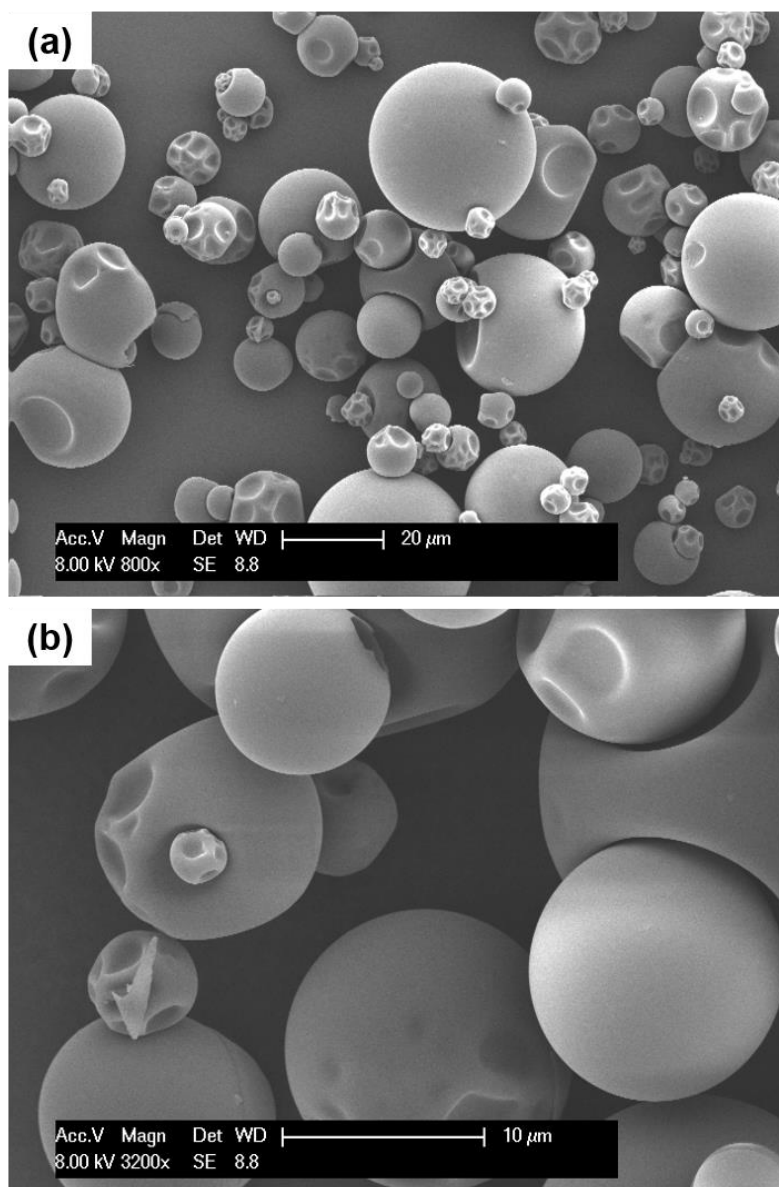


Figure 63. SEM images of raw PM in magnifications (a) 800x, (b) 3200x.

Additionally, this morphology has been typically observed for spray-dried powders in previously published studies with different drugs belonging to the same antibiotic family (aminoglycoside) of PM. Ballesteros and co-workers (2008) analyzed the use of trileucine to produce low-density spray-dried microparticles of raffinose, gentamicin and netilmicin. They observed a smooth shriveled spherical morphology of gentamicin spray-dried microparticles without trileucine. The same morphology of gentamicin-leucine spray-dried microparticles was observed by Aquino and co-workers (2012). These literature

findings and the observation of the shape of the powder obtained by reprocessing the raw PM powder indicate that the raw PM was obtained by spray drying. As the spray-dried solid particles are produced by the fast evaporation of a liquid solution during spray drying, they can be amorphous. The solid states of raw and spray-dried powders of PM were investigated further in this work.

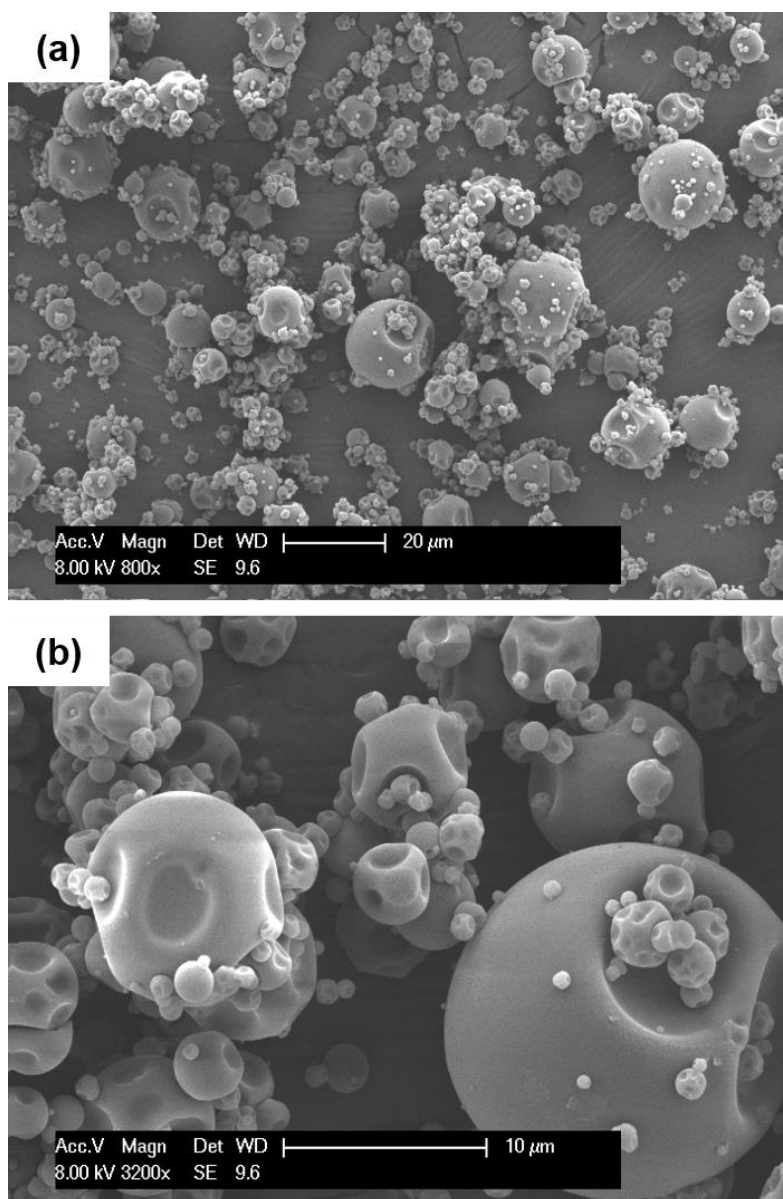


Figure 64. SEM images of atomized PM in magnifications (a) 800x, (b) 3200x.

4.4.1.2. Differential Scanning Calorimetry (DSC)

The MDSC curve of raw and spray-dried PM was shown in Figure 65.

The thermogram of raw and spray-dried PM present no endothermic melting peak through rev Heat Flow and Heat Flow analyses. The large endotherm event (between 25°C and 175°C) showed in non-reversible heat flow (nonrev Heat Flow) and Heat Flow analyses in both samples of PM probably corresponds to the loss of moisture of the drug, which is very hygroscopic. The spray-dried PM showed a higher loss of moisture than raw PM, what could be due to their smaller particle size (and then greater surface area) favoring increased water uptake. The MDSC analysis stopped at 200°C, because PM suffers degradation and the powder changes the color without melt as shown in Figure 66.

Little information on thermal properties of PM is found in the literature. However, we can mention few works that have observed a broad peak corresponding to loss of moisture between 30°C to 100°C during thermal analyses (DSC and TGA) of pure PM (KHAN & KUMAR, 2011a, b). A broad peak corresponding to loss of moisture between 30°C and 185°C was also measured for PM by Brugués and co-workers (2015).

In turn, some works have confirmed PM degradation above 210°C (KHAN & KUMAR, 2011a, b) or 230°C (BRUGUÉS *et al.*, 2015), attributed to PM pyrolysis.

At our knowledge, only one paper published in 2008 (KALIMOUTTOU *et al.*, 2008) have identified a melting point (T_m) for a crystalline sample of PM corresponding to an endothermic peak at 179.64°C. However, no data could be found related to the glass transition temperature (T_g) of the amorphous form of PM. Generally, the T_g of materials can be found in the interval between $\frac{2}{3}$ and $\frac{4}{5}$ of T_m (JÓJÁRT-LACZKOVICH & SZABÓ-RÉVÉSZ, 2010). From this statement, T_g of PM could be expected to be between 28°C ($\frac{2}{3} T_m$) and 89°C ($\frac{4}{5} T_m$). Nevertheless, DSC analyses did not detect any T_g on both, raw and reprocessed PM powders. A supplementary analysis was done increasing the interval of temperature from -90°C to 200°C (data not shown) in an attempt to investigate

the presence of T_g , but none was identified in this temperature range, either.

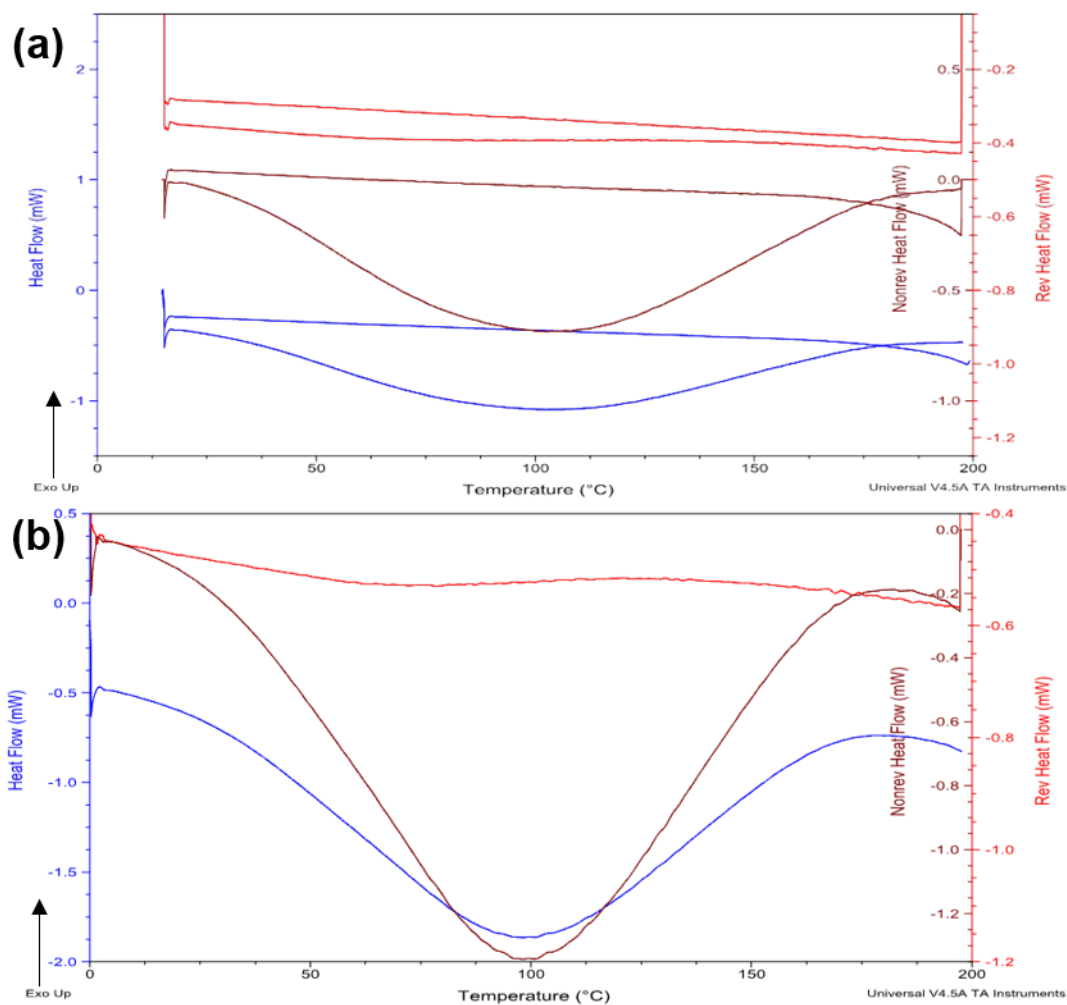


Figure 65. MDSC of (a) raw PM and (b) spray-dried PM with two heating cycles.

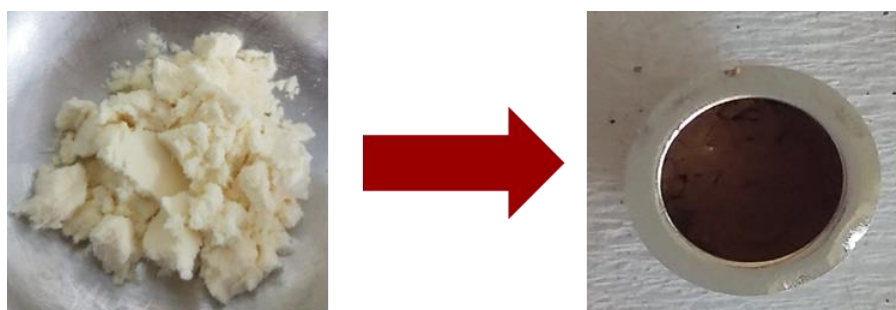


Figure 66. Color change of free PM: (a) light yellow powder before DSC analysis at room temperature, (b) dark brown powder after submitted to 200°C in DSC analysis.

4.4.1.3. X-ray Scattering Diffraction (XRD)

X-ray powder scattering diffraction patterns of raw and reprocessed PM powders are shown in Figure 67. It can be seen that the diffraction patterns did not show sharp Bragg peaks, which is characteristic of amorphous materials.

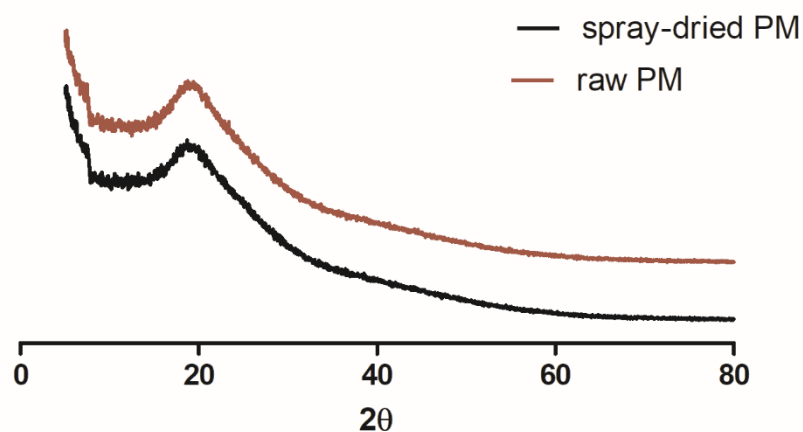


Figure 67. XR Diffractograms of PM powders.

4.4.1.4. Fourier Transform Infrared Spectroscopy (FTIR)

Figure 68 displays the FTIR spectra for raw PM powder. The PM spectrum shows characteristic peaks at 3408 cm^{-1} (NH_2 amine group), at 1632 cm^{-1} (N-H bending coupled with C-N stretch), at 1534 cm^{-1} (CH_2 bending) and at 1027 cm^{-1} (C-O-C stretch). The reprocessed PM sample presented a similar FTIR spectrum.

Khan and Kumar (2011a, b) described PM characteristic peaks at 1629 cm^{-1} (N-H bending coupled with C-N stretch), 1535 cm^{-1} (CH_2 bending) and at 1091 cm^{-1} (C-O-C stretch). Moreover, they observed two bands at 2928 cm^{-1} and at 3377 cm^{-1} corresponding to hydroxyl and NH_2 amine groups. Therefore, the PM FTIR spectrum presented in Figure 68 revealed similar PM characteristics peaks to those described in literature.

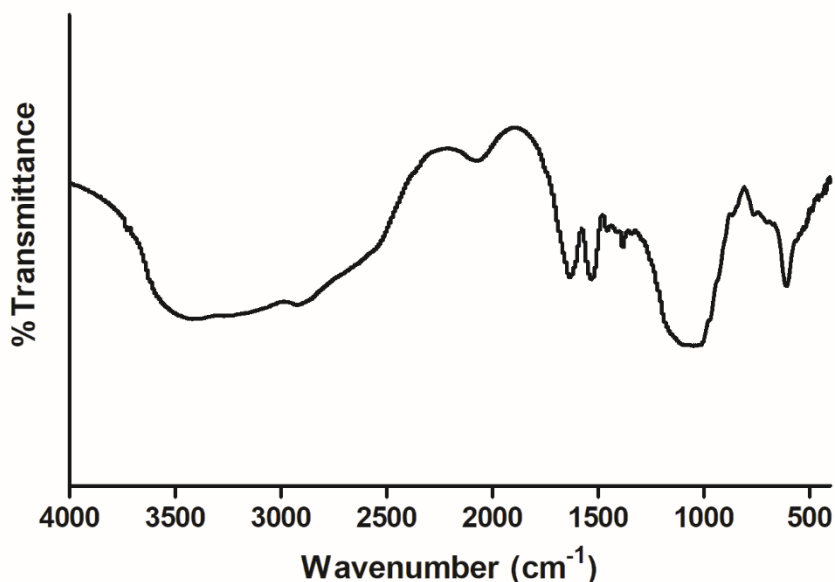


Figure 68. FTIR spectrum of PM.

4.4.1.5. Raman Spectroscopy

The Raman spectrum of PM is shown in Figure 69. It can be seen one peak around 1000 cm^{-1} and one peak between 2900 cm^{-1} and 3100 cm^{-1} . Also, it was observed that PM presents fluorescence. Raman and infrared are complementary techniques which identify the molecular structure. For this reason, the Raman spectrum and FTIR spectrum are linked (LARKAN, 2011). According to this information, the characteristic peak around 1000 cm^{-1} can be related to C-O-C stretch and peak around 3000 cm^{-1} can be related to NH_2 because hydroxyls have weak signal in Raman spectra (LARKAN, 2011). The two spectra (FTIR and Raman) provide the molecular structure “fingerprint” of PM. However, Raman spectrum of PM was not found in the literature.

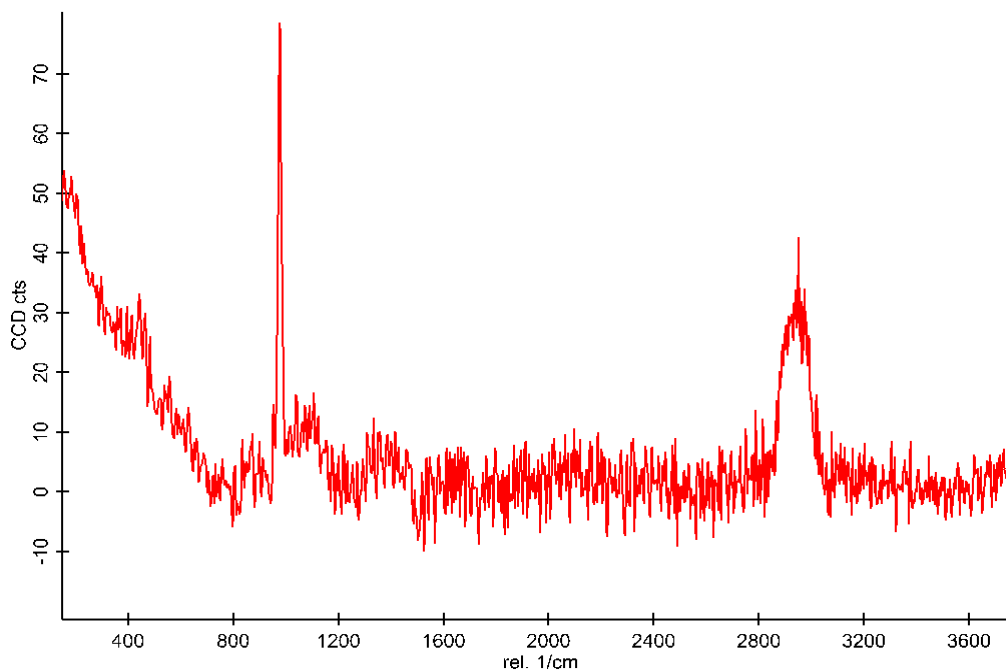


Figure 69. Raman spectrum of PM.

4.4.2. PAROMOMYCIN POLYMERIC MICROSPHERES DEVELOPMENT

4.4.2.1. Development of PM-loaded PLGA microspheres

The first series of tests aimed, on one hand, to select the organic solvent for the polymeric carrier, and on the other hand, to investigate the ability of the spray drying process to produce PM-loaded polymeric microspheres.

4.4.2.1.1. Solvent Choice

The most common solvent used to produce PLGA microspheres by the conventional emulsification-evaporation process is dichloromethane because it has low boiling point around 40°C, which allows fast extraction and evaporation under controlled conditions of temperature and pressure (SINGH & VAN DEN MOOTER, 2016; RE, 2006; WANG & WANG, 2003; WANG & WANG, 2002). However, the use of halogenated solvents (dichloromethane or chloroform) have regulatory restriction because they belong to the class II solvents (solvents to be limited) of ICH classification (ICH, 2016). In this work, two solvents belonging to the class III of ICH classification (solvents with low toxic potential) were selected

for the first tests: ethyl acetate and acetone.

Samples were then prepared with ethyl acetate (PM-MS01, PM-MS02 and PM-MS03 samples) or acetone (PM-MS06) to solubilize the polymeric carrier. Table 11 shows the formulation and process parameters fixed: PM was dispersed in the organic polymeric solution (dispersion type), the initial PM concentration in the formulation was fixed at 30%wt in relation to the total content of solids in the liquid formulation, the polymeric carrier was PLGA 50:50 and a two-fluid nozzle with a nozzle orifice diameter of 1.4 mm was used. The spray-dried products were characterized and compared in terms of particle shape (Figures 70 and 71) and yield (Table 11).

Table 11. Formulation conditions, process and product characteristics of PM-loaded microspheres: solvent effect.

Batch ¹	Solvent	Polymeric carrier	PM in the formulation	Yield (%)	Drug loading in the microspheres (%)	Encapsulation Efficiency (%)
PM-MS01	Ethyl acetate	PLGA 50:50	Dispersed ²	27.2	-	-
PM-MS02	Ethyl acetate	PLGA 50:50	Dispersed ²	11.0	-	-
PM-MS03	Ethyl acetate	PLGA 50:50	Dispersed ²	6.4	-	-
PM-MS06	Acetone	PLGA 50:50	Dispersed ²	35.3	6.9	23.0

Legend: ¹ process conditions: 1.4 mm two-fluid nozzle; ² Raw PM dispersed in the polymeric solution (0.65g PM in 99.35g organic solution, of which 1.5g PLGA in 97.85g organic solvent).

Figure 70 shows some SEM images of samples prepared with ethyl acetate and Figure 71 shows some SEM images of samples prepared with acetone, where, in both figures, raw PM was dispersed in the organic solution

containing PLGA. It can be observed that PM-MS microspheres generated in presence of ethyl acetate (Figure 70 a-d) contain large agglomerates with irregular shape, in which some spherical forms can be seen, although dispersed in a molten-like state. In contrast, PM-MS microspheres generated in presence of acetone (Figure 71 a-b) show the predominance of particles with spherical form, smooth surface, although also agglomerated.

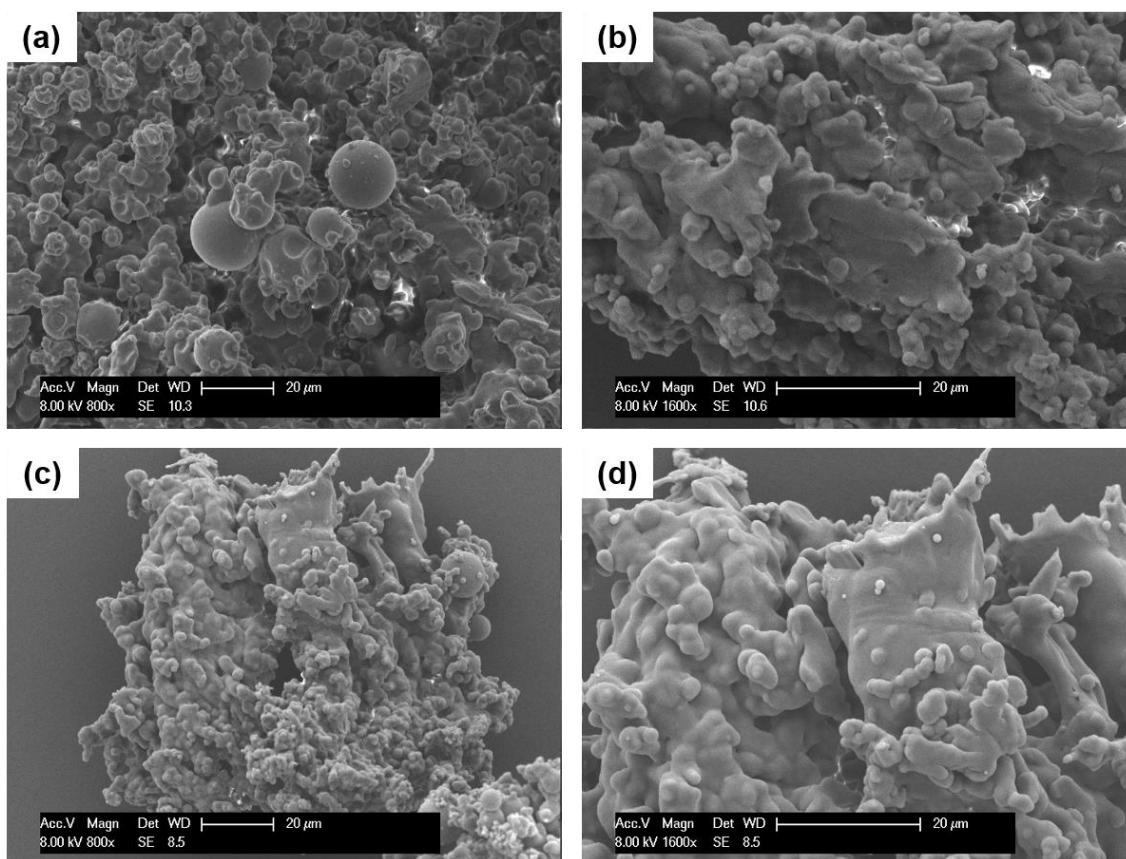


Figure 70. SEM Images of some batches prepared with ETHYL ACETATE in two different magnifications: (a) PM-MS01 800x, (b) PM-MS01 1600x, (c) PM-MS02 800x and (d) PM-MS02 1600x.

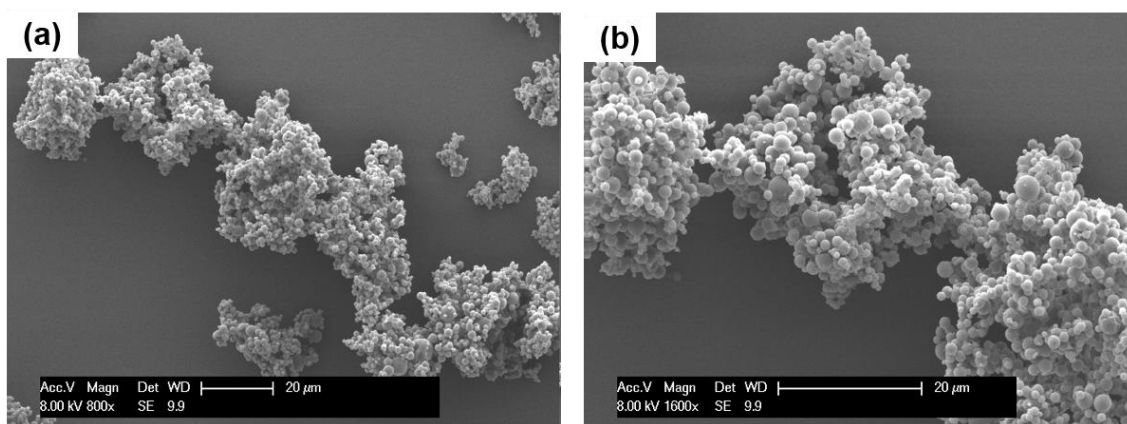


Figure 71. SEM Images of some batches prepared with ACETONE in two different magnifications: (a) PM-MS06 800x, (b) PM-MS06 1600x.

One of difficulties to generate drug-PLGA microspheres by spray drying is due to the low glass transition temperature (T_g) of amorphous PLGA (around 45°C) (SOSNIK & SEREMETA, 2015; ANSARY, AWANG, RAHMAN, 2014; WAN *et al.*, 2013a). If a spray-dried powder is exposed to high temperatures, it can move to a rubbery state, adhering to the spray drying chamber or cyclone walls and be hardly recovered, which explains the low yield of our batches (Table 11).

The production of PM-loaded PLGA microspheres employing ethyl acetate as solvent requires higher temperatures than acetone, since their boiling points are 77°C and 56°C, respectively. The outlet temperatures were kept in the range 65–67°C to evaporate ethyl acetate and in the range 42–46°C to evaporate acetone. The latter condition is more favorable to improve the yield production of PLGA microspheres by spray drying.

Indeed, using literature as basis, some works can be mentioned. Silva-Junior and colleagues (2009) prepared triamcinolone PLGA spray-dried microparticles using acetone as solvent with gas inlet temperature of 70°C and outlet temperature of 45°C. They obtained smooth spherical agglomerated microparticles similarly to those shown in Figure 71 (a and b). Oliveira and co-workers (2013) evaluated the physicochemical properties of methotrexate PLGA spray-dried microparticles prepared with different proportions drug/polymer using acetone as solvent. They observed that methotrexate microparticles had spherical smooth shape with some agglomerates and suggested that the

particles agglomeration is related to low T_g of the polymer.

Another option is a solvent mixture as proposed by Wan and colleagues (2013a, b). They tested different proportions of two organic solvents (acetone and methanol) to produce celecoxib PLGA spray-dried microparticles using gas inlet and outlet temperature of 45°C and 30°C, respectively. The SEM images showed microparticles with spherical and smooth surface.

Ethyl acetate has been used as solvent to produce Etanidazole-PLGA spray-dried particles with lower temperatures than that used in our tests. The authors kept the dryer outlet temperature in the range 40-46°C and also reported that the dry product stuck on the cyclone wall leading to low yields (WANG & WANG, 2002).

Therefore, based on the particles shape and yield of PM-MS batches with acetone and ethyl acetate, acetone was selected as solvent for PLGA-based polymers used in this work to produce PM-loaded polymeric microparticles.

4.4.2.1.2. Nozzle Orifice Diameter Effect

Other parameter evaluated during the development of PM-loaded PLGA microspheres was the nozzle orifice diameter, as indicated in Table 12. Generally, in a two-fluid nozzle, droplet size is a function of liquid formulation type, liquid flow rate, atomization gas flow rate and liquid orifice diameter (RÉ, MESSIAS, SCHETTINI, 2004).

Table 12. Formulation conditions, process and product characteristics of PM-loaded microspheres: nozzle orifice diameter effect.

Batch ¹	Polymeric carrier	PM in the formulation	Nozzle orifice diameter (mm)	Yield (%)	Drug loading in the microspheres (%)	Encapsulation Efficiency (%)
PM-MS05	PLGA 50:50	Dispersed ³	0.7	24.5	3.7	12.5
PM-MS06	PLGA 50:50	Dispersed ³	1.4	35.3	6.9	23.0
PM-MS07	PLGA 50:50	Dispersed ³	2.0	44.5	18.3	61.1

Legend: ¹ process conditions: acetone is the solvent for the polymer, two-fluid nozzle; ² Raw PM dispersed in the polymeric solution (0.65g PM in 99.35g organic solution, of which 1.5g PLGA and 97.85g acetone).

SEM images of PM-loaded PLGA microspheres generated from two-fluid nozzles with different orifice diameters are shown in Figure 72. It is possible to verify that all particles are very similar in shape and degree of agglomeration. PM-MS05 batch (0.7 mm nozzle orifice diameter) has smaller particles in comparison to PM-MS06 and PM-MS07 batches. PM-MS07 batch (2.0 mm nozzle orifice diameter) seems to be constituted by particles of different sizes, which corresponds to a wider particle size distribution. In fact, bigger particles might be expected from the bigger nozzle orifice diameter, since it produces bigger liquid droplets during atomization. Bigger liquid droplets normally produce bigger dry particles (SOSNIK & SEREMETA, 2015).

Referring to literature data: drug-loaded PLGA microspheres have been generated from two-fluid nozzles with different orifice diameters. For example, Mok and Park (2008) developed spray-dried human growth hormone-loaded PLGA microspheres using 0.5 mm nozzle orifice diameter. Spray-dried rifampicin-loaded PLGA microspheres were also produced from 0.5 mm nozzle orifice

diameter (SON & McCONVILLE, 2012). In both studies the aim was to produce fine particles and they used the smaller orifice diameter existing for two-fluid nozzles operating with conventional bench spray dryers. Oliveira and co-workers (2013) used 0.7 mm nozzle orifice diameter to prepare methotrexate-loaded PLGA microspheres, while Nakashima and co-workers (2017) used 1.4 mm nozzle orifice diameter to produce spray-dried aripiprazole-loaded PLGA microparticles for injectable sustained release.

In this study, Table 12 shows that yield, drug loading and encapsulation efficiency increased with the increase of two-fluid nozzle orifice diameter from 0.7 to 2.0 mm. For the next steps of this work, the orifice diameter of 1.4 mm was chosen even if higher EE, drug loading and yield could be reached with the larger (2.0 mm) diameter orifice. The apparent larger particle size distribution obtained with the largest orifice diameter could impact the drug release from these microspheres as the release rate depends, among others, of the surface area exposed to the release medium.

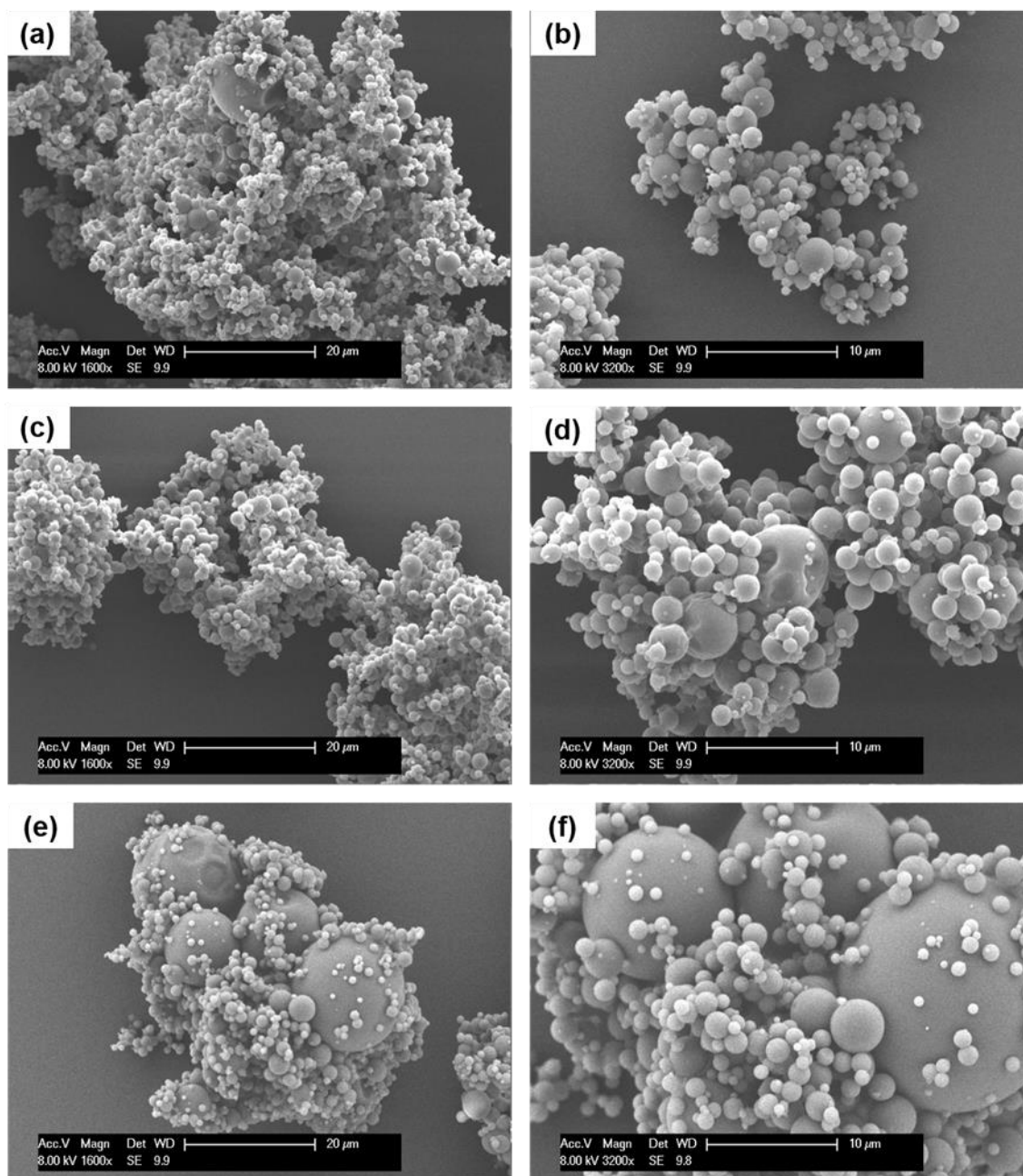


Figure 72. SEM Images of some batches prepared with acetone in two different magnifications varying the nozzle diameter size: (a) PM-MS05 1600x 0.7 mm, (b) PM-MS05 3200x 0.7 mm, (c) PM-MS06 1600x 1.4 mm, (d) PM-MS06 3200x 1.4 mm, (e) PM-MS07 1600x 2.0 mm and (f) PM-MS07 3200x 2.0 mm.

4.4.2.1.3. Paromomycin Concentration

Other parameter evaluated during the development of PM-loaded PLGA microspheres was the PM concentration, as indicated in Table 13.

Table 13. Formulation conditions, process and product characteristics of PM-loaded microspheres: effect of PM concentration in the initial liquid formulation.

Batch ¹	Initial Drug content ² (%wt.)	Polymeric carrier	PM in the formulation	Yield (%)	Drug loading in the microspheres (%)	Encapsulation Efficiency (%)
PM-MS07	30	PLGA 50:50	Dispersed ³	44.5	18.3	61.1
PM-MS08	70	PLGA 50:50	Dispersed ⁴	38.8	33.8	48.3

Legend: ¹ process conditions: acetone is the solvent for the polymer; 2.0mm two-fluid nozzle; ² Drug percentage in relation to total of solid contents; ³ Raw PM dispersed in the polymeric solution (0.65g PM in 99.35g organic solution containing 1.5%wt PLGA); ⁴ Raw PM dispersed in the polymeric solution (3.50g PM in 96.50g organic solvent containing 1.5%wt PLGA).

SEM images of PM-loaded PLGA microspheres generated from two-fluid nozzles with different PM concentrations are shown in Figure 73. It is possible to observe that the particles are similar in shape and degree of agglomeration. However, some differences can be verified in Table 13:

1. Reduced encapsulation efficiency and yield when increasing the PM concentration in the initial liquid formulation.
2. PM-MS07 batch (30% PM) showed higher yield and encapsulation efficiency than PM-MS08 batch (70% PM).

There are some studies described in literature with a similar correlation between drug content and encapsulation efficiency. Lin and co-workers (2005) evaluated the production of doxorubicin-loaded PLGA or PLLA/PLGA microparticles obtained by spray-drying. They observed that the encapsulation efficiency and yield decreased when increasing the drug content in the microparticles. It was explained by the drug insolubility in the organic solvent used. Prior and co-workers (2000) evaluated two different microencapsulation techniques (solvent evaporation and spray-drying) to produce gentamicin PLGA microparticles. Two batches were prepared from each technique, varying the gentamicin concentration. They also attributed the lower encapsulation efficiency

for more concentrated batches to gentamicin insolubility in the organic solvent. However, in our case, PM is dispersed and not dissolved in the organic solvent and the lower encapsulation efficiency and yield are not related to the recrystallization of PM in acetone but more probably to some loss of PM powder during the atomization step (segregation in the feeding pump).

3. Increased PM concentration in the initial liquid formulation leads to increased drug loading in the PM-MS batches.

Despite the losses, PM-MS08 batch has a drug loading higher than PM-MS07 batch. This trend has been reported with other drugs encapsulated in PLGA microspheres (WAN *et al.*, 2014a; OLIVEIRA *et al.*, 2013).

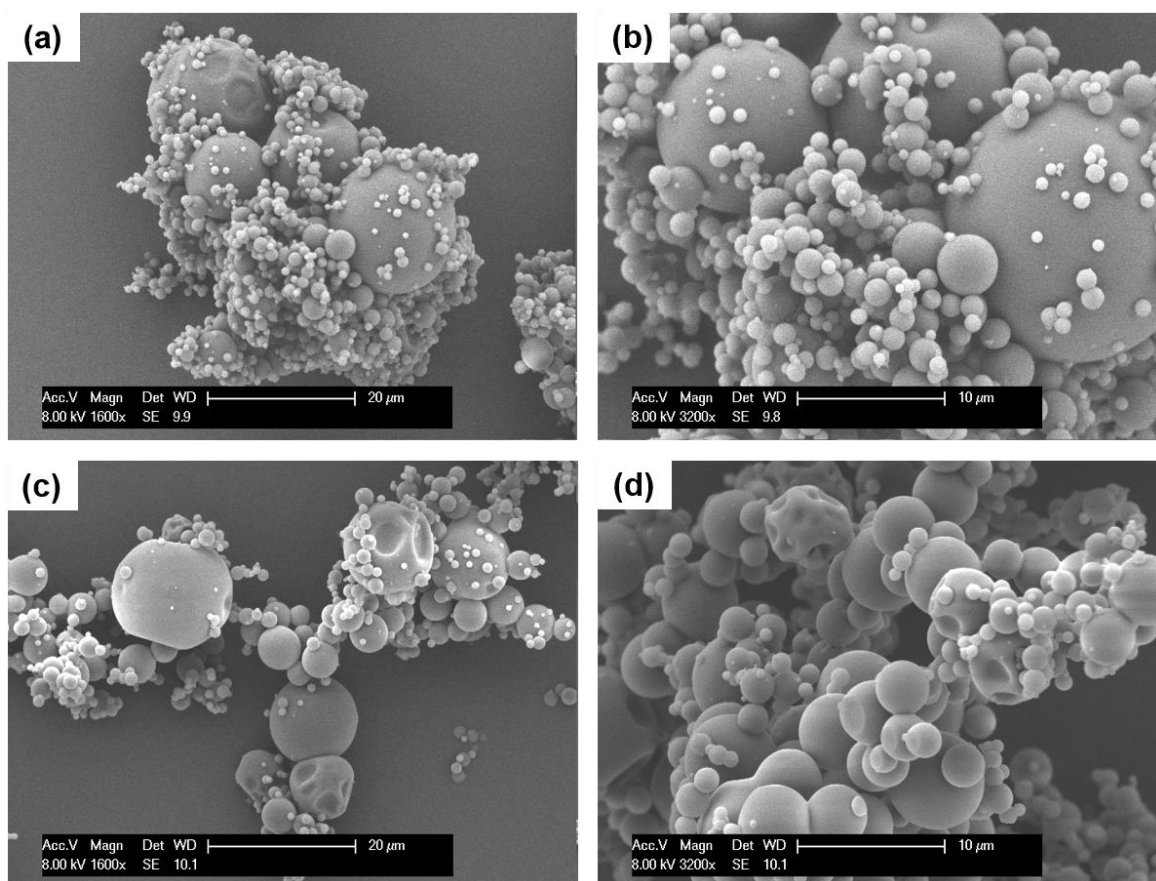


Figure 73. SEM Images of some batches prepared with acetone in two different magnifications varying the PM concentration in the initial formulation: (a) PM-MS07 1600x, (b) PM-MS07 3200x, (c) PM-MS08 1600x, (d) PM-MS08 3200x.

4.4.2.2. Development of PM-loaded core-shell PLGA microcapsules

In a second study, core-shell PLGA microcapsules were developed to encapsulate PM, thanks to a three-fluid nozzle. They are named PM-MC samples from this point of manuscript.

Table 14 presents all batches produced. The studied adjustable parameters were the initial PM concentration in the initial core formulation (from 15 to 60% PM); the shell composition (PLGA or a mixture of PLGA and PLA with varying PLA mass proportions); the physical state of PM in the initial core formulation (solubilized in water or dispersed in the organic solvent).

From these results, it could be concluded that:

- An increase in the PM concentration in the initial core formulation led to an increase the drug loading in the microcapsules (see PM-MC04, PM-MC12 and PM-MC13, then PM-MC14 and PM-MC15). The same effect could be observed in encapsulation efficiency (EE) for the first series MC04, MC12, MC13 but not for MC14 and MC15. The yield was less influenced by this parameter.

- PM, introduced in a solubilized form in the core formulation, allowed higher drug loading in the microcapsules compared to the powder form (see PM-MC15, PM-MC16). EE and yield seemed to be less influenced by this parameter.

- The change in the polymeric matrix from PLGA 50:50 to PLA (see PM-MC12 x PM-MC22) led to a reduction in drug loading in the microcapsules and EE, despite the yield increase.

- The use of a PLGA/PLA blend as polymeric carrier influenced the drug loading, EE and yield, being favored by the increase of the PLA proportion in the matrix (see PM-MC19 to PM-MC21).

Table 14. Formulation conditions, process and product characteristics of PM- loaded core-shell microcapsules.

Batch ¹	Initial drug content ² (%)	Core	Shell	Yield (%)	Drug loading in the microcapsules (%)	Encapsulation Efficiency (%)
PM-MC04	45	PM in water (solution)	PLGA	48.8	30.1	66.9
PM-MC12 PM-MC15	30	PM in water (solution)	PLGA	54.8±8.3	24.3±2.5	87.1±8.3
PM-MC13	15	PM in water (solution)	PLGA	40.8	7.0	46.7
PM-MC14	60	PM in water (solution)	PLGA	80.3	30.7	51.1
PM-MC16 PM-MC18	30	Raw PM powder	PLGA	31.7±12.0	25.4±4.9	80.6±22.2
PM-MC17	15	Raw PM powder	PLGA	45.1	1.4	28.8
PM-MC19	30	PM in water (solution)	PLGA (95%)-PLA (5%)	42.2	2.8	9.4
PM-MC20	30	PM in water (solution)	PLGA (90%)-PLA (10%)	32.1	18.1	60.3
PM-MC21	30	PM in water (solution)	PLGA (60%)-PLA (40%)	53.4	28.0	93.4
PM-MC22	30	PM in water (solution)	PLA	70.9	9.2	30.5
MC23	-	Water	PLGA (95%)-PLA (5%)		-	-
MC24	-	Water	PLGA (90%)-PLA (10%)		-	-
MC25	-	Water	PLGA (60%)-PLA (40%)		-	-

Legend: ¹ Process conditions: acetone as organic solvent; three-fluid nozzle (orifice diameter 1.4 mm); ² Drug percentage in relation to total solid content.

In general, and in quantitative terms, Table 14 shows that the yield of PM-microcapsules varied between 32.1% and 80.3%. The drug loading in all PM-MC

batches ranged from 1.4% to 30.7%. EE was also highly variable, from 9.4% up to 93.4%.

In comparison with PM-MS06, produced with same nozzle orifice size (1.4 mm), PM-microcapsules presented higher values of drug loading and EE. PM-MC16 showed the highest EE (93.4%), however, this batch changed of powder color (from white to light-yellow).

Some published data reflect the difficulty to reach high drug loadings in PLGA microspheres: Prior and co-workers (2004) developed spray-dried gentamicin-loaded PLGA microspheres with a low drug loading of 20 μg gentamicin/mg microspheres, compared to the expected loading of 100 μg gentamicin/mg microspheres. On the other hand, Guerrero and co-workers (2008) prepared spray-dried ketotifen-loaded microspheres using PLA or PLGA and obtained high values of EE and drug loadings: EE of 82% and a drug loading of 91% with PLGA and EE of 75% and drug loading of 83% with PLA.

Furthermore, others micro and nano systems have been described aiming PM encapsulation. These systems presented different EE values:

Kalimouttou and colleagues (2008) prepared PM-loaded PLGA nanoparticles by nanoprecipitation method and evaluated EE varying polymer and solvent amounts. The very low EE measured, lower than 4%, led the authors to conclude that was not possible to encapsulate PM in the nanoparticles.

Ghadiri and co-workers (2011) produced solid lipid nanoparticles containing PM with EE of 39%.

In another study performed by Jaafari and co-workers (2009), PM-loaded liposomes were produced by fusion method. The EE, measured by two different methods (direct and indirect), remained around 60%.

Khan and Kumar (2011a) prepared spray-dried PM-loaded Albumin microparticles with 1:9 drug/polymer ratio and a very high EE of approximately 100%.

Gaspar and colleagues (2015) prepared different PM-loaded liposomes by dehydration and rehydration technique, varying the lipid composition among

batches. EE of PM-loaded liposomes batches ranged from 58 to 97%, depending on the lipid composition.

The PM-MS batches produced in our study showed average values of EE in comparison of PM encapsulation efficiency described in literature using various encapsulation systems.

4.4.2.2.1. Differential Scanning Calorimetry (DSC)

Figure 74 displays the MDSC thermograms of PM-loaded PLGA microspheres (PM-MS06) compared to PM-loaded core-shell PLGA microcapsules (PM-MC12). The thermogram for pure PLGA is also displayed in this figure.

A T_g of 40.8°C was identified for PLGA through rev Heat Flow in the first heating cycle (Figure 74a), moving to 42.2°C in the second heating cycle. These values are close to values of T_g reported in the literature for PLGA 50:50 (ERBETTA *et al.*, 2012; PARK & JONNALAGADDA, 2006).

When analyzing the microparticles produced by spray drying the first cycle of heating reveals the thermal history from the process used to generate them. DSC thermograms for PM-MS06 revealed only a single T_g of 39.79°C in the first heating cycle and of 41.33°C in the second cycle, which is close to the T_g of pure PLGA.

PM-MC12 sample has a higher T_g of 44.08°C in the first heating cycle that moved to 45.68°C in the second cycle. No other thermal events were observed. According to these results, no differences in thermal properties were found between the MDSC thermograms of PM-loaded PLGA microspheres (PM-MS06) compared to PM-loaded core-shell PLGA microcapsules (PM-MC12).

Comparing to some published data, it can be seen that these values are close to the T_g measured during the preparation of PLGA microspheres loaded with another drug (aripiprazole). A T_g of 46.7°C was identified for pure PLGA with a displacement to 50.2°C in presence of the drug (NAKASHIMA *et al.*, 2017). In our case, for PM-MC12, it is difficult to attribute the displacement of T_g to the PM

presence, because the T_g of PM was not identified by our DSC analysis, as already shown in previous section of this chapter.

Table 15 presents the thermal properties of pure PLGA and PM-loaded PLGA microspheres (PM-MS06) and microcapsules (PM-MC12).

Table 15. Thermal properties of pure PLGA, PM-MS06 and PM-MC12.

Batch ¹	1st Heating Cycle		2nd Heating Cycle	
	T_g (°C)	ΔC_p J/g. °C	T_g (°C)	ΔC_p J/g. °C
PLGA	40.80	0.4726	42.24	0.5390
PM-MS06	39.79	0.4974	41.33	0.4533
PM-MC12	44.08	0.4925	45.68	0.4044

Legend: ¹ PM-MS06 was produced with two-fluid nozzle and PM-MC12 with three-fluid nozzle; PLGA 50:50 is the polymeric matrix in both samples; an aqueous solution of PM was introduced in the core liquid formulation.

Figure 75 shows the MDSC thermograms of PM-loaded core-shell PLGA/PLA microcapsules and corresponding blank formulation. The thermogram for pure PLA is also displayed in this figure.

The thermogram of PLA (Figure 75a) showed a single T_g at 59°C in rev Heat Flow analysis. In the nonrev Heat Flow and Heat Flow analyses can be observed an exothermic peak related to PLA crystallization at 73°C followed by an endothermic peak at 170°C, which corresponds to the melting of the polymer.

PM-MC20 and MC24 presented MSDC curves very similar: T_g of polymers around 45°C (rev Heat Flow) and one endothermic event at 169°C corresponding to the melting point of PLA (Heat Flow).

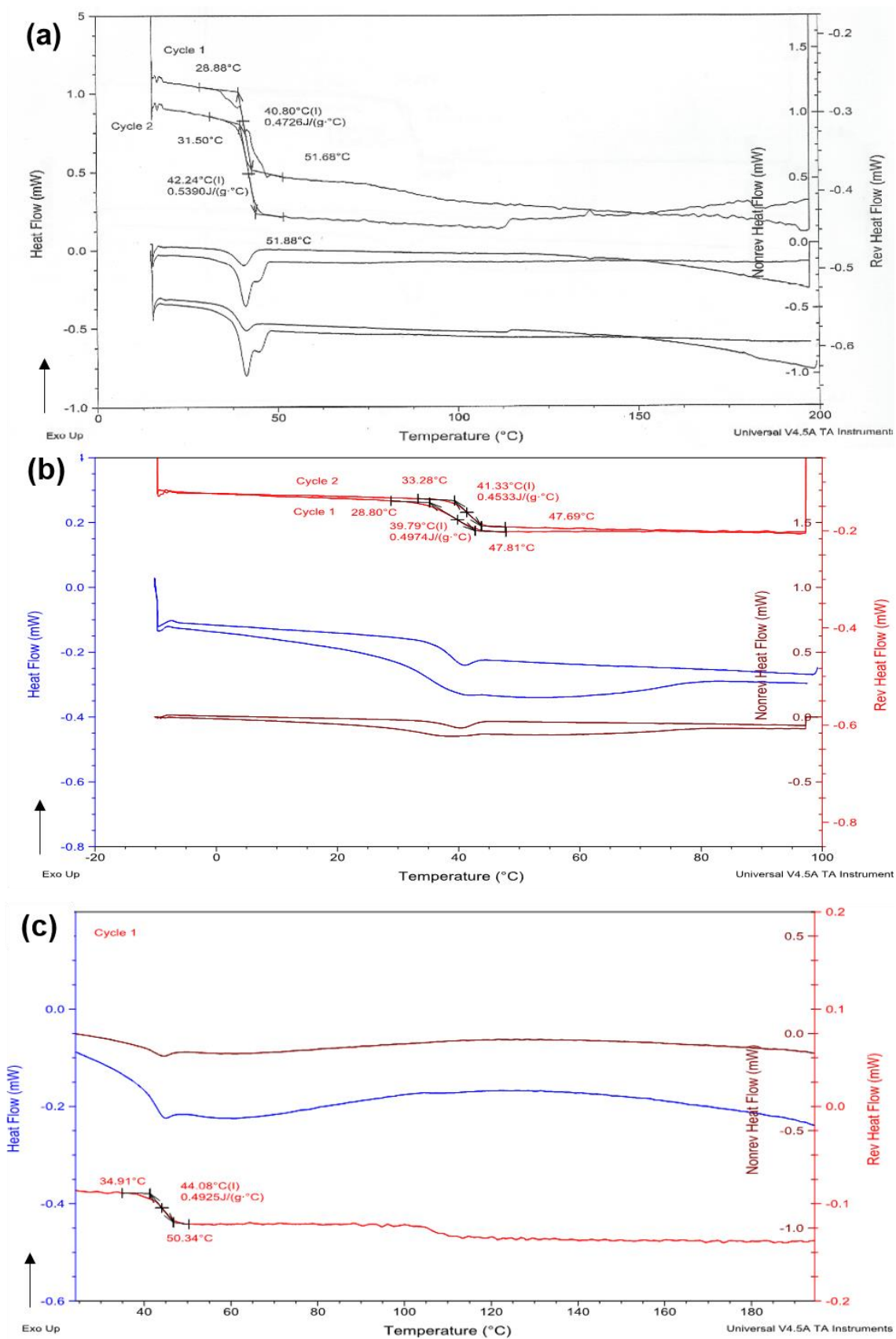


Figure 74. MDSC curves of (a) pure PLGA, (b) PM-loaded PLGA microspheres (PM-MS06) and (c) PM-loaded core-shell PLGA microcapsules (PM-MC12).

Table 16 shows the thermal properties of PM-MC and MC (blank) batches prepared with PLGA/PLA blends. PM-MC22 prepared only with PLA showed the highest T_g (58.89°C in the first cycle) close to the T_g of pure PLA (59.81°C). PLGA-PLA microparticles showed higher T_g than PLGA microcapsules, which could represent an improvement of physical stability under storage conditions.

Table 16. Thermal properties of PM-MC and MC (blank) batches prepared with PLGA/PLA as polymeric matrix.

Batch	1st Heating Cycle		2nd Heating Cycle		T cryst (°C)	ΔH cryst J/g. °C	T fusion (°C)	ΔH fusion J/g. °C
	T_g (°C)	ΔC_p J/g. °C	T_g (°C)	ΔC_p J/g. °C				
PLGA	40.80	0.47	42.24	0.54	-	-	-	-
PLA	59.81	0.45	61.90	0.22	68.54	18.36	170.88	58.02
PM-MC19	43.84	0.59	44.14	0.56	-	-	170.83	2.08
PM-MC20	45.07	0.57	44.56	0.56	-	-	169.96	5.26
PM-MC21	45.88	0.34	43.56	0.39	74.73	1.523	170.23	16.99
PM-MC22*	58.89	0.34	67.51	0.12	69.14	11.22	170.64	37.65
MC23	41.92	1.16	43.19	0.62	-	-	169.16	3.05
MC24	42.93	0.51	42.81	0.55	-	-	169.02	6.83
MC25	46.01	0.42	44.91	0.35	66.74	8.110	169.99	24.76

Legend: * Batch prepared only with PLA

Miscibility between any two polymers in the amorphous state is detected by the presence of a single glass-transition temperature (T_g) intermediate between those of the two component polymers. Immiscibility of two polymers is demonstrated by the retention of the T_g values of both individual components. In Figure 75, the PLGA-PLA blend exhibit a single T_g , as all studied blends. As shown in Table 16, the T_g of the blends (PM-MC219 to PM-MC21) appears to be more or less proportional to the composition of the blend, since the value of the single T_g detected increases by increasing the proportion of PLA (individual

component with a higher T_g). A single T_g could be an indicative of miscibility of the amorphous phase in in the blends. However, DSC curves showed that PLA is partially crystalline (T_m) in these samples.

The thermal properties of PLA and PLGA have been reported in the literature. For example, Lu and Mikos (1999) described that PLA has two enantiomers and can be found in three forms: PDLA (stereoisomer D), PLLA (stereoisomer L) and PDLLA (racemic mixture). PLLA has a T_g between 52.85-63.85°C and a melting point between 144.85-185.85°C.

Kim and Park (2004) investigated the sustained release of human growth hormone encapsulated in PLA, PLGA and PLGA-PLA blend prepared by solvent evaporation method. They identified a T_g of PLA at 32°C with melting point at 145°C and a T_g of PLGA at 28°C. However, they did not characterize the thermal properties of the PLGA-PLA blends.

Farah and co-workers (2016) described a T_g for PLLA at 55-65°C and the melting point between 170-200°C. Our data (T_g and T_m for PLA) shown in Table 16 are falling within this range.

In contrast, the study of Park and Jonnalagadda (2006) showed T_g values of PLA (41.9°C in first heating cycle and 45.3°C in second heating cycle) lower than those given in Table 16. This difference could be related to intrinsic viscosity of the PLA used (0.39 dl/g for Park's study and between 0.8 dl/g and 1.2 dl/g for PM-MC batches).

Some PLGA blends have been reported in the literature: Lin and co-workers (2012) evaluated a novel risperidone-loaded PLGA-sucrose acetate isobutyrate for sustained release injection depot. A polymer mixture composed of PDLLA, PGA and PCL (40:40:20) was used in another study. The experimental value of T_g found for this blend was 21.8 °C (LIU, BAI, LIANG, 2016).

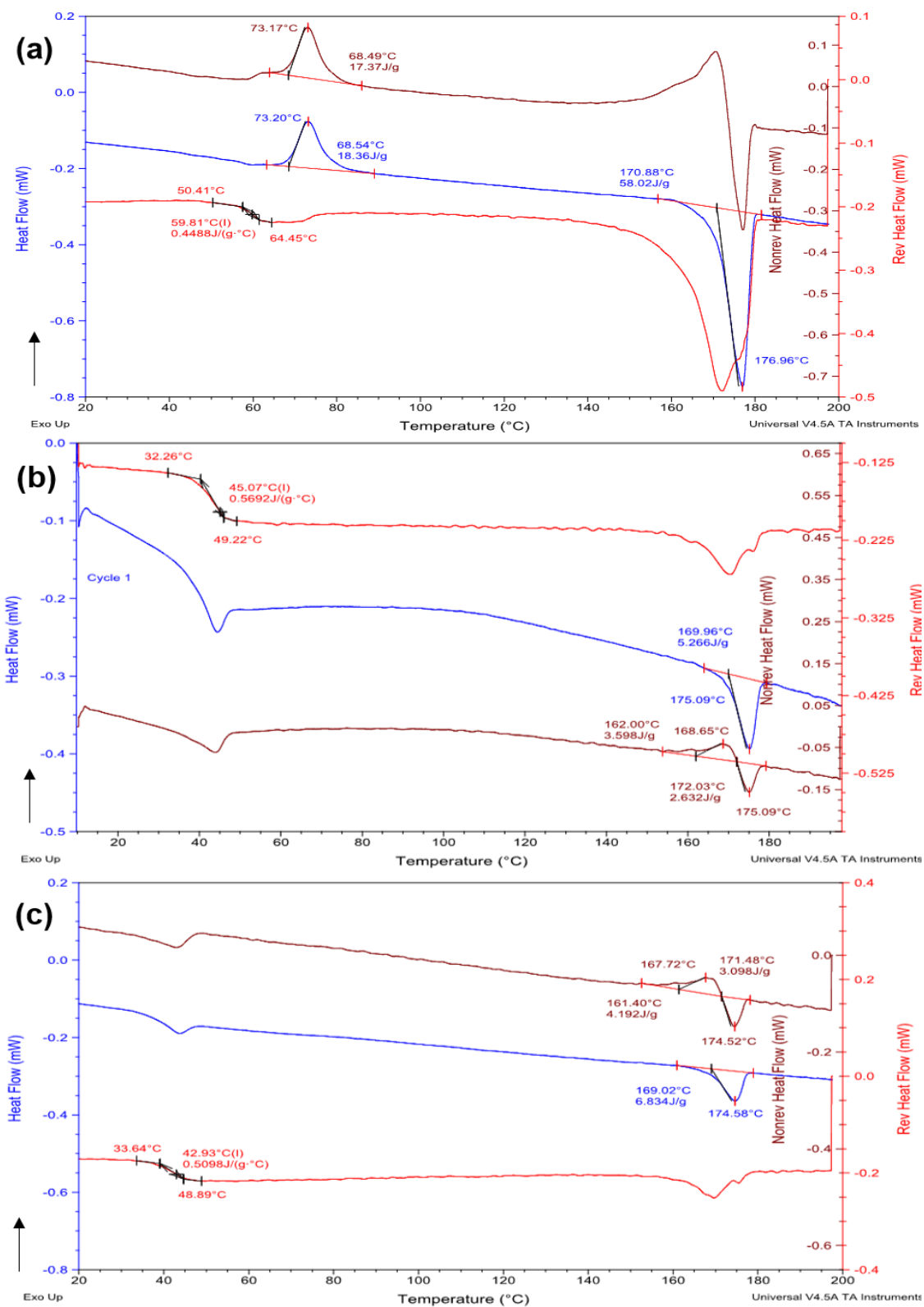


Figure 75. MDSC curves of (a) pure PLA, (b) PM-loaded core-shell PLGA/PLA microcapsules (PM-MC20) and (c) PLGA/PLA blend microparticles (MC24).

4.4.2.2.2. Scanning Electron Microscopy (SEM)

Figure 76 shows SEM images of PM-loaded PLGA microspheres (PM-MS06) compared to PM-loaded core-shell PLGA microcapsules (PM-MC12 and PM-MC16). The difference between PM-MC12 and PM-MC16, both produced with the three-fluid nozzle, was the PM solid state in the feed solution: PM-MC12 was produced from PM dissolved in water in the core feed, while PM-MC16 was produced from a liquid core containing PM dispersed in acetone. PM-C18 contains a higher load of PM (28.9%wt) than PM-MS06 (6.9%).

SEM images show particles very similar to raw PM particles (see Figure 63) in both MC and MS samples prepared from raw PM particles dispersed in acetone. They are mixed to smaller particles, which sometimes are adhered to their surface (see higher magnifications).

The sample PM-MC12, prepared from an aqueous solution of PM fed into the 3-fluid nozzle to generate the particle core, seems to be constituted by smaller particles, very agglomerated.

PM-loaded microcapsules were also generated using a blend of PLGA and PLA instead of PLGA alone. Three different compositions were tested, the PLA content varying from 5% to 40% in the polymeric mixture. Microcapsules prepared with PLGA-PLA blends are shown in Figure 77. It can be observed that they are characterized by smaller particles with smooth surface, also very agglomerated and the shape seemed to be influenced by the PLA content.

PM-MC22 was generated with PLA alone. The sample showed a distinct morphology (Figure 78), with irregular wrinkled shape and porous surface, and agglomerates. Similar morphologies were already found for other spray-dried PLA microparticles encapsulating sodium monofluorophosphate (ZUO *et al.*, 2017), methotrexate (OLIVEIRA *et al.*, 2017) or ketotifen (GUERRERO *et al.*, 2008).

These batches were investigated subsequently by other characterization techniques and the results will be discussed later in this chapter.

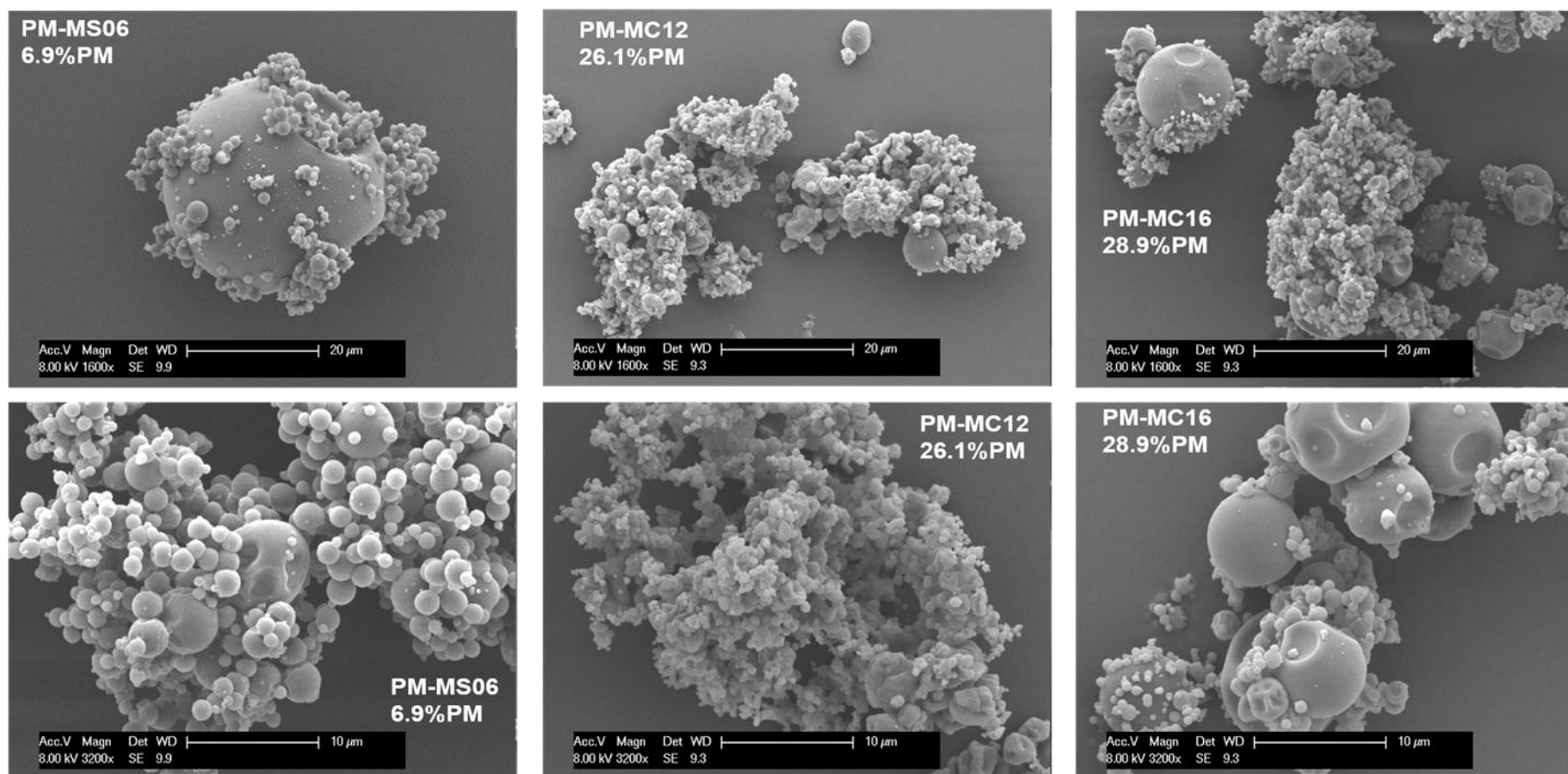


Figure 76. SEM Images of some batches prepared with acetone in two different magnifications varying the nozzle type: two-fluid PM-MS06 and three-fluid (PM-MC12 and PM-MC16).

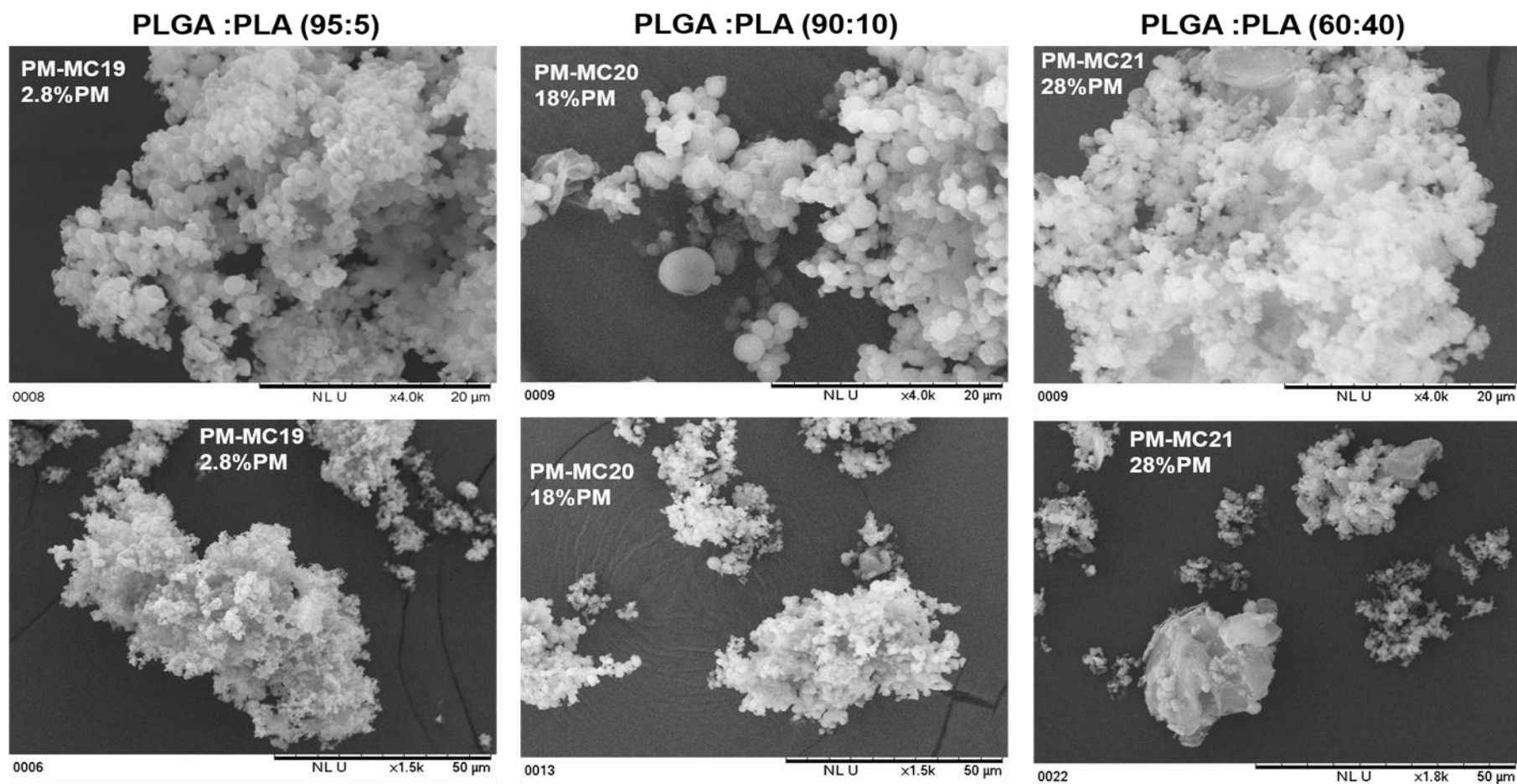


Figure 77. SEM images of some batches prepared from an aqueous of PM, three-fluid, with different compositions of PLGA/PLA blends: PM-MC19 (95:5), PM-MC20 (90:10) and PM-MC21 (60:40).

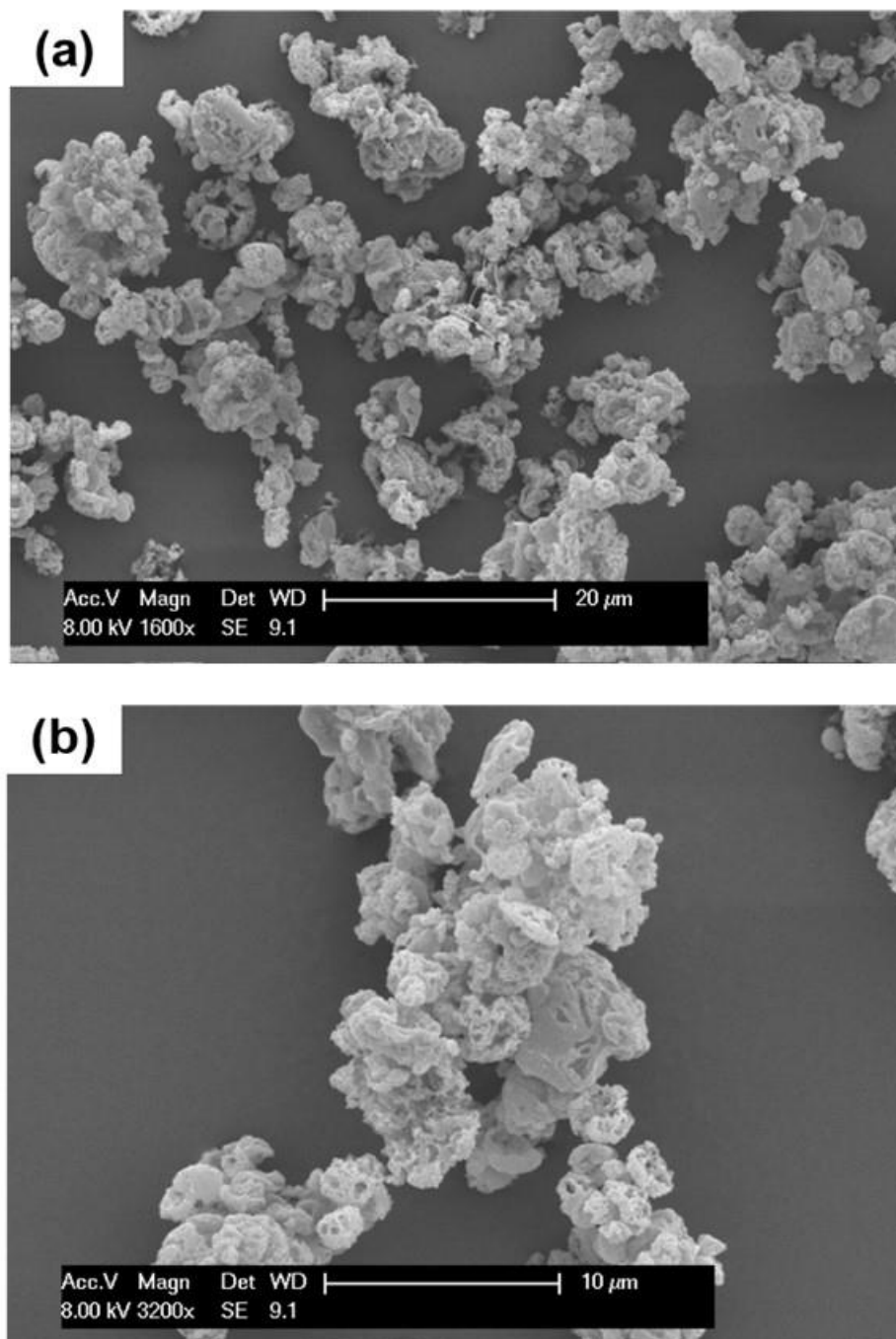


Figure 78. SEM Images of PM-MC22 prepared with dichloromethane: acetone in two different magnifications: (a) 1600x, (b) 3200x.

4.4.2.2.3. Fourier Transform Infrared Spectroscopy (FTIR)

Figure 79 shows the FTIR spectra of PLGA pure, PM pure, physical mixture PM+PLGA, PM-MS06 (produced by two-fluid nozzle), PM-MC12 (three-fluid nozzle, core fed by PM solubilized in water and shell fed by the organic solution) and PM-MC18 (three-fluid nozzle, core fed by PM dispersed in acetone and shell fed by the organic solution). These samples were chosen for comparison of PM-MS microspheres with PM-MC microcapsules.

The PLGA spectrum showed peaks at 2997 cm^{-1} and 2917 cm^{-1} (CH_2 stretch), 1750 cm^{-1} ($\text{C}=\text{O}$ stretch), 1380 cm^{-1} ($\text{CH}_2\text{-CH}$ wagging vibration) and at 1180 cm^{-1} and 1098 cm^{-1} (C-O stretch, ester group), similarly to characteristic peaks reported in the literature (ERBETTA *et al.*, 2012; SILVA-JUNIOR *et al.*, 2009). The PM spectrum showed characteristic peaks at 3408 cm^{-1} (NH_2 amine group), at 1632 cm^{-1} (N-H bending coupled with C-N stretch), at 1534 cm^{-1} (CH_2 bending) and at 1027 cm^{-1} (C-O-C stretch), also in line with characteristic peaks previously reported for PM (KHAN & KUMAR, 2011 a,b). Some characteristic peaks of both PM and PLGA can be seen in the PM-PLGA physical mixture.

PM-MS06 presented peaks at 3380 cm^{-1} (NH_2 amine group), 1080 cm^{-1} (C-O-C stretch) corresponding to PM peaks and at 2990 cm^{-1} , 2940 cm^{-1} (CH_2 stretch), 1750 cm^{-1} ($\text{C}=\text{O}$ stretch) corresponding to PLGA peaks ((b) in Figure 79). By its turn, PM-MC12 and PM-MC18 presented similar spectra when compare to PM-MS06 differing only in peaks intensity at 2990 cm^{-1} and 2940 cm^{-1} (CH_2 stretch, corresponding to PLGA peaks) ((a) in Figure 79) and in the range of 1380 cm^{-1} to 1040 cm^{-1} ((c) in Figure 79). These ranges presented peaks corresponding to PM and PLGA, in which PM-MS06 showed broader band than PM-MC12 and PM-MC18.

To conclude, the absence of new IR peaks and the maintenance of characteristics peaks of drug and polymer suggest no chemical interactions between PM and PLGA.

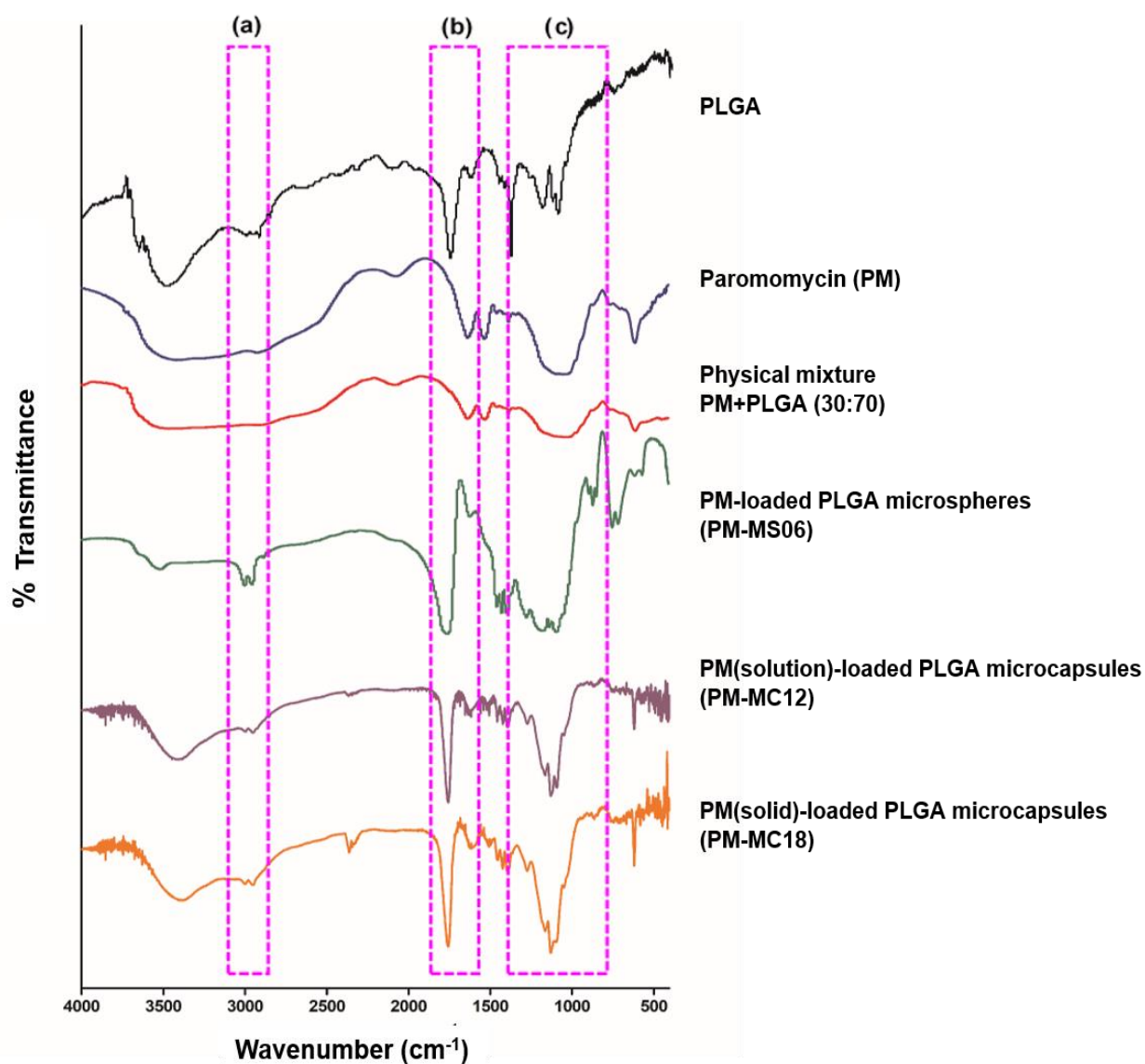


Figure 79. FTIR spectra of pure components (PLGA and PM), physical mixture PM+PLGA (30:70) and microparticles samples (PM-MS06, PM-MC12 and PM-MC18).

The effect of PLGA/PLA blends was also investigated by FT-IR analysis. Figure 80 shows the FTIR spectra of PLA pure, physical mixture PLA+PLGA, physical mixture PM+PLA+PLGA (30:5:65), PM-MC19 (produced with 5% of PLA) and MC23 (blank microparticles). These samples were chosen to represent the results found in PM-MS batches prepared with PLGA/PLA blend.

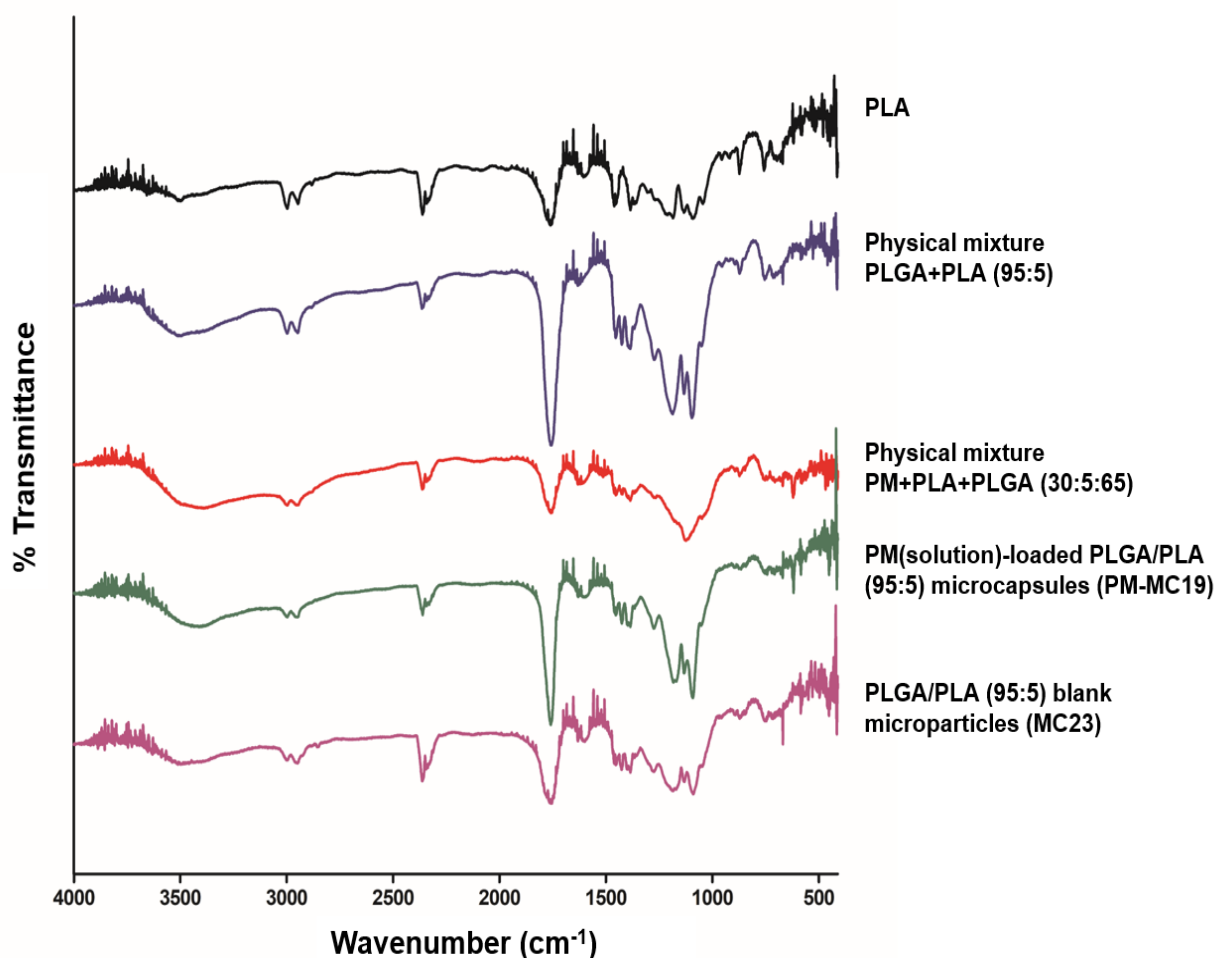


Figure 80. FTIR spectra of pure PLA, physical mixture PLGA+PLA (95:5), physical mixture PM+PLA+PLGA (30:5:65), PM microparticles (PM-MC19) and blank microparticles (MC23).

PLA spectrum showed characteristics peaks at 2989 cm^{-1} and 2939 cm^{-1} (CH_2 stretch), 1750 cm^{-1} ($\text{C}=\text{O}$ stretch), 1448 cm^{-1} and 1369 cm^{-1} ($\text{CH}_2\text{-CH}$ wagging vibration) and at 1175 cm^{-1} and 1077 cm^{-1} (C-O stretch, ester group), in accordance with literature (OLIVEIRA *et al.*, 2017; LU & MIKOS, 1999).

Physical mixtures (PLA+PLGA and PLA+PLGA+PM), PM-MC19 and MC23 showed FTIR spectra similar to PLA, varying only in intensity (especially at 1750 cm^{-1} corresponding to $\text{C}=\text{O}$). However, it is not possible to relate the peaks observed in samples to PLA or PLGA, because the polymers presented similar chemical structures and similar IR spectra as already reported by Kang and co-workers (2008). The results also suggested no chemical interactions between PLGA/PLA blends and PM.

4.4.2.2.4. Particle Size

The particle size of some batches was measured by laser granulometry as described in 4.3.2.3.5. All PM-MS/PM-MC batches presented small individual particles (lower than 10 μm), however, very agglomerated. Table 17 shows particle size distribution and span of some PM-MC batches prepared with three-fluid nozzle. As particles are hardly separated, the mean particle size should be viewed cautiously.

Table 17. Particle size distribution and Span of some PM-MC batches.

Batch	d_{10} (μm)	d_{50} (μm)	d_{90} (μm)	Span*
PM-MC12	2.24 ± 0.06	5.77 ± 0.17	19.5 ± 1.13	3.00 ± 0.10
PM-MC13	2.59 ± 0.01	7.26 ± 0.03	21.7 ± 0.21	2.62 ± 0.05
PM-MC14	1.76 ± 0.00	3.38 ± 0.01	6.53 ± 0.02	1.41 ± 0.00
PM-MC15	2.17 ± 0.01	5.58 ± 0.02	20.4 ± 0.64	3.30 ± 0.09
PM-MC16	2.95 ± 0.03	12.6 ± 0.28	44.6 ± 2.55	3.29 ± 0.12
PM-MC17	4.19 ± 0.02	23.7 ± 0.28	67.2 ± 0.85	2.66 ± 0.00
PM-MC18	3.78 ± 0.03	20.9 ± 0.14	62.7 ± 0.64	2.82 ± 0.06

Legend: * - Span = $(d_{90} - d_{10})/d_{50}$

Table 17 shows that batches prepared with PM dissolved in water (PM-MC12, PM-MC13, PM-MC14 and PM-MC15) had smaller mean particles size ($d_{50} < 7.3 \mu\text{m}$) than batches prepared with PM dispersed in acetone (PM-MC16, PM-MC17 and PM-MC18) ($d_{50} > 12 \mu\text{m}$).

PM-MC12 presented results very similar to PM-MC15, its replicate. However, comparing PM-MC16 and its replicate (PM-MC18), it was possible to observe different results. The trouble of particles agglomeration and difficulty of particles dispersion probably explain the difficulty to reproduce particle size and span results. This finding indicates that PM dissolved in water provides smaller microcapsules than PM dispersed in organic solvent.

The literature gives some information about particle size of spray-dried PLGA microparticles. Lin and co-workers (2005) evaluated the particle size distribution of spray-dried doxorubicin-loaded PLGA microparticles using a similar laser diffraction method adopted to PM-MS batches. They analyzed particles dispersed in deionized water under sonication and obtained particles in the range of 2-5 μm . Wan and co-workers (2014b) investigated the particle size distribution of spray-dried bovine serum albumin-loaded PLGA microparticles using a laser diffraction method. The particles were dispersed in water under sonication before measurement and got particles with d_{50} between 5 and 11 μm and span in the range 1-2.

Wang and co-workers (2015) evaluated the particle size distribution of gycyrrhetic acid PLGA microparticles obtained by oil-water emulsion. The particles were dispersed in water containing 0.5% of PVA and 0.1% of Tween[®] 80 under sonication and analyzed by laser diffraction method. They produced particles with mean size around 40 μm , which are bigger than microparticles obtained by spray-drying. Spray drying is seen as a technique available to reduce and control particle size compared to techniques such as emulsification-solvent evaporation also used to produce drug-loaded PLGA microparticles (SOLLOHUB & CAL, 2010).

4.4.3. IN VITRO RELEASE OF PAROMOMYCIN POLYMERIC MICROPARTICLES

Based on the characteristics of the batches produced in this study, the choice of PM-MS/PM-MC formulations was made for *in vitro* release study.

The batches selected were PM-MC15 (PM-MC12 replicated), PM-MC20, PM-MC18 and PM-MS06. Free drug and a physical mixture of PM and PLGA (30:70) were also subjected to the same *in vitro* test. For remembering, Table 18 summarizes the initial composition of PM-MS/PM-MC batches selected and some characteristics of the products.

Table 18. Composition of PM-MS/PM-MC batches selected and their characterization

Batch ¹	Composition of batches				Characterization		
	Inner solution		Outer solution		Yield (%)	EE ² (%)	DL ³ (%)
PM (g)	Solvent/ Volume (g)	Polymer (g)	Solvent/ Volume (g)				
PM-MS06	0.65	-	1.5 g PLGA	97.85 g ACE ⁴	35.30	23.01	6.90
PM-MC15	1.03	49.97 g Water	2.4 g PLGA	157.60 g ACE ⁴	60.65	75.27	22.58
PM-MC18	0.77	29.23 g ACE ⁴	1.8 g PLGA	118.20 g ACE ⁴	40.32	64.81	21.94
PM-MC20	1.03	49.97 g Water	2.16 g PLGA / 0.24 g PLA	137.60 g ACE ⁴ / 20.00 g DCM ⁵	32.11	60.29	18.09

Legend: ¹ PM-MS06 (raw PM powder fed into the 2-fluid nozzle); PM-MC15 (PM-MC12 replicated, PM in solution fed to the 3-fluid nozzle, PLGA), PM-MC18 (raw PM powder fed to the 3-fluid nozzle) and PM-MC20 (PM in solution fed to the 3-fluid nozzle, PLGA:PLA mixture 90:10); ² Encapsulation efficiency; ³ Drug loading content; ⁴ Acetone; ⁵ Dichloromethane.

The percentage of PM released for each sample per hour of released test is given in Table 19. Dissolution efficiencies at the end of the experimental test (DE_{4h}) are also given in Table 19.

PM-MS06, PM-MC15 and PM-MC18 showed fast release with higher than 66% of drug released in the first hour, corresponding to DE higher than 70% (see Table 19). The same behavior was observed for free PM and the physical mixture. Nonetheless, PM-MC20 displayed a slower PM release rate reaching approximately 34% of drug release in 4h (Table 19) and DE of 27.5%.

For comparative purposes, Khan and Kumar (2011a) verified a biphasic

release profile of PM from albumin microspheres with an initial burst release of 50-60% of drug released in 2 h.

Table 19. % PM released per hour of released test and dissolution efficiency after 4 hours (DE_{4h})

Batch ¹	Time (h)			DE _{4h}
	1	2	4	
Free PM	76.62 ± 4.75	90.33 ± 1.86	90.60 ± 2.46	75.68
PM: PLGA physical mixture	71.77 ± 9.58	94.72 ± 10.06	98.35 ± 4.89	78.05
PM-MS06	70.30 ± 2.37	83.91 ± 1.82	84.14 ± 3.50	70.08
PM-MC15	66.13 ± 1.98	98.68 ± 2.87	100.00 ± 1.58	78.54
PM-MC18	78.34 ± 12.24	98.88 ± 2.87	100.00 ± 1.58	81.66
PM-MC20	30.32 ± 0.35	30.11 ± 0.33	34.35 ± 0.42	27.46

Legend: ¹ Physical Mixture PM:PLGA (30:70); PM-MS06 (raw PM powder fed into the 2-fluid nozzle); PM-MC15 (PM-MC12 replicated, PM in solution fed to the 3-fluid nozzle, PLGA), PM-MC18 (raw PM powder fed to the 3-fluid nozzle) and PM-MC20 (PM in solution fed to the 3-fluid nozzle, PLGA:PLA mixture 90:10) (n=3).

To investigate the mechanism of drug release, the % cumulative PM from these different structures (MS and MC) were fitted in Korsmeyer-Peppas model. Nonlinear regressions were applied for cumulative dissolved PM. The coefficient of determination (R^2), root-mean-square error (RMSE) and Akaiik's information criterion (AIC) values were determined using Kinet DS 3.0 rev. 2010 software. The data obtained from Korsmeyer-Peppas for all dissolution experiments are listed in Table 20.

Table 20. Kinetic parameters of PM-MS/PM-MC batches using Korsmeyer-Peppas model.

Batch	Korsmeyer-Peppas model				
	K (min ⁻¹)	R ²	n	AIC ¹	RMSE ²
PM-MS06	41.19	0.9987	0.14	18.44	3.04
PM-MC15	25.02	0.9992	0.26	25.11	7.00
PM-MC18	41.15	0.9989	0.17	21.10	4.24
PM-MC20	17.37	0.9986	0.12	10.38	1.11

Legend: ¹ Akaike Information Criterion calculated from Equation 3, Table 10 (item 4.3.2.4.1); ² Root Mean Squared Error calculated from Equation 2, Table 10 (item 4.3.2.4.1).

The four PM-loaded batches showed high values of coefficient correlation ($r^2 > 0.9986$), which means a good correlation fit with experimental values and predicted values. Moreover, the AIC and RMSE values are small, which means that these criteria confirms Korsmeyer-Peppas as a good model to fit PM-MS/PM-MC batches. The comparison between predicted drug release and experimental drug release for each batch was shown in Annex 2 in this work.

According to Korsmeyer-Peppas model, it is possible to characterize the drug release mechanism based on release exponent (n) values. If n value is equal or lower than 0.5, the release mechanism follows Fickian diffusion. If n value is between 0.5 and 1, the release mechanism follows a non-Fickian model named anomalous transport. If n value is equal to 1, the release mechanism is Case-II transport, while n value higher than 1 corresponds to super Case-II transport (CARMELLO *et al.*, 2016; DASH *et al.*, 2010; COSTA, 2002; COSTA & LOBO, 2001).

The four samples showed “ n ” values lower than 0.5, which indicates that

PM release mechanism follows Fickian diffusion model (CARMELO *et al.*, 2016; DASH *et al.*, 2010; COSTA, 2002). Based on this model, the solvent diffusion into polymeric matrix is faster than polymer relaxation and drug get out of particles by diffusion (BRUSCHI, 2015). As introduced earlier in this chapter, PLGA is a bulk-eroding polymer and during the polymer erosion, the water uptake into the matrix is higher than polymer degradation rate (hydrolysis). Consequently, water uptake promotes drug diffusion from outside the particles (HAN *et al.*, 2016; KAPOOR *et al.*, 2015; MAKADIA & SIEGEL, 2011). In addition, formulations properties affecting release from PLGA microparticles include their size (large particles have small initial burst release with slow release than smaller particles) and drug load (low drug content allows slow burst release), besides the solubility of the drug in the release medium. A small individual particle size (in the order of a few microns) and a drug load of 18-24% could be in part responsible for the rapid release. Moreover, PM is a very water-soluble drug and its release will be fast if the drug is not protected by a polymeric matrix.

In an effort to explain the unexpected fast release from PLGA PM-MS06, PM-MC15 and PM-MC18 samples, additional characterizations were performed and are presented and discussed in the next section.

4.4.4. SPATIAL DISTRIBUTION OF CONSTITUENTS IN PM-MS AND PM-MC MICROPARTICLES

In order to investigate the spatial localization of polymer and drug in the microparticles, different techniques described in item 4.3.2.5 were associated: Raman mapping and SEM analyses after contact with water during 24h, aiming to remove PM not encapsulated.

Figures 81 to 83 display respectively SEM images of PM-M06 microspheres, PM-MC15 and PM-MC18 microcapsules, before and after contact with water during 24h. This test aimed to release PM not protected by PLGA and then allow the observation of the solid structure after the possible PM release.

Figure 81 shows some particles with more porous structure or voids that could be created by the release of PM. In Figures 82 and 83, in the samples

exposed to water, some bigger particles like the ones visible in Figure 82(top left), seem to have disappeared.

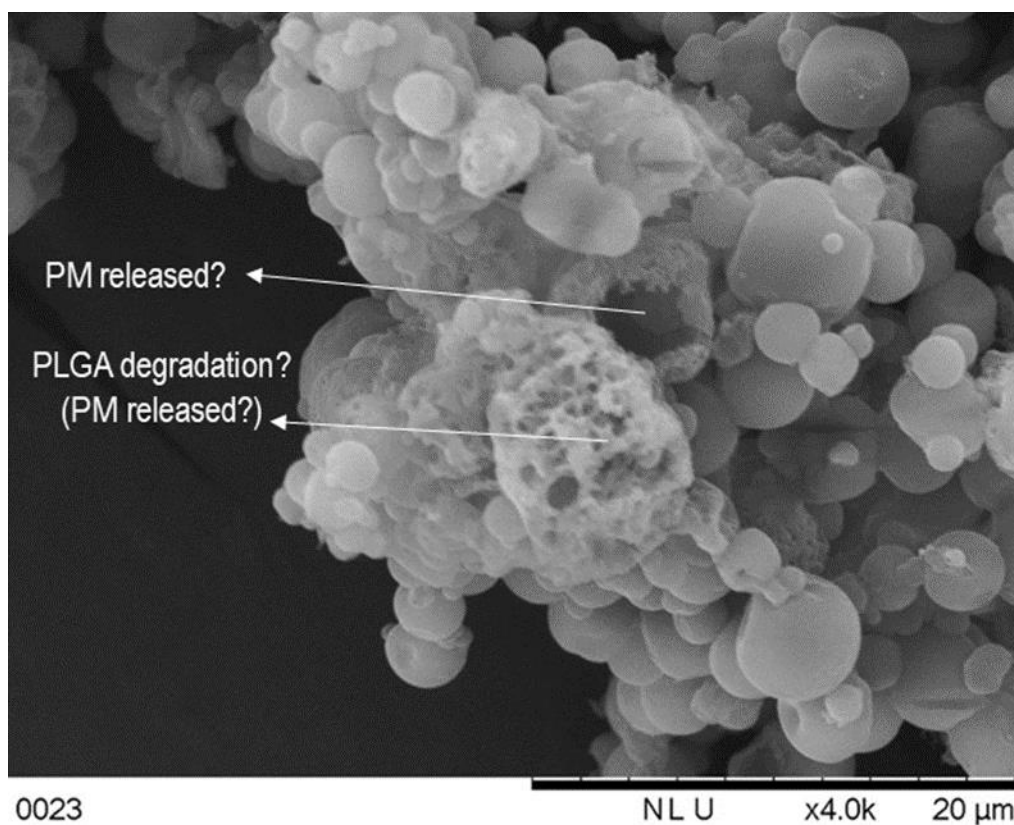


Figure 81. PM-MS06 microspheres, after contact with water for 24h.

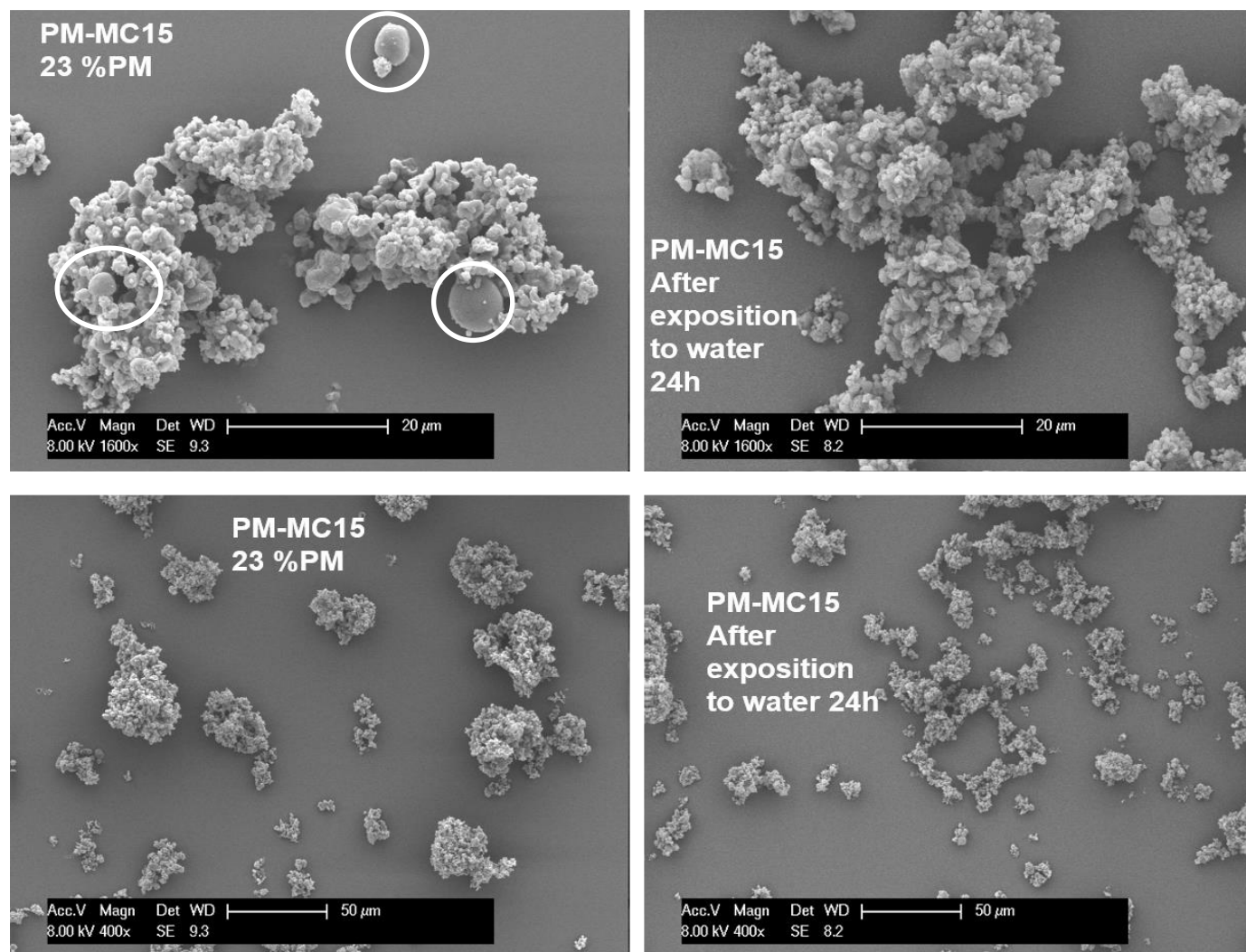


Figure 82. PM-MC15 microcapsules, before and after contact with water for 24h.

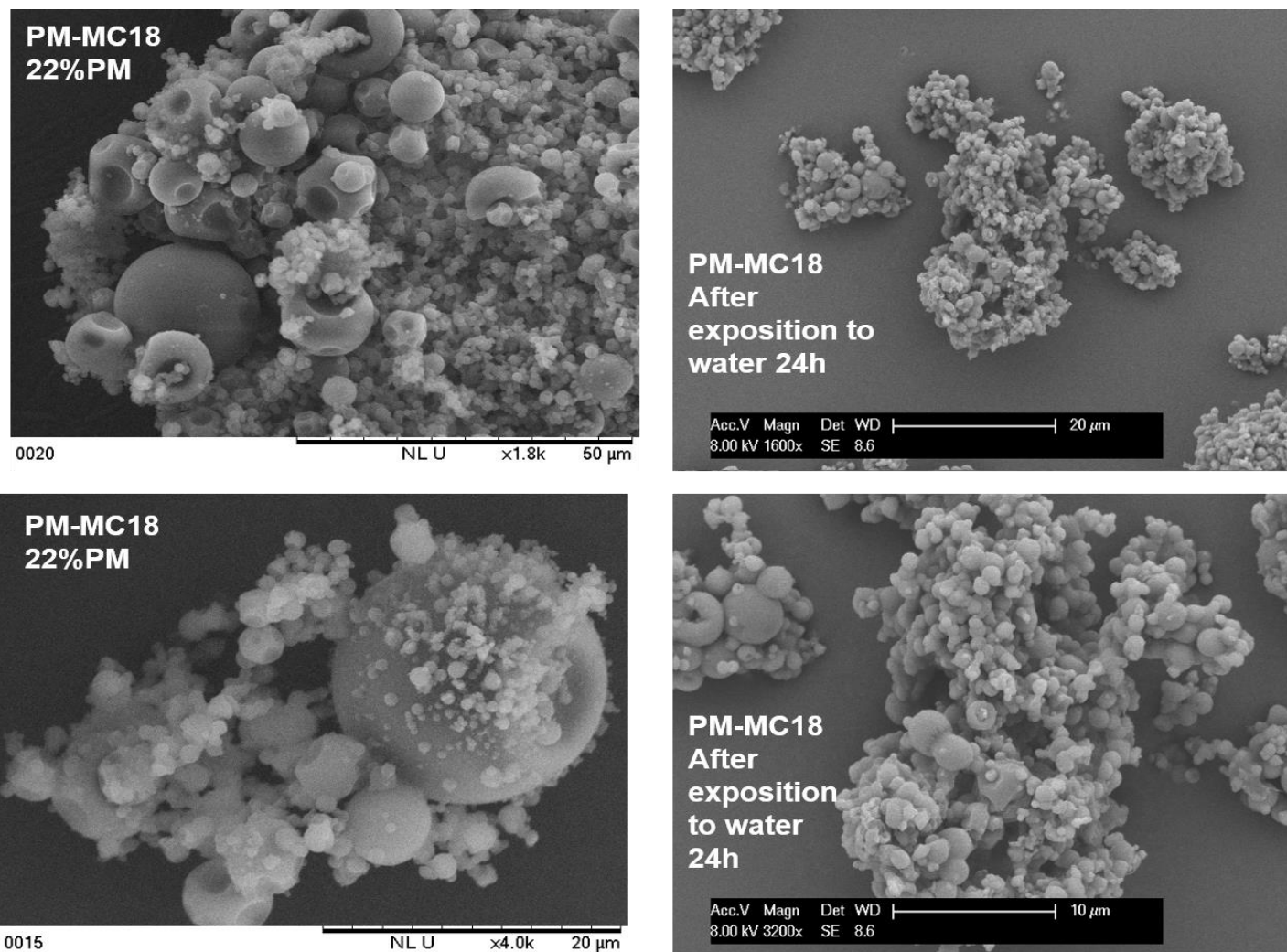


Figure 83. PM-MC18 microcapsules, before and after contact with water for 24h.

Figure 84 shows the spatial distribution of PM and polymer mapped by Raman spectroscopy in studied samples, PM-MS06, PM-MC12 (replicate of PM-MC15), PM-MC16 (replicate of PM-MC18) and PM-MC20. The Raman spectra of PLGA and PM are also presented in this figure.

PLGA Raman spectrum presented some characteristics peaks in the range of 800-1200 cm^{-1} , around 1400 cm^{-1} , between 1700-1800 cm^{-1} and strong peak between 2800-3100 cm^{-1} , corresponding to C-O stretch, C-H bend, C=O stretch, C-H stretch, respectively. These peaks can be related to peaks observed in PLGA IR spectrum. However, the strong peak in Raman is linked to C-H bond because OH⁻ has weak signal in Raman spectra (LARKAN, 2011).

Sanna and co-workers (2012) developed PLGA nanoparticles of resveratrol and analyzed the Raman spectra of components. The PLGA spectrum presented peaks at 2882 cm^{-1} , 2946 cm^{-1} and 3000 cm^{-1} related to C-H stretching, at 1766 cm^{-1} related to C=O bond stretching, peak at 1130 cm^{-1} and 1044 cm^{-1} corresponding to C-O stretching and one peak at 1453 cm^{-1} corresponding to C-H bend. Yan and co-workers (2015) investigated PLGA nanoparticles with hydrophobic drugs. The Raman spectrum of polymer showed peaks at 2930 cm^{-1} , 2960 cm^{-1} corresponding to CH₃ stretch of lactic acid, at 2884 cm^{-1} related to C-H stretch of lactic acid, at 2850 cm^{-1} related to CH₂ stretch of glycolic acid. It was also observed: - a peak at 1635 cm^{-1} corresponding to C=O stretch; - peaks between 1400-1500 cm^{-1} related to C-H bend; - peak at 1296 cm^{-1} related to C-H stretch and peaks between 1130-1000 cm^{-1} corresponding to C-O-C stretch. Wang and co-workers (2016) evaluated microspheres of PLGA or Pluronic® F127 + PEG containing exenatide and prepared by double emulsification and solvent evaporation. They evaluated the Raman spectra of pure substances and of the microparticles and observed that PLGA spectrum had a strong peak in the range of 2500-3000 cm^{-1} and six small peaks between 800 and 1500 cm^{-1} . These studies have identified the same Raman spectrum of PLGA showed in Figure 84.

Figure 84 allows the analysis of the spatial distribution of PLGA and PM in the microparticles prepared using two-fluid and three-fluid nozzle. The PM-loaded PLGA microspheres (MS06) (a) showed PM (in red) partially surrounded by the polymer (in blue). On the other hand, the batches of core-shell microcapsules

prepared with three-fluid nozzle (PM-MC12, PM-MC16 and PM-MC20) showed spherical spots of PM surrounded by PLGA, suggesting a core-shell structure. A core-shell structure should be advantageous for PM, since this drug presents some limitation as degradation susceptibility.

Raman mapping and analysis of SEM images after possible removal of PM of the solid structures give some information about them. The expected structures for PM-MS and PM-MC particles are schematically represented in Figure 85a and b, respectively.

PM-MS06 is the selected batch prepared with two-fluid nozzle to compare results with batches prepared with three-fluid nozzle. This batch presented a structure with low drug content and low encapsulation efficiency (%DL around 7%; %EE around 23%, see Table 18) and, in Raman analysis, drug and polymer appeared side by side, without the expected 'matrix' structuration illustrated by Figure 85a. PM-MS06 showed a fast release in the first hour. This release is, probably, related to how PM is dispersed in PLGA matrix. PM-MS06 has the possible structure showed in Figure 85c, in which small particles of PLGA, formed during spray drying, are not able to entrap the bigger particles of raw PM dispersed in the liquid formulation.

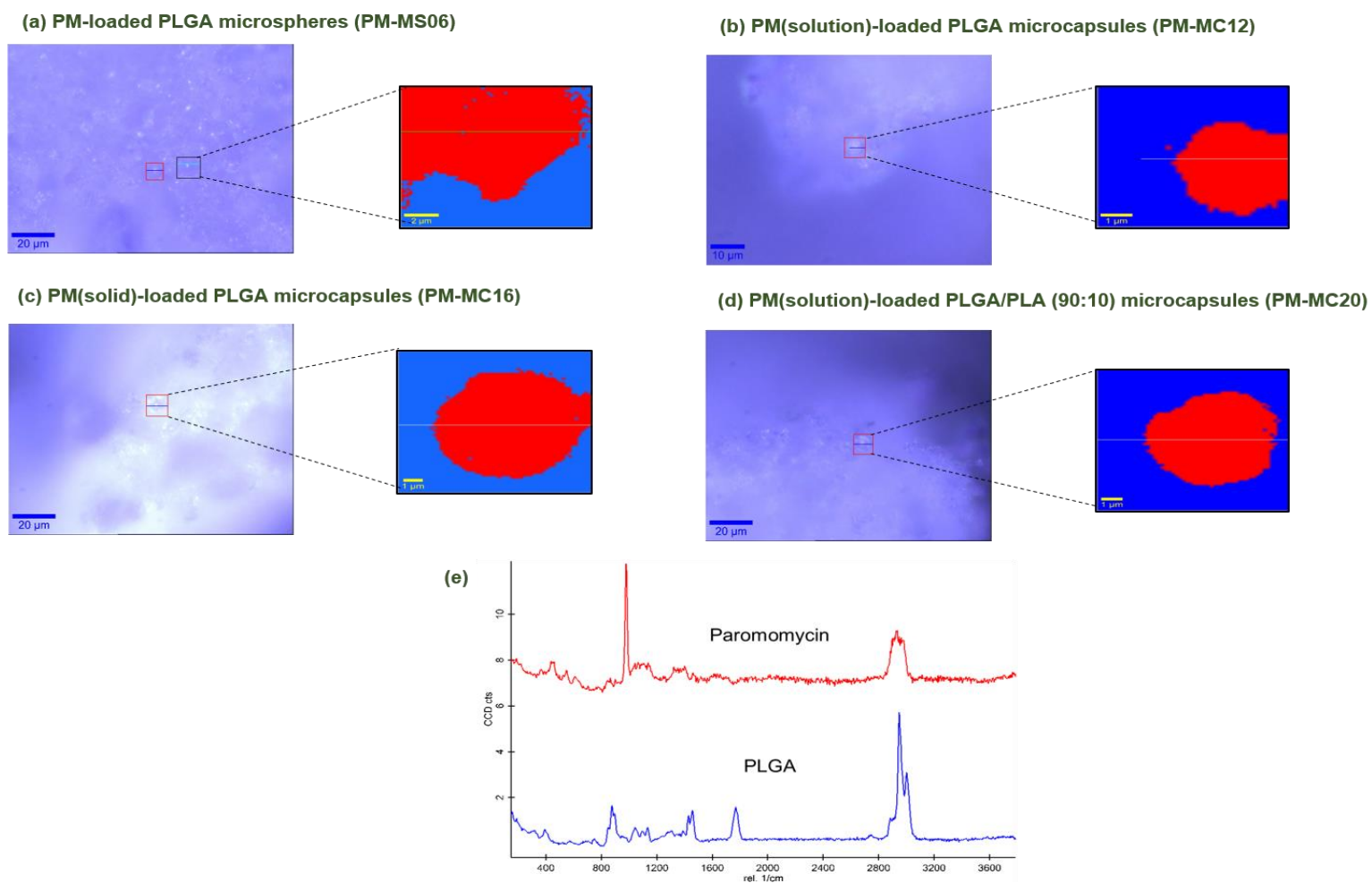


Figure 84. Raman images of spatial distribution of some PM-MS/PM-MC batches (a) PM-MS06, (b) PM-MC12, (c) PM-MC16 and (d) PM-MC20; (e) Raman spectra of Paromomycin (red) and PLGA (blue) with correspondent colors to identify polymer and drug in spatial distribution.

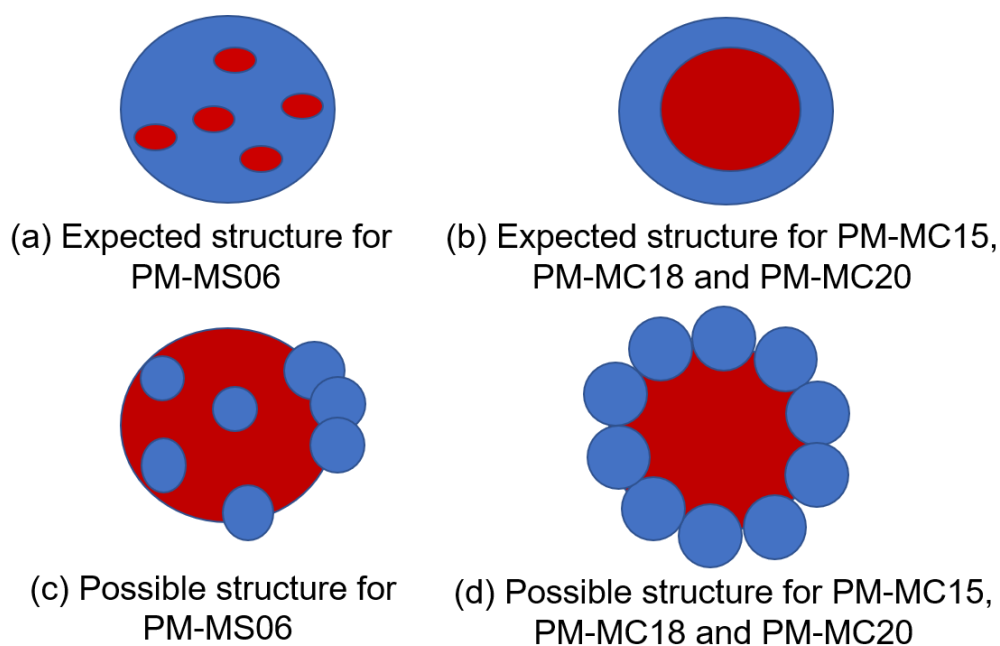


Figure 85. Possible structure of PM-MS/PM-MC batches based on Raman analysis. Legend: red – corresponding PM and blue – corresponding polymer.

Nonetheless, PM-MC15 and PM-MC18, both prepared with three-fluid nozzle (varying only in relation to drug solution/dispersion), presented similar release profiles with fast release in the first hour (between 66 and 78%). The microparticles structure of these two batches are probably core-shell like, as observed by Raman mapping. Apparently, the PLGA shells of PM-MC15 and PM-MC18 exhibited pores, as schematically represented in Figure 85d, which allow fast PM release in the beginning of release assay.

One of the theories proposed to describe the particle formation process via spray drying with a 3-fluid nozzle is that two liquids would form an 'emulsion mixture' upon atomization (WAN *et al.*, 2014a). When a miscible solvent like acetone is applied in the 3-fluid nozzle, the two feeds (inner and outer feed) mix intimately to make a 'transient film' which then break up into micro-droplets. According to this theory, particle formation is initiated by the formation of a transient liquid PLGA film at the interface between the aqueous (inner feed) and the organic solution (outer feed), which is a result of mass transfer between the organic solvent and water, leading to a decrease in the solubility of the polymer

in the solvents. In the case that the transitional liquid PLGA film appears instantaneously once the organic PLGA solution comes into contact with the aqueous solution, it forms irregular PLGA aggregates in the subsequent drying process. The use of organic solvent with a low surface tension and a certain degree of miscibility with water causes the instant phase separation of the PLGA film (WAN *et al.*, 2014a), which could explain the formation of a structure like that illustrated in Figure 85c. In other words, use of acetone as organic solvent produces more irregular PLGA aggregates resulted from lower surface tension between acetone and water, which promotes fast spreading rate of solvent on the aqueous droplets surface (WAN *et al.*, 2014a). Then, the particles produced with acetone from 3-fluid nozzles and PLGA solution (PM-MC15 and PM-MC18) were more porous. The pores provided PM passage for receptor chamber that is composed of water medium (PBS) being favorable for drug dissolution (PM is highly hydrophilic).

PM-MC20 was prepared with a polymer blend comprising PLGA (90%) and PLA (10%) and had a core-shell structure, possibly close to that illustrated in Figure 85b. The slow release of PM from this sample could be due to a slow diffusion through a polymeric barrier. Two factors have probably contributed to this effect:

1. The modification of the composition of the organic solution to a binary solvent mixture.

To solubilize PLA, dichloromethane was mixed to acetone leading to a mass ratio around 1:7 w/w in organic solution. Dichloromethane is immiscible with water and better solvent for PLA and PLGA and could prevent the formation of aggregates from the polymeric blend. Aggregates were unlikely to form on PLGA films when this solvent was used as observed previously (WAN *et al.*, 2014a). A more uniform polymeric membrane can promote an increase of the resistance of polymer matrix in release processes (WAN *et al.*, 2014a), which could explain the slow release of this batch (PM-MC20).

2. The polymeric composition

The release from a PLGA: PLA blend was influenced by its degradation rate, delayed by the presence of PLA. PLA increased hydrophobicity of the polymer blend, reducing water uptake, polymer hydrolysis and providing slow release.

4.4.4. BIOLOGICAL ASSAYS

The capacity of PM-loaded microparticles to induce cytotoxicity in BMDM cells and their antileishmanial activity against *L. amazonensis* promastigotes were investigated. Samples chosen for these tests were: PM-MC12 (PM in solution, microcapsules), PM-MC20 (PM in solution, PLGA/PLA mixture (90:10) microcapsules) and MC24 (blank batch for PM-MC20). Free drug was also submitted to the same assays.

4.4.4.1. Assessment of cytotoxicity of PM-loaded microparticles in BMDM cells

The cytotoxicity was evaluated in BMDM cells and the results was shown in Figure 86.

Firstly, Free PM (Figure 86a) showed a dose-dependent cytotoxicity and presented lower toxicity than PM-MC batches.

MC24, blank formulation, showed no cytotoxicity with no statistically significant differences ($P > 0.05$) among three concentrations (812 $\mu\text{g/mL}$, 1625 $\mu\text{g/mL}$, 3250 $\mu\text{g/mL}$) and Negative Control, suggesting that the cytotoxicity observed in microparticles batches with PM was due to the drug present in concentration between 26% wt. (PM-MC12) and 18% wt. (PM-MC20).

PM-MC12 presented no statistically significant differences ($P > 0.05$) among the three concentrations (1625 $\mu\text{g/mL}$, 3250 $\mu\text{g/mL}$, 7500 $\mu\text{g/mL}$) and the Positive Control (Triton). Moreover, the lower concentration of PM-MC12 analyzed (812 $\mu\text{g/mL}$) also demonstrated cytotoxicity.

PM-MC20 as well as PM-MC12 showed cytotoxicity in all concentrations

in comparison to the Negative Control. However, only the highest concentration (7500 $\mu\text{g/mL}$) had no statistically significant differences ($P > 0.05$) in relation to Positive Control.

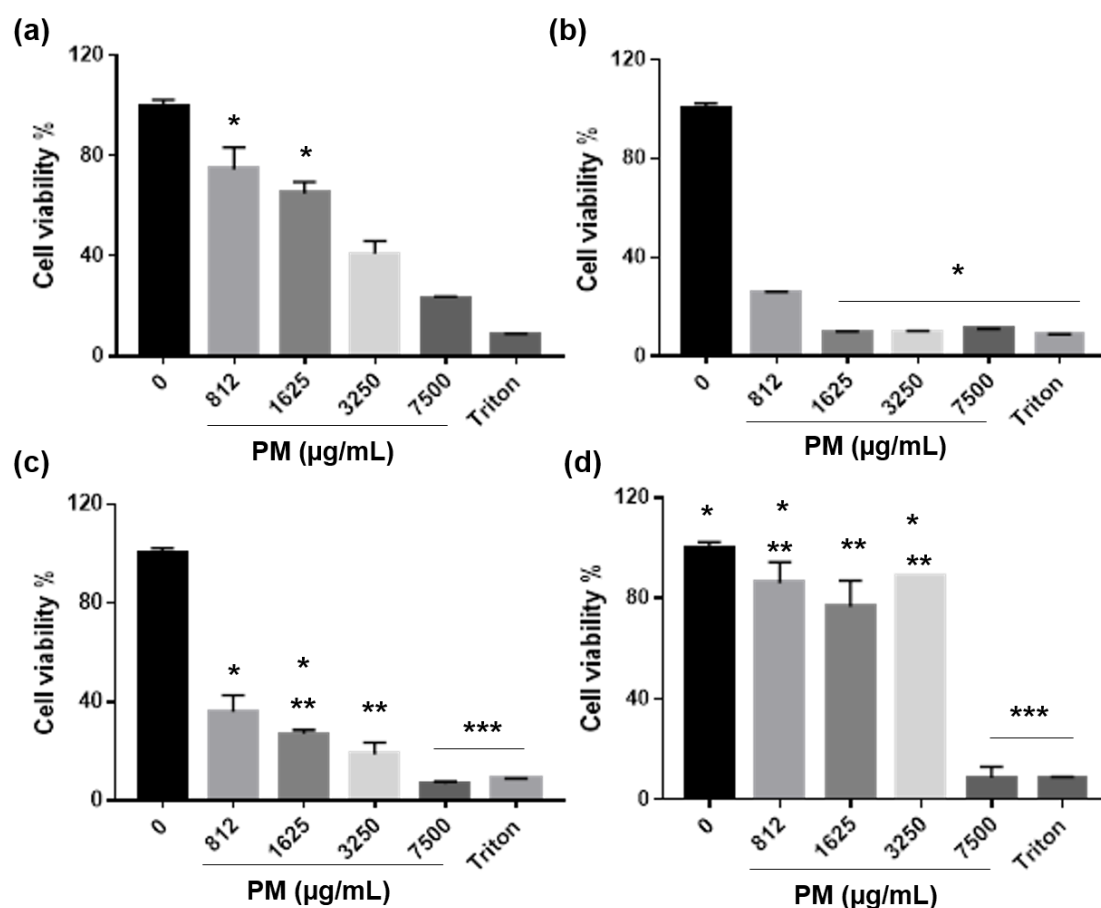


Figure 86. Cytotoxicity assay of (a) free PM, (b) PM-MC12, (c) PM-MC20 and (d) MC24 in BMDM cells. Legend: 0 – Negative Control without treatment, Triton – Positive Control (4% Triton 100x). * - No statistically significant differences ($P > 0.05$); ** - No statistically significant differences ($P > 0.05$); *** - No statistically significant differences ($P > 0.05$) according to One-way ANOVA with Tukey post-test.

Khan and co-workers (2013) developed PM albumin microspheres and investigated their cytotoxicity and PM in solution in peritoneal macrophages. The concentration ranged between 0.5-150 $\mu\text{g/mL}$ and it was observed that PM solution and PM microspheres promoted no cytotoxicity, suggesting that higher concentrations than 150 $\mu\text{g/mL}$ of PM solution and PM formulation should be tested to conclude about the cytotoxicity of this formulation. Our tests were

performed with very higher loads of PM (812 to 7500 $\mu\text{g}/\text{mL}$) compared with the concentrations tested for PM albumin microspheres.

Brugués and co-workers (2015) developed PM nanogel and evaluated its cytotoxicity in macrophages RAW 264.7, in comparison to the nanogel without PM (blank formulation) and an aqueous solution of PM (PM solution). The cytotoxicity was investigated in the concentration range of 0.8-25000 $\mu\text{g}/\text{mL}$. The results showed that PM nanogel presented higher cytotoxicity than the PM solution, while blank nanogel showed lower cytotoxicity than PM solution or nanogel. A similar trend was observed in our results.

Kharaji and co-workers (2015) developed solid lipid nanoparticles containing PM and evaluated the cytotoxicity of these formulations, blank nanoparticles and PM solution in human monocytic cell line (THP-1). The results showed no toxicity for blank nanoparticles and PM solution even in the highest concentration analyzed (6400 $\mu\text{g}/\text{mL}$). On the other hand, the nanoparticle size had some influence on cytotoxicity: the bigger PM solid lipid nanoparticles (980 nm and 1500 nm) have shown higher cytotoxicity than the smaller ones (120 nm and 240 nm).

In short, the results reported here with others different PM delivery systems (albumin microspheres, nanogel, solid lipid nanoparticles) confirmed that cytotoxicity depends on the range of PM concentration ($\mu\text{g}/\text{mL}$) tested and may be revealed for more concentrated formulations. Moreover, physical characteristics of these systems such as particle size may also influence the results. The higher cytotoxicity of PM-loaded microparticles (Figure 86 b and c) in relation to the free PM (Figure 86a) could be due to the polymer used, however it was not confirmed with the blank polymeric microparticles (Figure 86d). More studies are need to a better understanding of this biological behavior. However, compared to the literature, the PM-MC samples tested are in the same category of cytotoxicity found with other formulations aiming leishmaniasis treatment.

4.4.4.2. Antileishmanial Activity

The antileishmanial activity against *L. amazonensis* promastigotes was evaluated with the same PM-MC samples tested in cytotoxicity assay and the results are shown in Figure 87.

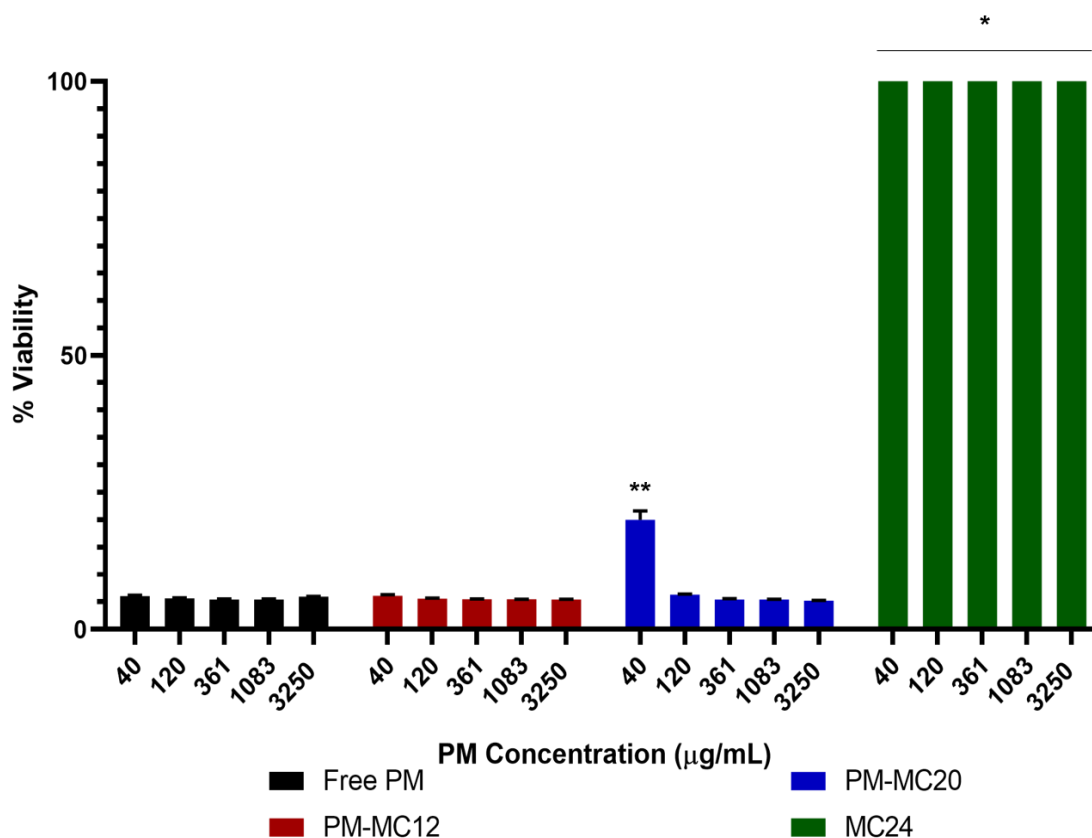


Figure 87. Antileishmanial activity in *L. amazonensis* promastigotes. Legend: *- MC24 is statistically significant different ($P < 0.05$) than the others, ** - Statistically significant differences ($P < 0.05$) according to One-way ANOVA with Tukey post-test.

Figure 87 shows that free PM, PM-MC12 and PM-MC20 presented similar antileishmanial activity, without statistically significant differences ($P > 0.05$), only in lower concentration (40 µg/mL) for PM-MC20 in relation to free PM and PM-MC12. The concentration range tested (40 to 3250 µg/mL) presented higher than 80% of *L. amazonensis* promastigotes death. Moreover, the blank formulation (MC24) had no antileishmanial activity.

In order to compare the cytotoxicity and antileishmanial activities, the following parameters were calculated: CC_{50} (for cytotoxicity); IC_{50} (for antileishmanial activity) and Selective Index (CC_{50}/IC_{50}) for free PM, PM-MC12, PM-MC20 and MC24. The results are given in Table 21.

Table 21 shows that free PM and MC24 presented higher values of CC_{50} than PM-MC batches. MC24 showed no antileishmanial activity with high value of IC_{50} ($> 3250 \mu\text{g/mL}$). PM-MS20 had IC_{50} value of $11.8 \mu\text{g/mL}$, slightly higher than the similar value of IC_{50} ($7.5 \mu\text{g/mL}$) of PM-MC12 and free PM.

Table 21. In vitro antileishmanial activity and cytotoxicity results for PM-MC formulations (CC_{50} , IC_{50} values and Selective Index of free PM and PM-MC batches) against *L. amazonensis* promastigotes

Formulation	CC_{50} *	IC_{50} **	Selective Index (SI)***
PM	2653 $\mu\text{g/mL}$	7.5 $\mu\text{g/mL}$	353.73
PM-MC12	308 $\mu\text{g/mL}$	7.5 $\mu\text{g/mL}$	41.06
PM-MC20	597 $\mu\text{g/mL}$	11.8 $\mu\text{g/mL}$	50.59
MC24	5437 $\mu\text{g/mL}$	$>3250 \mu\text{g/mL}$	<1.67

Legend: *- concentration in $\mu\text{g/mL}$ cytotoxicity for 50% of BMDM; ** - concentration in $\mu\text{g/mL}$ which reduces 50% of viability of *L. amazonensis* promastigotes; *** - Selective Index: CC_{50}/IC_{50} .

A key part of the development of PM-MS or PM-MC formulations is the characterization and optimization of their safety and efficacy and to identify which have an appropriately balanced safety-efficacy profile for intralesional or subcutaneous leishmaniasis treatment. The selectivity index (SI) which is usually considered as the highest drug's exposure that results in no toxicity to the exposure that produces the desired efficacy – is an important parameter in efforts to achieve this balance.

In the present study, the selectivity of the free PM and its formulation was expressed in terms of selectivity index (SI). To be a safe drug, SI should be

greater than 10 (KATSUNO *et al.*, 2015; NWAKA & HUDSON, 2006). Compared to free PM, PM-MC20 and PMC-12 had a decrease in the selectivity index, however, the SI values for both samples were approximately 50 and 41, respectively, indicating that they presented promising activity, which is higher than its cytotoxicity.

Taking the literature as reference, some results are cited here: Jaafari and co-workers (2009) developed topical PM liposomes with two different concentrations of drug (10% and 15%wt) and evaluated the efficacy of this formulation *in vitro*, against *L. major* promastigotes and amastigotes, and *in vivo* against BALB/c mice infected with *L. major*. No significant differences were observed in the antileishmanial activity of the two PM formulations. Nevertheless, PM liposomes showed higher activity (IC_{50} of 60-65 $\mu\text{g/mL}$) than the free drug (IC_{50} of 205 $\mu\text{g/mL}$).

Brugués and co-workers (2015) evaluated the CC_{50} of PM nanogel and PM solution in macrophages RAW 264.7 in concentrations varying from 0.8 $\mu\text{g/mL}$ to 25000 $\mu\text{g/mL}$. Blank formulation was evaluated in concentrations between 800 $\mu\text{g/mL}$ and 80000 $\mu\text{g/mL}$. The antileishmanial activity of PM nanogel, blank nanogel and PM solution, against *L. major* and *L. infantum* promastigotes, was evaluated in concentrations between 0.49 $\mu\text{g/mL}$ and 500 $\mu\text{g/mL}$ to obtain the IC_{50} values. The CC_{50} of blank formulation (80000 $\mu\text{g/mL}$) was higher than PM solution and PM nanogel. PM nanogel and PM solution presented similar CC_{50} values (> 1000 $\mu\text{g/mL}$ and 1210 $\mu\text{g/mL}$, respectively). In relation to IC_{50} values, nanogel without drug had no antileishmanial activity. PM nanogel and PM solution showed higher values of IC_{50} for *L. major* (12 $\mu\text{g/mL}$ and 20 $\mu\text{g/mL}$, respectively) than for *L. infantum* (23 $\mu\text{g/mL}$ and 37 $\mu\text{g/mL}$, respectively).

Kharaji and co-workers (2015) investigated the CC_{50} of PM liposomes, blank liposome and PM solution in THP-1 cells in concentrations between 25 $\mu\text{g/mL}$ and 6400 $\mu\text{g/mL}$. Moreover, the IC_{50} of these formulations for *L. major* and *L. tropica* promastigotes were evaluated in concentrations varying 25 $\mu\text{g/mL}$ to 3200 $\mu\text{g/mL}$. PM solution and blank liposomes presented no cytotoxicity and same CC_{50} value (6400 $\mu\text{g/mL}$). PM solution and blank liposomes presented no

cytotoxicity and same CC_{50} value (6400 $\mu\text{g}/\text{mL}$). PM liposomes with lower size had high CC_{50} (4000 – 4500 $\mu\text{g}/\text{mL}$) than PM liposomes with high size, but lower in comparison with PM solution. Liposome without drug had no effect against *Leishmania* species. The IC_{50} values, for *L. major*, of PM solution and PM liposomes were 3100 $\mu\text{g}/\text{mL}$ and 1600 $\mu\text{g}/\text{mL}$ (same value for the two formulations), respectively. The values for IC_{50} for *L. tropica* were similar than those observed for *L. major*, in which PM solution had 3200 $\mu\text{g}/\text{mL}$ and PM-liposomes 1600 and 1700 $\mu\text{g}/\text{mL}$. These results demonstrated that PM liposomes were more effective than PM solution.

Bavarsad and co-workers (2012) prepared several PM transfersomes varying their formulations and evaluated *in vitro* and *in vivo* activity. Transfersomes are elastic vesicles composed of phospholipids, cholesterol and single chain surfactant, which pass through skin under hydration gradient influence. The authors observed that, while blank transfersomes had no antileishmanial activity against *L. major* promastigotes, all PM transfersomes and PM solution developed antileishmanial activity with IC_{50} in the range of 18.60 $\mu\text{g}/\text{mL}$ to 124.67 $\mu\text{g}/\text{mL}$ and 205.70 $\mu\text{g}/\text{mL}$, respectively. The higher antileishmanial activity of PM transfersomes was attributed to a more efficient release of PM in parasites cytosol by the transfersomes compared with free PM.

It is difficult to compare our results with literature because the different tests were performed with different *Leishmania* species and, in general, for topical application. However, it could be verified that PM-MC batches presented attractive antileishmanial activity against *L. amazonensis*. In addition, it is the first time that the antileishmanial activity of polymeric microparticles containing PM are investigated against *Leishmania* species.

4.5. CONCLUSION

In this chapter, PLGA-based microparticles were proposed as systems for subcutaneous delivery of Paromomycin (PM) for leishmaniasis treatment. Spray drying was the manufacturing process chosen to this end.

The raw PM used in this study was commercially produced by spray drying. There are very few scientific publications on physicochemical properties of this molecule. DRX analysis confirmed the amorphous state of the sample, however its glass transition temperature (T_g) could not be determined by DSC analysis in the interval -90°C to 200°C .

PLGA 50:50 is the polymer of first choice for subcutaneous delivery due to its biodegradability and biocompatibility. However, the development of drug-loaded PLGA microparticles containing hydrophilic drug like PM represents a challenge due to low drug loadings often reached, low encapsulation efficiencies and initial burst release.

Different parameters were varied during the development of the spray-dried drug-loaded microparticles, among them: the type of organic solvent, drug concentration in the initial formulations, formulation and nozzle design (two-fluid and three-fluid nozzles, nozzle diameter orifice of the two-fluid nozzle) and composition of the polymeric carrier (PLGA or PLGA:PLA binary mixture). The spray-dried powders were characterized in terms of physicochemical properties, release behavior and biological assays.

Two different structures were expected: microspheres (matrix) and microcapsules (core-shell). The samples obtained were characterized by characteristics quite different in terms of drug loading (between 1.4% and 33.8%), EE (between 9.3% and 96.4%) and yield of production (between 6.4% and 80.5%).

Physicochemical characterizations (DSC, DRX, FT-IR analysis) revealed no interactions between the drug and polymeric carrier, which could be expected in the matrix structure (from two-fluid nozzle). *In vitro* release showed unexpected behaviors such as fast release from microspheres and PLGA microcapsules. These undesirable performances were attributed to the solid structure of the microparticles. A better understanding of the mechanism of particle formation from 3-fluid nozzles helps to identify ways to better control the physical core-shell structures formed. One way could be the mixture of polymers, PLGA and PLA as demonstrated by some of our results shown in this chapter (PM controlled release).

All spray-dried samples tested in biological assays, microspheres and microcapsules, presented safety with low toxicity detected in bone marrow-derived macrophages. Their Selective index was higher than 10, which confirms that these formulations were safe, with antileishmanial activity higher than cytotoxicity.

CHAPTER 5

GENERAL CONCLUSIONS AND PERSPECTIVES

The treatment for cutaneous leishmaniasis is a challenge since it is difficult to overcome problems such as the several side effects provoked by several drugs with antileishmanial activity. For this reason, formulation strategies and alternative administration routes have been increasingly studied looking for innovative treatments, with more efficacy and safety.

The aim of this study was to provide, for the treatment of cutaneous leishmaniasis, novel formulations for two drugs with well-known antileishmanial activity, amphotericin B and paromomycin.

Amphotericin B (AmB) is the most potent drug. However, its marketed formulations present high cytotoxicity, several side effects, high cost (for Ambisome®) and are available only for injectable use in hospital environment. There are several studies aiming novel formulations containing AmB and focusing in different routes of administration. Nonetheless, besides high toxicity, this drug presents low solubility and low permeability, which difficult the development of novel formulations.

Nanoemulsions were chosen as formulation strategy for AmB due to the presence of an oil phase, which in turn, should be able to entrap the drug and favor its permeation through the skin in topical application. Moreover, the use of topical formulation is a suitable alternative for decrease the toxicity, side effects and for self-application, increasing the patient's adhesion. In addition, nanoemulsions can generally be produced by simple manufacturing processes, which could be verified in this study. The formulations proposed here presented another advantage that is the use of a less toxic *solvent* (Class 3 ICH Guidelines) to solubilize AmB in the oil phase, DMSO, instead the most used in AmB nanoemulsions (dichloromethane), which is Class 2. Solvents in *Class 2* need to be limited in pharmaceutical products because of their inherent toxicity.

The AmB nanoemulsions developed here have demonstrated relevant characteristics like stability during 365 days under refrigeration (4°C), very slow release profile and slow drug permeation during *in vitro* tests. They also revealed good antileishmanial activity, however high cytotoxicity. The most promising formulation is AmB nanoemulsion prepared with surfactant Tween® 20 (Nanoemulsion B), which showed the lowest cytotoxicity with selective index

around 6. To be safe, formulations require SI values higher than 10. However, B-NE formulation has perhaps some potential in terms of composition to further improve its selectivity, which could be seen here as recommendations for future improvements: reduction of the amount of drug, novel formulations using others poloxamers, reduction of the amount or replacement of clove oil. Furthermore, the addition of an additional compound for accelerating the drug release could be another modification to improve nanoemulsion B performance.

In follow-up to this work, complementary studies for nanoemulsion B are required and are listed here:

- rheological properties, spreadability;
- antileishmanial activity against *L. amazonensis* amastigotes,
- antileishmanial activity against other *Leishmania* species that cause cutaneous leishmaniasis;
- *in vivo* studies in BALB/c mice model.

Paromomycin (PM) is another drug for which the parasite resistance, the few studies of PM efficacy in New World, the few numbers of clinical studies and the toxicity of formulations presented on the market are motivating the development of new PM formulations for leishmaniasis treatment. This drug has some physicochemical characteristics as high hydrophilicity and poor permeability that difficult the efficacy of topical formulations as already reported, besides susceptibility to degradation. Another route of administration not yet studied for paromomycin is the intralesional route. In addition to avoid problems of poor permeability through skin, the potential advantages of intralesional administration could be the use of lower total doses of the drug (and thus fewer toxic effects) and a more flexible schedule without the requirement of daily drug administration. PLGA-based formulations were chosen for PM because the use of biocompatible polymer allows injectable application. In addition, the manufacturing process chosen was spray drying, a rapid and one-step process that can be used for hydrophilic drug encapsulation.

The development of paromomycin microparticles involved the study of parameters influencing in physicochemical properties of formulations and the

structure of the delivery systems, microspheres or microcapsules. Different structures could be developed with PLGA or a mixture of PLGA and PLA as polymeric carriers. Microcapsules prepared with PLGA/PLA blend (PM-MC20) had the most interesting properties as core-shell structure and slow and controlled release. In addition, this batch presented low cytotoxicity with good antileishmanial activity and high selectivity for leishmanicidal effect.

Several other possibilities can be explored to modify the release profile of all PLGA-based microparticles generated in this study. Strategies for this aim in further studies could be:

- A better control of PLGA shell formation by modifying the interfacial tension at the interface core (water)-shell (organic solvent) with the use of other solvents for example.
- The investigation of other PLGA/PLA blend compositions.
- Moreover, some analyses are required to confirm the promising formulation (PM-MC20), such as: antileishmanial activity against *L. amazonensis* amastigotes, stability study, antileishmanial activity against other *Leishmania* species that cause cutaneous leishmaniasis and *in vivo* studies in BALB/c mice model.

To conclude, the two formulations proposed in this work could represent novel promising possibilities for cutaneous leishmaniasis treatment, one via topical administration of amphotericin B, and the other via intralesional administration of paromomycin.

CHAPTER 6

BIBLIOGRAPHY

ABADI, S. S. H.; MOIN, A. ; VEERABHADRAPPA, G. H. Review Article: Fabricated Microparticles : an innovative method to minimize the side effects of NSAIDs in arthritis. *Critical ReviewsTM in Therapeutic Drug Carrier Systems* v. 33, i. 5, p. 433-488, 2016.

ABULATEEFEH, S. R.; ALKILANY, A. M. Synthesis and characterization of PLGA shell microcapsules containing aqueous core prepared by internal phase separation. *AAPS PharmSciTech* v. 17, i. 4, p. 891-897, 2015.

AKBARI, M.; ORYAN, A.; HATAM, G. Application of nanotechnology in treatment of leishmaniasis: A review. *Acta Tropica* v. 172, p. 86-90, 2017.

ALI, H. H.; HUSSEIN, A. A. Oral nanoemulsions of candesartan cilexetil: formulation, characterization and in vitro drug release studies. *AAPS Open* v. 3, 2017. doi: 10.1186/s41120-017-0016-7

ALI, S. M.; YOSIPOVITCH, G. Skin pH: From basic science to basic skin care. *Acta Dermato Venereologica* v. 93, p. 261-267, 2013.

AL-QUADEIB, B. T.; RADWAN, M. A.; SILLER, L.; HORROCKS, B.; WRIGHT, M. C. Stealth amphotericin B nanoparticles for oral drug delivery: *In vitro* optimization. *Saudi Pharmaceutical Journal* v. 23, i. 3, p. 290-302, 2015.

ALVAREZ-LORENZO, C.; SOSNIK, A.; CONCHEIRO, A. PEO-PPO block copolymers for passive micellar targeting and overcoming multidrug resistance in cancer therapy. *Current Drug Targets* v. 12, i. 8, p. 1112-1130, 2011.

ALVAR, J.; VÉLEZ, I. D.; BERN, C.; HERRERO, M.; DESJEUX, P.; CANO, J.; JANNIN, J.; DEN BOER, M. Leishmaniasis worldwide and global estimates of its incidence, *PLOS One* v. 7, i. 5, p. 1-12, 2012. doi: 10.1371/journal.pone.0035671

ANGAMUTHU, M.; NANJAPPA, S. H.; RAMAN, V.; JO, S.; CEGU, P.; MURTHY, N. Controlled-release injectable containing terbinafine/PLGA microspheres for Onychomycosis treatment. *Journal of Pharmaceutical Sciences* v. 103, p. 1178-1183, 2014.

ANSARY, R. H.; AWANG, M. B.; RAHMAN, M. M. Biodegradable poly (D, L-lactico-glycolic acid) based micro/nanoparticles for sustained release of protein drugs – A review. *Tropical Journal of Pharmaceutical Research* v. 13, i. 7, p. 1179-1190, 2014.

AQUINO, R. P.; PROTA, L.; AURIEMMA, G.; SANTORO, A.; MENCHERINI, T.; COLOMBO, G.; RUSSO, P. Dry powders inhalers of gentamicin and leucine: formulation parameters, aerosol performance and *in vitro* toxicity on CuFi1 cells. *International Journal of Pharmaceutics* v. 462, p. 100-107, 2012.

ARANTES, P. O.; DOS SANTOS, Q. N.; FREITAS, Z. M. F.; PYRRHO, A. S.; CERQUEIRA-COUTINHO, C.; VILLA, A. L. V.; DOS SANTOS, E. P.; RICCI-JUNIOR, E. Promotion of cutaneous penetration of nifedipine for nanoemulsion. *Brazilian Journal of Pharmaceutical Sciences* v. 53, i. 2.; p. e15249, 2017. doi: 10.1590/s2175-97902017000215249

ARONSON, N. E.; WORTMANN, G. W.; BYRNE, W. R.; HOWARD, R. S.; BERNSTEIN, W. B.; MAROVICH, M. A.; POLHEMUS, M. E.; YOON, I. K.; HUMMER, K. A.; GASSER JUNIOR, R. A.; OSTER, C. N.; BENSON, P. M. A randomized controlled trial of local heat therapy versus intravenous sodium stibogluconate for the treatment of cutaneous *Leishmania major* infection. *PLoS Neglected Tropical Diseases* v. 4, i. 3, p. e628, 2010. doi: 10.1371/journal.pntd.0000628

BALLESTEROS, D. L.; CHARAN, C.; STULTS, C. L. M.; STEVENSON, C. L.; MILLER, D. P.; VEHRING, R.; TEP, V.; KUO, M. C. Trileucine improves aerosol performance and stability of Spray-dried powders for inhalation. *Journal of Pharmaceutical Sciences* v. 97, i. 1, p. 287-302, 2008.

BARI, H. A prolonged release parenteral drug delivery system – an overview. *International Journal of Pharmaceutical Sciences Review and Research* v. 3, i. 1, article 001 p. 1-11, 2010.

BATES, P. A. Transmission of *Leishmania* metacyclic promastigotes by phlebotomine sand flies, *International Journal for Parasitology* v. 37, p. 1097-1106, 2007.

BATISTA, A. J. S.; LIMA, W. P.; COSTA, N. A.; FALCÃO, C. A. B.; RÉ, M. I.; BERGMANN, B. R. Depot subcutaneous injection with chalcone CH8-loaded poly (lactic-co-glycolic acid) microspheres as a single dose treatment of cutaneous leishmaniasis. *Antimicrobial Agents and Chemotherapy* v. 62, i. 3, p. e01822-17, 2018. doi: 10.1128/AAC.01822-17

BAVARSAAD, N.; BAZZAZ, B. S. F.; KHAMESIPOUR, A.; JAAFARI, M. R. Colloidal, *in vitro* and *in vivo* anti-leishmanial properties of transfersomes containing paromomycin sulfate in susceptible BALB/c mice. *Acta Tropica* v. 124, p. 33-41, 2012.

BERMAN, J. D. Human leishmaniasis: clinical, diagnostic and chemotherapeutic developments in the last 10 years, *Clinical Infections Diseases* v. 24, p. 684-703, 1997.

BHOWMIK, D.; GOPINATH, H.; KUMAR, B. P.; DURAIVEL, S.; KUMAR, K. P. S. Recent advances in novel topical drug delivery system. *The Pharma Innovation* v. 1, i. 9, p. 12-31, 2012.

BLANCO-GARCIA, E.; GUERRERO-CALLEJAS, F.; BLANCO-MENDEZ, J.; GOMEZ-COUSO, H.; LUZARDO-ALVAREZ, A. Development of particulate drug formulation against *C. parvum*: Formulation, characterization and *in vivo* efficacy. *European Journal of Pharmaceutical Sciences* v. 92, p. 74-85, 2016.

BODRATTI, A. M.; ALEXANDRIDIS, P. Formulation of poloxamers of drug delivery. *Journal of Functional Biomaterials* v. 9, i. 1, 2018. doi: 10.3390/jfb9010011

BONIATTI, J.; PITALUGA, A. Jr.; SEICEIRA, R. C. Avaliação de diferentes tensoativos não iônicos na análise de distribuição granulométrica do insumo farmacêutico diazepam por espalhamento de luz laser. In: 5°ENIFARMED, 2011, São Paulo. Poster. São Paulo, 2011.

BONNER, D. P.; MECHLINSKI, W.; SCHAFFNER, C. P. Stability studies with amphotericin B and amphotericin B methyl ester. *The Journal of Antibiotics* v. 28, i. 2, p. 132-135, 1975.

BOS, J. D.; MEINARDI, M. M. H. M. The 500 Dalton rule for the skin penetration of chemical compounds and drugs. *Experimental Dermatology* v. 9, p. 165-169, 2000.

BRAVO-OSUNA, I.; ANDRES-GUERRERO, V.; PASTORIZA ABAL, P.; MOLINA-MARTINEZ, I. T.; HERRERO-VANRELL, R. Pharmaceutical microscale and nanoscale approaches for efficient treatment of ocular diseases. *Drug Delivery and Translational Research*, 2016. doi: 10.1007/s13346-016-0336-5.

BRITO, N. C.; RABELLO, A.; COTA, G. F. Efficacy of pentavalent antimoniate intralesional infiltration therapy for cutaneous leishmaniasis: a systematic review. *PLoS One* v. 12, i. 9, p. e0184777, 2017. doi: 10.1371/journal.pone.0184777

BRUSCHI, M. L. Mathematical Models of Drug Release. In: *Strategies to Modify the Drug Release from Pharmaceutical Systems*. Elsevier Woodhead Publishing, p. 63-86, 2015. doi: 10.1016/C2014-0-02342-8

BRYCESON, A. D. M.; MURPHY, A.; MOODY, A. H. Treatment of 'Old World' cutaneous leishmaniasis with aminosidine ointment: results of an open study in London. *Transactions of the Royal Society of Tropical Medicine and Hygiene* v. 84, p. 226-228, 1994.

BRUGUÉS, A. P.; NAVEROS, B. C.; CAMPMANY, A. C. C.; PASTOR, P. H.; SALADRIGAS, R.F.; LIZANDRA, C. R. Developing cutaneous applications of paromomycin entrapped in stimuli-sensitive block copolymer nanogel dispersions. *Nanomedicine* v. 10, i. 2, p. 227-240, 2015.

BUSATTO, C.; PESOA, J.; HELBLING, I.; LUNA, J.; ESTENOZ, D. Effect of particle size, polydispersity and polymer degradation on progesterone release from PLGA microparticles: Experimental and mathematical modeling. *International Journal of Pharmaceutics* v. 536, i. 1, p. 360-369, 2018.

BUTANI, D.; YEWALE, C.; MISRA, A. Amphotericin B topical microemulsion: Formulation, characterization and evaluation. *Colloids and Surface B: Biointerfaces* v. 116, p. 351-358, 2014.

CALDEIRA, L. R.; FERNANDES, F. R.; COSTA, D. F.; FRÉZARD, F.; AFONSO, L. C. C.; FERREIRA, L. A. M. Nanoemulsions loaded with amphotericin B: A new approach for the treatment of leishmaniasis. *European Journal of Pharmaceutical Sciences* v. 70, p. 125-131, 2015.

CAL, K.; SOLLOHUB, K. Spray drying technique. I: Hardware and process parameters. *Journal of Pharmaceutical Sciences* v. 99, i. 2, p.575-586, 2010.

CAMPOS, V. E. B.; RICCI-JUNIOR, E.; MANSUR, C. R. E. Nanoemulsions as a delivery system for lipophilic drugs, *Journal of Nanoscience and Nanotechnology* v. 12, i. 3, p. 2881-2890, 2012.

CAMPOS, V. E. B.; TEIXEIRA, C. A. A.; VEIGA, V. F.; RICCI-JUNIOR, E.; HOLANDINO, C. L-Tyrosine-loaded nanoparticles increase the antitumoral activity of direct electric current in a metastatic melanoma cell model. *International Journal of Nanomedicine* v. 5, p. 961-971, 2010.

CARDONA-ARIAS, J. A.; LÓPEZ-CARVAJAL, L.; TAMAYO-PLATA, M. P.; VÉLEZ, I. D. Comprehensive economic evaluation of thermotherapy for the treatment of cutaneous leishmaniasis in Colombia. *BMC Public Health* v. 18, 2018. doi: 10.1186/s12889-018-5060-2

CARDOSO, V. S.; VERMELHO, A. B.; RICCI-JUNIOR, E.; RODRIGUES, I. A.; MAZOTTO, A. M.; SUPURAN, C. T. Antileishmanial activity of sulphonamide nanoemulsions targeting the β -carbonic anhydrase from *Leishmania* species. *Journal of Enzyme Inhibition and Medicinal Chemistry* v. 33, i. 1, p. 850-857, 2018.

CARMELO, S. R. P.; FRANCESCHI, S.; PEREZ, S.; FULLANA, S. G.; RÉ, M. I. Factors influencing the erosion rate and the drug release kinetics from organogels designed as matrices for oral controlled release of hydrophobic drug. *Drug Development and Industrial Pharmacy* v. 24, i. 6, p. 985-997, 2016.

CARNEIRO, G.; SANTOS, D. C. M.; OLIVEIRA, M. C.; FERNANDES, A. P.; FERREIRA, L. S.; RAMALDES, G. A.; NUNAN, E. A.; FERREIRA, L. A. M. Topical delivery and in vivo antileishmanial activity of paromomycin loaded liposomes for treatment of cutaneous leishmaniasis. *Journal of Liposome Research* v. 20, i. 1, p. 16-23, 2010.

CARNEIRO, G.; AGUIAR, M. G.; FERNANDES, A. P.; MIRANDA, L. A. M. Drug delivery systems for the topical treatment of cutaneous leishmaniasis. *Expert Opinion on Drug Delivery* v. 9, i. 9, p. 1083-1097, 2012.

CHAPPUIS, F.; SUNDAR, S.; HAILU, A.; GHALIB, H.; RIJAL, S.; PEELING, R. W.; ALVAR, J.; BOELAERT, M. Visceral leishmaniasis: what are the needs for diagnosis, treatment and control? *Nature Reviews Microbiology* v. 5, p. s7-s16, 2007.

CHATTOPADHYAY, A.; JAFURULLA, M. A novel mechanism for an old drug: Amphotericin B in the treatment of visceral leishmaniasis, *Biochemical and Biophysical Research Communications* v. 416, p. 7-12, 2011.

CHAUHAN S.; BATRA, S. Development and in vitro characterization of nanoemulsion embedded thermosensitive in-situ ocular gel of diclofenac sodium for sustained delivery. *International Journal of Pharmaceutical Sciences and Research* v. 9, i. 6, p. 2301-2314, 2018.

CHEMID PLUS. United States National Library of Medicine. Available at: <http://chem.sis.nlm.nih.gov/chemidplus/> Accessed in: January 2016.

CHHONKER, Y. S.; PRASAD, Y. D.; CHANDASANA, H.; VISHVKARMA, A.; MITRA K.; SHUKLA, P.K.; BHATTA, R. S. Amphotericin B entrapped lecithin/chitosan nanoparticles for prolonged ocular application. *International Journal of Biological Macromolecules* v. 72, p. 1451-1458, 2015.

CHOUDHURY, H.; GORAIN, B.; PANDEY, M.; CHATTERJEE, L. A.; SENGUPTA, P.; DAS, A. MOLUGULU, N.; KESHARWANI, P. Recent uptake on nanoemulgel as topical drug delivery system. *Journal of Pharmaceutical Sciences* v. 106, i. 7, p. 1736-1751, 2017.

CONNORS, K. A.; AMIDON, G. L.; STELLA, V. J. *Chemical Stability of Pharmaceuticals: A Handbook for Pharmacists*. 2nd Ed., John Wiley & Sons, Inc. Amphotericin B monography p. 193-197, 1986.

COSTA, P. J. C. Avaliação in vitro da bioequivalência de formulações farmacêuticas. *Brazilian Journal of Pharmaceutical Sciences* v. 38, i. 2, p. 141-153, 2002.

COSTA, P.; LOBO, J. M. S. Modeling and comparison of dissolution profiles. *European Journal of Pharmaceutical Sciences* v. 13, p. 123-133, 2001.

CSEPREGI, R.; LEMLI, B.; KUNSÁGI-MÁTÉ, S.; SZENTE, L.; KÖSZEGI, T.; NÉMETI, B.; POÓR, M. Complex formation of resorufin and resazurin with β -cyclodextrins: Can cyclodextrins interfere with a resazurin cell viability assay? *Molecules* v. 23, i. 2, 2018. doi: 10.3390/molecules23020382

DANHIER, F.; ANSORENA, E.; SILVA, J. M.; COCO, R.; LE BRETON, A.; PRÉAT, V. PLGA-based nanoparticles: An overview of biomedical applications. *Journal of Controlled Release* v. 161, p. 505-522, 2012.

DASH, S.; MURTHY, P. N.; NATH, L.; CHOWDHURY, P. Kinetic modeling on drug release from controlled drug delivery systems. *Acta Poloniae Pharmaceutica – Drug Research* v. 97, i. 3, p. 217-223, 2010.

DAS, S. K.; DAVID, S. R. N.; RAJABALAYA, R.; MUKHOPADHYAY, H. K.; HALDER, T.; PALANISAMY, M.; KHANAM, J.; NANDA, A. Microencapsulation techniques and its practice. *International Journal of Pharmaceutical Science and Technology* v. 6, i. 2, p.1-23, 2011.

DATE, A. A.; DESAI, N.; DIXIT, R.; NAGARSENKER, M. Self-nanoemulsifying drug delivery systems: formulation insights, applications and advances. *Nanomedicines* v. 5, i. 10, p. 1595-1616, 2010.

DATE, A. D.; JOSHI, M. D.; PATRAVALE, V. B. Parasitic diseases: Liposomes and polymeric nanoparticles versus lipid nanoparticles. *Advanced Drug Delivery Reviews* v. 59, p. 502-521, 2007.

DAVIDSON, R. N.; DEN BOER, M.; RITMEIJER, K. Paromomycin. *Transactions of the Royal Society of Tropical Medicine and Hygiene* v. 103, p. 653-660, 2009.

DESHMUKH, R.; WAGH, P.; NAIK, J. Solvent evaporation and spray drying technique for micro- and nanospheres particles preparation: A review. *Drying Technology* v. 34, i. 15, p. 1758-1772, 2016.

DEVI, D. R.; SANDHYA, P.; HARI, B. N.V. Poloxamer: A novel functional molecule for drug delivery and gene therapy. *Journal of Pharmaceutical Sciences and Research* v. 5, i. 8, p. 159-165, 2013.

DHIFI, W.; BELLILI, S.; JAZI, S.; BAHLOUL, N. ; MNIF, W. Essential oils' chemical characterization and investigation of some biological activities: a critical review. *Medicines* v. 3, i. 4, 2016. doi: 10.3390/medicines3040025

DING, D.; ZHU, Q. Recent advances of PLGA micro/nanoparticles for the delivery of biomacromolecular therapeutics. *Materials Science & Engineering C*, 2018. doi: 10.1016/j.msec.2017.12.036

DOWLING, A. P. Development of nanotechnologies. *Materials Today – Nano today*, v. 7, i. 12, p. 30-35, 2004.

DRUG FOR NEGLECTED DISEASES INITIATIVE (DNDi). Diseases & Projects. About Leishmaniasis. Current Treatments. Available at: <https://www.dndi.org/diseases-projects/leishmaniasis/leish-current-treatments/>
Accessed in: March 2018.

DUEÑAS-ROMERO, A. M.; LOISEAU, P. M.; CHAZALET, M. S.P. Interactions of sitamaquine with membrane lipids of *Leishmania donovani* promastigotes, *Biochimica et Biophysica Acta* v. 1768, p. 246-252, 2007.

DUQUE, M. C. O.; VASCONCELLOS, E. C. F.; PIMENTEL, M. I. F.; LYRA, M. R.; PACHECO, S. J. B.; MARZOCHI, M. C. A.; ROSALINO, C. M. V.; SCHUBACH, A. O. Standardization of intralesional meglumine antimoniate treatment for cutaneous leishmaniasis. *Journal of the Brazilian Society of Tropical Medicine* v. 49, i. 6., p. 774-776, 2016.

EID, A. M.; EL-ENSHASY, H. A.; AZIZ, R.; ELMARZUGI, N. A. The preparation and evaluation of self-nanoemulsifying systems containing *Swietenia* oil and an examination of its anti-inflammatory effects. *International Journal of Nanomedicine* v. 9, p. 4685-4695, 2014.

EL-ON, J.; JACOBS, G. P; WITZTUM, E.; GREENBLATT, C. L. Development of topical treatment for cutaneous Leishmaniasis caused by *Leishmania major* in experimental animals. *Antimicrobial Agents and Chemotherapy* v. 26, i. 5, p. 745-51, 1984.

ERBETTA, C. D. C.; ALVES, R. J.; RESENDE, J. M.; FREITAS, R. F. S.; SOUSA, R. G. Synthesis and characterization of poly (D, L-lactide-co-glycolide) copolymer. *Journal of Biomaterials and Nanobiotechnology* v. 3, p. 208-225, 2012.

EUROPEAN PHARMACOPEIA 7.0, v. 2, Monography amphotericin B, p. 1391-1393, 2009.

ESPUELAS, M. S.; LEGRAND, P.; LOISEAU, P. M.; BORIES, C.; BARRATT, G.; IRACHE, J. M. In vitro antileishmanial activity of amphotericin B loaded in poly (ϵ -caprolactone) nanospheres, *Journal of Drug Targeting* v. 10, p. 593-599, 2003.

FAKHARI, A.; CORCORAN, M.; SCHWARZ, A. Thermogelling properties of purified poloxamer 407. *Heliyon* v. 3, p. e00390, 2017. doi: 10.1016/j.heliyon.2017.e00390

FARAH, S.; ANDERSON, D. G.; LANGER, R. Physical and mechanical properties of PLA, and their functions in widespread applications – A comprehensive review. *Advanced Drug Delivery Reviews* v. 107, p. 367-392, 2016.

FAROUK, F.; AZZAZY, H. M. E.; NIESSEN, W. M. A. Challenges in the determination of aminoglycoside antibiotics, a review. *Analytical Chimica Acta* v. 890, p. 21-43, 2015.

FREDENBERG, S.; WAHLGREN, M.; RESLOW, M.; AXELSSON, A. The mechanism of drug release in poly(lactic-co-glycolic acid)-based drug delivery systems – A review. *International Journal of Pharmaceutics* v. 415, p. 34-52, 2011.

FILIPPIN, F. B.; SOUZA, L. C.; MARANHÃO, R. C. Amphotericin B associated with triglyceride-rich nanoemulsion: Stability studies and in vitro antifungal activity. *Química Nova* v. 31, n. 3, p. 591-594, 2008.

FRANZINI, C. M. *Complexos de inclusão de anfotericina B com derivados de ciclodextrinas e sua incorporação em microemulsões lipídicas biocompatíveis*. 2010. Thesis (Doutorado em Ciências Farmacêuticas). Universidade Estadual Paulista Júlio de Mesquita Filho. Araraquara, 2010.

FREITAS, E. O.; NICO, D.; GUAN, R.; MEYER-FERNANDES, J. R.; CLINCH, K.; EVANS, G. B.; TYLER, P. C.; SCHRAMM, V. L.; PALATNIK-DE-SOUSA, C. B. Immucillins impair *Leishmania (L.) infatum chagasi* and *Leishmania (L.) amazonensis* multiplication in vitro. *PLOS One* v. 10, i. 4, 2015. doi: 10.1371/journal.pone.0124183

FUKUI, H.; KOIKE, T.; SAHEKI, A.; SONOKE, S.; SEKI, J. A novel delivery system for amphotericin B with lipid nano-sphere (LNS®). *International Journal of Pharmaceutics* v. 265, p. 37-45, 2003.

GARNIER, T.; CROFT, S. L. Topical treatment for cutaneous leishmaniasis. *Current Opinion in Investigational Drugs* v. 3, i. 4, p. 538-544, 2002.

GASPAR, M. M.; CALADO, S.; PEREIRA, J.; FERRONHA, H.; CORREIA, I.; CASTRO, H.; TOMAS, A. M.; CRUZ, M. E. M. Targeted delivery of paromomycin in murine infectious diseases through association to nano lipid systems. *Nanomedicine: Nanotechnology, Biology and Medicine* v. 11, p. 1851-1860, 2015.

GASPARINI, G.; HOLDICH, R. G.; KOSVINTSEV, S. R. PLGA particle production for water-soluble drug encapsulation: degradation and release behavior. *Colloids and Surfaces B: Biointerfaces* v. 75, p. 557-564, 2010.

GHADIRI, M.; VATANARA, A.; DOROUD, D.; NAJAFABADI, A. R. Paromomycin loaded solid lipid nanoparticles: characterization of production parameters. *Biotechnology and Bioprocess Engineering* v. 16, p. 617-623, 2011.

GHADIRI, M.; FATEMI, S.; VATANARA, A.; DOROUD, D.; NAJAFABADI, A. R.; DARABI, M.; RAHIMI, A. A. Loading hydrophilic drug in solid lipid media as nanoparticles: Statistical modeling of entrapment efficiency and particle size. *International Journal of Pharmaceutics* v. 424, p. 128-137, 2012.

GHOSH, S.; DAS, S.; DE, A. K.; KAR, N.; BERA, T. Amphotericin B-loaded mannose modified poly (D, L- lactide-co-glycolide) polymeric nanoparticles for the treatment of visceral leishmaniasis: *in vitro* and *in vivo* approaches. *RSC Advances* v. 7, p. 29575-29590, 2017. doi: 10.1039/C7RA04951J

GONÇALVES, G. S.; FERNANDES, A. P.; SOUZA, R. C. C.; CARDOSO, J. E.; OLIVEIRA-SILVA, F.; MACIEL, F. C.; RABELLO, A.; FERREIRA, L. A. M. Activity of a paromomycin hydrophilic formulation for topical treatment of infections by *Leishmania (Leishmania) amazonensis* and *Leishmania (Vianna) braziliensis*. *Acta Tropica* v. 93, p. 161-167, 2005.

GOLENSER, J.; DOMB, A. New formulations and derivatives of amphotericin B for treatment of leishmaniasis. *Mini-Reviews in Medicinal Chemistry* v. 6, p. 153-162, 2006.

GOTO, H.; LINDOSO, J. A.L. Current diagnosis and treatment of cutaneous and mucocutaneous leishmaniasis. *Expert Review of Anti-infective Therapy* v. 8, i. 4, p. 419-433, 2010.

GUERRERO, S.; MUÑÍZ, E.; TEIJÓN, C.; OLMO, R.; TEIJÓN, J. M.; BLANCO, M. D. Ketotifen-loaded microspheres prepared by spray-drying poly (D, L – lactide) and poly (D, L-lactide-co-glycolide) polymers: Characterization and *in vivo* evaluation. *Journal of Pharmaceutical Sciences* v. 97, i. 8, p. 3153-3169, 2008.

HALNOR, V. V.; PANDE, V. V.; BORAWAKE, D. D.; NAGARE, H. S. Nanoemulsion: A novel platform for drug delivery system. *Journal of Materials Science & Nanotechnology* v. 6, i. 1, p.104, 2018.

HAMILL, R. J. Amphotericin B formulations: A comparative review of efficacy and toxicity. *Drugs* v. 73, i. 9, p. 919-934, 2013.

HANDLER, M. Z.; PATEL, P. A.; KAPILA, R.; AL-QUBATI, Y.; SCHWARTZ, R. A. Cutaneous and mucocutaneous leishmaniasis: Differential diagnosis, diagnosis, histopathology and management. *Journal of the American Academy of Dermatology* v. 73, i. 6, p. 911-926, 2015.

HAN, F. Y.; THRURECHT, K. J.; WHITTAKER, A. K.; SMITH, M. T. Bioerodable PLGA-based microparticles for production sustained-release drug formulations and strategies for improving drug loading. *Frontiers in Pharmacology* v. 7, p. 185, 2016. doi: 10.3389/fphar.2016.00185

HASSAN, I.; DORJAY, K.; ANWAR, P. Pentoxifylline and its applications in dermatology. *Indian Dermatology Online Journal* v. 5, i. 4, p. 510-516, 2014.

HEPBURN, N. C. Cutaneous leishmaniasis, *Clinical and Experimental Dermatology* v. 25, p. 363-370, 2000.

HERRERO-VANRELL, R.; DE LA TORRE, M. V.; ANDRES-GUERRERO, V.; BARBOSA-ALFARO, D.; MOLINA-MARTINEZ, I. T.; BRAVO-OSUNA, I. Nano and microtechnologies for ophthalmic administration, an overview. *Journal of Drug Delivery Science and Technology* v. 23, i. 2, p. 75-102, 2013.

HUBERT, D. J.; CÉLINE, N.; MICHEL, N.; GOGULAMUDI, V. R.; FLORENCE, N. T.; JOHNSON, B. N.; BONAVENTURE, N. T.; SINGH, I. P.; SEHGAL, R. *In vitro* leishmanicidal activity of some Cameroonian medicinal plants, *Experimental Parasitology* v. 134, p. 304-308, 2013.

HUSSAIN, A.; SAMAD, A.; SINGH, S. K.; AHSAN, M. N.; HAQUE, M. W.; FARUK, A.; AHMED, F. J. Nanoemulsion gel-based topical delivery of an antifungal drug: in vitro activity and in vivo evaluation. *Drug Delivery* v. 23, i. 2, p. 642-657, 2016a.

HUSSAIN, A.; SINGH, V. K.; SINGH, O. P.; SHAFAT, K.; KUMAR, S.; AHMED, F. J. Formulation and optimization of nanoemulsion using antifungal lipid and surfactant for accentuated topical delivery of amphotericin B. *Drug Delivery* v. 23, i. 8, p. 3101-3110, 2016b.

HUSSAIN, A.; SAMAD, A.; NAZISH, I.; AHMED, F. J. Nanocarrier-based topical drug delivery for an antifungal drug. *Drug Development and Industrial Pharmacy* v. 40, i. 4, p. 527-541, 2013.

IBRAHIM, F.; GERSHKOVICH, P.; SIVAL, O.; WASAN, E. K.; WASAN, K. M. Assessment of novel oral lipid-based formulations of amphotericin B using in vitro lipolysis model. *European Journal of Pharmaceutical Sciences* v. 46, p. 323-328, 2012.

ICH. International Council for Harmonization of Technical Requirements for Pharmaceuticals for Human Use. *ICH Harmonized Guideline. Impurities: Guideline for Residual Solvents Q3C(R6)*. 2016.

IMBERT, L.; COJEAN, S.; LIBONG, D.; CHAMINADE, P.; LOISEAU, P. M. Sitamaquine resistance in *Leishmania donovani* affects drug accumulation and lipid metabolism. *Biomedicine & Pharmacotherapy* v. 68, p. 893-897, 2014.

INAL, O. YAPAR, E. A. Effect of mechanical properties on the release of meloxicam from poloxamer gel bases. *Indian Journal of Pharmaceutical Sciences* v. 75, i. 6, p. 700-706, 2013.

ISLAN, G. A.; DÚRAN, M.; CACICEDO, M. L.; NAKAZATO, G.; KOBAYASHI, R. K. T.; MARTINEZ, D. S. T.; CASTRO, G. R.; DÚRAN, N. Nanopharmaceuticals as a solution to neglected diseases: It is possible? *Acta Tropica* v. 170, p. 16-42, 2017.

ISOHERRANEN, N; SOBACK, S. Chromatographic methods for analysis of aminoglycoside antibiotics. *Journal of AOAC International* v. 82, i. 5, p. 1017-1045, 1999.

JAAFARI, M. R.; BAVARSAD, N.; BAZZAZ, B. S. F.; SAMIEI, A.; SOROUSH, D.; GHORBANI, S.; HERVAI, M. M. L.; KHAMESIPOUR, A. Effect of topical liposomes containing paromomycin sulfate in the course of *Leishmania major* infection in susceptible BALB/c mice. *Antimicrobial Agents and Chemotherapy* v. 53, i. 6, p. 2259-2265, 2009.

JAIN, A.; KUNDURU, K. R.; BASU, A.; MIZRAHI, B.; DOMB, A. J.; KHAN, W. Injectable formulations of poly (lactic acid) and its copolymers in clinical use. *Advanced Drug Delivery Reviews* v. 107, p. 213-227, 2016.

JAISWAL, M.; DUDHE, R.; SHARMA, P. K. Nanoemulsion: an advance mode of drug delivery system. *3 Biotech* v. 5, p. 123-127, 2015.

JAMEKHORSHID, A.; SADRAMELI, S. M.; FARID, M. A review of microencapsulation methods of phase change materials (PCMs) as a thermal energy storage (TES) medium. *Renewable and Sustainable Energy Reviews* v. 31, p. 531-542, 2014.

JHINGRAN, A.; CHAWLA, B.; SAXENA, S.; BARRET, M. P.; MADHUBALA, R. Paromomycin: uptake and resistance in *Leishmania donovani*. *Molecular and Biochemical Parasitology* v.164, i. 2, p. 111-117, 2009.

JÓJÁRT-LACZKOVICH, O.; SZABÓ-RÉVÉSZ, P. Amorphization of a crystalline active pharmaceutical ingredient and thermoanalytical measurements on this glassy form. *Journal of Thermal Analysis and Calorimetry* v. 102, p. 243-247, 2010.

JUG, M.; HAFNER, A.; LOVRIĆ, J.; KREGAR, M. L.; PEPIĆ, I.; VANIĆ, Z.; CETINA-ČIŽMEK, B.; FILIPOVIĆ-GRČIĆ. An overview of *in vitro* dissolution/release methods for novel mucosal drug delivery systems. *Journal of Pharmaceutical and Biomedical Analysis* v. 147, p. 350-366, 2018.

JYOTHI, N. V. N.; PRASANNA, P. M.; SAKARKAR, S. N.; PRABHA, K. S.; RAMAIAH, P. S.; SRAWAN, G. Y. Microencapsulation techniques, factors influencing encapsulation efficiency. *Journal of Microencapsulation* v. 27, i. 3, p. 187-197, 2010.

KALIMOUTTOU, S.; LAHIANI-SKIBA, M.; NAOULI, N.; LIN, V. S.; SKIBA, M. Evaluation of the paromomycin loading characteristics in nanoprecipitated PLGA nanospheres. *Nano Science and Technology Institute – Nanotech* v. 2, p. 407-410, 2008.

KANG, Y.; WU, J.; YIN, G.; HUANG, Z.; YAO, Y.; LIAO, X.; CHEN, A.; PU, X.; LIAO, L. Preparation, characterization and in vitro cytotoxicity of indomethacin-loaded PLLA/PLGA microparticles using supercritical CO₂ technique. *European Journal of Pharmaceutics and Biopharmaceutics* v. 70, p. 85-97, 2008.

KAPOOR, D. N.; BHATIA, A.; KAUR, R.; SHARMA, R.; KAUR, G.; DHAWAN, S. PLGA: a unique polymer for drug delivery. *Therapeutic Delivery* v. 6, i. 1, p. 41-58, 2015.

KAŠPAR, O.; JAKUBEC, M.; ŠTĚPÁNEK, F. Characterization of spray dried chitosan-TPP microparticles formed by two- and three-fluid nozzles. *Powder Technology* v. 240, p. 31-40, 2013a.

KAŠPAR, O.; TOKÁROVÁ, V.; NYANHONGO, G. S.; GÜBITZ, G.; ŠTĚPÁNEK, F. Effect of cross-linking method on the activity of spray-dried chitosan microparticles with immobilized laccase. *Food and Bioproducts Processing* v. 91, i. 4, p. 525-533, 2013b.

KATOUZIAN, I.; JAFARI, S. M. Nano-encapsulation as a promising approach for targeted delivery and controlled release vitamins. *Trends in Food Science & Technology* v. 56, p. 34-48, 2016.

KATSUNO, K.; BURROWS, J. N.; DUNCAN, K.; VAN HUIJSDUIJNEN, R. H.; KANEKO, T.; KITA, K.; MOWBRAY, C. E.; SCHMATZ, D.; WARNER, P.; SLINGSBY, B. T. Hit and lead criteria in drug discovery for infectious diseases of the developing world. *Nature Reviews Drug Discovery* v. 14, p. 751-758, 2015.

KAUPPINEN, A.; BROEKHUIS, J.; GRASMEIJER, N.; TONNIS, W.; KETOLAINEN, J.; FRIJLINK, H. W. ; HINRICHS, W. L. J. Efficient production of solid dispersions by spray drying solutions of high solid content using a 3-fluid nozzle. *European Journal of Pharmaceutics and Biopharmaceutics* v. 123, p. 50-58, 2018.

KEMPE, S.; MÄDER, K. In situ forming implants – an attractive formulation principle for parenteral depot formulations. *Journal of Controlled Release* v. 161, p. 668-679, 2012.

KHAN, W.; KUMAR, N. Drug targeting to macrophages using paromomycin-loaded albumin microspheres for treatment of visceral leishmaniasis: an in vitro evaluation. *Journal of Drug Targeting* v. 19, i. 4, p. 239-250, 2011a.

KHAN, W.; KUMAR, N. Characterization, thermal stability studies, and analytical method development of Paromomycin for formulation development. *Drug Testing and Analysis* v. 3, p. 363-372, 2011b.

KHAN, W.; KUMAR, R.; SINGH, S.; ARORA, S. K.; KUMAR, N. Paromomycin-loaded albumin microspheres: efficacy and stability studies. *Drug Testing and Analysis* v. 5, p. 468-473, 2013.

KHARAJI, M. H.; DOROUD, D.; TAHERI, T.; RAFATI, S. Drug targeting to macrophages with solid lipid nanoparticles harboring paromomycin: an in vitro evaluation against *L. major* and *L. tropica*. *AAPS PharmSciTech* v. 17, i. 5, p. 1110-1119, 2015.

KHARAJI, M. H.; TAHERI, T.; DOROUD, D.; HABIBZADEH, S.; BADIRZADEH, A.; RAFATI, S. Enhanced paromomycin efficacy by solid lipid nanoparticle formulation against Leishmania in mice model. *Parasite Immunology* v. 38, p. 599-608, 2016.

KHATAMI, A.; FIROOZ, A.; GOROUHI, F.; DOWLATI, Y. Treatment of acute Old World cutaneous leishmaniasis: a systematic review of the randomized controlled trials. *Journal of the American Academy of Dermatology* v. 57, i. 2, p. 335.e1-335.e29, 2007.

KIM, D. H.; CHUNG, H. J.; BLEYS, J.; GHOHESTANI, R. F. Is paromomycin an effective and safe treatment against cutaneous leishmaniasis? A meta-analysis of 14 randomized controlled trials. *PLOS Neglected Tropical Diseases* v. 3, i. 2, p. e381, 2009. doi: 10.1371/journal.pntd.0000381

KIM, H. K.; PARK, T. G. Comparative study on sustained release of human growth hormone from semi-crystalline poly (L-lactic acid) and amorphous poly (D, L-lactic-co-glycolic acid) microspheres: morphological effect on protein release. *Journal of Controlled Release* v.98, p. 115-125, 2004.

KOLEY, D.; BARD, A. J. Triton X-100 concentration effects on membrane permeability of a single HeLa cell by scanning electrochemical microscopy (SECM). *Proceedings of the National Academy of Sciences of the United States of America (PNAS)* v. 107, i. 39, p. 16783-16787, 2010. doi: 10.1073/pnas.1011614107

KONDO, K.; NIWA, T.; DANJO, K. Preparation of sustained-release coated particles by novel microencapsulation method using three fluid nozzle spray drying technique. *Journal of Pharmaceutical Sciences* v. 51, p. 11-19, 2014.

KOUIDHI, B.; ZMANTAR, T.; BAKHROUF, A. Anticariogenic and cytotoxic activity of clove essential oil (*Eugenia caryophyllata*) against a large number of oral pathogens. *Annals of Microbiology* v. 60, p. 599-604, 2010.

KULSHRESTHA, A.; BHANDARI, V.; MUKHOPADHYAY, R.; RAMESH, V.; SUNDAR, S.; MAES, L.; DUJARDIN, J. C.; ROY, S.; SALOTRA, P. Validation of a simple resazurin-based promastigote assay for the routine monitoring of miltefosine susceptibility in clinical isolates of *Leishmania donovani*. *Parasitology Research* v. 112, p. 825-828, 2013.

KULSHRESTHA, A.; SINGH, R.; KUMAR, D.; NEGI, N. S.; SALOTRA, P. Antimony-resistant clinical isolates of *Leishmania donovani* are susceptible to paromomycin and sitamaquine. *Antimicrobial Agents and Chemotherapy* v. 55, i. 6, p. 2916-2921, 2011.

LAMBERS, H.; PIESENS, S.; BLOEM, A.; PRONK, H.; FINKEL, P. Natural skin surface pH is on average below 5, which is beneficial for its resident flora. *International Journal of Cosmetic Science* v. 28, p. 359-370, 2006.

LARKAN, P. *Infrared and Raman Spectroscopy: Principles and Spectral Interpretation*. United States: Elsevier Inc., 2011.

LARRAÑETA, E.; LUTTON, R. E. M.; WOOLFSON, A. D.; DONNELLY, R. F. Microneedle arrays as transdermal and intradermal drug delivery systems: Materials science, manufacture and commercial development. *Material Science and Engineering R* v. 104, p. 1-32, 2016.

LI, H.; KOCHHAR, J. S.; PAN, J.; CHAN, S. Y.; KANG, L. Nano/microscale technologies for drug delivery. *Journal of Mechanics in Medicine and Biology* v. 11, i. 2, p. 337-367, 2011.

LIN, R.; NG, L. S.; WANG, C. H. In vitro study of anticancer doxorubicin in PLGA-based microparticles. *Biomaterials* v. 26, p. 4476-4485, 2005.

LIN, X.; YANG, S.; GOU, J.; ZHAO, M.; ZHANG, Y.; QI, N.; HE, H.; CAI, C.; TANG, X. ; GUO, P. A novel risperidone-loaded SAIB-PLGA mixture matrix depot with a reduced burst release: effects of solvents and PLGA on drug release behaviors in vitro/in vivo. *Journal of Materials Science: Materials in Medicine* v. 23, p. 443-455, 2012.

LINDOSO, J. A. L.; COSTA, J. M. L.; QUEIROZ, I. T.; GOTO, H. Review of the current treatments of leishmaniases. *Research and Reports in Tropical Medicine* v. 3, p. 69-77, 2012.

LIU, Y.; BAI, X.; LIANG, A. Synthesis, properties, and in vitro hydrolytic degradation of poly(d,l-lactide-co-glycolide-co- ϵ -caprolactone). *International Journal of Polymer Science*, 2016. doi: 10.1155/2016/8082014

LOBO, I. M. F.; SOARES, M. B. P.; CORREIA, T. M.; FREITAS, L. A. R.; OLIVEIRA, M. I.; NAKATANI, M.; NETTO, E.; BADARO, R.; DAVID, J. R. Heat therapy for cutaneous leishmaniasis elicits a systemic cytokine response similar to that of antimonial (Glucantime) therapy. *Transactions of the Royal Society of Tropical Medicine and Hygiene* v. 100, p. 642-649, 2006.

LÓPEZ, L. ROBAYO, M.; VARGAS, M.; VÉLEZ, I. D. Thermotherapy. An alternative for the treatment of American cutaneous leishmaniasis. *Trials* v. 13:58, 2012. doi: 10.1186/1745-6215-13-58.

LÜ, J. M.; WANG, X.; MARIN-MULLER, C.; WANG, H.; LIN, P. H.; YAO, Q.; CHEN, C. Current advances in research and clinical applications of PLGA-based nanotechnology. *Expert Reviews of Molecular Diagnostics* v. 9, i. 4, p.325-341, 2009.

LU, L.; MIKOS, A. G. Poly (lactic acid) In: *Polymer Data Handbook*. Oxford University Press, New York, p. 627-633, 1999.

LU, W. C.; HUANG, D. W.; WANG, C. C. R.; YEH, C. H.; TSAI, J. C.; HUANG, Y. T.; LI, P. H. Preparation, characterization and antimicrobial activity of nanoemulsions incorporating citral essential oil. *Journal of Food and Drug Analysis* v. 26, p. 82-89, 2018.

MAKADIA, H. K.; SIEGEL, S. J. Poly lactic-co-glycolic acid (PLGA) as biodegradable controlled drug delivery carrier. *Polymers* v. 3, p. 1377-1397, 2011.

MANSUETO, P.; SEIDITA, A.; VITALE, G.; CASCIO, A. Leishmaniasis in travelers: A literature review. *Travel Medicine and Infectious Disease* v.12, p. 563-581, 2014.

MARIM, F. M.; SILVEIRA, T. N.; LIMA JUNIOR, D. S.; ZAMBONI, D. S. A method for generation of bone marrow-derived macrophages from cryopreserved mouse bone marrow cells. *PLOS One* v. 5, i. 12, p. e15263, 2010. doi: 10.1371/journal.pone.0015263

MARQUES, T. Z. S.; SANTOS-OLIVEIRA, R.; SIQUEIRA, L. B. O.; CARDOSO, V. S.; FREITAS, Z. M. F.; BARROS, R. C. S. A.; VILLA, A. L. V.; MONTEIRO, M. S. S. B.; DOS SANTOS, E. P.; RICCI-JUNIOR, E. Development and characterization of a nanoemulsion containing propranolol for topical delivery. *International Journal of Nanomedicine* v. 13, p. 2827-2837, 2018.

MATTOS, C. B.; ARGENTA, D. F.; MELCHIADES, G. L.; CORDEIRO, M. N. S.; TONINI, M. L.; MORAES, M. H.; WEBER, T. B.; ROMAN, S. S.; NUNES, R. J.; TEIXEIRA, H. F.; STEINDEL, M.; KOESTER, L. S. Nanoemulsions containing a synthetic chalcone as an alternative for treating cutaneous leishmaniasis: optimization using a full factorial design. *International Journal of Nanomedicine* v. 10, i. 1, p. 5529-5542, 2015.

MEDEIROS, S. F.; LOPES, M. V.; ROSSI-BERGMANN, B.; RÉ, M. I.; SANTOS, A. M. Synthesis and characterization of poly(N-vinylcaprolactam)-based spray-dried microparticles exhibiting temperature and pH-sensitive properties for controlled release of ketoprofen. *Drug Development and Industrial Pharmacy* v. 43, i. 9, p. 1519-1529, 2017.

MEI, L.; ZHANG, Z.; ZHAO, L.; HUANG, L.; YANG, X. L.; TANG, J.; FENG, S. S. Pharmaceutical nanotechnology for oral delivery of anticancer drugs. *Advanced Drug Delivery Reviews* v. 65, p. 880-890, 2013.

MENDONÇA, D. V. C.; LAGE, L. M. R.; LAGE, D. P.; CHÁVEZ-FUMAGALLI, M. A.; LUDOLF, F.; ROATT, B. M.; MENEZES-SOUZA, D.; FARACO, A. A. G.; CASTILHO, R. O.; TAVARES, C. A. P.; BARICHELLO, J. M.; DUARTE, M. C.; COELHO, E. A. F. Poloxamer 407 (Pluronic® F127)- based polymeric micelles for amphotericin B: In vitro biological activity, toxicity and in vivo therapeutic efficacy against murine tegumentary leishmaniasis. *Experimental Parasitology* v. 169, p. 34-42, 2016.

MENEZES, J. P. B.; GUEDES, C. E. S.; PETERSEN, A. L. O. A.; FRAGA, D. B. M.; VERAS, P. S. T. Advances in development of new treatment for leishmaniasis. *BioMed Research International*, 2015. doi: 10.1155/2015/815023. Available at: <https://www.hindawi.com/journals/bmri/2015/815023>

MINISTÉRIO DA SAÚDE. Secretaria de Vigilância em Saúde. Manual de Vigilância e Controle da Leishmaniose Visceral, 1ª Ed., Brasília, Editora do Ministério da Saúde, 2006.

MINISTÉRIO DA SAÚDE. Secretaria de Vigilância em Saúde. Manual de Vigilância da Leishmaniose Tegumentar Americana, 2ª Ed., Brasília, Editora do Ministério da Saúde, 2017.

MIR, M.; AHMED, N.; REHMAN, A. Recent applications of PLGA based nanostructures in drug delivery. *Colloids and Surface B: Interfaces* v. 159, p. 217-231, 2017.

MITROPOULOS, P.; KONIDAS, P.; DURKIN-KONIDAS, M. New World cutaneous leishmaniasis: updated review of current and future diagnosis and treatment. *Journal of the American Academy of Dermatology* v. 63, i. 2, p. 309-322, 2010.

MOK, H.; PARK, T. G. Water-free microencapsulation of proteins within PLGA microparticles by spray drying using PEG-assisted protein solubilization technique in organic solvent. *European Journal of Pharmaceutics and Biopharmaceutics* v. 70, p. 137-144, 2008.

MOMENI, A.; MORTEZA, R.; MOMENI, A.; NAVAEI, A.; EMANI, S.; SHAKER, Z.; MOHEBALI, M.; KHOSHDEL, A. Development of liposomes loaded with anti-leishmanial drugs for the treatment of cutaneous leishmaniasis. *Journal of Liposome Research* v. 23, i. 2, p. 134-144, 2013.

MONTENEGRO, L.; LAI, F.; OFFERTA, A.; SARPIETRO, M. G.; MICICCHÈ, L.; MACCIONI, A. M.; VALENTI, D.; FADDA, A. M. From nanoemulsions to nanostructured lipids carriers: A relevant development in dermal delivery of drugs and cosmetics. *Journal of Drug Delivery Science and Technology* v. 32, p. 100-112, 2016.

MORAIS, S. M.; VILA-NOVA, N. S.; BEVILAQUA, C. M. L.; RONDON, F. C.; LOBO, C. H.; MOURA, A. A. A. N.; SALES, A. D.; RODRIGUES, A. P. R.; FIGUEREIDO, J. R.; CAMPELLO, C. C.; WILSON, M. E.; ANDRADE JUNIOR, H. F. Thymol and eugenol derivatives as potential antileishmanial agents. *Bioorganic & Medicinal Chemistry* v. 22, n. 21, p. 6250-6255, 2014.

MORONKEJI, K.; TODD, S.; DAWIDOWSKA, I.; BARRET, S. D.; AKHTAR, R. The role of subcutaneous tissue stiffness on microneedle performance in a representative in vitro model of skin. *Journal of Controlled Release* v. 265, p. 102-112, 2017.

MOU, D.; CHEN, H.; DU, D.; MAO, C.; WAN, J.; XU, H.; YANG, X. Hydrogel-thickened nanoemulsion system for topical delivery of lipophilic drugs. *International Journal of Pharmaceutics* v. 353, p. 270-276, 2008.

MUNGURE, T. E.; ROOHINEJAD, S.; BEKHIT, A. E. D.; GREINER, R.; MALLIKARJUNAN, K. Potential application of pectin for the stabilization of nanoemulsions. *Current Opinion in Food Science* v. 19, p. 72-76, 2018.

NAKASHIMA, A.; IZUMI, T.; OHYA, K.; KONDO, K.; NIWA, T. Design of highly dispersible PLGA microparticles in aqueous fluid for the development of long-acting release injectables. *Chemical and Pharmaceutical Bulletin* v. 65, p. 157-165, 2017.

NASSIF, P. W.; MELLO, T. F. P.; NABASCONI, T. R.; MOTA, C. A.; DEMARCHI, I. G.; ARISTIDES, S. M. A.; LONARDONI, M. V. C.; TEIXEIRA, J. J. V.; SILVEIRA, T. G. V. Safety and efficacy of current alternatives in the topical treatment of cutaneous leishmaniasis: a systematic review. *Parasitology*, doi:10.1017/S0031182017000385, 2017.

NOGUEIRA, I. R. L.; CARNEIRO, G.; YOSHIDA, M. I.; OLIVEIRA, R. B.; FERREIRA, L. A. M. Preparation, characterization, and topical delivery of paromomycin ion pairing. *Drug Development and Industrial Pharmacy* v. 37, i. 9, p. 1083-1089, 2011.

NO, J. H. Visceral leishmaniasis: Revisiting current treatments and approaches for future discoveries. *Acta Tropica* v. 155, p. 113-123, 2016.

OLIVEIRA, A. R.; MOLINA, E. F.; MESQUITA, P. C.; FONSECA, J. L. C.; ROSSANEZI, G.; FERNANDES-PEDROSA, M. F.; OLIVEIRA, A. G.; SILVA-JUNIOR, A. A. Structural and thermal properties of spray-dried methotrexate-loaded biodegradable microparticles. *Journal of Thermal Analysis and Calorimetry* v. 112, p. 555-565, 2013.

OLIVEIRA, E. G.; CALAND, L. B.; OLIVEIRA, A. R.; MACHADO, P. R. L.; FARIAS, K. J. S.; COSTA, T. R.; MELO, D. M. A.; CORNÉLIO, A. M.; FERNANDES-PEDROSA, M. F.; SILVA-JÚNIOR, A. A. Monitoring thermal, structural properties, methotrexate release and biological activity from biocompatible spray-dried microparticles. *Journal of Thermal Analysis and Calorimetry* v. 130, p. 1481-1490, 2017.

PACE, D. Leishmaniasis. *Journal of Infection* v. 69, p. s10-s18, 2014.

PARK, P. I. P.; JONNALAGADDA, S. Predictors of glass transition in the biodegradable poly-lactide and poly-lactide-co-glycolide polymers. *Journal of Applied Polymer Science* v. 100, p. 1983-1987, 2006.

PARVEEN, S.; MISRA, R.; SAHOO, S. K. Nanoparticles: a boon to drug delivery, therapeutics, diagnostics and imaging. *Nanomedicine: Nanotechnology, Biology and Medicine* v. 8, p. 147-166, 2012.

PATEL, B. B.; PATEL, J. K.; CHAKRABORTY, S.; SHUKLA, D. Revealing facts behind spray dried solid dispersion technology used for solubility enhancement. *Saudi Pharmaceutical Journal* v. 23, p. 352-365, 2015.

PATEL, H. R.; PATEL, R. P.; PATEL, M. M. Poloxamers: A pharmaceutical excipients with therapeutic behavior. *International Journal of PharmTech Research* v. 1, i. 2, p. 299-303, 2009.

PAUDEL, A.; WORKU, Z. A.; MEEUS, J.; GUNS, S.; VAN DEN MOOTER, G. Manufacturing of solid dispersions of poorly water-soluble drugs by spray-drying: Formulation and process considerations. *International Journal of Pharmaceutics* v. 453, p. 253-284, 2013.

PEREIRA, G. G.; DIMER, F. A.; GUTERRES, S. S.; KECHINSKI, C. P.; GRANADA, J. E.; CARDOZO, N. S. M. Formulation and characterization of poloxamer 407®: thermoreversible gel containing polymeric microparticles and hyaluronic acid. *Química Nova* v. 36, i. 8, p. 1121-1125, 2013.

PEREZ, A. P.; ALTUBE, M. J.; SCHILRREFF, P.; APEZTEGUIA, G.; CELES, F. S.; ZACCHINO, S.; OLIVEIRA, C. I.; ROMERO, E. L.; MORILLA, M. J. Topical amphotericin B in ultradeformable liposomes: Formulation, skin penetration study, antifungal and antileishmanial activity *in vitro*. *Colloids and Surface B: Biointerfaces* v. 139, p. 190-198, 2016.

PILANIYA, U.; KHATRI, K.; PATIL, U. K. Depot based drug delivery system for the management of depression. *Current Drug Delivery* v. 8, i. 5, p. 483-493, 2011.

PINERO, J.; TEMPORAL, R. M.; GONÇALVES, A. J. S.; JIMÉNEZ, I. A.; BAZZOCCHI, I. L.; OLIVA, A.; PERERA, A.; LEON, L. L.; VALLADARES, B. New administration model of trans-chalcone biodegradable polymers for the treatment of experimental leishmaniasis. *Acta Tropica* v. 98, p. 59-65, 2006.

PINHEIRO, I. M.; CARVALHO, I. P.; CARVALHO, C. E.; BRITO, L. M.; SILVA, A. B.; CONDE JÚNIOR, A. M.; CARVALHO, F. A.; CARVALHO, A. L. Evaluation of the *in vivo* leishmanicidal activity of amphotericin B emulgel: An alternative for the treatment of skin leishmaniasis. *Experimental Parasitology* v. 164, p. 49-55, 2016.

POLYCHNIATOU, V.; TZIA, C. Study of formulation and stability of co-surfactant free water-in-olive oil nano- and submicron emulsions with food grade non-ionic surfactants. *Journal of the American Oil Chemists' Society* v. 91, p. 79-88, 2014.

PRASHAR, A.; LOCKE, I. C.; EVANS, C. S. Cytotoxicity of clove (*Syzygium aromaticum*) oil and its major components to human skin cells. *Cell Proliferation* v. 39, p. 241-248, 2006.

PRIOR, S.; GAMAZO, C.; IRACHE, J. M.; MERKLE, H. P.; GANDER, B. Gentamicin encapsulation in PLA/PLGA microspheres in view of treating *Brucella* infections. *International Journal of Pharmaceutics* v. 196, p. 115-125, 2000.

PRIOR, S.; GANDER, B.; LECÁROZ, C.; IRACHE, J. M.; GAMAZO, C. Gentamicin-loaded microspheres for reducing the intracellular *Brucella abortus* load in infected monocytes. *Journal of Antimicrobial Chemotherapy* v. 53, p. 981-988, 2004.

PUJOL-BRUGUÉS, A.; CALPENA-CAMPMANY, A. C.; RIERA-LIZANDRA, C.; HALBAULT-BELLOWA, L.; CLARES-NAVEROS, B. Development of a liquid chromatographic method for the quantification of paromomycin. Application to in vitro release and ex-vivo permeation studies. *Spectrochimica Acta Part A: Molecular and Biomolecular Spectroscopy* v. 133, p. 657-662, 2014.

RAI, V. K.; MISHRA, N.; YADAV, K. S.; YADAV, N. P. Nanoemulsion as pharmaceutical carrier for dermal and transdermal drug delivery: Formulation development, stability issues, basic considerations and applications. *Journal of Controlled Release* v. 270, p. 203-225, 2018.

RAMAZANI, F.; CHEN, W.; VAN NOSTRUM, C. F.; STORM, G.; KIESSLING, F.; LAMERS, T.; HENNINK, W. E.; KOK, R. J. Strategies for encapsulation of small hydrophilic and amphiphilic drugs in PLGA microspheres: state-of-the-art and challenges. *International Journal of Pharmaceutics* v. 499, i. 1-2, p. 358-367, 2016.

RAMPERSAD, S. N.; Multiple applications of Alamar Blue as an indicator of metabolic function and cellular health in cell viability bioassays. *Sensors* v. 12, p. 12347-12360, 2012.

RAMTEKE, K.H.; DIGHE, P. A.; KHARAT, A. R.; PATIL, S. V. Mathematical models of drug dissolution: a review. *Scholars Academic Journal of Pharmacy* v. 3, i. 5, p. 388-396, 2014.

REITHINGER, R.; DUJARDIN, J. C.; LOUZIR, H.; PIRMEZ, C.; ALEXANDER, B.; BROOKER, S. Cutaneous leishmaniasis, *The Lancet Infectious Diseases* v. 7, i.7, p. 581-596, 2007.

RE, M. I. Microencapsulation by Spray Drying. *Drying Technology* v. 16, i. 6, p. 1195-1236, 1998.

RE, M. I. Formulating drug delivery systems by Spray Drying. *Drying Technology* v. 24, i. 4, p. 433-446, 2006.

RE, M. I.; MESSIAS, L. S.; SCHETTINI, H. The influence of the liquid properties and the atomizing conditions on the physical characteristics of the spray-dried ferrous sulfate microparticles. *Paper presented at the annual International Drying Symposium*, August 22-25, 2004, in Campinas, Brazil.

RODRIGUES, C. D.; CASA, D. M.; DALMOLIN, L. F.; CAMARGO, L. E. A.; KHALIL, N. M.; MAINARDES, R. M. Amphotericin B-loaded poly(lactide)-poly(ethylene glycol)-blend nanoparticles: Characterization and in vitro efficacy and toxicity. *Current Nanoscience* v. 9, p. 594-598, 2013.

RODRÍGUEZ, A. C. M. *Desarrollo farmacéutico de formulaciones de poliagregados de anfotericina B*. 2011. Thesis (Doctoral em Farmacia y Tecnología Farmacéutica). Universidad Complutense de Madrid. Madrid, 2011.

ROLÓN, M.; VEGA, C.; ESCARIO, J. A.; GÓMEZ-BARRIO, A. Development of resazurin microtiter assay for drug sensibility testing of *Trypanosoma cruzi* epimastigotes. *Parasitology Research* v. 99, p. 103-107, 2006.

ROWE, R. C.; SHESKEY, P. J.; QUINN, M. E. *Handbook of Pharmaceutical Excipients*. United States: Pharmaceutical Press and the American Pharmacist Association, Six Edition, 2009.

RUELA, A. L. M.; PERISSINATO, A. G.; LINO, M. E. S.; MUDRIK, P. S.; PEREIRA, G. R. Evaluation of skin absorption of drugs from topical and transdermal formulations. *Brazilian Journal of Pharmaceutical Sciences* v. 52, i. 3, p.527-544, 2016.

RYAN, J. A. Colorimetric Determination of Gentamicin, Kanamycin, Tobramycin and Amikacin Aminoglycosides with 2,4-dinitrofluorobenzene. *Journal of Pharmaceutical Sciences* v. 73, i. 9, p. 1301-1302, 1984.

SALAH, A. B.; BUFFET, P. A.; MORIZOT, G.; BEN MASSOUD, N.; ZÂATOUR, A.; BEN ALAYA, N.; HAMIDA, N. B. H.; EL AHMADI, Z.; DOWNS, M. T.; SMITH, P. L.; DELLAGI, K.; GRÖGL, M. WR279,996, a third generation aminoglycoside ointment for the treatment of Leishmania major cutaneous leishmaniasis: A phase 2, randomized, double blind, placebo controlled study. *PLOS Neglected Tropical Diseases* v. 3, i. 5, e432, p. 1-9, 2009.

SALAH, A. B.; MESSAOUD, N. B.; GUEDRI, E.; ZAA TOUR, A.; ALAYA, N. B.; BETTAIED, J.; GHARBI, A.; HAMIDA, N. B.; BOUKTHIR, A.; CHLIF, S.; ABDELHAMID, K.; AHMADI, Z. E.; LOUZIR, H.; MOKNI, M.; MORIZOT, G.; BUFFET, P.; SMITH, P. L.; KOPYDLOWSKI, K. M.; KREISHMAN-DEITRICK, M.; SMITH, K. S.; NIELSEN, C. J.; ULLMAN, D. R.; NORWOOD, J. A.; THORNE, G. D.; McCARTHY, W. F.; ADAMS, R. C.; RICE, R. M.; TANG, D.; BERMAN, J.; RANSOM, J.; MAGILL, A. J.; GROGL, M. Topical paromomycin with or without gentamicin for cutaneous leishmaniasis. *The New England Journal of Medicine* v. 368, i. 6, p. 524-532, 2013.

SANNA, V.; ROGGIO, A. M.; SILIANI, S.; PICCININI, M.; MARCEDDU, S.; MARIANI, A.; SECHI, M. Development of novel cationic chitosan- and anionic alginate-coated poly (D,L-lactide-co-glycolide) nanoparticles for controlled release and light protection of resveratrol. *International Journal of Nanomedicine* v.7, p. 5501-5516, 2012.

SANTOS, D. C. M.; SOUZA, M. L. S.; TEIXEIRA, E. M.; ALVES, L. L.; VILELA, J. M. C.; ANDRADE, M.; CARVALHO, M. G.; FERNANDES, A. P.; FERREIRA, L. A. M.; AGUIAR, M. M. G. A new nanoemulsion formulation improves antileishmanial activity and reduces toxicity of amphotericin B. *Journal of Drug Targeting*, 2017. doi: 10.1080/1061186X.2017.1387787

SANTOS, C. M.; OLIVEIRA, R. B.; ARANTES, V. T.; CALDEIRA, L. R.; OLIVEIRA, M. C.; EGITO, E. S. T.; FERREIRA, L. A. M. Amphotericin B-loaded nanocarriers for topical treatment of cutaneous leishmaniasis: development, characterization, and *in vitro* skin permeation studies. *Journal of Biomedical Nanotechnology* v. 8, p. 322-329, 2012.

SENGUPTA, P.; CHATTERJEE, B. Potential and future scope of nanoemulgel formulation for topical delivery of lipophilic drugs. *International Journal of Pharmaceutics* v. 526, i. 1-2, p. 353-365, 2017.

SETYA, S.; TALEGAONKAR, S.; RAZDAN, B. K. Nanoemulsions: Formulation methods and stability aspects. *World Journal of Pharmacy and Pharmaceutical Science* v. 3, i. 2, p. 2214-2228, 2014.

SHAHAVI, M. H.; HOSSEINI, M.; JAHANSHAHI, M.; MEYER, R. L.; DARZI, G. N. Evaluation of critical parameters for preparation of stable clove oil nanoemulsion. *Arabian Journal of Chemistry*, 2015. doi: <https://doi.org/10.1016/j.arabjc.2015.08.024>

SHARMA, M.; MANN, B.; SHARMA, R.; BAJAJ, R.; ATHIRA, S.; SARKAR, P.; POTHURAJU, R. Sodium caseinate stabilized clove oil nanoemulsion: Physicochemical properties. *Journal of Food Engineering* v. 212, p. 38-46, 2017.

SHARMA, S.; PARMAR, A.; KORI, S.; SAHNDHIR, R. PLGA-based nanoparticles : A new paradigm in biomedical applications. *Trends in Analytical Chemistry* v. 80, p. 30-40, 2016.

SILVA, A. E.; BARRAT, G.; CHÉRON, M.; EGITO, E. S. T. Development of oil-in-water microemulsions for the oral delivery of amphotericin B. *International Journal of Pharmaceutics* v. 454, p. 641-648, 2013.

SILVA, R. E.; CARVALHO, J. P.; RAMALHO, D. B.; SENNA, M. C. R.; MOREIRA, H. S. A.; RABELLO, A.; COTA, E.; COTA, G. Towards a standard protocol for antimony intralesional infiltration technique for cutaneous leishmaniasis treatment. *Memórias do Instituto Oswaldo Cruz* v. 113, i. 2, p. 71-79, 2018.

SILVA-JUNIOR, A. A.; MATOS, J. R.; FORMARIZ, T. P.; ROSSANEZI, G.; SCARPA, M. V.; EGITO, E. S. T.; OLIVEIRA, A. G. Thermal behavior and stability of biodegradable spray-dried microparticles containing triamcinolone. *International Journal of Pharmaceutics* v. 368, p. 45-55, 2009.

SILVERSTEIN, R. M.; WEBSTER, F. X.; KIEMLE, D. J. *Spectrometric identification of organic compounds*. United States: John Wiley & Sons. Seventh Edition, 2005.

SINGH, A.; VAN DEN MOOTER, G. Spray drying formulation of amorphous solid dispersions. *Advanced Drug Delivery Reviews* v. 100, p. 27-50, 2016.

SINGH, M. N.; HEMANT, K. S. Y.; RAM, M. SHIVAKUMAR, H. G. Microencapsulation: A promising technique for controlled drug delivery. *Research in Pharmaceutical Sciences* v.5, i. 2, p. 65-77, 2010.

SINGH, N.; KUMAR, M.; SINGH, R. K. Leishmaniasis: Current status of available drugs and new potential drug targets, *Asian Pacific Journal of Tropical Medicine*, p. 485-497, 2012.

SINGH, S.; SIVAKUMAR, R. Challenges and new discoveries in the treatment of leishmaniasis. *Journal of Infection and Chemotherapy* v.10, i. 6, p. 307-315, 2004.

SINGH, Y.; MEHER, J. G.; RAVAL, K.; KHAN, F. A.; CHAURASIA, M.; JAIN, N. K.; CHOURASIA, M. K. Nanoemulsion: concepts, development and applications in drug delivery. *Journal of Controlled Release* v. 252, p. 28-49, 2017.

SIQUEIRA, L. B. O.; CARDOSO, V. S.; RODRIGUES, I. A.; VASQUEZ-VILLA, A. L.; SANTOS, E. P.; GUIMARÃES, B. C. L. R.; COUTINHO, C. S. C.; VERMELHO, A. B.; RICCI-JUNIOR, E. Development and evaluation of zinc phthalocyanine nanoemulsions for use in photodynamic therapy for *Leishmania* spp. *Nanotechnology* v. 28, 2017 doi: 10.1088/1361-6528/28/6/065101.

SOARES, D. C.; PEREIRA, C. G.; MEIRELES, M. A.; SARAIVA, E. M. Leishmanicidal activity of a supercritical fluid fraction obtained from *Tabernaemontana catharinensis*. *Parasitology International* v. 56, p. 135-139, 2007.

SOLANS, C.; SOLÉ, I. Nano-emulsions: Formation by low energy methods. *Current Opinion in Colloid & Interface Science* v. 17, p. 246-254, 2012.

SOLLOHUB, K.; CAL, K. Spray drying technique: II. Current applications in pharmaceutical technology. *Journal of Pharmaceutical Sciences* v. 99, i. 2, p. 586-597, 2010.

SON, Y. J.; McCONVILLE, J. T. Preparation of sustained release rifampicin microparticles for inhalation. *Journal of Pharmacy and Pharmacology* v. 64, p. 1291-1302, 2012.

SOSA, L.; CLARES, B.; ALVARADO, H. L.; BOZAL, N.; DOMENECH, O.; CALPENA, A. C. Amphotericin B releasing topical nanoemulsion for the treatment of candidiasis and aspergillosis. *Nanomedicine: Nanotechnology, Biology and Medicine* v. 13, p. 2303-2312, 2017.

SOSNIK, A.; SEREMETA, K. P. Advantages and challenges of spray-drying technology for the production of pure drug particles and drug-loaded polymeric carries. *Advances in Colloid and Interface Science* v. 223, p. 40-54, 2015.

SOUSA-BATISTA, A. J.; PACIENZA-LIMA, W.; ARRUDA-COSTA, N.; FALCÃO, C. A. B.; RÉ, M. I.; ROSSI-BERGMANN, B. Depot subcutaneous injection with chalcone CH8-loaded poly(lactic-co-glycolic acid) microspheres as a single-dose treatment of cutaneous leishmaniasis. *Antimicrobial Agents and Chemotherapy* v. 62, i. 3, p. e01822-17, 2018. doi: 10.1128/AAC.01822-17.

STEVENSON, C. L.; SANTINI JUNIOR, J. T.; LANGER, R. Reservoir-based drug delivery systems utilizing microtechnology. *Advanced Drug Delivery Reviews* v. 64, p. 1590-1602, 2012.

SUNDAR, S.; CHAKRAVARTY, J. An update on pharmacotherapy for leishmaniasis. *Expert Opinion on Pharmacotherapy* v. 16, i. 2, p. 237-252, 2015.

SUNDERLAND, T.; KELLY, J. G.; RAMTOOLA, Z. Application of a novel 3-fluid nozzle spray drying process for the microencapsulation of therapeutic agents using incompatible drug-polymer solutions. *Archives of Pharmacal Research* v. 38, i. 4, p. 566-573, 2015.

SWIDER, E.; KOSHINA, O.; TEL, J.; CRIZ, L. J.; DE VRIES, J. M.; SRINIVAS, M. Customizing poly(lactic-co-glycolic acid) particles for biomedical applications. *Acta Biomaterialia* v. 78, p. 38-51, 2018.

TANG, S. T.; MANICKAM, S.; WEI, T. K.; NASHIRU, B. Formulation development and optimization of a novel Cremophore EL-based nanoemulsion using ultrasound cavitation. *Ultrasonics Sonochemistry* v. 19, p. 330-345, 2012.

TAO, S. L.; DESAI, T. A. Microfabricated drug delivery systems: from particles to pores. *Advanced Drug Delivery Reviews* v.55, p. 315-328, 2003.

TEIXEIRA, R. R.; GAZOLLA, P. A. R.; SILVA, A. M.; BORSODI, M. P. G.; BERGMANN, B. R.; FERREIRA, R. S.; VAZ, B. G.; VASCONCELOS, G. A.; LIMA, W. P. Synthesis and leishmanicidal activity of eugenol derivatives bearing 1,2,3-trialoze functionalities. *European Journal of Medicinal Chemistry* v. 146, p. 274-278, 2018.

THE INTERNATIONAL PHARMACOPEIA, 7th Ed., Monographs: Pharmaceutical substances: Amphotericin B (Amphotericinum B), 2017a. Available at: <http://apps.who.int/phint/en/p/docf/> Accessed in: January 2018.

THE INTERNATIONAL PHARMACOPEIA, 7th Ed., Monographs: Pharmaceutical substances: Paromomycin sulfate (Paromomycini sulfas), 2017b. Available at: <http://apps.who.int/phint/en/p/docf/> Accessed in: January 2018.

TIUMAN, T. S.; SANTOS, A. O.; UEDA-NAKAMURA, T.; DIAS FILHO, B. P.; NAKAMURA, C. V. Recent advances in leishmaniasis treatment, *International Journal of Infectious Diseases* v. 15, p. e525-e532, 2011.

TOMARO-DUCHESNEAU, C.; SAHA, S.; MALHOTRA, M.; KAHOU LI, I.; PRAKASH, S. Microencapsulation for the therapeutic delivery of drugs, live mammalian and bacterial cells, and other biopharmaceutics: Current status and future directions. *Journal of Pharmaceutics*, 2013 doi: 10.1155/2013/103527

TORRES-SANTOS, E. C.; SAMPAIO-SANTOS, M. I.; BUCKNER, F. S.; YOKOYAMA, K.; GELB, M.; URBINA, J. A.; ROSSI-BERGMANN, B. Altered sterol profile induced in *Leishmania amazonensis* by a natural dihydroxymethoxylated chalcone. *Journal of Antimicrobial Chemotherapy* v. 63, p. 469-472, 2009.

TRAN, V. T.; BENOÎT, J. P.; VENIER-JULIENNE, M. C. Why and how to prepare biodegradable, monodispersed, polymeric microparticles in the field of pharmacy? *International Journal of Pharmaceutics* v. 407, p. 1-11, 2011.

UNITED STATES PHARMACOPEIA (USP) 35, v. 2, Amphotericin B, p. 2206-2207, 2012a.

UNITED STATES PHARMACOPEIA (USP) 35, v. 2, Paromomycin, p. 4223-4224, 2012b.

UNITED STATES PHARMACOPEIA (USP) 35, v. 1, Buffer Solutions, p. 1067-1068, 2012c.

WALKER, S.; TAILOR, S. A. N.; LEE, M.; LOUIE, L.; LOUIE, M.; SIMOR, A. E. Amphotericin B in lipid emulsion: stability, compatibility, and *in vitro* antifungal activity. *Antimicrobial Agents and Chemotherapy* v. 42, i. 4, p. 762-766, 1998.

WAN, F.; BOHR, A.; MALTESEN, M. J.; BJERREGAARD, S.; FOGED, C.; RANTANEN, J.; YANG, M. Critical solvent properties affecting the particle formation and characteristics of celecoxib-loaded PLGA microparticles via spray-drying. *Pharmaceutical Research* v. 30, p. 1065-1076, 2013a.

WAN, F.; WU, J. X.; BOHR, A.; BALDURSDOTTIR, S. G.; MALTESEN, M. J.; BJERREGAARD, S.; FOGED, C.; RANTANEN, J.; YANG, M. Impact of PLGA molecular behavior in the feed solution on the drug release kinetics of spray dried microparticles. *Polymer* v. 54, p. 5920-5927, 2013b.

WAN, F.; MALTESEN, M. J.; ANDERSEN, S. K.; BJERREGAARD, S.; FOGED, C.; RANTANEN, J.; YANG, M. One-step production of protein-loaded PLGA microparticles via spray drying using 3 fluid nozzle. *Pharmaceutical Research* v. 31, p. 1967-1977, 2014a.

WAN, F.; MALTESEN, M. J.; ANDERSEN, S. K.; BJERREGAARD, S.; BALDURSDOTTIR, S. G.; FOGED, C.; RANTANEN, J.; YANG, M. Modulating protein release profiles by incorporation hyaluronic acid into PLGA microparticles via spray dryer equipped with a 3-fluid nozzle. *Pharmaceutical Research* v. 31, 2940-2951, 2014b.

WANG, F. J.; WANG, C.H. Sustained release of etanidazole from spray dried microspheres prepared by non-halogenated solvents. *Journal of Controlled Release* v. 81, p. 263-280, 2002.

WANG, F. J.; WANG, C. H. Etanidazole-loaded microspheres fabricated by spray-drying different poly(lactide/glycolide) polymers: effects on microspheres properties. *Journal of Biomaterials Science, Polymer Edition* v. 14, i. 2, p. 157-183, 2003.

WANG, F.; YANG, M. Design of PLGA-based depot delivery systems for biopharmaceuticals prepared by spray drying. *International Journal of Pharmaceutics* v. 498, p. 82-95, 2016.

WANG, H.; ZHANG, G.; SUI, H.; LIU, Y.; PARK, K.; WANG, W. Comparative studies on the properties of glycyrrhetic acid-loaded PLGA microparticles prepared by emulsion and template methods. *International Journal of Pharmaceutics* v. 496, p. 723-731, 2015.

WANG, L.; WANG, Y. S.; CHEN, R. Y.; FENG, C. L.; WANG, H.; ZHU, X. W.; YU, J. N.; XU, X. M. PLGA microspheres as a delivery vehicle for sustained release of tetracycline: biodistribution in mice after subcutaneous administration. *Journal of Drug Delivery Science and Technology* v. 23, i. 6, p. 547-553, 2013.

WANG, P.; WANG, Q.; REN, T.; GONG, H.; GOU, J.; ZHANG, Y.; CAI, C.; TANG, X. Effects of Pluronic F127-PEG multi-gel-core on the release profile and pharmacodynamical of exenatide loaded in PLGA microspheres. *Colloids and Surface B: Biointerfaces* v. 147, p. 360-367, 2016.

WEN, M. M.; EL-SALAMOUNI, N. S.; EL-REFAIE, W. M.; HAZZAH, H. A.; ALI, M. M.; TOSI, G.; FARID, R. M.; BLANCO-PRIETO, M. J.; BILLA, N.; HANAFY, A. S. Nanotechnology based drug delivery systems for Alzheimer's disease management: Technical, industrial and clinical challenges. *Journal of Controlled Release* v. 245, p. 95-107, 2017.

WISCHKE, C.; SCHWENDEMAN, S. P. Principles of encapsulating hydrophobic drugs in PLA/PLGA microparticles. *International Journal of Pharmaceutics* v. 364, p. 298-327, 2008.

WORLD HEALTH ORGANIZATION (WHO). Leishmaniasis. Available at: <http://www.who.int/mediacentre/factsheets/fs375/en/> Accessed in May 2017.

WORLD HEALTH ORGANIZATION (WHO). Control of the Leishmaniasis. WHO Technical Report Series n. 949, Geneva, 2010.

YAHYA, M.; FATEMEH, G.; ABDOLHOSEIM, D.; ZOHREH, S.; ZUHAIR, H. Effect of cantharidin on apoptosis of the *Leishmania major* and on parasite load in BALB/c mice, *Research Journal of Parasitology* v.8, i. 1, p. 14-25, 2013.

YAN, H.; HOU, Y. F.; NIU, P. F.; SHOJI, T.; TSUBOI, Y.; YAO, F. Y.; ZHAO, L. M.; CHANG, J. B. Biodegradable PLGA nanoparticles loaded with hydrophobic drugs: confocal Raman microspectroscopic characterization. *Journal of Materials Chemistry B* v. 3, p. 3677-3680, 2015.

YAO, S.; LIU, H.; YU, S.; LI, Y.; WANG, X.; WANG, L. Drug-nanoencapsulated PLGA microspheres prepared by emulsion electrospray with controlled release behavior. *Regenerative Biomaterials* v. 3, i. 5, p. 309-317, 2016. doi: 10.1093/rb/rbw033

ZHENG, Y.; OUYANG, W. Q.; SYED, S. F.; HAO, C. S.; WANG, B. Z.; SHANG, Y. H. Effects of carbopol® 934 proportion on nanoemulsion gel for topical and transdermal drug delivery: a skin permeation study. *International Journal of Nanomedicine* v. 11, p. 5971-5987, 2016.

ZIA, Q.; MOHAMMAD, O.; RAUF, M. A.; KHAN, W.; ZUBAIR, S. Biomimetically engineered Amphotericin B nano-aggregates circumvent toxicity constraints and treat systemic fungal infection in experimental animals. *Nature Scientific Reports* 2017. doi: 10.1038/s41598-017-11847-0

ZULFIQAR, B.; SHELPER, T. B.; AVERY, V. M. Leishmaniasis drug discovery: recent progress and challenges in assay development. *Drug Discovery Today* v. 22, i. 10, p. 1516-1531, 2017.

ZUO, J.; ZHAN, J.; LUO, C.; DONG, B.; XING, F.; CHEN, D. Characteristics and release property of polylactic acid/sodium monofluorophosphate microcapsules prepared by spray drying. *Advanced Powder Technology* v. 28, i. 11, p. 2805-2811, 2017.

ZU, Y.; SUN, W.; ZHAO, X.; WANG, W.; LI, Y.; GE, Y.; LIU, Y.; WANG, K. Preparation and characterization of amorphous amphotericin B nanoparticles for oral administration through liquid antisolvent precipitation. *European Journal of Pharmaceutical Sciences* v. 53, p. 109-117, 2014.

CHAPTER 7

RÉSUMÉ LONG EN FRANÇAIS

La leishmaniose est une maladie infectieuse, non contagieuse, négligée causée par des parasites protozoaires du genre *Leishmania* et transmis par la piqûre d'un phlébotome. Cette maladie affecte 98 pays, 12 millions de personnes, 350 millions risquent de développer la leishmaniose dans plusieurs pays. Par ailleurs, la co-infection *Leishmania*/ VIH (virus de l'immunodéficience humaine) a été identifiée dans 35 pays et présente une tendance de croissance. Cette maladie peut être de type cutanée (LC), muco-cutanée (LMC) et viscérale (LV), en fonction de l'espèce infectieuse et de la réponse immunologique de l'hôte.

La leishmaniose cutanée (LC) ou la leishmaniose tégumentaire américaine (ATL) est caractérisée par des lésions sur la peau, apparaissant principalement au niveau local de la piqûre d'insecte. La première lésion est en général unique et indolore. Après une période de 1 à 12 semaines, une lésion apparaît sous la forme d'une papule érythémateuse qui se développe en un nodule avec une base nécrotique et des bords surélevés en une période de deux semaines à six mois. Cette manifestation clinique est endémique dans plus de 70 pays et est considérée comme l'une des six maladies infectieuses les plus importantes, car la LC présente une grande capacité à causer des déformations et un coefficient de détection élevé.

Le traitement de premier choix consiste en une administration intraveineuse, intralésionnelle ou intramusculaire d'antimomiate pentavalent. Le traitement de second choix implique l'administration intraveineuse ou intramusculaire d'amphotéricine B et de pentamidine. Le traitement actuel de la leishmaniose, en particulier de la LC, a de nombreux effets secondaires (médicaments toxiques), une résistance au parasite et une faible adhésion des patients (traitement injectable, douloureux et prolongé). Ces facteurs intensifient la recherche de nouvelles formulations pharmaceutiques et l'étude de différentes voies d'administration principalement pour le traitement de la LC, pour lesquelles des micro et nano-systèmes de délivrance de médicaments pourraient représenter des solutions technologiques intéressantes capables de moduler le relargage ou la biodisponibilité des principes actifs.

Un médicament important est l'amphotéricine B (AmB), un antibiotique macrolide injectable utilisé comme traitement de deuxième choix. L'AmB a une faible solubilité et une faible perméabilité et est classé dans la classe IV du SCB.

L'AmB est l'un des médicaments les plus étudiés pour le traitement de la leishmaniose. Elle est utilisée dans différents systèmes d'administration pour améliorer leur activité leishmanicide et réduire leurs effets secondaires. Comme l'AmB est très toxique, les formulations topiques contenant ce médicament peuvent être une option intéressante pour réduire sa toxicité.

Un des médicaments alternatifs étudiés pour le traitement de la LC est la paromomycine (PM), un antibiotique aminoglycoside utilisé par voie intraveineuse et topique. La PM est fortement soluble dans l'eau, mais présente une faible perméabilité, ce qui permet d'insérer ce médicament dans la classe III du système de classification biopharmaceutique (SCB). En raison de la faible perméabilité du médicament, les formulations topiques de PM ont un usage controversé, en particulier contre les espèces de *Leishmania* de «Nouveau Monde». Il existe peu d'études portant sur la caractérisation physicochimique de la PM ou sur les systèmes de libération de la PM. De plus, ce médicament n'a pas encore été approuvé pour le traitement de la leishmaniose dans des pays comme le Brésil, où cette maladie est présente.

Cette thèse porte sur le développement d'une nanoémulsion d'huile-dans-l'eau (HE) contenant AmB pour une administration topique et des microparticules polymériques contenant PM obtenues par séchage par atomisation pour une administration intralésionnelle pour le traitement de la LC. Les formulations ont été caractérisées en termes de taille et morphologie de particules et gouttelettes d'huile, contenu d'actif, stabilité, propriétés thermiques, relargage *in vitro*. L'activité biologique a été évaluée *in vitro* sur des macrophages et l'activité antileishmanienne sur des promastigotes de *Leishmania amazonensis*.

Les nanoémulsions HE contenant Amphotéricine B (AmB)

Les nanoémulsions HE contenant AmB ont été préparées par un procédé d'émulsification sous ultrasons. Les huiles essentielles (huile de girofle et huile de menthe) ont été sélectionnées pour la phase huileuse en raison de leur capacité à augmenter la perméation des médicaments.

Douze lots ont été préparés en modifiant leur composition comme l'huile essentielle utilisée, la présence de tensioactif (0 à 5% de Tween® 20 en masse), la quantité de polymère utilisée en phase aqueuse (10 à 15% de Pluronic® F127

en masse) et la présence d'AmB (0,5 mg/mL). Les étapes de préparation des nanoémulsions peuvent être visualisées sur la Figure 1. Les lots ont été caractérisés par la taille des gouttelettes, l'indice de polydispersité, le pH et la teneur d'AmB.

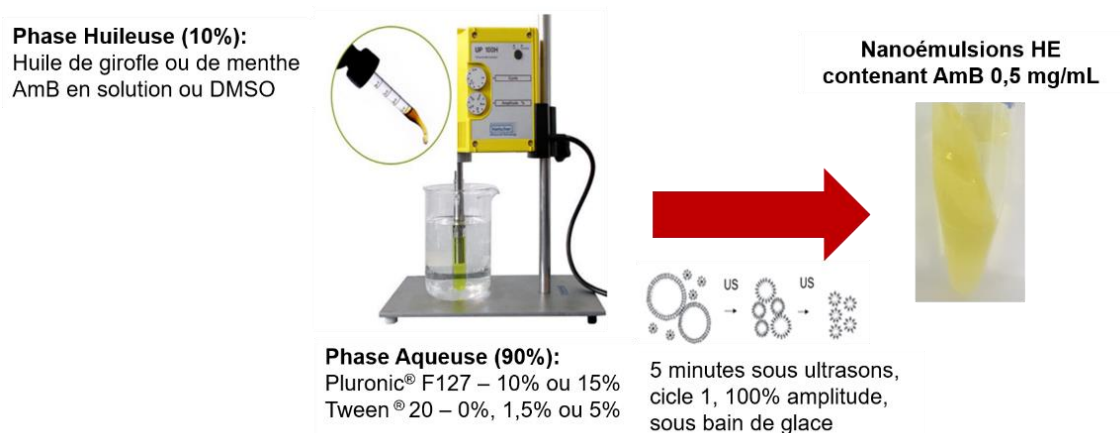


Figure 1 – Représentation schématique de la préparation des nanoémulsions. (DMSO – diméthylsulfoxyde et HE - huile-dans-l'eau).

Les nanoémulsions contenant AmB présentait une couleur jaune et un aspect physique de gel. Les lots produits avec de l'huile de menthe présentait une couleur jaune opaque, la taille de gouttelettes moyenne la plus élevée (entre 60 et 380 nm) et des valeurs élevées d'indice de polydispersité ($> 0,45$). Les échantillons préparés avec de l'huile de girofle étaient caractérisés par une taille moyenne de gouttelettes inférieure à 100 nm et un indice de polydispersité inférieur à 0,4. En ce qui concerne les valeurs de pH des nanoémulsions, les valeurs sont restées 4,5 et 5,0, ce qui correspond à un pH compatible avec le pH de la peau humaine. Les résultats de la teneur d'AmB ainsi que la taille moyenne des gouttelettes et l'indice de polydispersité ont permis de choisir les meilleures nanoémulsions AmB pour des caractérisations supplémentaires.

Deux nanoémulsions contenant AmB sélectionnées (B-NE avec Tween® 20 et F-NE sans Tween® 20) et deux formulations placebos (sans AmB) correspondantes, L-NE et H-NE, ont été soumises à un test de stabilité dans deux conditions de stockage (température ambiante - 28°C et chaîne du froid - 4°C). Les échantillons ont été analysés au cours des jours de stockage suivants: 0, 7, 15, 30, 60, 90, 180 et 365 jours. Les formulations contenant AmB et respectivement les formulations blanches ont montré une bonne stabilité et sont

restées stables jusqu'à 365 jours de stockage (tailles de gouttelettes d'huile de l'ordre d'environ 50 nm, avec un indice de polydispersité inférieur à 0,4). Il a également été observé que les nanoémulsions contenant le médicament présentaient une taille de gouttelette moyenne et un indice de polydispersité plus élevés que les formulations placebos. Par rapport à la teneur d'AmB, il a été vérifié que les nanoémulsions stockées à 4°C présentaient une concentration d'AmB inchangée (supérieure à 95%) sur toute la période de stockage, ne présentant qu'une réduction statistiquement significative à la fin de l'expérience (365 jours). Cependant, cette évolution était inférieure à celle observée pour les échantillons stockés à température ambiante, qui ont présenté une diminution de la teneur d'AmB au long du stockage. Par conséquent, les nanoémulsions d'AmB ont besoin d'être conservées à des températures de l'ordre de 4°C.

Le pH des nanoémulsions soumises à l'étude de stabilité est resté inchangé à 5,0 pendant toute la période de stockage, dans les deux conditions de stockage. De plus, ces nanoémulsions étaient constituées de gouttelettes de forme sphérique avec une taille moyenne inférieure à 100 nm, confirmé par une analyse dynamique de la diffusion de la lumière.

Après l'étude de stabilité, les nanoémulsions d'AmB ont été étudiées pour déterminer leur profil de relargage *in vitro* (Fig 24, chapitre 3). Les deux nanoémulsions sélectionnées (B-NE et F-NE) présentaient un profil de relargage similaire et très lent d'AmB. La toxicité de l'AmB est un verrou dans le traitement conventionnel de la leishmaniose. Un profil de relargage lent d'AmB devrait être plus adaptée, diminuant la toxicité du médicament. Les nanoémulsions semblent représenter une formulation convenable pour une administration topique d'AmB.

Les nanoémulsions d'AmB ont été soumises à une étude de perméation *in vitro* (Fig 26, chapitre 3), à travers la peau d'oreille de porc. Les quantités d'AmB dans le compartiment receveur, dans l'épiderme et dans le derme ont été déterminées après 8 heures d'expérience par analyse pour chromatographie en phase liquide à haute performance.

Les deux formulations présentaient une rétention d'AmB supérieure à 0,7 $\mu\text{g} / \text{cm}^2$ dans l'épiderme et comprise entre 0,16 et 0,36 $\mu\text{g} / \text{cm}^2$ dans le derme. Bien que ces résultats suggèrent une faible perméation de l'AmB par les nanoémulsions, il existe une certaine quantité de médicament retenue dans le

derme qui peut favoriser le traitement de la LC lorsque les parasites y sont localisés.

La quantité d'AmB pénétrée à partir des deux nanoémulsions (B-NE et F-NE) était inférieure à $2 \mu\text{g} / \text{cm}^2$ (ou inférieure à 0,2%) après 8 heures. Les valeurs plus faibles de médicament pénétré après 8 heures peuvent être liées au profil de relargage très lent obtenu. De plus, la faible quantité d'AmB pénétrée suggère une faible action systémique de ces formulations, diminuant la toxicité et les effets secondaires d'AmB, et renforçant l'action locale souhaitée pour ces formulations

La cytotoxicité de ces formulations a été étudiée dans les cellules de macrophages dérivés de la moelle osseuse. Une relation dépendante de la dose avec la cytotoxicité a été observée, en particulier pour l'AmB libre. L'AmB libre a présenté une toxicité élevée avec des concentrations supérieures à $0,2 \mu\text{g} / \text{mL}$, alors que les nanoémulsions d'AmB et la nanoémulsion sans AmB ont été toxiques à toutes concentrations testées. Cette toxicité élevée pourrait être liée à la présence d'huile de girofle (cytotoxique). Cependant, ce résultat est à considérer avec réserve car cette toxicité devrait être validée par des études *in vivo*.

L'activité antileishmanienne des nanoémulsions d'AmB a été étudiée contre les promastigotes de *Leishmania amazonensis*, avec l'activité des l'AmB et l'huile de girofle libres par référence. L'AmB libre a montré une activité antileishmanienne contre les promastigotes à des concentrations supérieures à $0,1 \mu\text{g}/\text{mL}$. L'huile de girofle a montré une activité antileishmanienne contre les promastigotes à des concentrations supérieures à $3 \mu\text{g}/\text{mL}$. L'activité anti leishmanicide de l'huile de girofle avait déjà été décrite dans la littérature, qui établissait une corrélation entre cet effet et l'eugénol, principal constituant de l'huile de girofle. F-NE et H-NE ainsi que B-NE et L-NE ont montré une activité antileishmaniale. Cependant, F-NE a montré un effet leishmanicide plus faible en comparaison avec B-NE; H-NE a montré un effet leishmanicide plus faible en comparaison avec L-NE. Cela peut être dû à la présence de Tween® 20 dans B-NE et L-NE, qui peut être cytotoxique. Bien que L-NE et H-NE aient été préparées sans médicament, ces nanoémulsions ont présenté un effet leishmanicide similaire à celui observé pour l'AmB libre, confirmant ainsi l'activité anti

leishmanicide de l'huile de girofle.

Sur la base du test de cytotoxicité et de l'activité leishmanicide, il a été calculé la CC_{50} , la CI_{50} et l'indice sélectif (IS) de l'AmB libre, de l'huile de girofle libre et des quatre nanoémulsions. L'indice sélectif a été calculé et les valeurs étaient inférieures à 10, ce qui établissait une corrélation entre le médicament libre, l'huile de girofle et les nanoémulsions avec ou sans AmB comme produits cytotoxiques avec une faible sélectivité pour l'effet leishmanicide. La formulation la plus favorable est la nanoémulsion AmB préparée avec le surfactant Tween® 20 (B-NE), qui a montré le meilleur indice de sélectivité (IS =6). Cependant, la formulation de B-NE présente peut-être un potentiel en termes de composition pour améliorer sa sélectivité.

Des améliorations futures pourront être envisagées : la réduction de la quantité d'AmB, des formulations nouvelles utilisant d'autres poloxamères, la réduction de la quantité de l'huile de girofle ou son remplacement dans la formulation par une autre huile. Par ailleurs, l'addition d'un composé supplémentaire pour accélérer le relargage du médicament pourrait être une autre modification permettant d'améliorer les performances de la B-NE.

Microparticules de PLGA contenant Paromomycine (PM)

Les microparticules polymériques contenant PM ont été générées par le procédé de séchage par atomisation. Vingt-cinq lots ont été générés avec différentes compositions et préparations avec deux différents atomiseurs (buse bi-fluide et buse tri-fluide, comme montre la Fig 2), du type de solvant organique utilisé, du type de polymère, la concentration en masse de PM et l'état physique de PM (dispersé dans un solvant organique ou solubilisé dans l'eau). Les PM-MS (microsphères PM) et les PM-MC (microcapsules PM) ont été caractérisées à l'aide d'un ensemble de techniques (DSC, DRX, MEB, FT-IR et Raman).

Le produit pur (PM commercial) a été initialement caractérisé (DRX, DSC), ce qui a dévoilé son caractère amorphe.

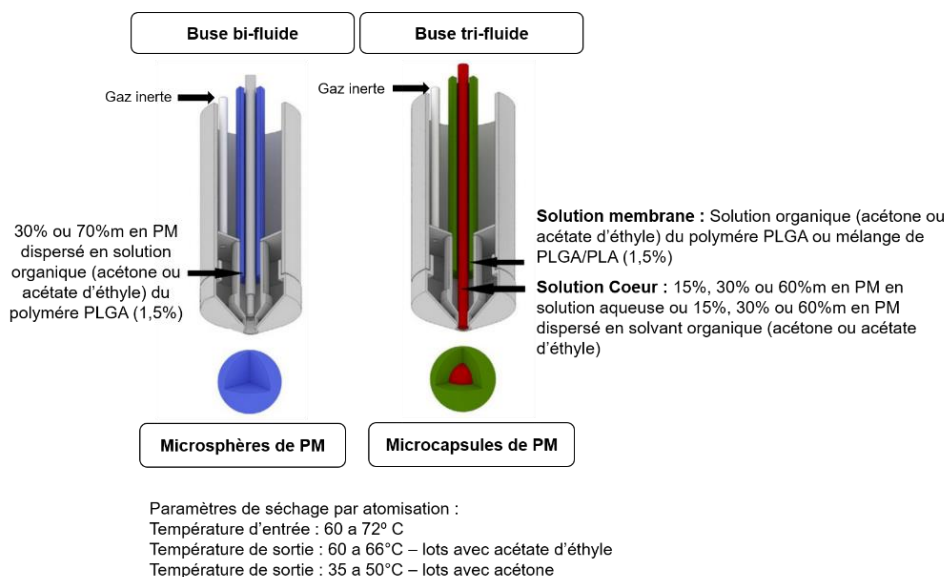


Figure 2 – Buses bi-fluide et tri-fluide utilisées lors de la préparation des microparticules de PM par séchage par atomisation

Les microcapsules de type matriciel (PM-MS) ont été développées utilisant une buse bi-fluide. Les lots ont été préparés en variant :

1) Le solvant organique, acétone ou acétate d'éthyle : les lots préparés avec de l'acétate d'éthyle présentaient de gros agglomérats, une morphologie irrégulière, avec un faible rendement du procédé, tandis que les lots produits avec de l'acétone présentaient une forme plus sphérique. Ces différences ont été attribuées aux conditions de séchage fixées afin d'évaporer les différents solvants. Comme l'acétate d'éthyle a un point d'ébullition plus élevé que l'acétone, la poudre a été exposée à des températures plus élevées lors du séchage et comme la poudre contenait du PLGA, polymère avec une température de transition vitreuse de l'ordre de 40°C, l'acétone a été choisie comme solvant pour produire des microparticules à des températures plus faibles.

2) Concentration du principe actif (30% et 70% m en PM) : le lot préparé avec la plus faible quantité de PM (30% m) a montré un rendement et une efficacité d'encapsulation plus élevés.

Les microcapsules de type coeur-membrane (PM-MC) ont été développées utilisant une buse tri-fluide. Les lots ont été préparés en variant :

1) La concentration initiale de principe actif dans la formulation (de 15 à 60% m PM) : comme espéré, l'augmentation de la concentration de PM conduisait à

une augmentation de la charge de médicament dans les microcapsules et de l'efficacité d'encapsulation.

2) L'état physique de PM dans le cœur (solubilisé dans l'eau ou dispersé dans le solvant organique) : Les lots produits avec PM solubilisé dans l'eau contenaient une charge plus élevée du principe actif dans les microcapsules que les lots produits avec PM dispersé dans l'acétone.

3) La composition du cœur (PLGA ou un mélange de PLGA / PLA avec différentes proportions massiques de PLA) : L'utilisation d'un mélange PLGA / PLA en tant que support polymérique a influencé la charge en médicament, l'efficacité d'encapsulation et le rendement, favorisés par l'augmentation de la proportion du PLA dans le mélange.

Nous avons également constaté qu'un lot produit avec la même taille d'orifice de buse (1,4 mm) et avec buse bi-fluide présentait des valeurs en principe actif et efficacité d'encapsulation inférieures à celles du lot préparé avec buse tri-fluide.

Les caractéristiques des produits (microparticules PM-MS et microcapsules PM-MC) ressorties des analyses thermiques et FT-IR sont les suivantes :

- Un seul événement thermique lié à la température de transition vitreuse du PLGA pour les particules ne contenant que PLGA comme polymère.
- Un seul événement correspondant à une température intermédiaire de transition vitreuse entre PLGA et PLA pour les lots préparés avec le mélange de ces deux polymères et un événement endothermique correspondant au point de fusion du PLA
- Aucune interaction chimique entre les particules et le PLGA ou entre le mélange de particules et de PLGA / PLA n'a été observée dans l'analyse FT-IR.

L'étude de relargage *in vitro* (Fig 61, chapitre 4) a été développée avec quatre lots sélectionnés: PM-MC15 (buse tri-fluide, PLGA seul, cœur contenant PM solubilisé dans l'eau), PM-MC20 (buse tri-fluide, mélange PLGA / PLA, cœur contenant PM solubilisé dans l'eau), PM-MC18 (buse tri-fluide, PLGA seule, cœur contenant PM dispersées dans de l'acétone) et PM-MS06 (buse bi-fluide, PLGA seule, PM dispersées dans de l'acétone). PM-MS06, PM-MC15 et PM-

MC18 ont montré un relargage rapide avec plus de 66% de principe actif libéré dans la première heure, ce qui correspond à une efficacité de dissolution supérieure à 70%. Le même comportement a été observé pour les particules libres et le mélange physique. Cependant, la PM-MC20 a présenté un relargage lent, atteignant environ 34% du relargage de PM en 4h et une efficacité de dissolution de 27,5%. Pour étudier le mécanisme de relargage de PM, les pourcentages cumulés de PM de ces différentes structures (MS et MC) ont été ajustés dans le modèle de Korsmeyer-Peppas. Les quatre lots ont montré des valeurs élevées de corrélation de coefficient ($r^2 > 0,9986$), qui signifie un bon ajustement de la corrélation entre les valeurs expérimentales et les valeurs prédites. De plus, le modèle de Korsmeyer-Peppas permet de caractériser le mécanisme de relargage du médicament en fonction des valeurs de l'exposant de libération (n). Les quatre échantillons ont montré des valeurs « n » inférieures à 0,5, qui indique que le mécanisme de relargage de PM suit le modèle de diffusion « fickienne ».

L'échantillon PM-MS06 (buse bi-fluide, PLGA seule, PM dispersées dans de l'acétone) a montré un relargage rapide, ce qui peut être lié à la façon dont les particules de PM sont dispersées dans la matrice de PLGA. Probablement, les petites particules de PLGA, formées pendant le séchage par atomisation, ne peuvent pas recouvrir les plus grosses particules de PM dispersées dans la formulation liquide et vérifié avec la microscopie Raman.

De même, les échantillons, PM-MC15 et PM-MC18, préparés avec la buse tri-fluide (variant uniquement en fonction de la forme dissoute ou dispersée du principe actif), présentaient des profils de relargage similaires et rapides dans la première heure (entre 66 et 78%). Ce résultat était surprenant car la structure attendue pour les particules est de type cœur-membrane. Vraisemblablement les membranes de PLGA formées autour du cœur présentaient des pores (Fig 85, chapitre 4) qui permettent une libération rapide du PM contenu dans le cœur tout au début de la dissolution *in vitro*.

L'échantillon PM-MC20 a été préparée avec un mélange de polymères comprenant du PLGA (90%*m*) et du PLA (10%*m*) afin de aussi générer une structure coeur-membrane et produire un relargage lent de PM, ce qui a été confirmé. Deux facteurs ont probablement contribué à cet effet: la modification

de la composition de la solution organique en un mélange de solvants binaires (dichlorométhane: acétone pour solubiliser le PLA) et la présence de PLA, ce qui augmente l'hydrophobicité du mélange de polymère.

Par ailleurs, la cytotoxicité de ces échantillons a été évaluée dans les cellules de macrophages dérivées de la moelle osseuse. La PM libre présentait une cytotoxicité liée à la dose et une toxicité inférieure à celles des lots de PM-MC. La formulation placebo (sans PM) n'a montré aucune cytotoxicité. La cytotoxicité plus élevée des microparticules par rapport au principe actif libre pourrait être due au polymère utilisé, mais cela n'a pas été confirmé avec les microparticules polymériques sans PM. Plusieurs études sont nécessaires pour mieux comprendre ce comportement biologique. Par rapport à la littérature, les lots de microcapsules PM-MC testés appartiennent à la même catégorie de cytotoxicité que celle trouvée dans d'autres formulations pour le traitement de la leishmaniose.

L'activité antileishmanienne contre les promastigotes de *L. amazonensis* a été évaluée avec les mêmes échantillons de PM-MC testés dans le cadre d'un essai de cytotoxicité. Les échantillons de PM libre et de PM-MC présentaient une activité antileishmanienne similaire. De plus, la formulation placebo (sans PM) n'avait aucune activité antileishmanienne.

Comme calculé pour les nanoémulsions, CC_{50} , IC_{50} et l'indice sélectif de PM libre, des échantillons de PM-MC et la formulation blanche ont été évalués. Il a été observé que la molécule libre de PM présentait une valeur d'indice sélectif élevée par rapport aux échantillons de PM-MC. Cependant, les valeurs d'indice sélectif pour les deux échantillons étaient d'environ 50 et 41, respectivement, indiquant qu'ils présentaient une activité prometteuse, supérieure à sa cytotoxicité.

En conclusion, les deux types de formulations étudiées dans cette thèse, nano émulsions HE contenant Amphotéricine B et microparticules de PLGA ou PLGA / PLA contenant Paromomycine, pourraient être considérées comme des nouvelles alternatives pour le traitement de la leishmaniose cutanée (LC). Néanmoins, pour le confirmer, d'autres études sont nécessaires comme l'activité antileishmanienne contre les amastigotes de *L. amazonensis* et des études *in vivo* sur des souris BALB/c.

CHAPTER 8

ANNEXES

ANNEX 1 - Certificate of Analysis



CERTIFICATE OF ANALYSIS

Product : Amphotericin B, non-sterile, USP intended for use in
preparing parenteral dosage forms
Batch no : A1960924
Manufactured : July 2013
Expires : June 2015
Stored below 8°C protected from light and moisture
Description : Yellow to orange powder

Tests	Results	Specifications
Identification	: Passes tests	Passes tests
Amphotericin A	: 0 %	NMT 5 %
Loss on drying	: 1.9 %	NMT 5.0 %
Heavy metals	: NMT 20 ppm	NMT 20 ppm
Sulphated ash	: 0.3 %	NMT 0.5 %
Residual solvents:		
Methanol	: 0.1 %	NMT 0.3 %
N-methyl-pyrrolidone	: 0.5 %	NMT 0.7 %
Content of EDTA	: NMT 0.1 %	NMT 0.1 %
Total viable aerobic count	: NMT 100 cfu/g	NMT 100 cfu/g
Bacterial endotoxins	: NMT 1.0 EU/mg	NMT 1.0 EU/mg
Assay (as is)	: 1089 µg/mg	
Assay (on dried basis)	: 1110 µg/mg	NLT 750 µg/mg

Complies with USP

2013-08-07

Date

Quality Release Team

Xellia Pharmaceuticals ApS
Dalslandsgade 11
2300 Copenhagen S
Denmark

P: +45 32 64 55 00
F: +45 32 64 55 01
www.xellia.com

CVR-Nr: 61 09 46 28

**BIOVET JSC**

Office 68a, Aprilsko vastanie Blvd., 7200 Razgrad, BULGARIA,
 Phone: (+359 84) 660 888, Fax: (+359 84) 661 515
 e-mail: office@biovet.com

CERTIFICATE OF ANALYSIS

Product Name:	PAROMOMYCIN SULFATE
Quantity:	0.760 kgA 1.000 kg
Destination:	Brazil
Manufacturing Date:	August, 2013
Re-test Date:	August, 2015
Date of Issue:	19 September, 2013
Certificate Number:	0482
Quality Standard:	USP 36

TEST CHARACTERISTICS	REQUIREMENTS	RESULTS
Batch No		13080816087
Appearance	Creamy white to light yellow hygroscopic powder	Corresponds
Identification	TLC Test for sulfates	Corresponds Corresponds
pH (3% w/v)	From 5.0 to 7.5	5.3
Specific optical rotation (5.0% w/v), dried substance	From +50.0 to +55.0	+53.4
Loss on drying, % (3h, 60°C, 0.7 kPa)	Not more than 5.0	4.1
Residue on ignition, %	Not more than 2.0	0.5
Assay (microbiological method), dried substance, µg/mg -on technical weight	Not less than 675	792 760
Size of granules, %:		
- 315 µm sieve, % of granules that pass		98.0
- 180 µm sieve, % of granules that pass		94.9

I hereby certify that the above information is authentic and accurate. This batch of product has been manufactured, including packaging and quality control at the above - mentioned site in full compliance with GMP requirements of the local Regulatory Authority. The batch processing, packaging and analysis records were reviewed and found to be in compliance with GMP.

Signed by:

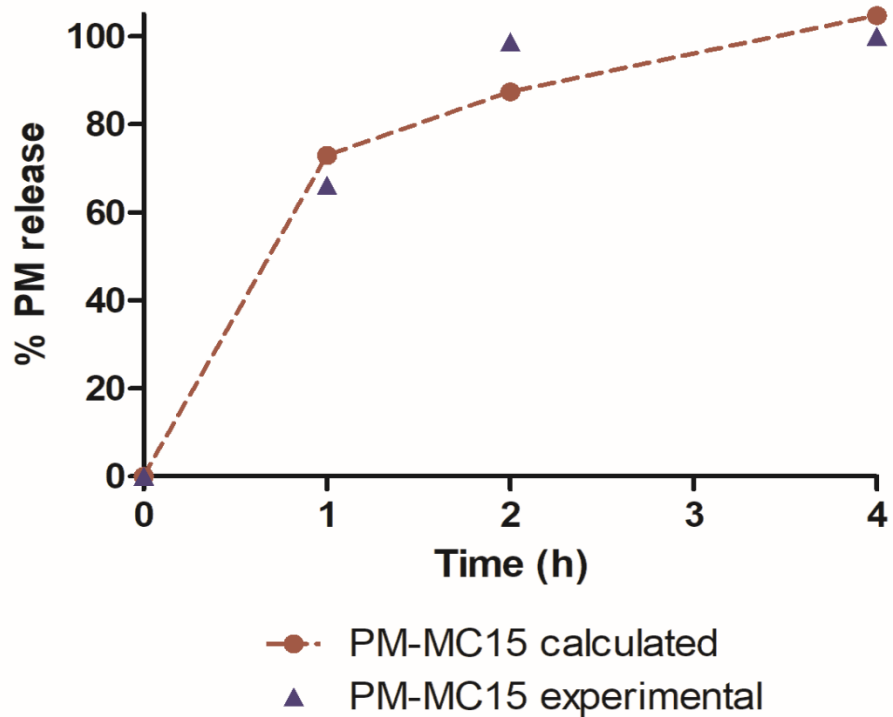
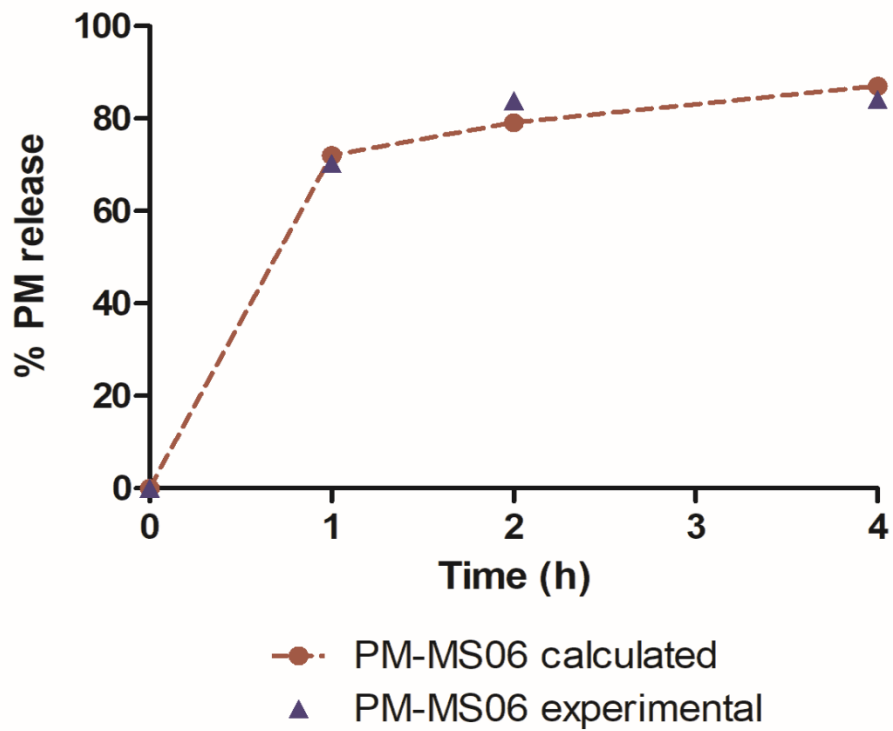
Elena GEORGIEVA
 Quality Control Lab. Manager

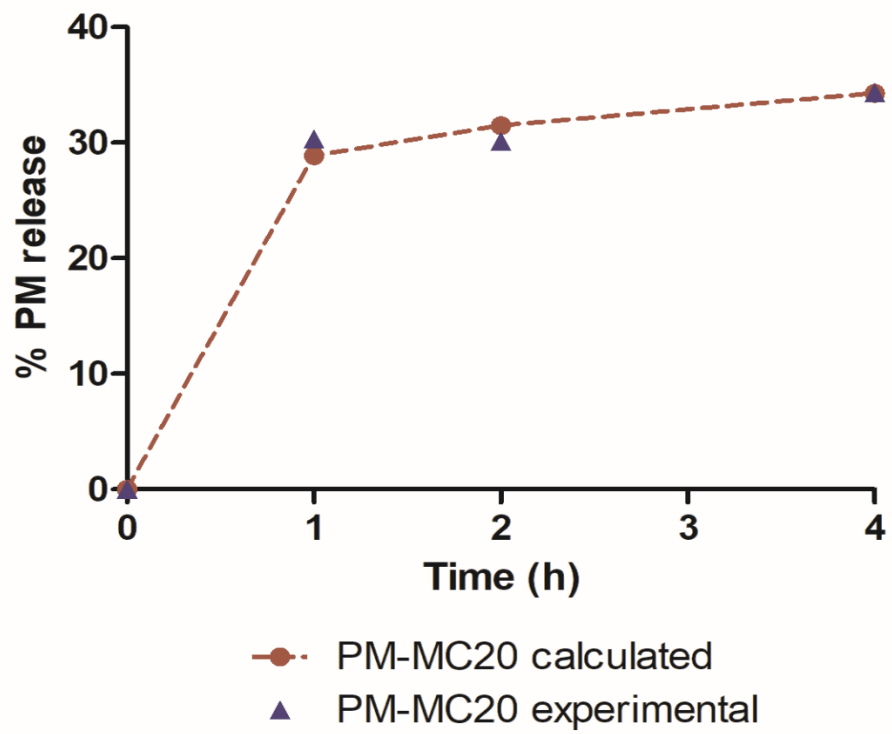
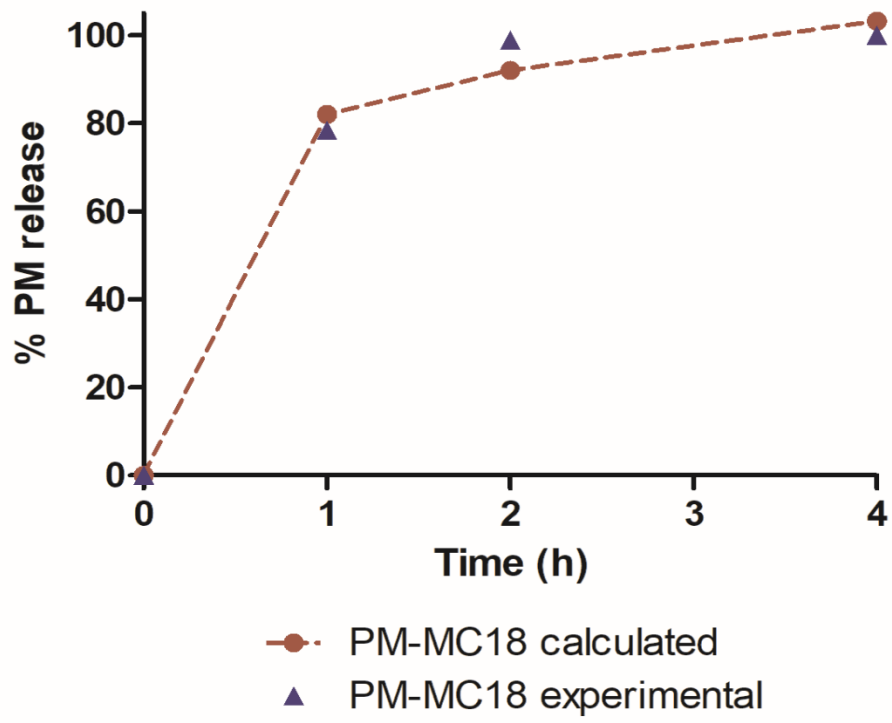
Approved by:

Nadezhda MIHAYLOVA Ph.D.
 Qualified Person



ANNEX 2 - PM release fitting described by mathematical Korsmeyer-Peppas model





CHAPTER 9

PUBLICATIONS RELATED

TO THIS WORK

Publications in International Journals

- ✓ Matos, A. P. S.; Viçosa, A.L.; Ré, M. I.; Ricci-Junior, E.; Holandino, C. A review of current treatments strategies based on paromomycin for leishmaniasis. – Under resubmission process
- ✓ Siqueira, L.B.O.; Matos, A. P. S.; Cardoso, V. S.; Villanova, J. C. O.; Guimarães, B. C. L. R.; dos Santos, E. P.; Vermelho, A. B.; Santos-Oliveira, R.; Ricci-Junior, E. Clove oil nanoemulsion showed potent inhibitory effect against *Candida* spp. – *Nanotechnology*, July 2019. doi: 10.1088/1361-6528/ab30c1
- ✓ Carvalho, S. G.; Siqueira, L. A.; Zanini, M. S.; Matos, A. P. S.; Quaresma, C. H.; Silva, L. M.; Andrade, S. F.; Severi, J. A.; Villanova, J. C.O. Physicochemical and in vitro biological evaluations of furazolidone-based β -cyclodextrin complexes in *Leishmania amazonensis*. – *Research in Veterinary Science*, v. 119, p. 143-153, 2018. doi: 10.1016/j.rvsc.2018.06.013

Publications in preparation

- Development and characterization of paromomycin polymeric microparticles for cutaneous leishmaniasis treatment;
- Development, characterization and leishmanicidal activity of topical amphotericin B nanoemulsions.

Publications in International Conferences

- ✓ Matos, A.P.S.; Azevedo, J.R.; Viçosa, A.L.; Ricci-Junior, E.; Holandino, C.; Ré, M.I. Development of paromomycin microparticles for cutaneous leishmaniasis treatment. In: 25th International Conference on Bioencapsulation. July 3-6, 2017, La Chapelle sur Erdre, France.
- ✓ Matos, A.P.S.; Leiras, T. G.; Campos, V. E. B.; Viçosa, A. L.; Ricci-Junior, E.; Holandino, C. Development, stability and leishmanicidal activity of nanoemulsions containing essential oil for cutaneous leishmaniasis treatment. In: III Congress ABCF. June 13-15, 2016, Porto Alegre, Brazil.
- ✓ Matos, A. P. S.; Campos, V. E.B.; Viçosa, A. L.; Ricci-Junior, E.; Holandino, C. Development of amphotericin B nanoemulsions for cutaneous leishmaniasis treatment. In: I International Symposium on Drug Delivery Systems. August 5-7, 2015, Maringá-Paraná, Brazil.
- ✓ Matos, A.P.S.; Campos, V. E.B.; Viçosa, A. L.; Ricci-Junior, E.; Holandino, C. Development of Paromomycin nanoparticles for cutaneous leishmaniasis treatment. In: 2nd Latin-America Symposium on Encapsulation, November 24-26, 2014, João Pessoa, Brazil.

ABSTRACT

ABSTRACT

Ana Paula dos Santos Matos. **Development of micro and nanostructured systems for cutaneous leishmaniasis treatment.** Rio de Janeiro, 2018. Thesis (PhD in Pharmaceutical Sciences), School of Pharmacy, Federal University of Rio de Janeiro, Brazil; (PhD in Process Engineering), IMT Mines Albi, Federal University of Toulouse, France, 2018.

Leishmaniasis is a neglected disease caused by protozoan parasites of the *Leishmania* genus and affects millions of people in several countries. The current treatment for cutaneous leishmaniasis (CL) has many side effects. Based on this scenario, there is an intensive search of new formulations and the study of different routes mainly for CL treatment. In this way, micro and nanotechnology are important technologies, which may be useful for modulation release profile of the drugs improving its bioavailability. One the most investigate drug for CL treatment is paromomycin (PM), an aminoglycoside antibiotic administered by the intravenous and topical route. Another important drug is intravenous amphotericin B (AmB), a macrolide antibiotic used as second-choice treatment. The aims of this study were to develop an oil-water (O/W) nanoemulsion containing AmB for topical administration and spray-dried polymeric microparticles containing PM for intralesional administration for CL treatment. Formulations were characterized mainly in terms of size and morphology of particles or oil droplets, thermal properties, drug content, stability and release behavior. Biological activity was evaluated by *in vitro* safety in macrophages and antileishmanial activity against *Leishmania amazonensis* promastigotes. O/W nanoemulsions containing AmB, were characterized by oil droplets of around 50 nm in size, with polydispersity index lower than 0.5 and drug content of 0.5 mg/mL. Nanoemulsions showed slow and controlled AmB release kinetic and low skin permeation. However, these formulations were cytotoxicity with good antileishmanial activity. Indeed, the best formulation showed stability until 365 days, but required stored in cold chain. For PM-loaded polymeric microparticles, different carriers were investigated (PLGA alone or a mixture of PLGA-PLA). It was found that PM release kinetic was influenced by the carrier composition, with a slow release for the blend of polymers. The investigated formulations were non-toxic and revealed good antileishmanial activity. Therefore, the O/W-AmB loaded nanoemulsions and the polymeric-PM loaded microparticles presented interesting results as novel alternatives for CL treatment. Nevertheless, more studies are required for their optimization as antileishmanial activity against *L. amazonensis* amastigotes and, further, *in vivo* studies in BALB/c mice.

Keywords: Cutaneous leishmaniasis, Amphotericin B, Paromomycin, Nanoemulsions, Microparticles, PLGA, PLA, Polymeric Blend, Spray Drying.